

A technical description of ACCESS-OM2, The Consortium of Ocean-Sea Ice Modelling in Australia's global ocean and sea ice model

Andrew Kiss, Andy Hogg, Kial Stewart, Adele Morrison, Aidan Heerdegen (ANU);
Nicholas Hannah (Double Precision); Marshall Ward (NCI);

Paul Spence, Matthew England, Ryan Holmes, Alfonso Acosta Goncalves (UNSW);
Russell Fiedler, Simon Marsland (CSIRO);

Fabio Dias, Abhishek Savita (UTas);

Petra Heil (AAD & ACE CRC, UTas);

Fanghua Wu (Beijing Climate Center);

Stephen Griffies (GFDL); James Munroe (Memorial U. Newfoundland)

TODO: consolidate author list and add anyone who's missing (order is arbitrary at this stage)

The latest version of this document is available from

GitHub: <https://github.com/COSIMA/ACCESS-OM2-1-025-010deg-report>

This version: typeset 2022-08-05 12:56:12 +10:00

Last commit: git hash: [315386c](#) 2022-02-18 12:19:56 +1100,

committed to branch "master" by Andrew Kiss

73 commit(s) since release 1.0

NB: git hash does not reflect any uncommitted changes to this document.

CONTRIBUTORS PLEASE NOTE:

- please sign up with GitHub and click "watch" on <https://github.com/COSIMA/ACCESS-OM2-1-025-010deg-report> to be kept informed of discussions
- to discuss aspects of the paper, please post an issue at <https://github.com/COSIMA/ACCESS-OM2-1-025-010deg-report/issues> instead of using email. You can tag relevant parts of the .tex file with \ISSUE{num} (where "num" is the issue number) to link to the issue page (change tag to \CISSUE{num} if the issue is closed, so it is easily changed back if the issue is reopened).
- note contributors for sections in the .tex file with \CONTRIBUTORS{...}
- add "to do" items to the .tex file with \TODO{...}
- note errors and problems with \FIXME{...} in the .tex file
- to make git diffs easier, please try to write each sentence in the .tex file on a separate line
- use a bare number (no leading v) if you do git tags (for compatibility with the gitinfo2 package used here)
- see <https://github.com/COSIMA/ACCESS-OM2-1-025-010deg-report> for how to add or edit figures



Contents

| | |
|---|-----------|
| 1 Purpose of this document | 7 |
| 2 Introduction | 7 |
| 3 Model Configuration | 7 |
| 3.1 Overview | 7 |
| 3.2 MOM configurations | 11 |
| 3.2.1 Vertical grid | 11 |
| 3.2.2 Horizontal grid | 13 |
| 3.2.3 Bathymetry | 13 |
| 3.2.4 Tracers | 17 |
| 3.2.5 Sub-grid scale lateral / neutral physics | 17 |
| 3.2.6 Sub-grid scale vertical physics | 18 |
| 3.2.7 Rayleigh drag | 21 |
| 3.2.8 Other model physical parameters | 23 |
| 3.2.9 Timestepping | 23 |
| 3.3 CICE sea ice model configurations | 24 |
| 3.3.1 Thickness redistribution | 25 |
| 3.3.2 Dynamics | 25 |
| 3.3.3 Thermodynamics | 26 |
| 3.4 Coupling | 26 |
| 3.5 Forcing | 27 |
| 3.5.1 JRA55-do interannual and repeat-year forcing | 28 |
| 3.5.2 Restoring | 30 |
| 3.5.3 Sea ice formation salt flux limiter | 31 |
| 3.5.4 Bulk formulas used | 31 |
| 3.5.5 YATM and libaccessom2 | 32 |
| 3.6 Initial conditions and spinup | 33 |
| 3.7 Model computational details and performance | 34 |
| 3.7.1 Resource requirements | 34 |
| 3.7.2 Tiling in MOM and CICE | 34 |
| 3.7.3 Parallel scaling | 34 |
| 3.8 Comparison with similar models | 37 |
| 3.8.1 OFAM3 | 37 |
| 3.8.2 ACCESS, ACCESS-CM2, ACCESS-ESM | 38 |
| 3.8.3 MOM-SIS-01 | 39 |
| 3.8.4 GFDL CM2, CM2.5, CM2.6 | 39 |
| 3.8.5 UKMO GO6, GO7, GC3.0, GC3.1 | 39 |
| 3.8.6 RASM and others? | 39 |
| 3.8.7 Whole Antarctic Ocean Model (formerly known as the Antarctic Tidal Ocean Model) | 40 |
| 4 Model evaluation | 41 |
| 4.1 Barotropic streamfunction | 41 |
| 4.2 Surface current speed and variability | 41 |
| 4.3 Deep circulation | 41 |
| 4.4 Transports through key straits and boundary currents | 41 |
| 4.4.1 ITF | 48 |
| 4.4.2 Drake Passage | 49 |
| 4.5 Equatorial current velocity and temperature structure | 49 |
| 4.6 Overturning | 49 |

CONTENTS

| | | |
|--------|--|----|
| 4.7 | Meridional heat transport | 49 |
| 4.8 | Model bias assessments | 49 |
| 4.9 | Water mass properties and structure | 51 |
| 4.10 | Mixed layer depth (MLD) | 51 |
| 4.10.1 | T/S diagrams | 52 |
| 4.10.2 | Deep water formation / transformation rates, locations, properties | 52 |
| 4.11 | Heat conservation, bias and drift | 52 |
| 4.11.1 | SST bias | 52 |
| 4.11.2 | lat/depth T sections and bias | 52 |
| 4.11.3 | Drift: depth/time T hovmollers | 52 |
| 4.11.4 | zonally averaged surface heat flux terms | 52 |
| 4.12 | Salt conservation, bias and drift | 52 |
| 4.12.1 | SSS bias | 52 |
| 4.12.2 | lat/depth S sections and bias | 53 |
| 4.12.3 | Drift: depth/time S hovmollers | 53 |
| 4.12.4 | zonally averaged surface salt/freshwater flux terms | 53 |
| 4.12.5 | Variation of ocean volume | 53 |
| 4.13 | Variability | 53 |
| 4.13.1 | Western boundary current variability | 53 |
| 4.13.2 | EKE spatial distribution and wavenumber spectrum | 53 |
| 4.14 | Sea level | 53 |
| 4.15 | Sea ice | 54 |
| 4.15.1 | Seasonal cycle of extent and area | 55 |
| 4.15.2 | Sea ice thickness and volume | 55 |
| 4.15.3 | Age | 56 |
| 4.15.4 | Formation rate | 56 |
| 4.15.5 | Drift | 56 |
| 4.15.6 | Ice deformation | 56 |
| 4.15.7 | Polynyas | 56 |
| 4.16 | Particularly important regions | 65 |
| 4.16.1 | ACC | 65 |
| 4.16.2 | Antarctic margins | 65 |
| 4.16.3 | East Australian Current | 65 |
| 4.16.4 | Leeuwin Current | 65 |
| 4.16.5 | North Atlantic | 65 |
| 4.16.6 | Arctic Ocean / Greenland-Iceland-Norway (GIN) Seas | 65 |
| 4.16.7 | Pacific | 65 |
| 4.16.8 | Agulhas | 66 |
| 5 | Changes made in new version | 67 |
| 5.1 | For all resolutions | 67 |
| 5.2 | At 0.1 degree | 69 |
| 6 | TODO for v2.0.0 | 69 |
| 6.1 | at 0.1 deg | 69 |
| 7 | Things to improve for next time | 70 |
| 7.1 | For all resolutions | 70 |
| 7.2 | At 1 degree | 71 |
| 7.3 | At 0.1 degree | 71 |
| 8 | Acknowledgments | 72 |

CONTENTS

| | |
|---|------------|
| A Namelists | 72 |
| A.1 ACCESS-OM2 namelist accessom2.nml | 72 |
| A.2 MOM namelist input.nml | 72 |
| A.3 CICE namelists | 80 |
| A.3.1 cice_in.nml | 80 |
| A.3.2 input_ice.nml | 87 |
| A.3.3 input_ice_gfdl.nml | 87 |
| A.3.4 input_ice_monin.nml | 88 |
| A.4 YATM namelist atm.nml | 88 |
| B Namelist changes within runs | 89 |
| B.1 ACCESS-OM2 namelist accessom2.nml | 89 |
| B.2 MOM namelist input.nml | 90 |
| B.3 CICE namelists | 90 |
| B.3.1 cice_in.nml | 90 |
| B.3.2 input_ice.nml | 91 |
| B.3.3 input_ice_gfdl.nml | 91 |
| B.3.4 input_ice_monin.nml | 91 |
| B.4 YATM namelist atm.nml | 91 |
| C Namelist differences from profiling runs | 91 |
| C.1 ACCESS-OM2 namelist accessom2.nml | 91 |
| C.2 MOM namelist input.nml | 92 |
| C.3 CICE namelists | 95 |
| C.3.1 cice_in.nml | 95 |
| C.3.2 input_ice.nml | 97 |
| C.3.3 input_ice_gfdl.nml | 97 |
| C.3.4 input_ice_monin.nml | 97 |
| C.4 YATM namelist atm.nml | 97 |
| D Namelist differences between old and new configs | 97 |
| D.1 ACCESS-OM2 namelist accessom2.nml | 98 |
| D.2 MOM namelist input.nml | 99 |
| D.3 CICE namelists | 104 |
| D.3.1 cice_in.nml | 104 |
| D.3.2 input_ice.nml | 108 |
| D.3.3 input_ice_gfdl.nml | 110 |
| D.3.4 input_ice_monin.nml | 111 |
| D.4 YATM namelist atm.nml | 111 |
| E Namelist differences between new configs | 111 |
| E.1 ACCESS-OM2 namelist accessom2.nml | 111 |
| E.2 MOM namelist input.nml | 112 |
| E.3 CICE namelists | 114 |
| E.3.1 cice_in.nml | 114 |
| E.3.2 input_ice.nml | 115 |
| E.3.3 input_ice_gfdl.nml | 115 |
| E.3.4 input_ice_monin.nml | 115 |
| E.4 YATM namelist atm.nml | 115 |

LIST OF FIGURES

| | | |
|-------------------|--|------------|
| F | Namelist differences from ACCESS, ACCESS-CM2, ACCESS-ESM, OFAM3 | 116 |
| F.1 | ACCESS-OM2-01 MOM compared to OFAM3 | 116 |
| F.2 | ACCESS-OM2-01 MOM compared to MOM-SIS-01 and GFDL | 124 |
| F.3 | ACCESS-OM2-01 CICE compared to RASM and NCAR | 124 |
| F.4 | ACCESS-OM2 MOM and CICE compared to ACCESS, ACCESS-CM2, ACCESS-ESM | 124 |
| F.4.1 | MOM namelist input.nml | 124 |
| F.4.2 | CICE namelist cice_in.nml | 130 |
| References | | 135 |
| Index | | 156 |

List of Figures

| | | |
|----|---|----|
| 1 | Coupling between model components. | 9 |
| 2 | Vertical grid spacing for the ACCESS-OM2 simulations. | 12 |
| 3 | Horizontal grid spacing for the ACCESS-OM2 simulations. The colorbar limits show the minimum and maximum values. Note the meridional refinement near the equator in the 1° grid. TODO: also plot aspect ratio? see Bi and Marsland (2010) | 14 |
| 4 | Land masks and T cell y-size in the Arctic tripolar region in the three resolutions. | 14 |
| 5 | Latitudinal variation of ocean cell dimensions (left), and cumulative histograms of horizontal grid spacing for ocean cells (right) in the ACCESS-OM2 simulations. Table 6 provides further statistics. | 15 |
| 6 | Scatter plots of partial cell thickness versus full cell thickness in the three configurations. The upper and lower lines have slopes of 1 and 0.2, respectively. For ACCESS-OM2-01 the cells are full-depth when thinner than 10 m (i.e. the points fall on the upper line). | 15 |
| 7 | Time-mean surface isotropic biharmonic viscosity A_4 in several western boundary regions. | 19 |
| 8 | Biharmonic western boundary current width $3.6(A_4/\beta)^{1/5}$ in several western boundary regions, based on the time-mean surface isotropic biharmonic viscosity A_4 (figure 7). | 20 |
| 9 | Rayleigh damping locations and magnitudes. | 22 |
| 10 | Sea ice volume (cumulative by category) in the RYF run used as the initial condition for the IAF run at 0.1°. | 34 |
| 11 | Ice spinup from initial condition | 35 |
| 12 | MOM5 and CICE5 scaling on Raijin. | 37 |
| 13 | Global barotropic streamfunction for ACCESS-OM2 simulations. TODO: averaged over what years? | 42 |
| 14 | Antarctic Circumpolar Current barotropic streamfunction for ACCESS-OM2 simulations. TODO: Compare with Colin de Verdière and Ollitrault (2016) figure 9: https://journals.ametsoc.org/na101/home/literatum/publisher/ams/journals/content/phoc/2016/15200485-46.1/jpo-d-15-0046.1/20160222/images/large/jpo-d-15-0046.1-f9.jpeg | 43 |
| 15 | Kuroshio barotropic streamfunction for ACCESS-OM2 simulations. TODO: Compare with Colin de Verdière and Ollitrault (2016) figure 7: https://journals.ametsoc.org/na101/home/literatum/publisher/ams/journals/content/phoc/2016/15200485-46.1/jpo-d-15-0046.1/20160222/images/large/jpo-d-15-0046.1-f7.jpeg | 43 |
| 16 | Gulf Stream barotropic streamfunction for ACCESS-OM2 simulations. TODO: Compare with Colin de Verdière and Ollitrault (2016) figure 3: https://journals.ametsoc.org/na101/home/literatum/publisher/ams/journals/content/phoc/2016/15200485-46.1/jpo-d-15-0046.1/20160222/images/large/jpo-d-15-0046.1-f3.jpeg | 43 |

LIST OF TABLES

| | | |
|----|--|----|
| 17 | East Australian Current surface speed from (a) observations (1979–2015 mean from drifters at 15 m; Laurindo et al., 2017) and snapshots FIXME: daily mean at 0.1 deg and annual mean at 0.25 and 1 deg? what date? from ACCESS-OM2 simulations at (b) 1° resolution; (c) 0.25° resolution and (d) 0.1° resolution. | 44 |
| 18 | Agulhas Current surface speed from (a) observations (1979–2015 mean from drifters at 15 m; Laurindo et al., 2017) and snapshots FIXME: daily mean at 0.1 deg and annual mean at 0.25 and 1 deg? what date? from ACCESS-OM2 simulations at (b) 1° resolution; (c) 0.25° resolution and (d) 0.1° resolution. | 44 |
| 19 | Kuroshio surface speed from (a) observations (1979–2015 mean from drifters at 15 m; Laurindo et al., 2017) and snapshots FIXME: daily mean at 0.1 deg and annual mean at 0.25 and 1 deg? what date? from ACCESS-OM2 simulations at (b) 1° resolution; (c) 0.25° resolution and (d) 0.1° resolution. | 45 |
| 20 | Gulf Stream surface speed from (a) observations (1979–2015 mean from drifters at 15 m; Laurindo et al., 2017) and snapshots FIXME: daily mean at 0.1 deg and annual mean at 0.25 and 1 deg? what date? from ACCESS-OM2 simulations at (b) 1° resolution; (c) 0.25° resolution and (d) 0.1° resolution. | 45 |
| 21 | East Australian Current surface speed from (a) observations (1979–2015 mean from drifters at 15 m; Laurindo et al., 2017) and climatology from ACCESS-OM2 simulations at (b) 1° resolution; (c) 0.25° resolution and (d) 0.1° resolution. | 46 |
| 22 | Agulhas Current surface speed from (a) observations (1979–2015 mean from drifters at 15 m; Laurindo et al., 2017) and climatology from ACCESS-OM2 simulations at (b) 1° resolution; (c) 0.25° resolution and (d) 0.1° resolution. | 46 |
| 23 | Kuroshio surface speed from (a) observations (1979–2015 mean from drifters at 15 m; Laurindo et al., 2017) and climatology from ACCESS-OM2 simulations at (b) 1° resolution; (c) 0.25° resolution and (d) 0.1° resolution. | 47 |
| 24 | Gulf Stream surface speed from (a) observations (1979–2015 mean from drifters at 15 m; Laurindo et al., 2017) and climatology from ACCESS-OM2 simulations at (b) 1° resolution; (c) 0.25° resolution and (d) 0.1° resolution. | 47 |
| 25 | Transports through key straits. TODO: update TODO: fix Lombok, fix ranges, include 1 deg, label panels (a), (b) etc FIXME: meridional transports are wrong - see https://github.com/COSIMA/ACCESS-OM2-1-025-010deg-report/issues/47 | 48 |
| 26 | Equatorial Pacific temperature and currents | 50 |
| 27 | Global overturning circulation on density surfaces (σ_2) for ACCESS-OM2 simulations at (a) 1° resolution; (b) 0.25° resolution and (c) 0.1° resolution. | 51 |
| 28 | Global mean sea surface height (left) and salinity (right) for the 3 runs. | 53 |
| 29 | Arctic ice concentration maps, March | 58 |
| 30 | Arctic ice concentration maps, September | 59 |
| 31 | Antarctic ice concentration maps, September | 60 |
| 32 | Antarctic ice concentration maps, February | 61 |
| 33 | Sea ice area timeseries. | 62 |
| 34 | Sea ice extent timeseries. | 62 |
| 35 | Sea ice volume timeseries. | 63 |
| 36 | Seasonal cycle of ice area and extent compared to climatology of NOAA/NSIDC G02135 Sea Ice Index v3 (Fetterer et al., 2017, updated daily, http://nsidc.org/data/g02135) | 64 |

List of Tables

| | | |
|---|---|----|
| 2 | Sources and paths to executables, inputs and outputs. | 10 |
| 4 | Vertical grid parameters. | 11 |
| 6 | Statistics of ocean T-cell horizontal dimensions and aspect ratios. | 13 |
| 8 | Computational details and resource requirements. | 36 |
| 9 | ACCESS-OM2 compared to ACCESS-OM and OFAM3. | 38 |

1 Purpose of this document

This document serves two purposes:

1. This is a technical report to document the configuration and performance of the ACCESS-OM2 suite of models at 1° , 0.25° and 0.1° horizontal resolution (<http://cosima.org.au/index.php/models/>), intended to be a resource for the user community (e.g. COSIMA) and readily updated. This approach was partly inspired by [Griffies \(2015\)](#).
2. It forms the basis of one or more journal papers to announce and assess the performance of these models, e.g. [Kiss et al. \(2020\)](#).

TODO: Auto-update figures by programatically running COSIMA notebooks, so you could have a jenkins job or somesuch checking the COSIMA tech paper notebooks are all up to date and working correctly <http://tritemio.github.io/smbits/2016/01/02/execute-notebooks/> and http://nbconvert.readthedocs.io/en/latest/execute_api.html

TODO: copy things from Nic's talk <http://cosima.org.au/wp-content/uploads/2018/06/COSIMA2018-Hannah.pdf>, Marshall's COSIMA 2018 workshop talk

2 Introduction

This technical report documents the ACCESS-OM2 ocean-sea ice model configurations at nominal horizontal resolutions of 1° , 0.25° and 0.1° developed by the Consortium for Ocean-Sea Ice Modelling in Australia (COSIMA, <http://cosima.org.au>). COSIMA is both a collaborative consortium within Australia's ocean and sea ice modelling community that integrates capability from different groups, and an ARC Linkage Project (involving the Australian National University, the University of New South Wales, the University of Tasmania, the Bureau of Meteorology, CSIRO and the Australian Antarctic Division) to develop the ACCESS-OM2 model suite described here, intended for nationwide use by Australia's ocean and sea ice modelling community, and to be incorporated into future versions of the Bluelink ocean reanalysis and forecasting system and the ACCESS coupled climate model.

The model configuration suite is designed to be accessible, well-documented and straightforward for new users to set up, run and analyse. Model development is public (<https://github.com/COSIMA/access-om2>) and all model code, configuration files and inputs are available to download and ready to run on NCI's Gadi supercomputer. Model run configurations are also tracked with git, with input files and executables tagged with git hashes for reproducibility. Output from all significant runs will be published on the NCI data repository, and the COSIMA Cookbook (<https://github.com/COSIMA/cosima-cookbook>) provides Python analysis tools to handle the large data volumes produced by the high-resolution runs.

3 Model Configuration

CONTRIBUTORS: Andrew Kiss to coordinate

TODO: incorporate things from <https://github.com/COSIMA/access-om2/wiki/System-description>

3.1 Overview

The ACCESS-OM2 model suite is described by [Kiss et al. \(2020\)](#); additional technical details are provided here. Model configurations at three horizontal resolutions have been developed, named

3.1 Overview

ACCESS-OM2 (nominally 1° horizontal resolution), ACCESS-OM2-025 (nominally 0.25°) and ACCESS-OM2-01 (nominally 0.1°). The suite of three resolutions is also collectively referred to as ACCESS-OM2. Configurations (e.g. run parameters and forcing) are as consistent as possible across the three resolutions (see Table 2 and Appendix A) to facilitate studies of resolution dependence and sub-gridscale parameterisations. The coarser models served as testbeds for developing correct configurations at higher resolutions, and are suitable for long experiments covering climatological timescales of hundreds of years, but are not eddy-resolving. They are intended for incorporation into future versions of the ACCESS-CM global coupled climate model. In contrast, the ACCESS-OM2-01 configuration resolves the first baroclinic deformation radius away from shelves and equatorward of about 50° (Hallberg, 2013), and therefore resolves the mesoscale in most of the world ocean. It is suitable for runs of several decades and is intended to form the basis of the next generation of the Bluelink operational ocean forecasting system.

ACCESS-OM2 consists of two-way coupled ocean and sea ice models driven by a prescribed atmosphere (see Figure 1). The model source code is hosted at <https://github.com/COSIMA/access-om2>. The ocean model component is the Modular Ocean Model (MOM) version 5.1 from the Geophysical Fluid Dynamics Laboratory (<https://mom-ocean.github.io>). The sea ice component (<https://github.com/COSIMA/cice5/>) is a fork from the Los Alamos sea ice model (CICE) version 5.1.2 from Los Alamos National Laboratories (<https://github.com/CICE-Consortium/CICE-svn-trunk/tree/cice-5.1.2>) which we keep up to date with <https://github.com/CICE-Consortium/CICE-svn-trunk>. **TODO:** cite CICE doi and let CICE consortium know of publications: <http://cice-consortium-cice.readthedocs.io/en/master/intro/citing.html> These components are forced by prescribed atmospheric conditions taken from the 55-year Japanese Reanalysis for driving oceans (JRA55-do, Tsujino et al., 2018a) via YATM (<https://github.com/COSIMA/libaccessom2/>). The model components are coupled together via Ocean Atmosphere Sea Ice Soil (OASIS3-MCT) version 2.0 from CERFACS and CNRS, France (<https://portal.enes.org/oasis>). The exact source code and inputs used for the experiments discussed here are listed in Table 2. The following subsections provide further details on these model components.

3.1 Overview

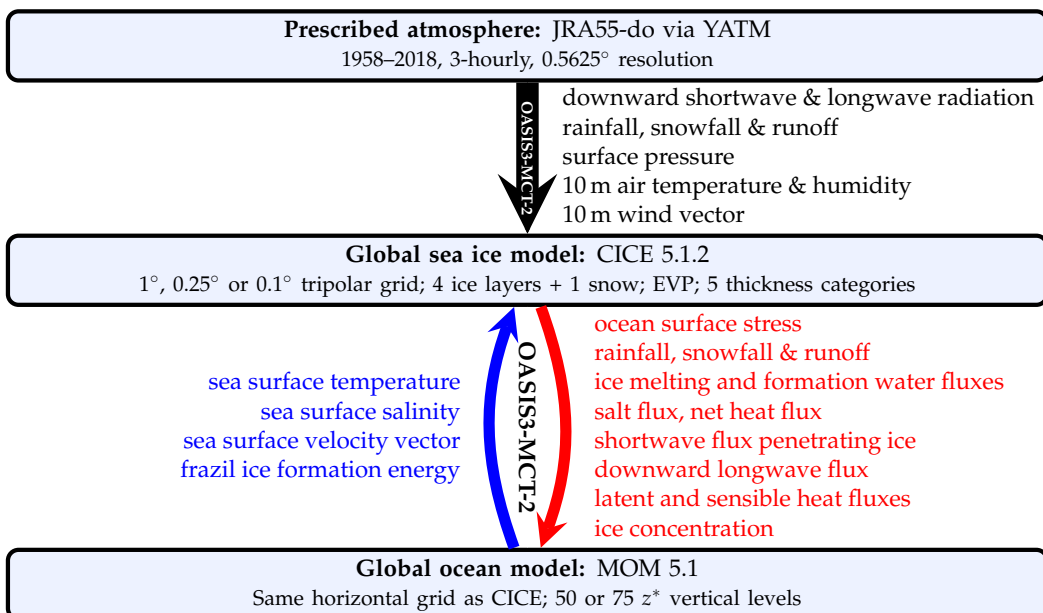


Figure 1: Coupling between model components by OASIS3-MCT-2 as specified in the namcouple file (which matches the atmosphere-CICE coupling fields specified in `atmosphere/forcing.json` and the CICE-MOM coupling fields specified in `mom_oasis3_interface_nml` in `ocean/input.nml`). Notice that MOM receives atmospheric forcing via CICE rather than directly from YATM (CICE has the same global domain as MOM). Surface pressure is used in the surface fluxes routines in CICE to calculate the saturated vapour pressure. It is also passed from CICE to MOM, but we don't show it here because MOM ignores it in the current configuration since `use_full_patm_for_sea_level=false` and `max_ice_thickness=0`. Similarly, the sea surface slope vector is passed from MOM to CICE but is unused (`use_ocnslope` is false, so the sea surface slope is instead calculated from the sea surface velocity vector, assuming geostrophy) so is not shown here. Also see <https://github.com/COSIMA/access-om2/wiki/System-description>.

3.1 Overview

| | ACCESS-OM2 | ACCESS-OM2-025 | ACCESS-OM2-01 |
|---------------|---|---|---|
| Experiment | 1deg_jra55v13_iaf_spinup1_B1 | 025deg_jra55v13_iaf_gmredi6 | 01deg_jra55v13_iaf |
| MOM source | https://github.com/mom-ocean/MOM5/tree/afe80bfd | https://github.com/mom-ocean/MOM5/tree/afe80bfd | https://github.com/mom-ocean/MOM5/tree/afe80bfd |
| executable | /g/data/ik11/inputs/access-om2/bin/fms_ACCESS-OM_afe80bfd.x | /g/data/ik11/inputs/access-om2/bin/fms_ACCESS-OM_afe80bfd.x | /g/data/ik11/inputs/access-om2/bin/fms_ACCESS-OM_afe80bfd.x |
| inputs | /g/data/ik11/inputs/access-om2/input_236a3011/mom_01deg | /g/data/ik11/inputs/access-om2/input_236a3011/mom_025deg | /g/data/ik11/inputs/access-om2/input_38570c62/mom_01deg |
| CICE source | https://github.com/COSIMA/cice5/tree/076b14f2 | https://github.com/COSIMA/cice5/tree/076b14f2 | https://github.com/COSIMA/cice5/tree/076b14f2 |
| executable | /g/data/ik11/inputs/access-om2/bin/cice_auscom_360x300_24p_-076b14f2.exe | /g/data/ik11/inputs/access-om2/bin/cice_auscom_1440x1080_480p_-076b14f2.exe | /g/data/ik11/inputs/access-om2/bin/cice_auscom_3600x2700_1392p_-076b14f2.exe |
| inputs | /g/data/ik11/inputs/access-om2/input_236a3011/cice_1deg | /g/data/ik11/inputs/access-om2/input_236a3011/cice_025deg | /g/data/ik11/inputs/access-om2/input_38570c62/cice_01deg |
| YATM source | https://github.com/COSIMA/libaccessom2/tree/e8ad3723 | https://github.com/COSIMA/libaccessom2/tree/e8ad3723 | https://github.com/COSIMA/libaccessom2/tree/e8ad3723 |
| executable | /g/data/ik11/inputs/access-om2/bin/yatm_e8ad3723.exe | /g/data/ik11/inputs/access-om2/bin/yatm_e8ad3723.exe | /g/data/ik11/inputs/access-om2/bin/yatm_e8ad3723.exe |
| inputs | /g/data/ik11/inputs/access-om2/input_236a3011/yatm_1deg | /g/data/ik11/inputs/access-om2/input_236a3011/yatm_025deg | /g/data/ik11/inputs/access-om2/input_38570c62/yatm_01deg |
| common inputs | /g/data/ik11/inputs/access-om2/input_236a3011/common_1deg_jra55 | /g/data/ik11/inputs/access-om2/input_236a3011/common_025deg_jra55 | /g/data/ik11/inputs/access-om2/input_38570c62/common_01deg_jra55 |
| outputs | /g/data/hh5/tmp/cosima/access-om2/1deg_jra55v13_iaf_spinup1_B1 | /g/data/hh5/tmp/cosima/access-om2/025/025deg_jra55v13_iaf_gmredi6 | /g/data/hh5/tmp/cosima/access-om2/01/01deg_jra55v13_iaf |
| run summary | /g/data/hh5/tmp/cosima/access-om2-run-summaries/run_summary_1deg_jra55v13_iaf_spinup1_B1.csv | /g/data/hh5/tmp/cosima/access-om2-run-summaries/run_summary_025deg_jra55v13_iaf_gmredi6.csv | /g/data/hh5/tmp/cosima/access-om2-run-summaries/run_summary_01deg_jra55v13_iaf.csv |

Table 2: Sources and NCI paths to executables, inputs and outputs for the experiments in this document. These are based on the final run of each experiment; consult run summary spreadsheets for information on any changes within these experiments and details on computational resource use. Namelist changes within runs are tabulated in Appendix B. Note that the last cycle of 1deg_jra55v13_iaf_spinup1_B1 was repeated with extra diagnostics in 1deg_jra55v13_iaf_spinup1_B1_lastcycle. The final source code and run configurations used here are at <https://doi.org/10.5281/zenodo.2653246> (or equivalently at <https://github.com/COSIMA/access-om2/releases/tag/GMD2019>). The individual final run configurations are at https://github.com/COSIMA/1deg_jra55_iaf/releases/tag/1.0, https://github.com/COSIMA/025deg_jra55_iaf/releases/tag/1.0 and https://github.com/COSIMA/01deg_jra55_iaf/releases/tag/1.0

3.2 MOM configurations

| Model | n | Δz_{\min} (m) | Δz_{median} (m) | Δz_{\max} (m) | H_{\max} (m) |
|----------------|-----|-----------------------|--------------------------------|-----------------------|----------------|
| ACCESS-OM2 | 50 | 2.3 | 93.0 | 219.6 | 5363.5 |
| ACCESS-OM2-025 | 50 | 2.3 | 93.0 | 219.6 | 5363.5 |
| ACCESS-OM2-01 | 75 | 1.1 | 42.6 | 198.4 | 5808.7 |

Table 4: Vertical grid parameters: n levels, with spacing of Δz_{\min} and Δz_{\max} at the surface and maximum depth H_{\max} , respectively, and median spacing Δz_{median} . Figure 2 shows the distribution with depth.

TODO: check that I'm correctly using the notation in Stewart et al. (2017)

3.2 MOM configurations

MOM parameters for the three model resolutions are tabulated in Appendix A.2. We discuss the choices of key parameters here.

The primary MOM5 reference is Griffies (2012). Griffies et al. (2008) provides many useful technical details (despite being for MOM4).

The ocean formulation is hydrostatic and Boussinesq (volume-conserving), with a free surface and z^* vertical coordinate.

The Boussinesq reference density is `rho0` = 1035.0 kg m⁻³, the default value.

3.2.1 Vertical grid

The configurations use a z^* vertical coordinate (`vertical_coordinate='zstar'`; Griffies, 2012, section 5.1.4), with partial cells (see section 3.2.3). The vertical grid is staggered, with vertical velocity points offset from tracer points. Vertical grid parameters are summarised in Tables 4 and 9 and Figure 2. The vertical grids are specified in the input file `ocean_vgrid.nc` for each configuration. Vertical grid data is also available in the `ocean.nc` output files (see variables `st_ocean`, `st_edges_ocean`, `sw_ocean`, `sw_edges_ocean`).

The vertical grids are optimised for resolving baroclinic modes (Stewart et al., 2017). The vertical grids in ACCESS-OM2 and ACCESS-OM2-025 are slightly modified versions of KDS50 (Stewart et al., 2017, table 1), with 50 levels and 2.3 m spacing at the surface, increasing smoothly to 219.6 m by the bottom at 5363.5 m. The vertical grid in ACCESS-OM2-01 is a slightly modified version of KDS75 (Stewart et al., 2017, table 1), with 75 levels and 1.1 m spacing at the surface, increasing smoothly to 198.4 m by the bottom at 5808.7 m. The 75 level vertical grid is finer than OFAM3 at all depths other than 100 – 260 m and finer at all depths than GFDL50 and NEMO46 (as defined by Stewart et al., 2017).

3.2 MOM configurations

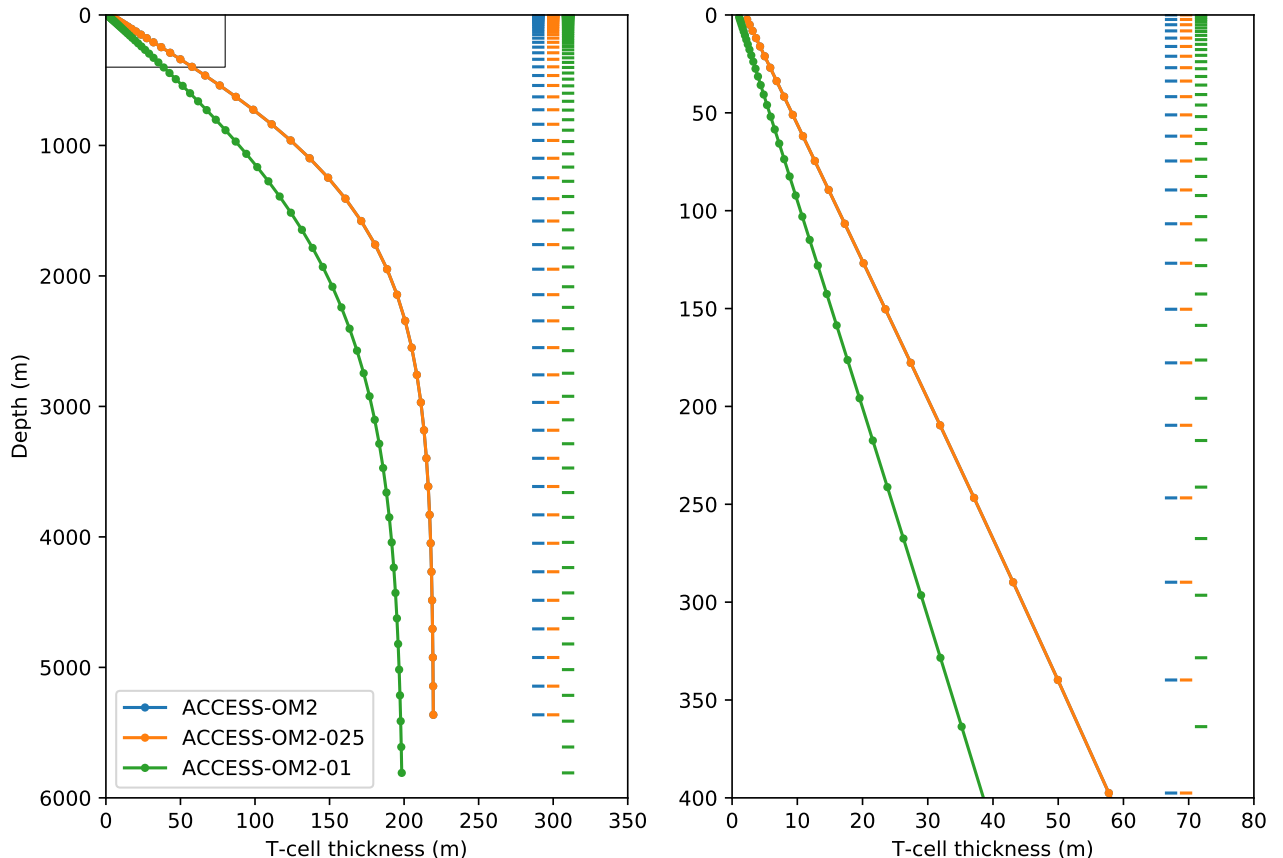


Figure 2: Vertical grid spacing for the ACCESS-OM2 simulations. ACCESS-OM2 and ACCESS-OM2-025 use the same vertical grid. Left: the full depth range. Right: the upper ocean. The horizontal lines show the top and bottom of T cells. Table 2 provides further details.

3.2 MOM configurations

| | Global | | | North of 60°N | | | South of 60°S | | |
|----------------------|--------|--------|-------|---------------|--------|------|---------------|--------|------|
| | min | median | max | min | median | max | min | median | max |
| ACCESS-OM2 dx | 23.8 | 91.7 | 111.2 | 24.7 | 32.7 | 54.8 | 23.8 | 43.0 | 54.6 |
| ACCESS-OM2 dy | 15.4 | 51.4 | 111.2 | 15.4 | 47.4 | 56.6 | 27.5 | 57.5 | 76.1 |
| ACCESS-OM2 dx/dy | 0.49 | 0.92 | 3.04 | 0.49 | 0.74 | 3.04 | 0.72 | 0.75 | 0.91 |
| ACCESS-OM2-025 dx | 6.0 | 18.1 | 27.8 | 6.2 | 8.1 | 13.9 | 6.0 | 11.3 | 13.9 |
| ACCESS-OM2-025 dy | 6.0 | 18.1 | 27.8 | 6.0 | 11.1 | 13.9 | 11.7 | 11.7 | 13.9 |
| ACCESS-OM2-025 dx/dy | 0.51 | 1.0 | 1.82 | 0.53 | 0.8 | 1.82 | 0.51 | 0.96 | 1.0 |
| ACCESS-OM2-01 dx | 2.19 | 7.16 | 11.12 | 2.47 | 3.29 | 5.55 | 2.19 | 4.52 | 5.55 |
| ACCESS-OM2-01 dy | 0.88 | 7.16 | 11.12 | 0.88 | 4.39 | 5.55 | 4.7 | 4.7 | 5.55 |
| ACCESS-OM2-01 dx/dy | 0.47 | 1.0 | 5.1 | 0.52 | 0.81 | 5.1 | 0.47 | 0.96 | 1.0 |

Table 6: Statistics of ocean T-cell horizontal dimensions (in km) and aspect ratios; global distributions are shown in Figure 5.

3.2.2 Horizontal grid

Grid parameters are summarised in Tables 6 and 9. The horizontal grids are specified in the file ocean_hgrid.nc for each configuration.

In the horizontal, MOM and CICE use the same orthogonal curvilinear Arakawa B-grid with velocity components co-located at the northeast corner of tracer cells. Model configurations have been developed with zonal resolutions of 1°, 0.25° and 0.1° south of 65°N. Figures 3, 4 and 5 and Table 6 show the grid spacing at the three resolutions. Globally, the median cell size is 92 km, 18.1 km and 7.2 km, respectively, at 1°, 0.25° and 0.1° resolution. Although the CICE model is global, the sea ice is mostly confined to latitudes higher than 60°, where most cell dimensions are finer than 47.4 km, 11.3 km and 4.5 km, respectively, at the three resolutions.

The horizontal meshes are 360×300 , 1440×1080 and 3600×2700 at 1°, 0.25° and 0.1°, respectively. In all cases the grid covers the global ocean, extending from the North Pole to the Antarctic shelf edge but omitting the Antarctic landmass. The T-grid extends to 77.8766233766234°S at 1°, 81.0770008338366°S at 0.25°, and 81.1297513555451°S at 0.1°. The ocean extends to the southernmost cell at 1°, but the other resolutions have a land mask covering the southernmost cells, giving southernmost ocean T-cell latitudes of 78.22584°S at 0.25°, and 79.58801°S at 0.1°.

The longitude range is -280° E to $+80^{\circ}$ E, placing the join in the middle of the Indian Ocean. In all configurations the grid is tripolar (Murray, 1996) north of 65°N (so the grid directions are not zonal and meridional in this region), with the tripoles placed on land at 65°N, -100° E and 65°N, 80° E. In the 0.25° and 0.1° configurations the grid is Mercator (i.e. the meridional spacing scales as the cosine of latitude) between 65°N and 65°S; south of 65°S, the meridional grid spacing is held at the same value (in km) as at 65°S. The meridional variation of meridional grid spacing is more complicated in the 1° model (Figure 5), and incorporates a refinement to $1/3^{\circ}$ (of latitude) within 10° of the Equator (Bi et al., 2013b; Bi and Marsland, 2010).

The 0.1° configuration had a misaligned CICE grid in both the IAF run and the preceding RYF spinup — see <https://github.com/COSIMA/access-om2/issues/190>.

TODO: maps of grid spacing divided by local 1st baroclinic Rossby radius from CheltonDeSzekeSchlaxEl-NaggarSiwertz1998a [http://www-po.coas.oregonstate.edu/research/po/research/rossby_radius/index.html?](http://www-po.coas.oregonstate.edu/research/po/research/rossby_radius/index.html)

3.2.3 Bathymetry

CONTRIBUTORS: Russ Fiedler

Topography tools:

3.2 MOM configurations

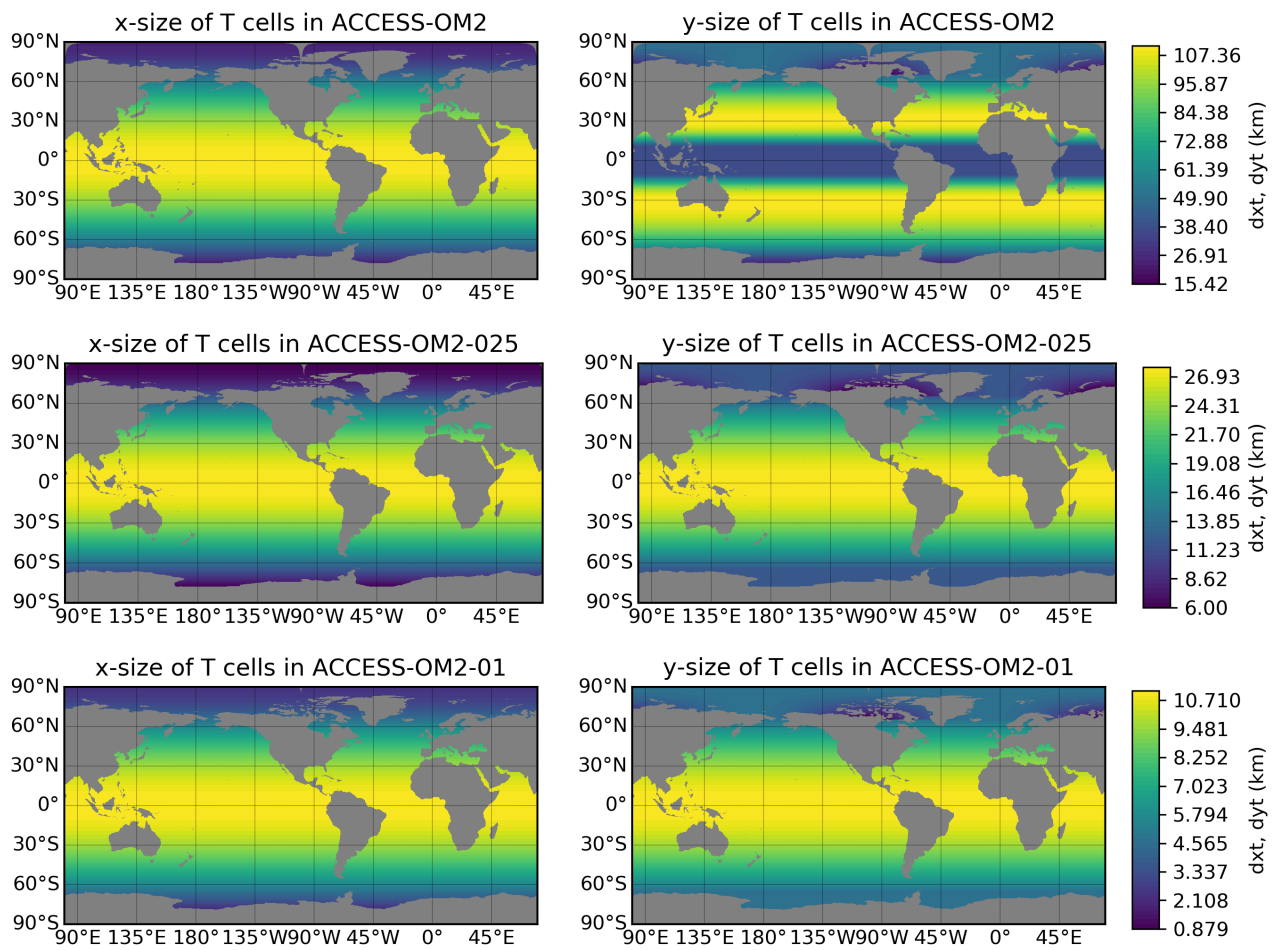


Figure 3: Horizontal grid spacing for the ACCESS-OM2 simulations. The colorbar limits show the minimum and maximum values. Note the meridional refinement near the equator in the 1° grid. **TODO:** also plot aspect ratio? see Bi and Marsland (2010)

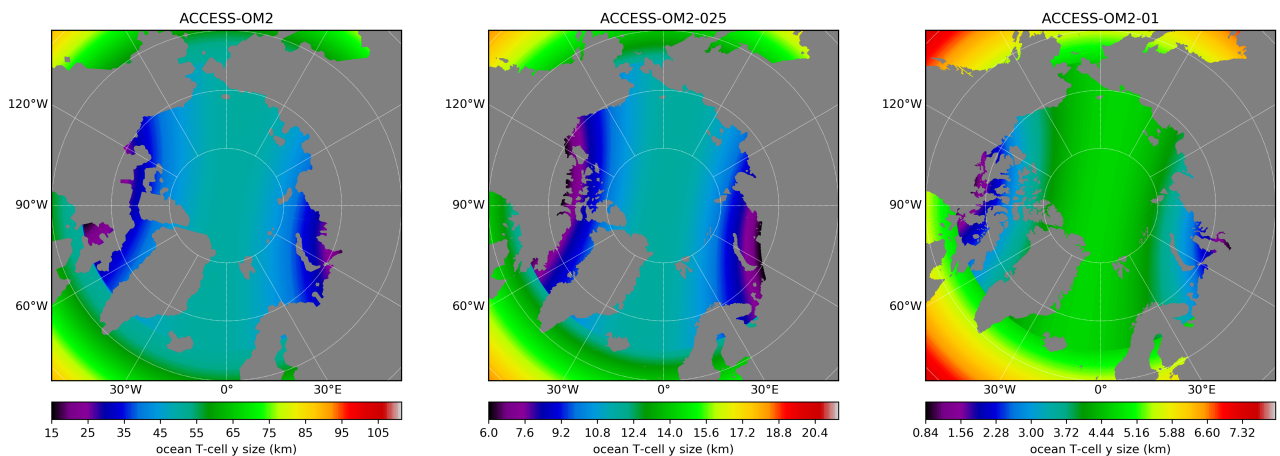


Figure 4: Land masks and T cell y-size in the Arctic tripolar region in the three resolutions.

3.2 MOM configurations

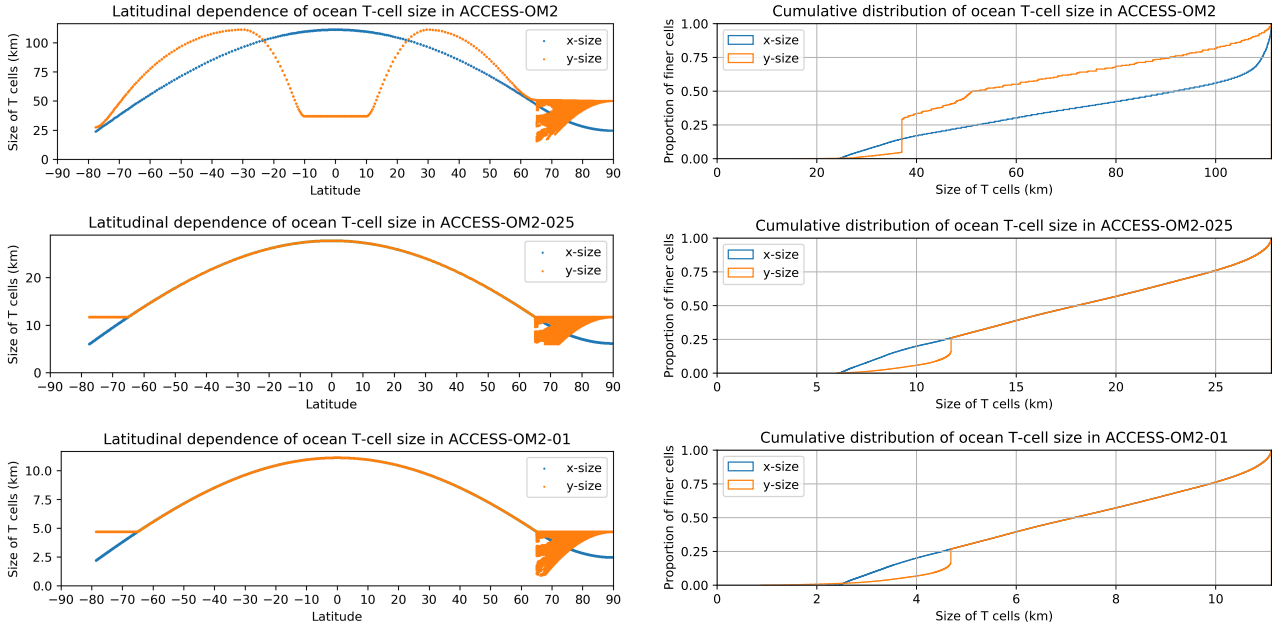


Figure 5: Latitudinal variation of ocean cell dimensions (left), and cumulative histograms of horizontal grid spacing for ocean cells (right) in the ACCESS-OM2 simulations. Table 6 provides further statistics.

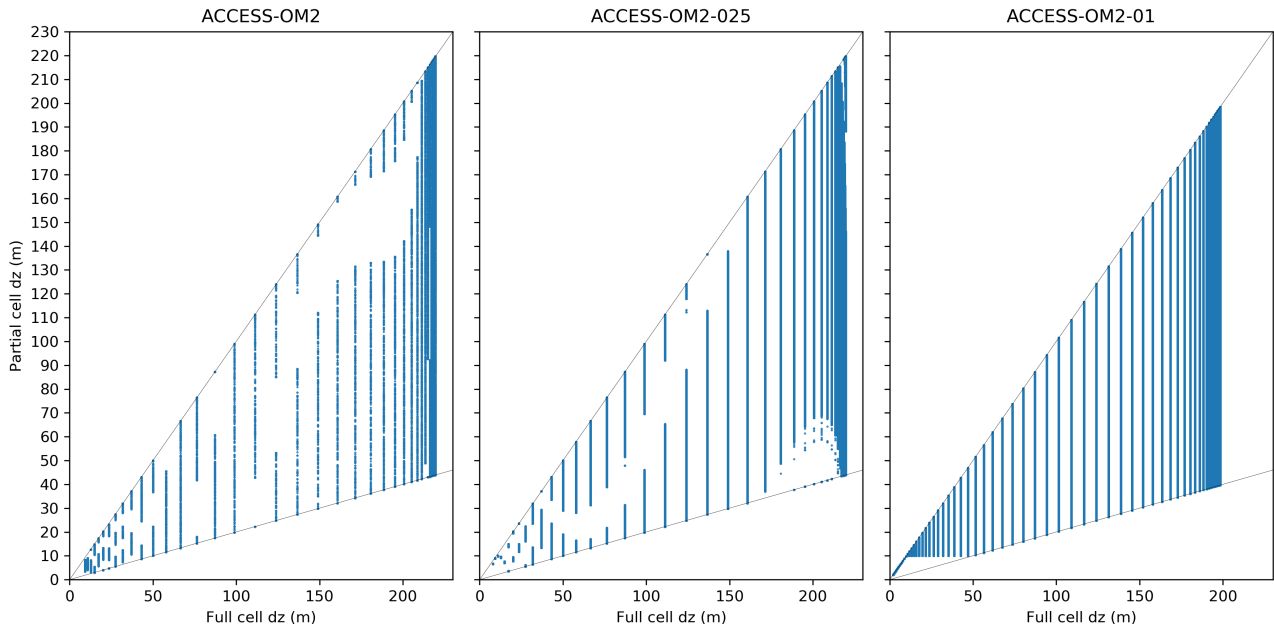


Figure 6: Scatter plots of partial cell thickness versus full cell thickness in the three configurations. The upper and lower lines have slopes of 1 and 0.2, respectively. For ACCESS-OM2-01 the cells are full-depth when thinner than 10 m (i.e. the points fall on the upper line).

3.2 MOM configurations

Various iterations of the 0.1° bathymetry are in /g/data/hh5/tmp/cosima/bathymetry; see /g/data/hh5/tmp/cosima/bathymetry and /short/v45/ae156/access-om2/input/mom_01deg/README-topog.txt and /home/156/ae156/payu/01deg_jra55v13_rf8485_-spinup6/README-topog.txt.

kmt_min: minimum number of vertical cells

The topog.nc seafloor topography (bathymetry) files were set up at each resolution with the help of <https://github.com/COSIMA/topogtools> and https://github.com/mom-ocean/MOM5/blob/master/src/tools/make_topog/topog.c and are read in by https://github.com/mom-ocean/MOM5/blob/master/src/mom5/ocean_core/ocean_topog.F90 at runtime. This reads work/ocean/INPUT/topog.nc which points to /short/v45/ae156/access-om2/input/mom_01deg/topog.nc - OR DOES IT? This in turn is the same as /g/data/hh5/tmp/cosima/bathymetry/topog_13_06_2018.baffin.nc. At 0.1° /short/v45/ae156/access-om2/control/01deg_jra55_ifa/config.yaml specifies /short/public/access-om2/input_38570c62/mom_01deg/topog.nc, which is the same as /g/data/hh5/tmp/cosima/bathymetry/topog_13_06_2018.baffin.nc. At 0.25° the topography is specified in /home/157/amh157/payu/jra55_ifa_gmredi/config.yaml as /g/data/ua8/MOM/grids/025/topog/KDS50/ **TODO: what's the 1 deg topog? FIXME: update all this**

The land mask in the two coarser resolutions was enlarged near the tripoles to remove small wet points, but this was not done at 0.1° (figure 4). Consequently the 0.1° bathymetry retains the Gulf of Ob in Siberia and many channels in the Canadian Archipelago which are absent at coarser resolution.

There are no ice shelf cavities as these are not supported in MOM5.1.

Mention the integrity checks and scripts used to generate the data (e.g. in /g/data/hh5/tmp/cosima/bathymetry/tools/com — should these be made publicly available? Also <https://github.com/aeckiss/notebooks/blob/master/non-advection.ipynb>.

The minimum depth is 45.11 m (10 levels) in ACCESS-OM2, 40.36 m (9 levels) in ACCESS-OM2-025, and 10.43 m (7 levels) in ACCESS-OM2-01 — see

⚠️ 1° and 0.25° The 1° and 0.25° topography files originate from the OCCAM model, from which they inherit a number of flaws such as anomalous ‘pits’ on the shelves (for example excessive depth in the Gulf of Carpentaria and also the East Siberian and Chukchi seas south of Wrangel Island); see <https://github.com/mom-ocean/MOM5/issues/172>. They also have land masks that differ from each other and also from the 0.1° topography; see <https://github.com/COSIMA/access-om2/issues/158>. The 1° and 0.25° topography files were based on previously-generated files with the GFDL50 vertical grid and a (presumably 20%) minimum partial cell thickness. When adapted to KDS50 the GFDL50 minimum cell thickness produces gaps in the thickness distribution (figure 6), i.e. the small terraces produced by the GFDL minimum partial cell thickness are inherited by the topography on the KDS50 vertical grid. See <https://github.com/COSIMA/access-om2/issues/141>.

0.1° The 0.1° bathymetry was generated from scratch by Russ Fiedler, and is therefore unaffected by the flaws that afflict the topography at 1° and 0.25° . It is based on GEBCO 2014 30 arcsecond gridded data **FIXME: which version?** http://www.gebco.net/data_and_products/gridded_bathymetry_data/gebco_30_second_grid/ GEBCO has 1 m vertical resolution but this is averaged within each model grid cell, so the model topography is smoother (at least, before later processing). The topography data used in the runs is /short/v45/ae156/access-om2/input/mom_01deg/topog.nc also /g/data/hh5/tmp/cosima/bathymetry/topog_latest.nc **FIXME: update**

Topography ends at a vertical wall at the ice shelf edge (the calving line, not the grounding line). A narrow strip along the southern boundary of the model is all land because the latitude range of the model was chosen for consistency with the previous MOM-SIS bathymetry which stopped at the grounding line.

TODO: plot or stats on how much model bathy differs from gebco plot bathymetry for the 3 resolutions – incl difference from gebco and from 0.1deg as maps, scatter plots, histograms, and differences between the 3 resolutions, eg in Canadian archipelago

TODO: mention main places where bathy tweaks were made – see /g/data/hh5/tmp/cosima/bathymetry/README

3.2 MOM configurations

/g/data/hh5/tmp/cosima/bathymetry/README: “Enforced minimum of 7 levels (approx 10m). Excavated not filled in so land mask kept. Partial cells: Enforced thickness of max(10,0.2*dz). If partial cell were thinner than half this then the cell was removed.”

We use partial cells (Adcroft et al., 1997; Pacanowski and Gnanadesikan, 1998) to obtain a more accurate representation of bottom topography. For ACCESS-OM2-01 the minimum height of partial cells is 20% of the full cell height, or min(10m, Δz), whichever is greater (depth:min_thick=10 in topog.nc; this modification is done by https://github.com/mom-ocean/MOM5/blob/master/src/tools/make_topog/topog.c#L858). This means the minimum thickness is greater than 20% of the full cell thickness if this is less than 50 m (i.e. for depths shallower than 543 m) and the cells are full-depth if they thinner than 10 m (i.e. for depths shallower than 103 m) — see figure 6 and <https://github.com/COSIMA/access-om2/issues/99>). This produces terraces in shallow water. This problem is fixed in more recent versions. ⚠️

3.2.4 Tracers

CONTRIBUTORS: Ryan Holmes

At all three resolutions tracers (salt, temperature and age) are advected horizontally and vertically by the multidimensional piecewise parabolic method (Colella and Woodward, 1984), with a monotonicity-preserving flux limiter following Suresh and Huynh (1997) (horizontal-advection-scheme=vertical-advection-scheme='mdppm' and ppm_hlimiter=ppm_vlimiter=3 for temp, salt and age in ocean/field_table; also see https://github.com/mom-ocean/MOM5/blob/master/src/mom5/ocean_tracers/ocean_tracer_advect.F90). **TODO:** check: is this monotonicity-preserving under all conditions? https://github.com/mom-ocean/MOM5/blob/99168b44ab45f4f5b4fa2544a0c3f644f0afb666/src/mom5/ocean_tracers/ocean_tracer_advect.F90 As the 0.1° configuration does not include a mesoscale eddy parameterization or explicit isopycnal or lateral diffusion (see section 3.2.5), the suppression of large lateral tracer gradients near the grid-scale in this configuration is achieved solely through spurious numerical mixing in this tracer advection scheme. **TODO:** Reference to Holmes et al numerical mixing article/

3.2.5 Sub-grid scale lateral / neutral physics

CONTRIBUTORS: Ryan Holmes

A sub-grid scale parameterization for mesoscale eddies is included in the 1° and 0.25° models (`ocean_nphysics_nml use_this_module=true`), but not at 0.1° as this resolution is considered “eddy-resolving”. In the two coarser configurations the Gent and McWilliams (1990) (GM) parameterization is used to represent the down-gradient isopycnal thickness flux associated with mesoscale eddies, and the along-isopycnal eddy tracer transport is parameterised by a Redi diffusivity (Redi, 1982). The namelist group `ocean_nphysics_util_nml` controls these parameterisations; see Griffies (2012, section 23.8) for further explanation. Note that the namelists are a bit confusing, as many ignored parameters are specified — see <https://github.com/COSIMA/access-om2/issues/197>. Their parameters are recalculated from scratch for each run, rather than being picked up from restarts (`nphysics_util_zero_init=true`).

The GM parameterization is implemented as a skew diffusive flux (Griffies, 1998). In common with many GFDL configurations, we use the `ocean_nphysicsC` formulation (`use_nphysicsc=true`) which differs from the default (`use_nphysicsa`) in that the skew diffusive flux calculation is based on a vector streamfunction built from a sum of baroclinic modes. The associated diffusivity is depth-independent but flow-dependent (`agm_closure=true`, `agm_closure_baroclinic=true`), and is the product of `agm_closure_scaling`, an inverse timescale, a squared length scale, and a grid scaling factor (see https://github.com/mom-ocean/MOM5/blob/4d60fad0e56/src/mom5/ocean_param/neutral/ocean_nphysics_util.F90#L2860). The length scale (`agm_closure_length`) is 50 km at 1° and 20 km at 0.25° (`agm_closure_length` is used because `agm_closure_baroclinic=true` — see https://github.com/mom-ocean/MOM5/blob/4d60fad0e5619fe15a630732ace4f0e3b3c6f23e/src/mom5/ocean_param/neutral/ocean_nphysics_util.F90#L2756). The inverse timescale is an Eady growth rate determined from the horizontal density gradient averaged between `agm_closure_upper_depth=100 m` and `agm_closure_lower_depth=2000 m` using a constant buoyancy frequency of `agm_closure_buoy_freq=0.004 s⁻¹` (these three values are the defaults). The Eady growth rate

3.2 MOM configurations

is subject to a limiter (`agm_closure_eady_cap`) and is smoothed both vertically and horizontally (`agm_closure_eady_smooth_horz=true`, `agm_closure_eady_smooth_vert=true`) and vertically averaged in the mixed layer (`agm_closure_eady_ave_mixed=true`). The grid scaling (`agm_closure_grid_scaling=true`) reduces the GM diffusivity in proportion to how well the numerical grid resolves the first baroclinic Rossby radius (or the equatorial Rossby radius within $\pm 5^\circ$ latitude), as suggested by (Hallberg, 2013). The GM diffusivity is limited to the ranges $50\text{--}600 \text{ m}^2\text{s}^{-1}$ at 1° and $1\text{--}200 \text{ m}^2\text{s}^{-1}$ at 0.25° set by `agm_closure_min` and `agm_closure_max`. It is not smoothed in space (`agm_smooth_space=false`) or time (`agm_smooth_time=false`).

The along-isopycnal Redi tracer diffusion (Redi, 1982) in the two coarser configurations has a diffusivity that differs from GM (`aredi_equal_agm=false`). A constant coefficient of `aredi=600 \text{ m}^2\text{s}^{-1}` is used at 1° . At 0.25° the Redi coefficient is scaled by the resolution of the grid relative to either the first baroclinic Rossby radius, or the equatorial Rossby radius for latitudes between $\pm 5^\circ\text{N}$ (`aredi_diffusivity_grid_scaling=true`), with a diffusivity no greater than `aredi=200 \text{ m}^2\text{s}^{-1}`.

`drhodz_mom4p1` is true at 1° but false at 0.25° .

Further testing of spatially- and temporally-dependent Redi and GM schemes has not yet been undertaken. However, given the sensitivity of the overturning circulation in the Southern Ocean and the formation of bottom water to the presence of these schemes exposed in a preliminary study in the 0.25° configuration, such a sensitivity study should be high on the agenda.

All three configurations include a parameterization for re-stratification in the surface mixed layer due to submesoscale eddies (Fox-Kemper et al., 2008); see namelist group `ocean_submesoscale_nml`. This parameterization applies an overturning circulation dependent on the horizontal buoyancy gradients within the mixed layer. The optional horizontal diffusive portion of this parameterization is not used (`submeso_diffusion=false`, so `submeso_diffusion_biharmonic` and `submeso_diffusion_scale` are ignored).

Horizontal friction is implemented with a biharmonic operator and an isotropic Smagorinsky scaling (`k_smag_iso=2.0`, `k_smag_aniso=0.0`) for the viscosity coefficient (Griffies and Hallberg, 2000); also see Griffies (2012, chapter 25). The 1° configuration also has a grid spacing-dependent isotropic (`vel_micom_aniso=0.0`) biharmonic background viscosity set by the velocity scale `vel_micom_iso=0.04 \text{ ms}^{-1}`; there is no background viscosity at the other resolutions. The NCAR viscosity scheme is also applied at 1° (`ncar_boundary_scaling=true`), to enhance the background horizontal viscosity at western boundaries in order to ensure the western boundary currents are resolved (`ncar_boundary_scaling=true` at 0.25° and 0.1° but this has no effect because `vel_micom_iso` and `vel_micom_aniso` are both zero). This increases the background viscosity at 1° by a factor that is 4 on the i-maximum side of land cells at each depth, and decreases to 1 as a function of distance in the i direction (NB: this is not eastward distance in the tripole), with a profile that is a Gaussian with length scale 500 km (the inverse of `ncar_vconst_4` in cm), raised to the power `ncar_rescale_power=2`. The background viscosity is inconsistent along the tripole seam with `ncar_boundary_scaling=true` — see <https://github.com/mom-ocean/MOM5/issues/282>. At 1° there is also background Laplacian viscosity at the bottom set by the velocity scale `vel_micom_bottom=0.01 \text{ ms}^{-1}` and calculated by a 5-point Laplacian operator (`bottom_5point=true`). The overall biharmonic viscosity is limited to `visc_crit_scale=25%` of the numerical instability threshold in ACCESS-OM2, or 100% in the other two configurations (see Griffies, 2004, equation (18.26)). The Smagorinsky biharmonic viscosity A_4 varies spatially by orders of magnitude (Figure 7). A viscous western boundary current has a width of about 3.6 times the length scale $(A_4/\beta)^{1/5}$ (see Haidvogel et al., 1992, Appendix B). This thickness is about 350 km in ACCESS-OM2, 100 km in ACCESS-OM2-025, and 60 km in ACCESS-OM2-01 (Figure 8), which is well-resolved by the grid in all cases. The lateral boundary condition for velocity is no-slip, as a consequence of using a B-grid (Griffies, 2012). ⚠️

3.2.6 Sub-grid scale vertical physics

CONTRIBUTORS: Ryan Holmes

Vertical diffusion of both tracers and momentum is parameterized using the K-profile parameterization (KPP, Large et al., 1994, `vert_mix_scheme='kpp_mom4p1'`), which governs mixing within the

3.2 MOM configurations

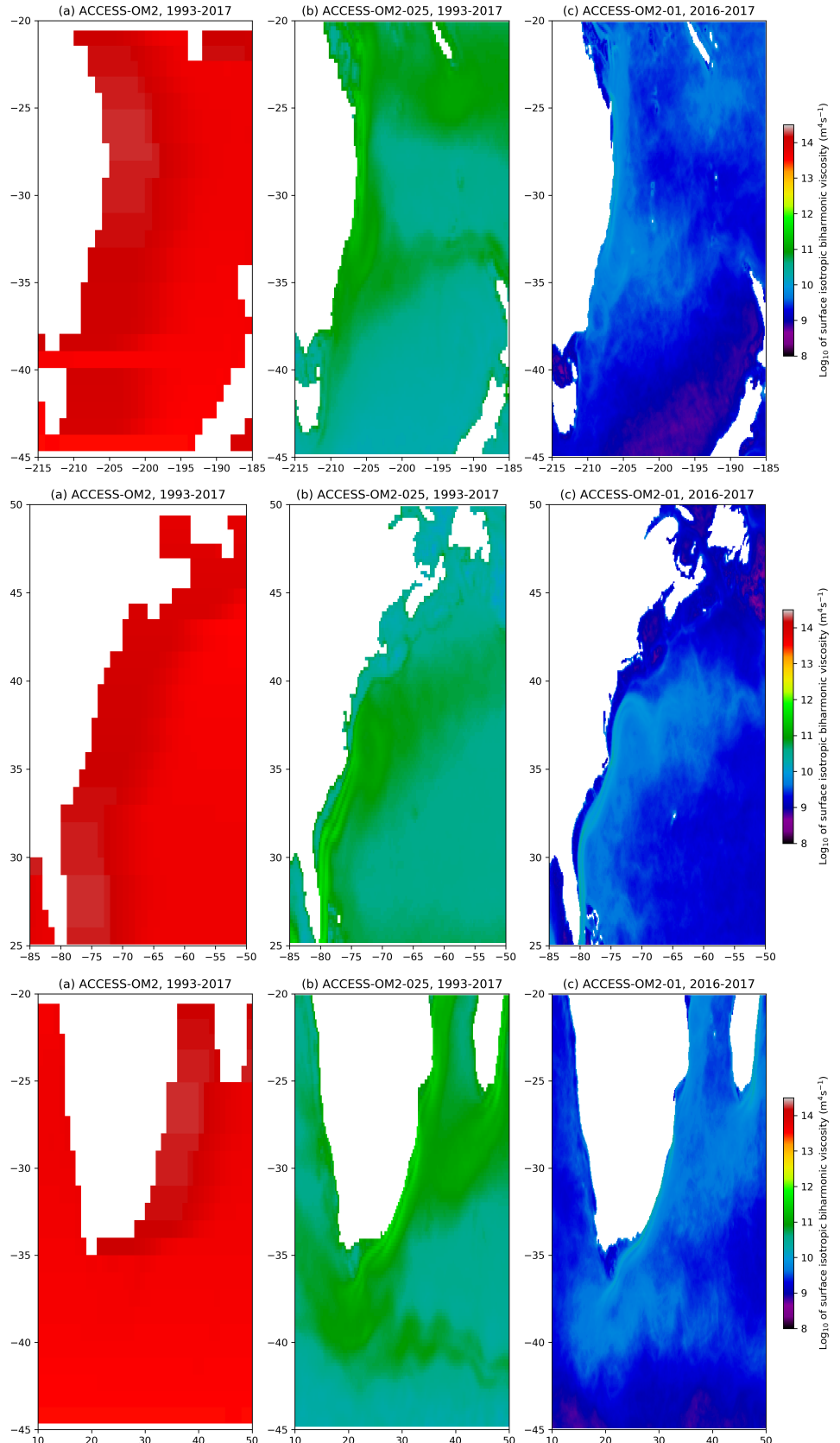


Figure 7: Time-mean surface isotropic biharmonic viscosity A_4 in several western boundary regions.

3.2 MOM configurations

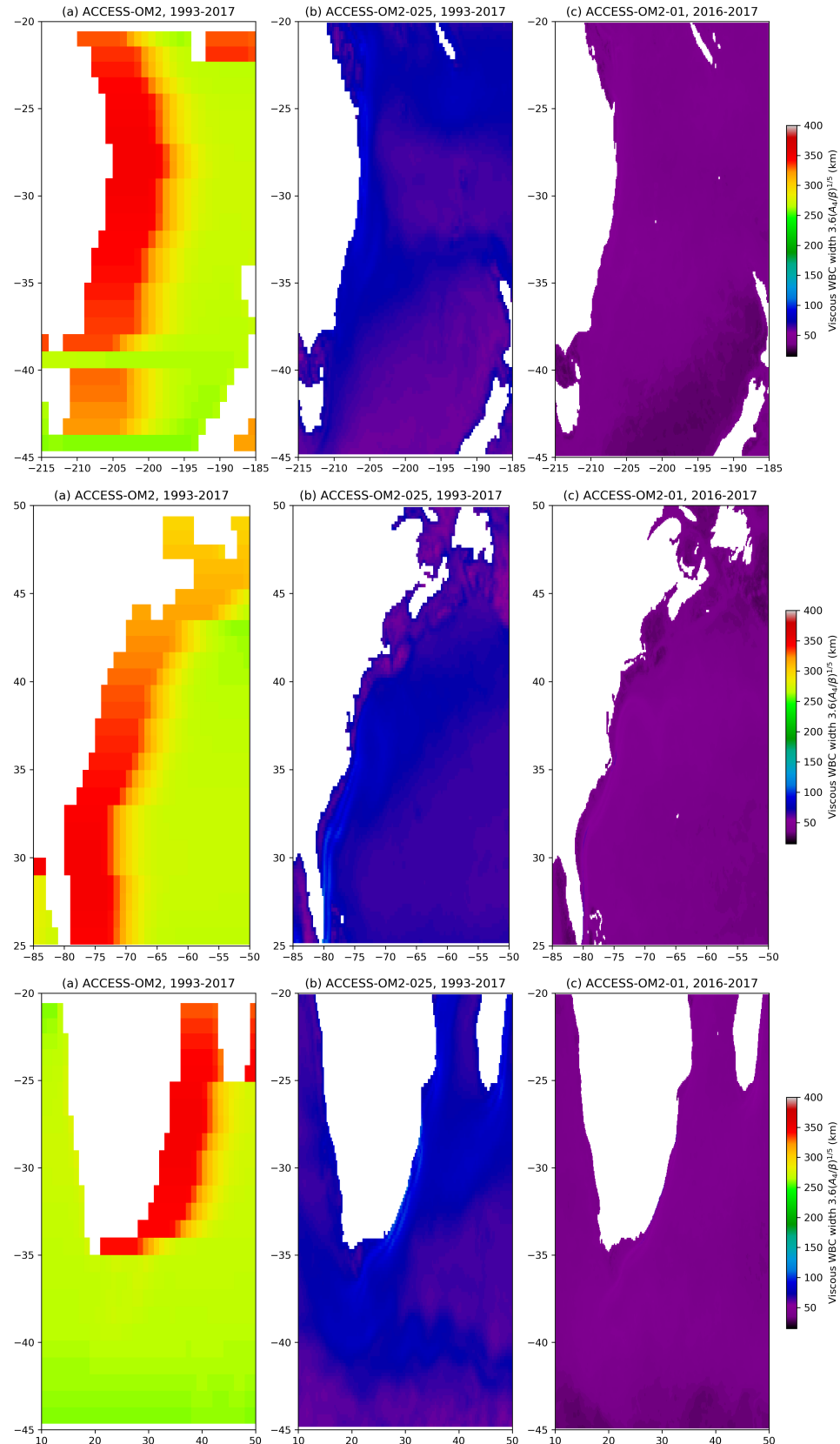


Figure 8: Biharmonic western boundary current width $3.6(A_4/\beta)^{1/5}$ in several western boundary regions, based on the time-mean surface isotropic biharmonic viscosity A_4 (figure 7).

3.2 MOM configurations

surface boundary layer, as well as interior convection (when the stratification is unstable), Richardson number-based shear instability (active mainly in the equatorial undercurrents), internal wave breaking, and double-diffusion. **TODO:** Comment on applicability of KPP at our high vertical resolution - see Van Roekel et al. (2018) KPP maintains static stability by applying large vertical diffusivity in regions with small or negative Richardson number; therefore explicit convective adjustment is not used at any resolution (see `ocean_convect_nml`). At 1° the Jochum (2009) latitudinally-dependent, depth-independent background vertical tracer diffusivity scheme is used (`j09_diffusivity=true`), with diffusivity $j09_bgmax=5 \times 10^{-6} \text{ m}^2\text{s}^{-1}$ poleward of $j09_lat=\pm 20^\circ\text{N}$, reducing to $j09_bgmin=1 \times 10^{-6} \text{ m}^2\text{s}^{-1}$ at the equator via a cosine profile, similar to observations (Gregg et al., 2003). The background vertical tracer diffusivity is zero in ACCESS-OM2-025 and ACCESS-OM2-01 (`j09_diffusivity` is unspecified, and the default is false). There is no additional non-tidal, non-KPP background vertical diffusivity at any resolution (`background_diffusivity=0.0`).

There are no explicit tides, but we include vertical tracer diffusivity and vertical viscosity from parameterised internal and barotropic tidal processes. Turbulent mixing and viscosity due to breaking internal tides is parameterised by the Simmons et al. (2004) scheme (`use_wave_dissipation=true`) with a vertical decay scale `decay_scale=500` m, zero background vertical diffusivity (`background_diffusivity=0.0`), a constant background vertical viscosity of `background_viscosity=1 \times 10^{-4} \text{ m}^2\text{s}^{-1}`, tidal current speed read from the file `tideamp.nc` (`read_tide_speed`) and bottom roughness amplitude read from the file `roughness_amp.nc` (`read_roughness=true` and `reading_roughness_amp=true`). The Lee et al. (2006) scheme is used to parameterise vertical mixing and viscosity due to the drag of barotropic tides on the bottom (`use_drag_dissipation`). Further parameters are in the `ocean_vert_tidal_nml` namelist group. **TODO:** investigate whether newer dissipation estimates/methods should be used, e.g. are de Lavergne et al. (2019) and <https://doi.org/10.17882/58105> relevant?

Bottom drag is calculated from the law of the wall using prescribed spatially-varying bottom roughness and tidal current speed (`cdbot_roughness_uamp=true`), with residual current `uresidual=0.05 \text{ ms}^{-1}`. Tidal current speed is read from the file `tideamp.nc` and bottom roughness is read from the file `roughness_cdbot.nc`. The bottom drag coefficient is restricted to the range `cdbot_lo` to `cdbot_hi`, where `cdbot_lo` takes its default value 0.001 and `cdbot_hi=0.007` (larger than the default value 0.003). `cdbot` is unused, since `cdbot_law_of_wall=false` (the default).

The tidal speed data in `tideamp.nc` probably originates from Jayne and St. Laurent (2001) if it came from GFDL. **TODO:** try to confirm this? The bottom roughness files seem basically the same, except that `roughness_amp.nc` is on T points and `roughness_cdbot.nc` is on U points. They probably originate from Jayne and St. Laurent (2001) or Jayne (2009), which in turn are derived from Smith and Sandwell (1997). **TODO:** try to confirm this?

TODO: What is `drag_coeff` in `ocean_grid.nc`??

3.2.7 Rayleigh drag

Rayleigh drag is a velocity tendency term proportional to the velocity, with a negative coefficient whose inverse magnitude is the e -folding time for velocity decay. It is a momentum sink that is employed as an engineering fix to improve model stability and/or realism in a few selected locations in the 1° and 0.1° configurations, specified in `ocean/field_table`, as shown in figure 9. At 1° it is used to improve the Indonesian Throughflow transport; a damping timescale of 1.5 hr is applied at all but the bottom 2 (3) U-cells in Lombok (Ombai) Strait and for 3/4 of the width of the Torres Strait at all depths (these omissions were not intended, and could be corrected in `ocean/field_table` in new configurations: <https://github.com/COSIMA/access-om2/issues/156>). At 0.1° a damping timescale of 1.5 hr is used at all depths across the full width of Kara Strait to constrain the velocity, which otherwise leads to numerical instability unless an unfeasibly small timestep is used. There is no Rayleigh drag in the 0.25° configuration.



3.2 MOM configurations

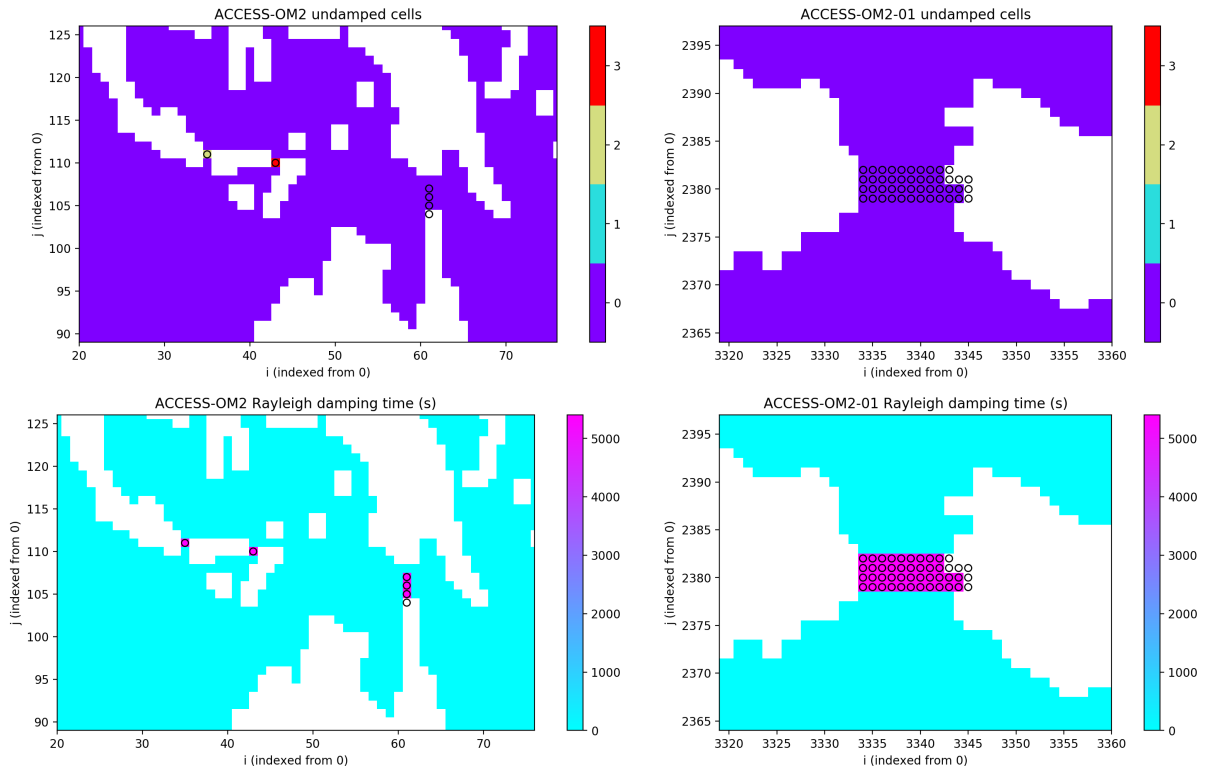


Figure 9: Rayleigh damping locations and magnitudes. Circles indicate where Rayleigh damping is defined in `ocean/field_table` and white cells are the U-grid land mask. Top row: Rayleigh damping locations at 1° (left; in the Lombok, Ombai and Torres Straits) and 0.1° (right; in the Kara Strait); colours in the circled cells indicate how many U-cells are not damped in each column. Bottom row: Rayleigh damping timescale (or zero if not defined) at 1° (left) and 0.1° (right). Where defined, damping timescales are all 5400 s. There is no Rayleigh damping at 0.25° .

3.2 MOM configurations

3.2.8 Other model physical parameters

We use the [Jackett et al. \(2006\)](#) pre-TEOS-10 seawater equation of state and freezing temperature (`eos_preteos10=true` and `freezing_temp_preteos10=true`). The prognostic temperature variable is conservative temperature in the 1° and 0.25° configurations (`temperature_variable='conservative_temp'`), and potential temperature¹ in the 0.1° configuration (`temperature_variable='potential_temp'`). However the 1° and 0.25° configurations mistakenly had `pottemp_equal_contemp=true`, which meant that incorrect temperatures were passed to the coupler <https://github.com/COSIMA/access-om2/issues/148>. The 0.1° simulation also had `pottemp_equal_contemp=true`, but the coupler fluxes are correct (since it used `temperature_variable='potential_temp'`) but the conservative temperature output diagnostic is actually potential temperature. Since we use pre-TEOS-10, practical salinity is the prognostic variable for salt for all the ACCESS-OM2 configurations (https://github.com/mom-ocean/MOM5/blob/99168b44ab45f4f5b4fa2544a0c3f644f0afb666/src/mom5/ocean_core/ocean_density.F90#L209). If we switched to TEOS-10 ([Roquet et al., 2015](#)) we'd need to use two salinity variables (Pre-formed Salinity and Absolute Salinity anomaly) instead of practical salinity: see https://github.com/mom-ocean/MOM5/blob/99168b44ab45f4f5b4fa2544a0c3f644f0afb666/src/mom5/ocean_tracers/ocean_tempsalt.F90#L60 and https://github.com/mom-ocean/MOM5/blob/99168b44ab45f4f5b4fa2544a0c3f644f0afb666/src/mom5/ocean_core/ocean_density.F90#L203 and <https://github.com/COSIMA/access-om2/issues/140>. Frazil production is not confined to the top model layer (`frazil_only_in_surface=false`) **TODO: check - ignored since we use auscom?** and uses the pre-TEOS-10 freezing temperature (`freezing_temp_preteos10=true`).

The Red Sea fix was not used (`redsea_gulfbay_sfix=false` or unspecified).

Overflow schemes are not used (see `ocean_overflow_nml` and `ocean_overexchange_nml`). Downslope transport and mixing schemes are only used at 1° , where we have sigma transport ([Beckmann and Döscher, 1997](#); [Campin and Goosse, 1999](#); [Döscher and Beckmann, 2000](#)) with default parameters (`ocean_sigma_transport_nml`) and downslope mixing (`ocean_mixdownslope_nml`) with `mixdownslope_npts=4` (the default is 1).

Ice is massless / levitating (`max_ice_thickness=0`) to avoid coupled ice-ocean instabilities ([Hallberg, 2014](#)), but this alters the pressure applied to the ocean by the sea ice and precludes exact mass conservation in the coupled ocean and sea ice system (although mass is conserved within MOM5 itself, i.e. mass change rate equals net mass flux **TODO: strictly speaking, should "mass" be "volume"?**). See https://github.com/mom-ocean/MOM5/blob/7c8bb96/src/mom5/ocean_core/ocean_sbc.F90#L321. We also have `use_full_patm_for_sea_level=false`. In combination with `max_ice_thickness=0` this eliminates the inverse barometer and ice mass signals from `eta_t`: https://github.com/mom-ocean/MOM5/blob/ac2aeaab3753f1170f8dc9d1db4c7a5f3bbf7359/src/mom5/ocean_core/ocean_sbc.F90#L3936

3.2.9 Timestepping

The MOM baroclinic timestep is `ice_ocean_timestep` in `accessom2.nml`. `ice_ocean_timestep` is also the CICE thermodynamic timestep, overriding `dt` in `cice_in.nml`. `ice_ocean_timestep` is chosen to be a factor of the JRA55-do forcing period of 3 hr = 10800 s, for example one of 100, 108, 120, 135, 144, 150, 180, 200, 216, 225, 240, 270, 300, 360, 400, 432, 450, 540, 600, 675, 720, 900, 1080, 1200, 1350, 1800, 2160, 2700, 3600 or 5400 s. Typical values are given in Table 8. We use split timestepping, with the baroclinic timestep `barotropic_split` = 80 times longer than the barotropic timestep. Note that in going from baroclinic timestep n to $n+1$ the barotropic solver integrates over a time interval covering baroclinic steps n to $n+2$ in order to give a centred time-average at baroclinic step $n+1$; thus there are 160 times more barotropic timesteps than baroclinic timesteps ([Griffies, 2012](#), section 11.6).

The barotropic dynamics use a predictor-corrector method ([Griffies, 2012](#), sections 11.2.5 and 11.5), with the recommended method (`barotropic_time_stepping_a=true`; see [Griffies, 2012](#), section 11.8.1) and default dissipation parameter `pred_corr_gamma=0.2` and smoothing `smooth_eta_t_laplacian=true`, `vel_micom_lap=0.05 ms-1`. (`smooth_eta_diag_laplacian` and `smooth_pbot_t_laplacian` are ignored since we use a depth-based (z^*) vertical coordinate, and `eta_max` and `frac_crit_cell_height` are ignored because `truncate_eta` is false.)

Two-level volume- and tracer-conserving timestepping schemes are used for the baroclinic dy-

¹This was an oversight: <https://github.com/COSIMA/access-om2/issues/97>, and has been corrected in the new 0.1° RYF configuration, which uses conservative temperature: <https://github.com/COSIMA/access-om2/projects/1>.

3.3 CICE sea ice model configurations

namics (`time_tendency`=‘twolevel’), with a staggered second-order forward method (tracer advection and lateral mixing of tracer and velocity calculated at timestep n and pressure gradients calculated at timestep $n + \frac{1}{2}$) **TODO: check - see Griffies (2012, chapter 11)**, implicit vertical mixing (`aidif`=1.0) and bottom drag (`bmf_implicit`=true), and semi-implicit Coriolis (`acor`=0.5) calculations. The tracer timestep is the same as the baroclinic dynamics timestep (`baroclinic_split` = 1). Velocity advection uses a second-order centred operator in space (`velocity_advect_centered`=true by default) and third-order Adams-Bashforth timestepping (`adams_bashforth_third`=true). See Griffies (2012, sections 11.3–11.6 and 11.8.1).

3.3 CICE sea ice model configurations

The sea-ice component in the ACCESS-OM2 suite is based on CICE version 5.1.2 (<https://github.com/CICE-Consortium/CICE-svn-trunk/tree/cice-5.1.2>). We have maintained our own fork at <https://github.com/COSIMA/cice5> which includes additional code such as the auscom drivers used in these runs. We periodically update this fork to match the latest from the CICE consortium <https://github.com/CICE-Consortium/CICE-svn-trunk>. The model runs reported here used commit 076b14f2 (table 2; <https://github.com/COSIMA/cice5/commit/076b14f2>) which was the 117th commit in our fork after an import of CICE 5.1.2 on 24 June 2015 (<https://github.com/COSIMA/cice5/commit/1110bae87>). Commit 076b14f2 did not include several bug fixes which we have since imported from the CICE consortium (see commits cbf4c62 through to 320a796 at <https://github.com/COSIMA/cice5/commits/master>). **TODO: check whether these bugs were relevant to our configs** ⚠

The primary CICE5 reference is Hunke et al. (2015). CICE parameters for the three model resolutions are tabulated in Appendix A.3; see https://ncar.github.io/CICE/users_guide/ice_nml_var.html for additional details. We discuss the choices of key parameters here. The parameters are based on those of ACCESS-OM **TODO: check** (Bi et al., 2013b), which used CICE4.1 and was the ocean-sea ice component of the ACCESS-CM coupled climate model (Bi et al., 2013a; Dix et al., 2013). ACCESS-CM has now been superseded by ACCESS-CM2; CICE namelist differences between our ACCESS-OM2 1° configuration and ACCESS-CM2 are are tabulated in Appendix F.4.2.

CICE5 uses the same horizontal grid as MOM (see section 3.2.2). Its thermodynamic timestep is `ice_ocean_timestep`, the same as the MOM baroclinic timestep, but its dynamic and elastic timesteps are reduced by the factors `ndtd` and `ndte` \times `ndtd` (respectively) as explained below.

Bailey et al. (2018)?

CICE parameter sensitivities: Hunke (2010).

Parameter sensitivities: Uotila et al. (2012) found that sea ice volume and area are sensitive to albedo, snow patchiness, turning angle, ocean-ice heat transfer coefficient, and a ridging parameter. Miller et al. (2006) documented a sensitivity of ice thickness, speed and extent to ice strength and the air-ice drag coefficient, whilst Kim et al. (2006) found sensitivity of ice thickness to ice density, conductivity, maximum salinity, ice-ocean drag coefficient and ridging parameters. Urrego-Blanco et al. (2016) found a sensitivity to snow parameters and melt pond drainage. Also see Massonnet et al. (2014) (NEMO-LIM3).

cf. Andrew Roberts RASM cice namelist (Petra email 6 June) **TODO: get permission** which was used in Roberts et al. (2015); Cassano et al. (2017); Hamman et al. (2017); Jin et al. (2018); Roberts et al. (2018) see Appendix F.3

See Andrew Roberts’ comments on Roberts et al. (2015) in email from Petra email 6 June — inertial coupling can be essential for stability

The CICE biogeochemistry code (group `zbgc_nml`) is not used.

3.3 CICE sea ice model configurations

3.3.1 Thickness redistribution

We use 5 thickness categories (specified at compile time in build.sh by NICECAT). We use `kcatbound`=0, so the lower bound of ice categories is 0, 0.6445072, 1.391433, 2.470179 and 4.567288 m (from NCAT in CICE output files), as in Hunke et al. (2015, table 2).

We use the Lipscomb et al. (2007) ridging scheme (`krdg_partic`=1), with an e -folding scale parameter $\mu_{rdg}=3\text{ m}^{1/2}$, which is the default value and matches ACCESS-CM2 (Appendix F.4.2) but is smaller than the value $2\text{ m}^{1/2}$ used in ACCESS-OM (Bi et al., 2013b, table 2). `maxraft` (the maximum thickness of rafted ice) takes the default value of 1.0 m in ACCESS-OM2, ACCESS-OM and ACCESS-CM.

3.3.2 Dynamics

TODO: check I (AK) haven't misunderstood anything here – this is based on only a quick skim of most of these papers

We are currently using “classic EVP”² (`kdyn`=1, `revised_evp` = false) (Hunke and Dukowicz, 1997, 2002; Hunke, 2001). This represents the internal ice stresses by a visco-plastic (VP) rheology (Hibler, 1979), to which a fictitious elastic term is added to facilitate efficient numerical convergence to the visco-plastic solution via damped elastic waves which are supposed to decay to negligible amplitude during `ndte`=120 sub-timesteps within each dynamic timestep (Hunke et al., 2015, sections 3.5.2 and 4.4; note that Δt should be replaced by Δt_{dyn} throughout section 3.5: see <https://github.com/CICE-Consortium/CICE/pull/83>).

There is an ongoing debate regarding the suitability of visco-plastic ice rheology, particularly to represent sea ice on fine scales (Nye, 1973; Weiss et al., 2007; Lindsay et al., 2003; Kwok et al., 2008; Girard et al., 2009; Dansereau et al., 2016; Hutter et al., 2018; Weiss and Dansereau, 2017; Hutter et al., 2018). An alternative supported by CICE is the elastic-anisotropic-plastic (EAP) model (Weiss and Schulson, 2009; Wilchinsky and Feltham, 2006; Tsamados et al., 2013), but this seems relatively untested and uncalibrated at this stage.

If we accept the VP formulation, there is also the question of how well the EVP sub-timestepping converges to the VP solution with no residual elastic wave effects. Like many comparable models we use `ndte`=120 sub-timestep iterations, but Losch and Danilov (2012); Lemieux et al. (2012); Kimmritz et al. (2017, 2015) show that full convergence may take thousands of iterations even with the revised EVP method (particularly at high resolution), which would be prohibitively expensive unless an accelerated method (e.g. Koldunov et al., 2019b) was used. We must therefore expect our sea ice stress distribution to contain artefacts due to residual elastic waves. These artefacts may include spurious grid-scale noise and long linear features in the shear and divergence fields (Lemieux et al., 2012). We note that the default `ndte` has been increased to 240 in CICE6.

see Lemieux and Tremblay (2009)

Horizontal advection of conserved properties is handled by the incremental remapping scheme of Dukowicz and Baumgardner (2000) and Lipscomb and Hunke (2004), documented in Hunke et al. (2015, section 3.2). We find that the CFL condition associated with this method usually sets the maximum CICE dynamic timestep, which is shorter than the CICE thermodynamic timestep (and MOM baroclinic timestep) by the factor `ndtd`. This CFL condition becomes very restrictive at 0.1° due to the very fine grid spacing in ocean cells near the tripole (table 6 and figures 3 and 5) so we set `ndtd`=3 to allow MOM to run with a longer timestep. We have not found this to be necessary in the coarser configurations, so these have `ndtd`=1. Using `ndtd`=3 slows down CICE relative to MOM, altering the load balance. We mitigate this by increasing the proportion of cores allocated to CICE

²Another CICE option is the “revised EVP” method (Bouillon et al., 2013; Hunke et al., 2015, section 3.5.3) which corrects an error in the “classic EVP” stress formulation and may also improve the convergence rate of the elastic sub-timesteps and reduce the incidence of spurious grid-aligned linear kinematic features (“leads”). **TODO:** try this out? Bouillon et al. (2013) argue that this is superior to using “classic EVP”, but see warnings by Kimmritz et al. (2017, 2015) that numerical instability may dominate over convergence as the greatest source of error. **FIXME:** wrong references? they don't say this as far as I can see.

3.4 Coupling

in the 0.1° configuration (table 8 and figure 12) so that MOM does not spend so much time waiting for CICE, but this configuration still appears to be CICE-bound. Newer configurations have greatly improved efficiency, partly by altering the bathymetry to eliminate the very smallest ocean cells.

In all three configurations the vertical grid resolution is fine enough to resolve the surface Ekman layer (Table 4), so we use a turning angle of zero (`cosw=1.0, sinw=0.0`), consistent with ACCESS-OM (Bi et al., 2013b, table 2) and ACCESS-CM2 (appendix F.4.2; values unspecified but `cosw=1.0, sinw=0.0` are the defaults). (Is zero turning angle reasonable? see Uotila et al. (2012); Park and Stewart (2016); McPhee (2008); Leppäranta (2011) — we are using 10m ageostrophic winds and can resolve the ocean Ekman layer.)

We use an ice-ocean drag coefficient of `dragio=0.00536`, consistent with ACCESS-OM (Bi et al., 2013b, table 2) and very close to the value of 0.0054 measured at 0.5 m below first-year landfast ice by Shirasawa and Ingram (1997). A wide range of values have been used in the literature (Lu et al., 2011; Martinson and Wamser, 1990; Leppäranta, 2011, table 5.3), but the coefficient also depends on the water velocity and depth at which it is measured, the ice roughness, and the upper ocean stratification (Leppäranta, 2011; Waters and Bruno, 1995). Sensitivity to this parameter has been investigated by Uotila et al. (2012); Urrego-Blanco et al. (2016); Kim et al. (2006).

Sea ice drag coefficients and turning angles: Heorton et al. (2019)

3.3.3 Thermodynamics

The albedo configuration is described in section 3.5.

We use 4 ice layers and one snow layer (specified at compile time in build.sh by NICELYR and NSNWLYR, respectively).

We use the mushy ice formulation of Turner et al. (2013) (`ktherm=2, tfrz_option='mushy'`) at 0.1° . At other resolutions we use the Bitz and Lipscomb (1999) formulation (`ktherm=1, tfrz_option='linear_salt'`). In both cases the freezing point depends on salinity. We also use a constant freezing temperature `tocnfrz=-1.8C` — should we switch to having a function of SSS that is consistent with `tfrz_option`? — see Uotila et al. (2012). These freezing points also differ from the frazil freezing point in MOM, for which we use `freezing_temp_preteos10 = true`. See Andrew Roberts' comments on mushy thermo in email from Petra email 6 June 2018 "First, we are using mushy-layer thermodynamics, and this needs to be carefully coupled so that the temperature in the ocean model's upper layer matches the liquidus temperature in CICE, but the ocean model still conserves salt." **TODO: make freezing points consistent?**

We use the NCAR CCSM3 shortwave distribution method (`shortwave='default'`), which has implicit melt ponds. Explicit melt ponds require the delta-Eddington radiation (`shortwave='dEdd'`), so the parameters in `ponds_nml` are ignored in our configuration **TODO: check**. See Andrew Roberts' comments on melt ponds in email from Petra email 6 June 2018.

Do we include lateral melting? see Roach et al. (2018).

Consistent with ACCESS-OM (Bi et al., 2013b, table 2) we use the Pringle et al. (2007) thermal conductivity parameterisation (`conduct='bubbly'`), which improves the otherwise slow Antarctic ice growth rate (Hunke, 2010), and an ice-ocean heat transfer coefficient of `chio=0.006` (this is the value actually used, since the namelist value `chio=0.004` was ignored — see <https://github.com/COSIMA/cice5/issues/55>) with minimum friction velocity `ustar_min=5 \times 10^{-3} ms^{-1}`.

3.4 Coupling

See <https://github.com/COSIMA/access-om2/wiki/System-description>

Figure 1 shows the fields that are transferred between the coupled model components. The prescribed atmosphere drives the global ice model, which is two-way coupled to the ocean model. Cou-

3.5 Forcing

pling is implemented using the Ocean Atmosphere Sea Ice Soil (OASIS3-MCT, Valcke et al., 2013) coupler version 2.0, developed at CERFACS and CNRS, France (<https://portal.enes.org/oasis>), which uses the Model Coupling Toolkit (MCT, <https://www.mcs.anl.gov/research/projects/mct/>) for routing between individual processors in each model component. The OASIS3-MCT-2 user guide is here: http://www.cerfacs.fr/oa4web/papers_oasis/oasis3mct_UserGuide_2.0.pdf. The coupling strategy is based on the ACCESS-OM model (Bi and Marsland, 2010), but we use a newer version of OASIS which is capable of parallel coupling.

The default remapping method used within OASIS3-MCT-2 (SCRIP <https://github.com/SCRIP-Project/SCRIP>) does not scale to 0.1° . Instead the grid remapping interpolation weights are calculated using the RegridWeightGen application which is part of the ESMF framework <https://www.earthsystemcog.org/projects/esmf/>. Conservative interpolation is used to remap flux fields (2nd order at 1° and 0.25° , first order for 0.1° : <https://github.com/COSIMA/access-om2/issues/71>). For scalar fields we use a technique called patch recovery (Kritsikis et al., 2017a; Khoei and Gharehbaghi, 2007) to produce very smooth destination fields. This is particularly important for the the 0.25° and 0.1° configurations because they have finer resolution than the forcing dataset. However the 2nd order conservative remapping method produces spurious extrema (including nonsensical incorrect signs such as negative runoff or negative downwelling shortwave fluxes): <https://github.com/COSIMA/access-om2/issues/74#issuecomment-454660871>. The creation of interpolation weights is documented at <https://github.com/COSIMA/access-om2/wiki/Technical-documentation#creating-remapping-weights>.

The atmosphere-to-ice coupling timestep is determined by the frequency of the atmospheric forcing dataset (i.e. 3 hourly for JRA55-do). Ice-to-ocean coupling takes place on every timestep (`ice_ocean_timestep`, the ocean baroclinic timestep and ice thermodynamic timestep), since `baroclinic_split=1`.

3.5 Forcing

There is no direct coupling from YATM to MOM5. Surface forcing is handled globally by CICE5, which obtains atmospheric data from YATM, interpolates it in time **TODO: check!**, and calculates various forcing fluxes to pass on to MOM5 via the OASIS3-MCT coupler (figure 1).

The entire 0.1° deg run was affected by a forcing bug: <https://github.com/marshallward/payu/issues/138> and <https://github.com/COSIMA/access-om2/issues/123>. The coarser model runs discussed here were not affected.

We have mass exchange of surface freshwater fluxes as in Bi et al. (2013b) **TODO: confirm**

JRA55-do v1.3 atmospheric forcing (1984-5, 1990-1 or 2003-4 repeat-year, 0.5625° ($\sim 55\text{km}$), 3-hourly) in addition to CORE NYF (2° ($\sim 200\text{ km}$), 6-hourly)

JRA-55-do v1.3 forcing is supported at all three resolutions, and CORE2 forcing is supported at 1 degree resolution. JRA-55-do repeat-year forcing forcing (RYF) and interannual forcing (IAF) are currently supported.

Ocean surface roughness following Beljaars (1995) (CICE parameter `rough_scheme='beljaars'`; note that this is also specified in MOM in `ocean_rough_nml`, but this is for SIS and is therefore ignored).

The sea ice roughness `iceruf`= 5×10^{-3} m matches that used in ACCESS-OM (Bi et al., 2013b, table 2).

Ocean albedo is constant (`cst_ocn_albedo=true`), with the value `ocn_albedo=0.1`, which is larger than the value 0.06 used in ACCESS-OM (Bi et al., 2013b). (This has been changed to the Large and Yeager (2009) latitude-dependent ocean albedo (`cst_ocn_albedo=false`) in more recent versions.) The MOM parameter `ocean_albedo_option` is ignored. In CICE5 we use the same NCAR CCSM3 shortwave distribution method (`shortwave='default'`), ice and snow albedos in the visible ($\leq 700\text{ nm}$) and infrared ($\geq 700\text{ nm}$) bands (`albicev`, `albicei`, `albsnowy`, `albsnowi`) and melt albedo parameters (`dalb_mlt` and `ahmax`) **TODO: explain these** as in ACCESS-OM (Bi et al., 2013b, their table 2), but we use the default snow patchiness parameter `snowpatch` = 0.02 m instead of the value 0.01 m used in ACCESS-OM. (We also set the same `dt_mlt`= 1.0°C as ACCESS-OM but this Delta-Eddington parameter is ignored since `shortwave='default'`.) The albedo parameters differ from those in Hunke et al. (2015) and in JRA-55 (Kobayashi et al., 2015). We use the default CCSM3 albedo type (`albedo_type='default'`). **TODO: explain what this does**

3.5 Forcing

Shortwave penetration into the ocean is handled by the GFDL scheme (`ocean_shortwave_gfdl_nml`), with Manizza et al. (2005) optics (`optics_manizza=true`). The Manizza et al. (2005) scheme splits the shortwave radiation flux equally into red and blue/green bands, and determines separate exponential decay scales for each band, with a term depending on chlorophyll-a concentration and a constant term for the absorption by pure seawater. We use a prescribed monthly surface chlorophyll-a climatology (`read_chl=true`) from the file `chl.nc`. This climatology is based on SeaWiFS data from 1998–2006 **TODO: check: Griffies (2015, sec 3.14.2) says 1998–2007** and is presumably **TODO: check** the same as used in GFDL’s CM2.5 and CM2.6 (Delworth et al., 2012; Griffies et al., 2015) based on the method of Sweeney et al. (2005). In the GFDL implementation this surface chlorophyll-a concentration is crudely approximated as independent of depth. We also set a maximum penetration of `zmax_pen=300 m`. This limit is unlikely to have a noticeable effect, since even the slowest-decaying component (the blue/green band in clear water) has a decay scale $k = 0.0232 \text{ m}^{-1}$, so the neglected fraction is at most $\frac{1}{2} \exp(-k \text{ zmax_pen}) = 4.7 \times 10^{-4}$, and probably very much less. **TODO: set `zmax_pen` to 1e6? see comments in code**

There is no representation of geothermal heating (`use_geothermal_heating=false`).

3.5.1 JRA55-do interannual and repeat-year forcing

The ACCESS-OM2 configurations are forced with the JRA55-do v1.3 atmospheric reanalysis (Tsujino et al., 2018a, and <http://www.cesm.ucar.edu/events/wg-meetings/2018/presentations/omwg/kim.pdf> and <https://climate.mri-jma.go.jp/~htsujino/jra55do.html>) which has significantly improved bias, spatial and temporal resolution (55 km, 3-hourly), temporal extent (1958–2018), and dynamical self-consistency compared to the CORE dataset (200 km, 6-hourly, 1948–2009) used in many previous studies. We use recent calving and basal melt estimates from Depoorter et al. (2013), which are spatially variable and somewhat larger than the uniform values in CORE (Tsujino et al., 2018a). JRA55-do will also be regularly updated, allowing real-time experiments. The improved spatial resolution of wind is important for better representation of coastal polynyas (Stössel et al., 2011; Zhang et al., 2015). JRA55-do has higher spatial and temporal resolution and longer temporal extent than ERA-Interim (80 km, 6-hourly, 1979–present) but is coarser and somewhat shorter than the upcoming ERA5 reanalysis (31 km, 3-hourly, 1950–present): <https://confluence.ecmwf.int/pages/viewpage.action?pageId=74764925>.

JRA55-do data are available from https://esgf-node.llnl.gov/search/input4mips/?institution_id=MRI. It has been downloaded to NCI in a few places: /g/data/qv56/replicas/input4MIPs/CMIP6/OMIP/MRI/ (note that MRI-JRA55-do-1-3 is actually v1.3.1) and also /g/data/ua8/JRA55-do/v1-3 (note that 1-3 is actually 1.3.0; this is what was used for the ACCESS-OM2 v1.0 runs). Also see <http://climate-cms.unsw.wikispaces.net/JRA55-do> and <https://github.com/COSIMA/access-om2/issues/120>.

The JRA55-do forcing file paths are constructed from the paths in `atmosphere/forcing.json`, with INPUT replaced by the paths in the atmosphere input section of `config.yaml` and `\{\{year\}\}` replaced by the model years over the range set in `accessom2.nml`.

See `JRA55_RYF_justification.ipynb` for biases in each RYF year.

JRA55-do (Tsujino et al., 2018a) is a surface-atmospheric reanalysis product derived from the 55-year Japanese reanalysis (JRA55, http://jra.kishou.go.jp/JRA-55/index_en.html) and intended for driving oceans models. We use JRA55-do version 1.3 to drive our ice and ocean models. The temporal coverage is from 1st January 1958 to 1st February 2018, but it is regularly updated to near present day.

JRA55-do v1.3 user manual: [Tsujino et al. \(2018b\)](#)

For the latest information on the dataset status and citation: <http://goo.gl/r8up31>.

see http://amaterasu.ees.hokudai.ac.jp/~tsujino/JRA55-do-v1.3/00README_v1_3.1st JRA-55: Kobayashi et al. (2015) JRA55-do: Tsujino (2015b,a, 2016); Tsujino et al. (2018a), Tsujino et al. (2016), Kim et al. (2018)

<http://www.clivar.org/omdp/japan2016>

JRA55-do version 1.3 provides 3-hourly liquid and solid precipitation, downwelling surface long-

3.5 Forcing

wave and shortwave radiation, sea level pressure, 10m wind velocity components, 10m specific humidity and 10m air temperature (NB: humidity and temperature are shifted from 2m in JRA55 to 10m in JRA55-do — see [Tsujino et al., 2018a](#), , appendix A2) on a TL319 grid (0.5625° resolution), and daily river flux at 0.25° resolution.

TODO: check: what do we use for glacier runoff? groundwater? evaporation? upwelling longwave radiation?

"Runoff from Greenland and Antarctica are replaced by climatological runoff. Greenland runoff is based on [Bamber et al. \(2012\)](#) and Antarctica runoff is based on [Depoorter et al. \(2013\)](#)." (http://amaterasu.ees.hokudai.ac.jp/~tsujino/JRA55-do-v1.3/00README_v1_3.1st)

The Antarctic runoff is spatially variable in JRA55-do ([Tsujino et al., 2018a](#)), in contrast to CORE . we made a start on this: <https://github.com/COSIMA/matm/issues/5> currently fresh water is input at the ice shelf edges.

cf. runoff (iceberg discharge scheme) used in ACCESS-CM2 - see AMOS2018 notes on Dave Bi's talk and <https://accessdev.nci.org.au/trac/wiki/CMIP6workshop> — this is discharged only at the surface. See Siobhan's email 2018-06-04

Runoff - incl distributed iceberg melt? Ask Adele? basal melt needs to be at depth - notebook p561, [Mathiot et al. \(2017\)](#). We have the data but waiting on it being published. Veronique has regridded this - see email 2017-11-16 [Merino et al. \(2016\)](#) and [Depoorter et al. \(2013\)](#) Paul: "The Antarctic ice berg data is published and the data is publicly available here: <http://neinch.github.io/personalweb/publications/> However, the Antarctic basal melt fluxes are not published yet and the data has not been made public." Also see [Merino et al. \(2018\)](#); [Donat-Magnin et al. \(2017\)](#); [Mathiot et al. \(2017\)](#); [Hammond and Jones \(2016\)](#); [Stössel et al. \(2015\)](#)

JRA55-do river runoff is from [Suzuki et al. \(2018\)](#); this is daily, interannually varying runoff from the JRA55 land surface model at 0.25° resolution, adjusted to match the observational estimates of [Dai et al. \(2009\)](#). River runoff is combined with climatological monthly solid runoff for Greenland ([Bamber et al., 2012](#)) and spatially-variable annual mean climatological basal melt and calving from Antarctica ([Depoorter et al., 2013](#)). Calving and liquid runoff are combined (`discharge_combine_runoff -calve` defaults to true). River discharge is inserted at the coast in the top `river_insertion_thickness=40 m`, but other runoff is inserted only at the surface (`runoff_insertion_thickness` and `calving_insertion_thickness` default to zero) at the ice shelf edge. Total runoff is remapped (and spread horizontally if needed to keep the flux below a threshold) in real time by YATM — see section 3.5.5.

runoff tools: https://github.com/COSIMA/runoff_tools

RYF: cite ([Stewart et al., 2019](#)); cf. [Röske \(2006\)](#).

discuss choice of year for RYF — will use 1984-5 for high-res runs – refer to Kial's paper

RYF generated by https://github.com/aidanheerdegen/make_rjf.

These 12-month periods were identified as particularly "neutral": 1 May 1984 - 30 April 1985, 1 May 1990 - 30 April 1991, 1 May 2003 - 29 April 2004 (we keep 29 Feb 2004 and ditch 30 April 2004 so as to keep 365 days per year). We have run ocean-sea ice spinups forced by all three JRA55-do v1.3 repeat years at 1° but we are concentrating on 1984-5 for the 0.1° spinup as it has less of the warming signal and also gives us more of the JRA55 dataset for subsequent interannual runs.

Kial's email 2018-03-05:

-1st of January is in the peak of the northern winter and southern summer, meaning the variability in forcing fields (ie. weather) is quite high. This is a problem for surface buoyancy fluxes in the north Atlantic and Labrador & Nordic Sea regions, where NADW formation is notoriously sensitive to changes in surface forcing. The day of the year with lowest variability (least weather) is going to be closer to the equinoxes, and in JRA55 DO it turns out to be 1 May.

3.5 Forcing

-The three candidate years have been selected as the 12-month periods with climate indices closest to neutral. The climate indices of interest are the SOI, SAM and NAO. Removing the criteria that a 12-month period follows the calendar year allows us to find "years" that are closer to climatologically neutral.

-Having the jump at 1 May allows us to run the model harder. The model tends to fall over at 1 Jan if the jump is there, meaning we have to back off the timestep and nurse it through. Having the jump at 1 May does not require any such nursing. Currently we are running the ACCESS-OM2 1° with 5400 sec timesteps from initialization and getting through 90 years per day.

TODO: plots of anomalies from climatology for the time-mean (or seasonal-mean) RYF forcing fields

see <https://github.com/COSIMA/access-om2/issues/52> and [http://www.earthsystemmodeling.org/esmf_releases/last_builtin/ESMF_refdoc/node3.html#SECTION0302000000000000000000000000000000](http://www.earthsystemmodeling.org/esmf_releases/last_builtin/ESMF_refdoc/node3.html#SECTION03020000000000000000000000)

All versions of JRA55-do up to and including (at least) v1.4.0 had some tropical cyclones in the Northeast Pacific and the North Atlantic from 1959 to 1987 erroneously represented as anti-cyclonic vortices: <https://github.com/COSIMA/access-om2/issues/186>. RYF8485 (1 May 1984 - 30 April 1985) has four faulty North Atlantic storms but RYF9091 and RYF0304 are OK. ⚠️

SST suddenly gets worse at end of 1990's at all resolutions, and stays that way ([Kiss et al., 2020](#), figure 3b) — is there a persistent problem with JRA55-do? Or is it just that the 18°C offset is wrong?

The new IAF configuration will use JRA55-do 1.4.0 from /g/data/qv56/replicas/input4MIPs/CMIP6/OMIP/MRI/MRI-JRA55-do-1-4-0. At present this extends to 5 Jan 2019, which is as much as is currently available from <https://esgf-node.llnl.gov/search/input4mips/> but this will be extended close to the present day from time to time — e.g. there is a beta version v1.4.0.1beta extending to 11 Jan 2020: <https://climate.mri-jma.go.jp/~htsujino/jra55do.html>. The JRA55-do v1.4.0 user manual is here: https://climate.mri-jma.go.jp/~htsujino/docs/JRA55-do/v1_4-manual/User_manual_jra55_do_v1_4.pdf ([Tsujino et al., 2019](#)).

3.5.2 Restoring

The only restoring we apply is to surface salinity. This is restored to interpolated **TODO: state interpolation method – Smoothing at 0.1deg to deal with spurious discontinuities and noise in WOA13v2**: <https://github.com/COSIMA/access-om2/issues/103> World Ocean Atlas 2013 v2 monthly climatology (<https://www.nodc.noaa.gov/OC5/woa13/>); the interpolated salinity file is salt_sfc_restore.nc. The restoring timescale is set by salt_restore_tscale; we use 10 days at 0.1° and 21.28 days for the coarser resolutions. The “piston velocity” (surface vertical grid spacing divided by restoring timescale) is more physically relevant than the restoring timescale. This is 0.11 m/day at all resolutions due to the differing vertical resolution (see Table 4). This piston velocity is within the range of values used for CORE-II models, but is somewhat weaker restoring than the 50 m/300 days (i.e. 0.167 m/day) used for GFDL’s MOM simulations ([Danabasoglu et al., 2014](#), table 2).

We apply salinity restoring via a salt flux (`use_waterflux = true`, `salt_restore_as_salt_flux = true`) and restore everywhere, including under ice (`salt_restore_under_ice = true`). A spatially constant offset is added to the salt restoring to ensure that the net salt restoring flux is zero for each timestep (`zero_net_salt_restore = true`). In order to avoid excessively large fluxes the SSS mismatch is limited to `max_delta_salinity_restore = 0.5 psu` for the purposes of calculating the restoring flux. We don’t use `salinity_restore_limit_lower` or `salinity_restore_limit_upper`, so `max_delta_salinity_restore` applies even in regions of extremely low or high salinity (see <https://github.com/mom-ocean/MOM5/Issues/203>). We impose a constraint of zero net water flux into the ocean from the coupler (`zero_net_water_coupler = true`) by removing the area-mean of P-E+R from P-E so that the area-integrated P-E+R=0 at each timestep; this does not constrain water exchanges with the sea ice (see section 4.12.5). **FIXME: how does this work, given that some of the precip falls as snow on ice to be released later, but zero_net_water_coupler is a MOM thing?** see <https://arccss.slack.com/archives/C9Q7Y1400/p1572993155004300> These choices are typical of CORE-II models ([Danabasoglu et al., 2014](#), table 2).

3.5 Forcing

See Griffies et al. (2016, section 2.3) and Danabasoglu et al. (2014, Appendix C). Sensitivity to restoring: Behrens et al. (2013).

2nd order conservative interpolation: Kritsikis et al. (2017b)

3.5.3 Sea ice formation salt flux limiter

The model sea ice has a fixed bulk salinity; we use the default `ice_salt_concentration` = 0.005 kg salt / kg ice, matching the CICE5 parameter `ice_ref_salinity` defined in `drivers/auscom/ice_constants.F90` (but differing from the ACCESS-OM value of 0.004 kg salt / kg ice, Bi et al., 2013b, table 2). This salt is obtained from the seawater when sea ice is formed, and we found this could drive ocean salinity below zero in regions fresher than `ice_salt_concentration`, for example during the spring melt in the shallow Siberian gulfs that are resolved in the 0.1° model bathymetry. This problem was resolved by setting the local ocean-ice salt flux to zero in regions where the seawater salinity is less than `ocean_ice_salt_limit` = 0.006 kg salt / kg ice. Since we use `zero_net_salt_restore` = true, in these regions the sea ice salt is instead obtained from the global surface ocean at large. Over a sea ice formation and melt cycle this produces a small unphysical transport of salt from the global surface ocean to regions where such sea ice melts. Sea ice formed in regions saltier than `ocean_ice_salt_limit` obtains its salt locally as usual. **TODO:** get Russ to check this <https://github.com/mom-ocean/MOM5/commit/2d76b70ca66173f8dfcfdb0597c9b148ef4a7510> This limiter is only applied in the 0.1° model.

3.5.4 Bulk formulas used

These are specified in the AUSCOM ocean drivers for CICE5.

see https://github.com/COSIMA/cice5/blob/master/source/ice_atmo.F90, https://github.com/COSIMA/cice5/blob/master/source/ice_forcing.F90, https://github.com/COSIMA/cice5/blob/master/drivers/auscom/surface_flux_mod.F90 https://github.com/COSIMA/cice5/blob/master/drivers/auscom/cpl_forcing_handler.F90

The stress applied to the ocean surface is a mixture of the air-ocean and ice-ocean stresses, weighted in proportion to the ice concentration (see [here](#), lines 725–6).

We use Large and Yeager (2004) turbulent flux bulk formulas (`ncar_ocean_flux=true`, `ncar_ocean_flux_orig=false`), for the air-ocean drag coefficient, evaporative transfer coefficient and sensible heat transfer coefficient (eq. 6–10 in Large and Yeager, 2004). This is implemented in https://github.com/COSIMA/cice5/blob/master/drivers/auscom/surface_flux_mod.F90#L824. The calculation uses the air-ocean velocity difference with an additional component to account for gustiness (the gust component is derived from **FIXME: what?** and is not modified: `alt_gustiness`, `gust_const`, `gust_min`). Note that the implementation differs from Large and Yeager (2004) in having a 0.5 m·s⁻¹ floor for the 10 m relative windspeed, a ceiling of 10 for the absolute value of the stability parameter ζ , and a floor of 1 for the parameter $X = (1 - 16\zeta)^{\frac{1}{4}}$ (though the last of these should have no effect). We used `n_itts=2` Monin-Obukhov iterations, which Large and Yeager (2004) state is appropriate for over the ocean, but less than their suggested value of 5 for over sea ice. **FIXME: or is this only applied over the ocean?**

TODO: comment on whether bulk formula is still applicable despite the fine vertical resolution – see Van Roekel et al. (2018)

Large and Yeager (2009)

- relative or absolute wind? See Abel et al. (2017). We use relative wind over ocean: https://github.com/COSIMA/cice5/blob/master/drivers/auscom/surface_flux_mod.F90#L558 - relative to ice as well as ocean? Relative winds are used over ocean, but absolute winds over ice: <https://github.com/COSIMA/access-om2/issues/138>.

We don't use high-frequency coupling (we don't specify `highfreq` in group `forcing_nml` so it defaults to false). `highfreq` implements the RASM coupling method of Roberts et al. (2015, 2011); also see http://www.oc.nps.edu/NAME/RASM_overview.pdf. It uses relative ice-atmosphere velocities for calculating stresses, so 

3.5 Forcing

should probably be turned on for consistency, since relative velocity is used for the ocean.³ **TODO:** check this is correct - ssuo is passed to surface_flux as u_surf There is now an option to use absolute winds to force the ocean via the boolean `absolute_wind` in namelist `surface_flux_nml` — see <https://github.com/COSIMA/access-om2/issues/137>. So absolute wind on both ocean and ice requires `absolute_wind=true` and `highfreq=false`, whereas relative wind on both ocean and ice requires `absolute_wind=false` and `highfreq=true`.

See [Tsujino et al. \(2018a\)](#), section 3.4.3): raw JRA55 winds have been adjusted in JRA55-do to agree with time-mean scatterometer and radiometer winds, which are relative to the ocean current. So subtracting the ocean surface current may be unnecessary. [Tsujino \(2018\)](#) recommend adding the [Rio et al. \(2014\)](#) climatological surface current distributed with the forcing dataset to better approximate the absolute wind. see [Wu et al. \(2017\)](#) and https://arccss.slack.com/archives/C6PP0GU9Y/p1511825314000106?thread_ts=1511802000.000465&cid=C6PP0GU9Y and <https://jra55-do.slack.com/archives/C7LEZT4KY/p1511963905000047> and <https://github.com/COSIMA/access-om2/issues/79>. In addition to the adjustment in JRA55-do, the underlying JRA55 reanalysis ingests scatterometer winds ([Kobayashi et al., 2015](#)), so presumably includes the imprint of eddies. This would not be corrected by adding climatological mean ocean currents. There may be significant impacts of western boundary currents — see [Renault et al. \(2019a, 2016\)](#).

We follow current recommended practice to calculate wind stress from relative wind, but this is still a matter of debate. The issue is that the JRA55-do mean winds are set to equal the scatterometer mean, and this is a relative measurement so includes the effect of mean currents. But if absolute wind is used in the stress calculation it will omit eddy stress damping. This is quite a complex issue, particularly since ocean-only models also lack important feedbacks that modulate the stresses (e.g. [Renault et al., 2020](#)).

TODO: should bulk formulas match what was used in JRA55-do? do we need something like `ncar_ocean_fluxes` but for JRA-55? https://github.com/COSIMA/cice5/blob/master/drivers/auscom/surface_flux_mod.F90#L820 NB: [Tsujino et al. \(2018a\)](#) use formulas from [Gill \(1982\)](#) and recommend using these rather than [Large and Yeager \(2004, 2009\)](#). Also see [Brodeau et al. \(2017\)](#).

see [Roberts et al. \(2015\)](#) appendix A - RASM uses nonzero ice velocity for stress calculation cf. appendix C of [Griffies et al. \(2009\)](#).

3.5.5 YATM and libaccessom2

CONTRIBUTORS: Nic Hannah

ACCESS-OM2 uses a new atmospheric driver, known as YATM, which implements a file-based atmosphere and replaces MATM used in ACCESS-OM ([Bi et al., 2013b](#)). Its purpose is to track model time and, when necessary, read the appropriate forcing fields from files and deliver them to the coupler. This is implemented via an associated library (libaccessom2, <https://github.com/COSIMA/libaccessom2>) that is linked into YATM, CICE and MOM to provide shared functionality and an interface to inter-model communication and synchronisation tasks.

YATM is also responsible for remapping runoff (combined river, calving and basal melt) in real-time. This is done separately from the other forcing fields because it is difficult to do in a distributed memory setting — ensuring runoff is on coastal points may require interprocess communication. Remapping is done in two steps: firstly it is moved to the destination grid using conservative interpolation, and then distributed from land to coastal points using an efficient nearest neighbour algorithm based on a pre-computed k-dimensional tree (k-d tree) data structure ([Bentley, 1975](#)). The Fortran k-d tree implementation is called KDTREE2 (<https://github.com/jmhodges/kdtree2>).

To prevent high concentrations of runoff a method for spatially variable conservative flux limiting has been implemented. Values are set by `runoff_caps` in units of $\text{kg m}^{-2} \text{s}^{-1}$; i -index start and end regions are set by `runoff_caps_is` and `runoff_caps_ie`, and j -index start and end regions are set by `runoff_-`

³This has been corrected in the new 0.1° RYF configuration, which uses relative velocities for both ice and ocean: <https://github.com/COSIMA/access-om2/projects/1>.

3.6 Initial conditions and spinup

`caps_js` and `runoff_caps_je`. The 0.25° and 1° configurations use the default runoff cap of $0.03 \text{ kg} \cdot \text{m}^{-2} \text{s}^{-1}$ globally. At 0.1° there are reduced caps of 0.001 and $0.003 \text{ kg} \cdot \text{m}^{-2} \text{s}^{-1}$ at the mouths of some Arctic rivers to produce broader spreading and avoid excessively low salinity, and a cap of $0.03 \text{ kg} \cdot \text{m}^{-2} \text{s}^{-1}$ everywhere else. **TODO:** Tabulate / plot runoff caps or runoff distribution in all models

YATM parameters for the three model resolutions are tabulated in Appendix A.4.

3.6 Initial conditions and spinup

The ACCESS-OM2 and ACCESS-OM2-025 runs were started at rest, with zero sea level, with temperature and salinity from World Ocean Atlas 2013 v2 (WOA13, Locarnini et al., 2013; Zweng et al., 2013, <https://www.nodc.noaa.gov/OC5/woa13/>) and run for five 60-year cycles (1 Jan 1958 – 31 Dec 2017) of JRA55-do. The temperature and salinity initial condition is created by the script `/g/data/hh5/tmp/cosima/observations/postprocessing/woa13/WOA_initial_conditions.py`. It is composed of the January 0.25° climatology `/g/data/v45/akm157/data/WOA13v2/averaged_-decades/woa13_decav_s01_04v2.nc` over the full range of depths for which it is available (0–1500 m) and the boreal Winter (January–March) 0.25° climatology `/g/data/v45/akm157/data/WOA13v2/averaged_decades/woa13_-decav_s13_04v2.nc` below that, with in-situ temperature converted to potential temperature referenced to 0 dbar via the TEOS-10 formulas as implemented in <https://pypi.org/project/gsw/>. Note that an initial condition of potential temperature was mistakenly used, which does not match the model prognostic conservative temperature used at 1° and 0.25° — see section 3.2.8 and <https://github.com/COSIMA/access-om2/issues/206>. We use the “decav” WOA13 product, which is the average of the decadal averages, so uses data from 1955–2012: <https://data.nodc.noaa.gov/woa/WOA13/DOC/woa13documentation.pdf>. Since it’s the average of the decadal averages it won’t be biased towards recent data. This initial condition is the same as for OMIP (Griffies et al., 2016), except that we use potential temperature and practical salinity rather than conservative temperature and absolute salinity. ⚠

The ACCESS-OM2-01 experiment `01deg_jra55v13_iaf` ran for 33 years from 1 Jan 1985 – 31 Dec 2017. It was started on 1 January from restart 431 from `01deg_jra55v13_rjf8485_spinup6`, i.e. after 40 years of JRA55-do 1 May 1984 – 30 April 1985 repeat-year forcing (RYF, Stewart et al., 2019), which in turn began from the same World Ocean Atlas 2013 v2 initial condition as the coarser runs. The `01deg_jra55v13_rjf8485_spinup6` RYF spinup contained some parameter changes, detailed in `/g/data/hh5/tmp/cosima/access-om2-run-summaries/run_summary_01deg_jra55v13_rjf8485_spinup6.csv`. The most significant of these was changing the ice turning angle from 16.26° **TODO:** in which direction? presumably depends on hemisphere (`cosw=0.96, sinw=0.28`) to zero (`cosw=1.0, sinw=0.0`) at the start of August in the 12th year (run 113). Before this change the Arctic ice volume was building up significantly (and unrealistically) in the thickest category, but it began a slow decline when the turning angle was set to zero (figure 10) which persisted into the first ~ 6 years of the IAF run (figure 35). This change in the turning angle also caused a small increase in Antarctic sea ice thickness which rapidly stabilised at its new level. The 1984–85 repeat-year forcing contained some biases relative to climatology; for example, biases in the North Pacific wind stress curl produced late separation of the Kuroshio Current. For details see Stewart et al. (2019).

The sea ice and snow initial conditions are set in subroutine `set_state_var` in `ice_init.F90` — see https://github.com/COSIMA/cice5/blob/5583ce54fd8822c1b8aef0549090167ca5f36d10/source/ice_init.F90#L1412. The first run has `restart=false` (see Appendix B.3.1), so uses `ice_ic='default'`. This sets a uniform ice concentration and thickness (100% and around 2.5 m, respectively) in regions north of 70°N and south of 60°S where the sea surface temperature is less than 1°C above freezing (see `aice` and `hi` in `/g/data/hh5/tmp/cosima/access-om2-01/01deg_jra55v13_rjf8485_spinup6/output000/ice/OUTPUT/iceh.0001-01-01.nc`). Ice area has a parabolic distribution across the five ice thickness categories. The initial snow thickness in each category is 0.2 m or 20% of the ice thickness in that category, whichever is smaller. The total sea ice and snow volumes in this initial condition are very close to the adjusted state (figure 11, top eight panels), displaying only a small reduction of ice mass in category 4 in both hemispheres, and an increase in category 5 in the Arctic. Consequently there is no significant drift in total ocean salt as the sea ice spins up (figure 11 bottom row).

3.7 Model computational details and performance

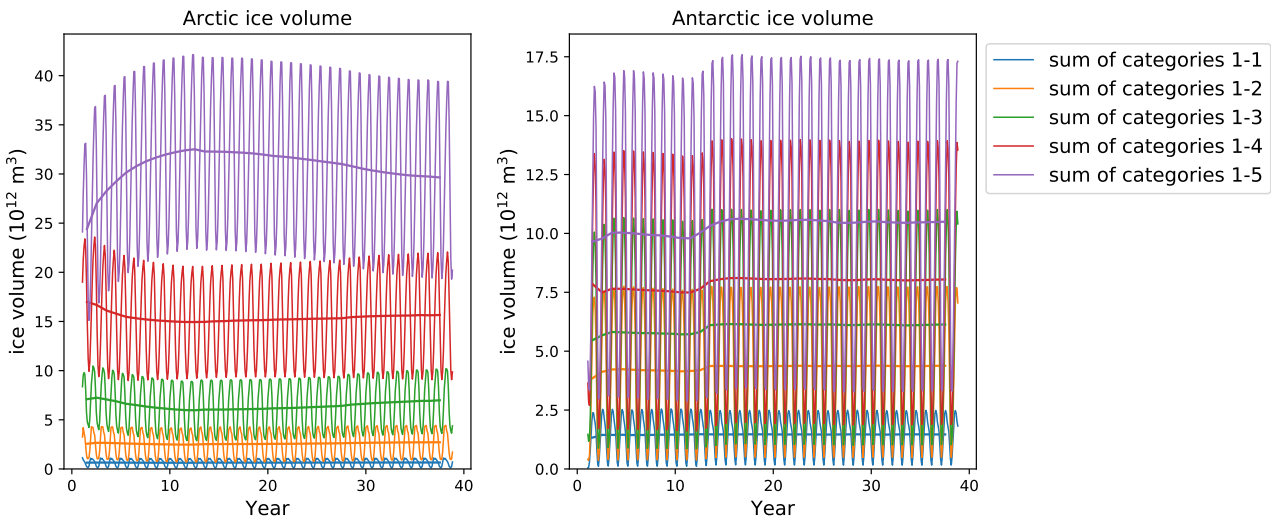


Figure 10: Sea ice volume (cumulative by category) in the RYF run used as the initial condition for the IAF run at 0.1° .

3.7 Model computational details and performance

CONTRIBUTORS: Marshall, Nic

3.7.1 Resource requirements

Typical model computational resource requirements are shown in Table 8; further details are provided in the run summary spreadsheets (see Table 2).

Some of the factors underlying these parameter choices are discussed in section 3.3.2. Newer configurations have greatly improved efficiency than is shown here.

This demonstrates efficient scaling well beyond the 512 cores investigated by Schmidt (2007).

cf. MOM-SIS-01: 50–60kSU/day?

cf. Matt Chamberlain's 2016 talk: global MOM-SIS at 0.1° and 50 levels, 960 CPUs (50x23 layout, 200 masked), dt=720s, month \sim 100min: http://cosima.org.au/wp-content/uploads/2016/06/ofam_global.mac_.pdf — this is as fast as ACCESS-OM2-01 but about 6x cheaper!

3.7.2 Tiling in MOM and CICE

mom tile layout: /short/v45/raf599/masking/procno_045x036_5000.nc

plot MOM tiling, showing dry tiles and bathymetry for each resolution?

plot CICE tiling, showing idle tiles for each resolution?

See table 8. CICE5 has the ability to subdivide the computational domain horizontally into tiles (termed “blocks”), and then parallelise by allocating one or more blocks to each CPU. This can improve load balancing if a similar number of ice-containing and ice-free blocks are allocated to each CPU. The maximum number of blocks per CPU is given by the environment variable MXBLCKS which is calculated from the CPU count⁴ (NTASK) by the build.sh compilation script: <https://github.com/COSIMA/cice5/blob/076b14f2/bld/build.sh#L72>; the actual number of blocks is reported in the output file ice_diag.d. NTASK is included in the executable name, with a ‘p’ suffix. There are tools for investigating load balance with various masking and CPU choices at <https://github.com/russfiedler/masking> (currently only for distribution_type='roundrobin').

The final CICE5 configurations of the runs reported here used distribution_type='roundrobin' with processor_shape='square-ice' at 0.25° and 0.1° (Craig et al., 2015), which omits land-only blocks and also improves the load balance. At 1° we use distribution_type='cartesian' and processor_shape='slenderX1', which allocates pole-to-pole meridional strips to each processor in the interests of load balancing. We also use halo masking at all resolutions (maskhalo_bound, maskhalo_dyn and maskhalo_remap are all true),

3.7 Model computational details and performance

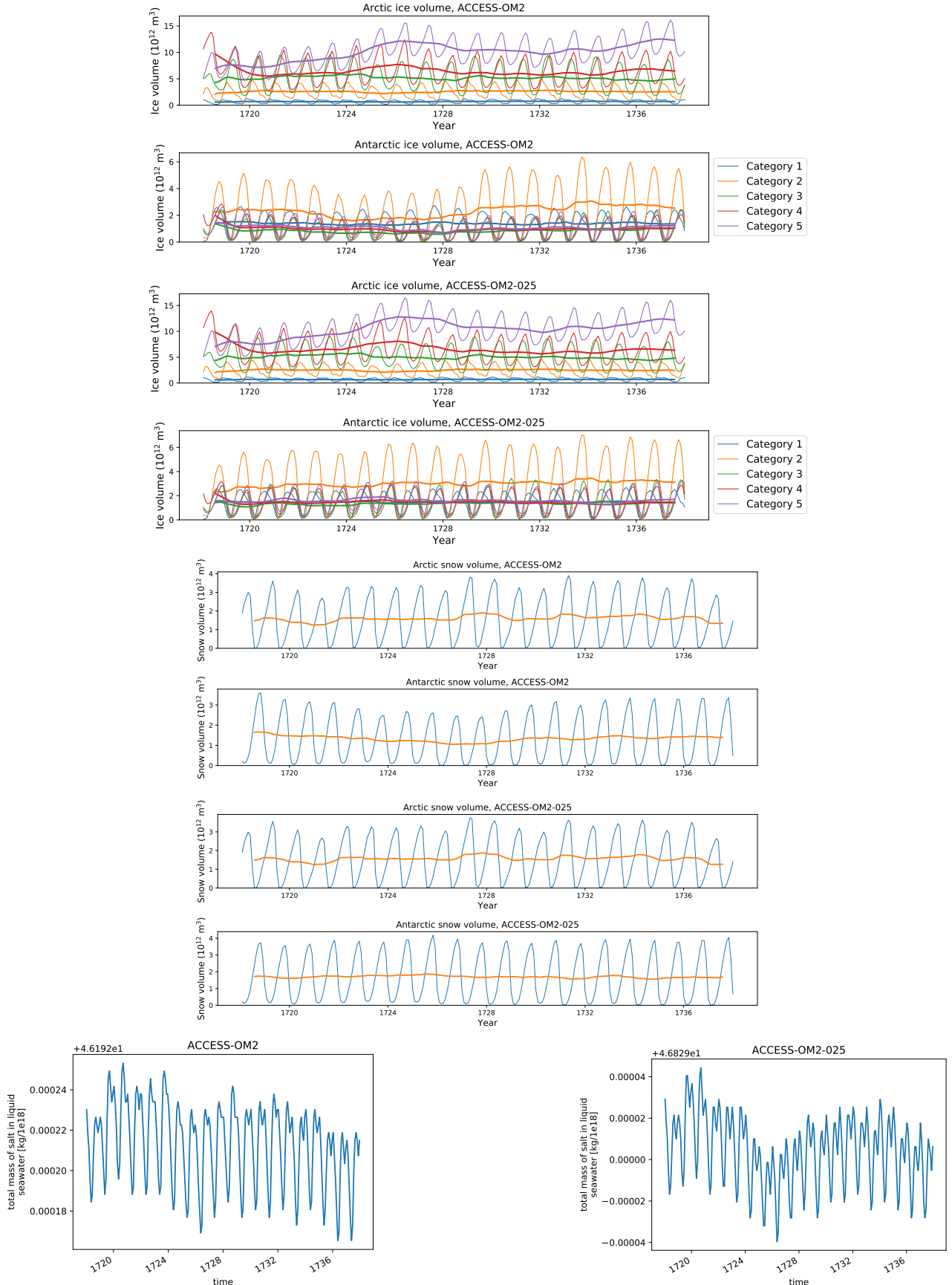


Figure 11: Top four plots: Arctic and Antarctic sea ice volume by category in initial spinup at 1° and 0.25° . Next four plots: Arctic and Antarctic snow volume in initial spinup at 1° and 0.25° . Bottom row: monthly mean total mass of ocean salt in the first several years at 1° (left) and 0.25° (right). The top eight plots show monthly means and 12-month rolling means. The ocean salt plots have large offsets indicated at the top of the y-axes. The annual cycles are due to sea ice formation and melting, which vary the total ocean salt by less than one part in 10^6 .

3.7 Model computational details and performance

| | ACCESS-OM2 | ACCESS-OM2-025 | ACCESS-OM2-01 |
|--------------------------------------|----------------|------------------|------------------|
| Zonal resolution | 1° | 0.25° | 0.1° |
| Ocean grid | 360 × 300 × 50 | 1440 × 1080 × 50 | 3600 × 2700 × 75 |
| MOM5 tile size | 23 × 20 | 30 × 27 | 45 × 36 |
| MOM5 number of tiles | 240 | 1920 | 6000 |
| MOM5 cores | 216 | 1455 | 4358 |
| CICE5 block size | 15 × 300 | 30 × 27 | 36 × 30 |
| CICE5 number of blocks | 24 | 1920 | 9000 |
| CICE5 cores (NTASK) | 24 (24) | 361 (480) | 1600 (1392) |
| CICE5 <code>processor_shape</code> | 'slenderX1' | 'square-ice' | 'square-ice' |
| CICE5 <code>distribution_type</code> | 'cartesian' | 'roundrobin' | 'roundrobin' |
| Queue | normalbw | normal | normal |
| Timestep (s) | 5400 | 1350–1800 | 450 |
| CPU hr / model year | 118 | 4,700 | 118,000* |
| Walltime hr / model year | 0.38 | 2.6 | 19.9* |
| Memory (Gb) | 83 | 522 | 2689 |

Table 8: Typical computational details and resource requirements for the three configurations. Full details are given in the run summary spreadsheets in Table 2, and namelist changes within runs are tabulated in Appendix B. Total core count in the spreadsheets is rounded up to a multiple of the cores per node (24 in the normalbw queue, 16 in the normal queue). The number of tiles (blocks) includes land-only tiles (blocks), but these are not allocated to a processor core. Multiple CICE5 blocks are allocated to each core at 0.25° and 0.1°. MOM5 tile size is determined by the horizontal grid dimension divided by the number of tiles in that direction as set by `layout`. CICE5 block size (`BLCKX`×`BLCKY`) and NTASK are defined at compile time via <https://github.com/COSIMA/cice5/blob/076b14f2/bld/config.nci.auscom.360x300>, <https://github.com/COSIMA/cice5/blob/076b14f2/bld/config.nci.auscom.1440x1080> and <https://github.com/COSIMA/cice5/blob/076b14f2/bld/config.nci.auscom.3600x2700> in ACCESS-OM2, ACCESS-OM2-025 and ACCESS-OM2-01, respectively. The timestep is the MOM5 baroclinic timestep, equal to the CICE5 thermodynamic timestep. *More recent configuration improvements have halved the ACCESS-OM2-01 walltime and SU cost.

In all cases the initial condition was 1st January from spun-up runs (1 January 2003 in 5th cycle at 1°, 1 January 2000 in 5th cycle at 0.25°, and 1 January 2000 at 0.1°).

See figure 12.

cf. [Koldunov et al. \(2019a\)](#)

The profiling runs were nearly identical to the final configurations of the production runs (Appendix A), in particular having the same `ndtd`=3 and mushy ice (`ktherm`=2), but they did have a few differences which are tabulated in Appendix C. We note here the main differences that may affect runtime.

- The profiled runs used executables compiled with Intel compiler suite 2019 and OpenMPI 3.0.3, whereas the production runs used Intel compiler suite 2017 (17.0.1.132) and OpenMPI 1.10.2.
- The profiled runs used Sandy Bridge nodes, whereas the production runs used the faster Broadwell nodes.
- The profiled 1° MOM5 runs used `redsea_gulfbay_sf`, but this wasn't used in production runs. This is expected to be insignificant as it used Russ' fixed version which has a negligible impact on runtime.
- The profiled CICE5 runs used `distribution_type`='sectrobin' at both 0.25° and 0.1°, but the production runs used 'roundrobin' at both resolutions (apart from the first 114 runs at 0.1° which used 'cartesian'). 'sectrobin' has a smaller communication overhead than 'roundrobin' but may have poorer load balancing ([Hunke et al., 2015](#)).

3.8 Comparison with similar models

- The profiled 1° CICE5 runs used an ice-ocean stress turning angle of 16.26° (`cosw`=0.96, `sinw`=0.28), instead of zero.
- `ice_ocean_timestep` was 1800 s and 400 s at 0.25° and 0.1° (respectively) in the profiled runs; these differ from 1350 s and 450 s in Appendix A, but are within the range of the values used in the production runs (Appendix B).

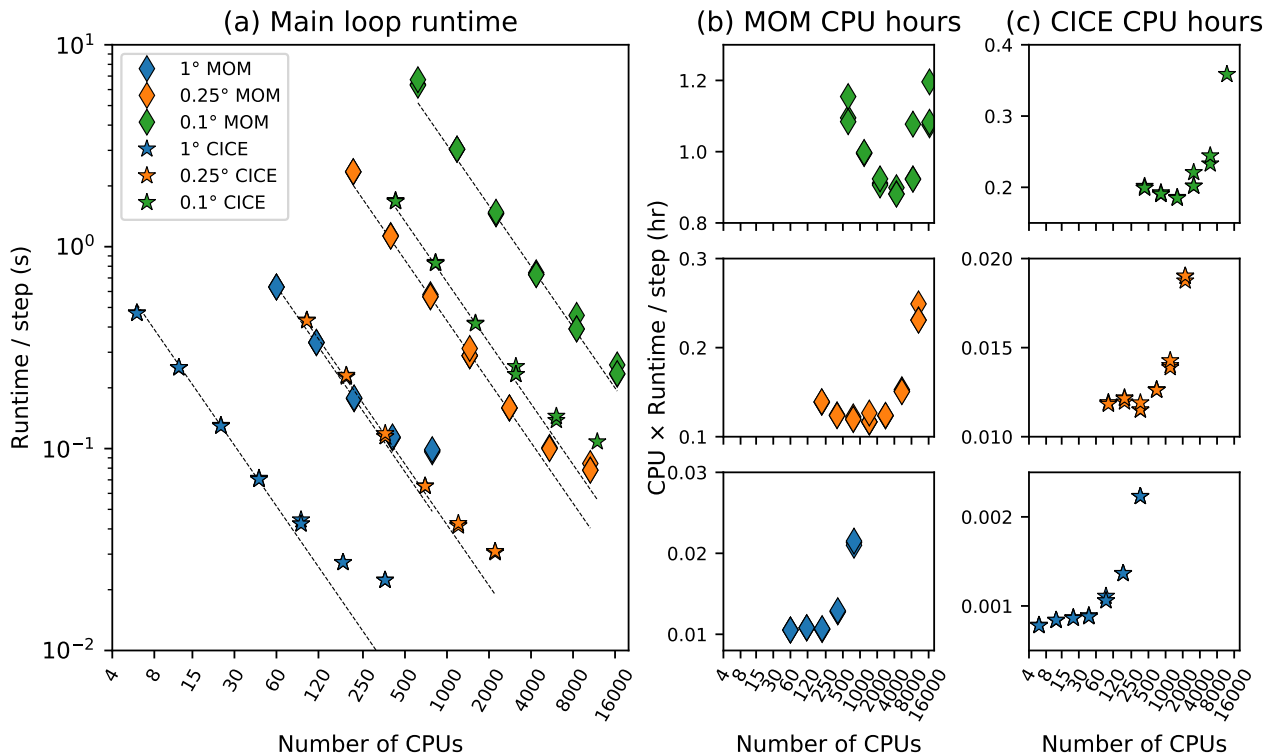


Figure 12: MOM5 and CICE5 scaling on Raijin.

3.8 Comparison with similar models

Iovino et al. (2016)

Namelists of MOM-based models are compared in Appendix F.

3.8.1 OFAM3

TODO: make the links point to the relevant appendix

ACCESS-OM2-01 MOM namelist differences from OFAM3 are shown in Appendix F.1, and Table 9 summarises differences in their grids. Also see Matt Chamberlain's email 28 May 2018.

`monin_obukhov_nml neutral` is false for OFAM2017 but true for the others.

The biharmonic Smagorinsky parameters differ. ACCESS-OM2-01 uses `k_smag_aniso`=0.0 and `k_smag_iso`=2.0, so is less viscous than the two OFAM configurations which use `k_smag_aniso`=3.0 and `k_smag_iso`=3.0, as well as background anisotropic and isotropic viscosities (set by `vel_micom_aniso` and `vel_mico_iso`). Although `vel_micom_bottom` is nonzero in the OFAM configurations, it is ignored because `bottom_5point`=false.

cf. oceanMAPS3.0 http://cosima.org.au/wp-content/uploads/2016/06/Brassington_Ocean_modelling_and_forecasting_v3.pptx.pdf

3.8 Comparison with similar models

Table 9: ACCESS-OM2 compared to ACCESS-OM and OFAM3.

| | ACCESS-OM | OFAM3 | ACCESS-OM2 |
|------------|--|---|--|
| Ocean | MOM 4.1 | MOM 4.1 | MOM 5.1 |
| Sea ice | CICE 4.1 | — | CICE 5.1 |
| Coupler | OASIS 3.25 | — | OASIS3-MCT-2 |
| Grid | global tripolar, z^* | 75°S–75°N only, z^* | global tripolar, z^* |
| Resolution | 1° , $360 \times 300 \times 50$ | 0.1° , $3600 \times 1500 \times 51$, $\Delta z = 5 - 1000$ m | 1° , $360 \times 300 \times 50$, $\Delta z = 10.0 - 334.7$ m or 0.25° , $1440 \times 1080 \times 50$, $\Delta z = 2.3 - 219.6$ m or 0.1° , $3600 \times 2700 \times 75$, $\Delta z = 1.1 - 198.4$ m |

The vertical resolution has also been improved relative to OFAM3 (Oke et al., 2013). The resolution is finer than OFAM3 at all depths other than 100–260 m, particularly at the surface and in the deep ocean, with 75 levels ranging from 1.1 m thick at the surface to 198 m thick at 5808 m (compared to 51 levels ranging from 5 m to 1000 m thick currently in OFAM3/Bluelink). Of particular relevance for coastal studies is the improved vertical resolution in the upper ocean, with 31 levels in the top 200 m and a minimum water depth of 10 m (rather than 24 levels and a minimum depth of 15 m for OFAM3), providing better resolution of shelf processes and a closer match to coastlines. Vertical spacing is optimised for resolving baroclinic modes, considerably reducing the error in their representation compared to the 51-level OFAM3 grid (Stewart et al., 2017, table 1).

Feng et al. (2016)

3.8.2 ACCESS, ACCESS-CM2, ACCESS-ESM

See Appendix F.4.

ACCESS-OM2 uses the same MOM, CICE and OASIS versions as ACCESS-CM2 (1°) Bi et al. (2016), <http://cosima.org.au/wp-content/uploads/2016/06/BI-COSIMA-Hobart-20160526.ppt.pdf>

In ACCESS-OM and ACCESS-CM2 the `ocean_sigma_transport_nml` parameters `sigma_advection_sgs_only`, `sigma_umax`, `thickness_sigma_layer`, `thickness_sigma_min`, `tracer_mix_micom` and `vel_micom` differ from the default values used in ACCESS-OM2 at 1° .

ACCESS-CM2 also uses Langmuir circulation parameterization in KPP (`do_langmuir`), which helps with getting realistic AAIW (Bi et al., 2019).

ACCESS-CM2 uses a different 50-level vertical grid from ACCESS-OM2, with 10 m spacing at the surface rather than 2.3 m.

ACCESS-CM2 code harmonised with ACCESS-OM2: <https://github.com/mom-ocean/MOM5/releases/tag/CM2-0.1>

https://www.dropbox.com/s/lktfwl3da0jpzp6/Fabio2018_Namelist_meeting_final.pdf?dl=0 section 2 shows that Rayleigh drag (see section 3.2.7) is also weaker in the Lombok and Torres Straits (longer timescale: 3600 s instead of 5400 s) in ACCESS-OM and (presumably) doesn't have any undamped cells at the bottom (unlike ACCESS-OM2 — see figure 9 (a)), since it uses the GFDL50 grid.

See <https://accessdev.nci.org.au/trac/wiki/CMIP6workshop> There's an ACCESS-CM2 report available - ask Arnold Sullivan. And data is available on NCI to members of p66 and NCI access groups

3.8 Comparison with similar models

cf. ACCESS [Bi et al. \(2013a,b\)](#); [Dix et al. \(2013\)](#). The ocean and sea ice components are essentially the same in ACCESS 1.0 and 1.3, which are based on MOM4p1 and CICE4.1 (<https://confluence.csiro.au/display/ACCESS/Home>). Also see https://accessdev.nci.org.au/trac/wiki/access/ACCESS_AMIP_testcases.

[Bi et al. \(2013b\)](#)

cf. ACCESS-ESM https://www.google.com.au/url?sa=t&rct=j&q=&esrc=s&source=web&cd=2&ved=0ahUKEwjvjsmH0rjZAhWEnpQKHb7VC-EQFgg0MAE&url=https%3A%2F%2Faccessdev.nci.org.au%2Ftrac%2Fraw-attachment%2Fwiki%2FscienceDay%2Fziehn_access_esm1.pdf&usg=A0vVaw1bYwLzey6vpy7g6v7W0aF0

3.8.3 MOM-SIS-01

cf. MOM-SIS-01 [Spence et al. \(2017\)](#) - forced by 2° CORE NYF - 75 levels; ACCESS-OM2-01 has newer bathy, CICE, JRA55-do, and probably different vertical grid

ACCESS-OM2-01 has newer forcing and bathymetry, and a different sea ice model than MOM-SIS-01 [Spence et al. \(2017\)](#).

3.8.4 GFDL CM2, CM2.5, CM2.6

cf. CM2-1deg CM2.5 CM2.6 (they were MOM v5) and discuss resolving eddies: [Griffies et al. \(2015\)](#) [Delworth et al. \(2012\)](#) [Dunne et al. \(2012\)](#) [Griffies \(2015\)](#)

cf. CORE ([Griffies et al., 2009](#)), CORE-II ([Danabasoglu et al., 2014](#))

minimum depth = 40m ?

3.8.5 UKMO GO6, GO7, GC3.0, GC3.1

cf. UKMO GO6, GO7 [Storkey et al. \(2018\)](#) - based on NEMO.

GO7 has cavities under the ice shelves, whereas GO6 is similar to ACCESS-OM2-x in having no cavities and fresh water input at the ice shelf edges.

cf. UKMO GC3.0, GC3.1 [Williams et al. \(2018\)](#)

cf. UKMO HadGEM3-GC3.1 [Ridley et al. \(2018\)](#); [Roberts et al. \(2019\)](#)

cf. UKMO Global Sea Ice 6.0 CICE configuration used in the Met Office global coupled configuration GC2.0 ([Rae et al., 2015](#))

3.8.6 RASM and others?

[Cassano et al. \(2017\)](#); [Hamman et al. \(2017\)](#); [Jin et al. \(2018\)](#); [Roberts et al. \(2018\)](#), http://www.oc.nps.edu/NAME/RASM_overview.pdf

Key RASM differences from ACCESS-OM2-01:

- `ndte`=600 (cf 120)
- `highfreq=true`
- differing pond parameters `hs0` and `rfracmax` — presumably ignored, since we don't use `short-wave='dEdd'`
- lots of differences in `shortwave_nml` — NB: we use `shortwave='default'` rather than '`dEdd`'
- differing thermo parameter `dSdt_slow_mode=-1.5e-07` (cf. `-5e-08`)

3.8 Comparison with similar models

RASM is $1/12^\circ$ but on a rotated-pole grid so the Arctic resolution is ~ 9 km (Roberts et al., 2015), considerably coarser than ACCESS-OM2-01 (Table 6).

Also RIOPS http://science.gc.ca/eic/site/063.nsf/eng/h_97632.html, GIOPS http://science.gc.ca/eic/site/063.nsf/eng/h_97631.html, https://www.godae.org/~godae-data/GOVST-VIII/presentations/5.9-GOVST8_Nov18_ScienceDay_GSmith.pdf

3.8.7 Whole Antarctic Ocean Model (formerly known as the Antarctic Tidal Ocean Model)

The Whole Antarctic Ocean Model (Richter et al., 2020) is a regional circum-Antarctic model based on ROMS. Key differences from ACCESS-OM2-01 include: circulation within cavities under ice shelves, tidal forcing, shelf melting and higher resolution (2km, 31 sigma layers). There is no sea ice model component.

4 Model evaluation

CONTRIBUTORS: Andy Hogg to coordinate

Kiss et al. (2020) present evaluations of the ACCESS-OM2 model suite; additional details are provided here.

Data from all experiments are stored on NCI in `/g/data/hh5/tmp/cosima` and can be accessed and analysed via the COSIMA Cookbook (<https://github.com/COSIMA/cosima-cookbook>). Table 2 specifies the subset of these experiments used for the comparisons in this section. Run configuration details are available on NCI in `/g/data/hh5/tmp/cosima/access-om2-run-summaries` for hh5 group members (apply for group membership if interested). Data are also publicly available at <https://doi.org/10.4225/41/5a2dc8543105a> and <https://researchdata.ands.org.au/cosima-model-output-collection/993052>. **TODO:** put data here

resolution dependence: Kirtman et al. (2012)

use obs dataset and methods from CLIVAR Repository for Evaluating Ocean Simulations? <http://www.clivar.org/clivar-panels/omdp/reos>

cf Ocean Modelling CORE-II Special Issue (Virtual) <http://www.sciencedirect.com/science/journal/14635003/vsi/10PSR6J3BV4>

OMIP - Griffies et al. (2016) - does BOM/CSIRO already have code to do this for CMIP6? ask Marsland

cf Oke et al. (2013) - reproduce some of these obs comparisons

cf http://www.cesm.ucar.edu/working_groups/Ocean/metrics.html?

cf esmvaltool <https://www.esmvaltool.org/>?

See Fanghua's observation comparison notebooks (should be on github) and also her presentation from 2018-01-25 and <https://github.com/FanghuaWu/cosima-cookbook/tree/master/notebooks>

see HighResMIP (Haarsma et al., 2016)

cf. <http://www.globcurrent.org/>?

4.1 Barotropic streamfunction

4.2 Surface current speed and variability

FIXME: we calculate magnitude of time-mean velocity which is not the same as time-mean speed. Is this what Lumpkin et al do, or should we save speed in `diag_table`?

Laurindo et al. (2017) Archer et al. (2017a,b, 2018) Wijeratne et al. (2018)

See figures 17–24.

Mean Gulf Stream separation is poor (late) at 0.25deg (Figure 24), and too variable.

Mean Gulf Stream separation is OK at 0.1deg, but separation location is too variable, occasionally separating 2-3 degrees too far north.

4.3 Deep circulation

Ollitrault and Colin de Verdière (2014)

4.4 Transports through key straits and boundary currents

See Figure 25

4.4 Transports through key straits and boundary currents

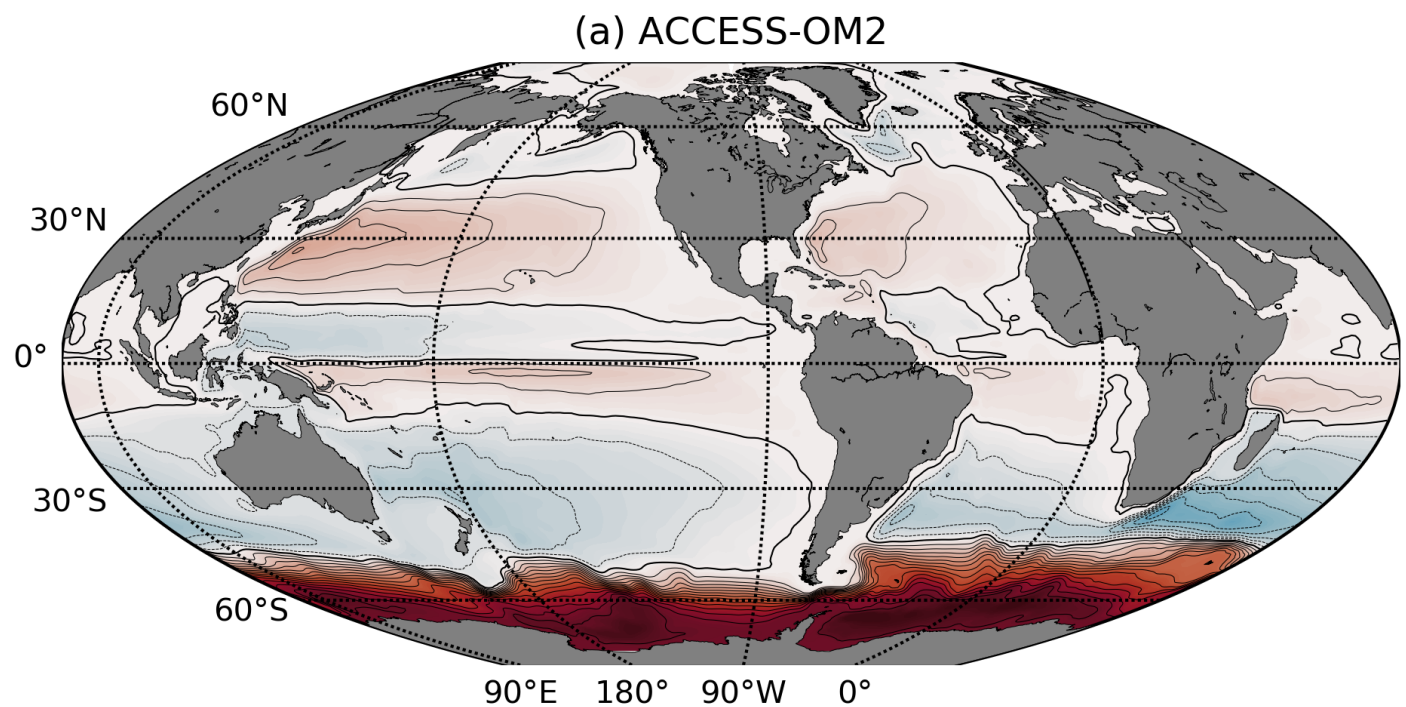


Figure 13: Global barotropic streamfunction for ACCESS-OM2 simulations. **TODO:** averaged over what years?

4.4 Transports through key straits and boundary currents

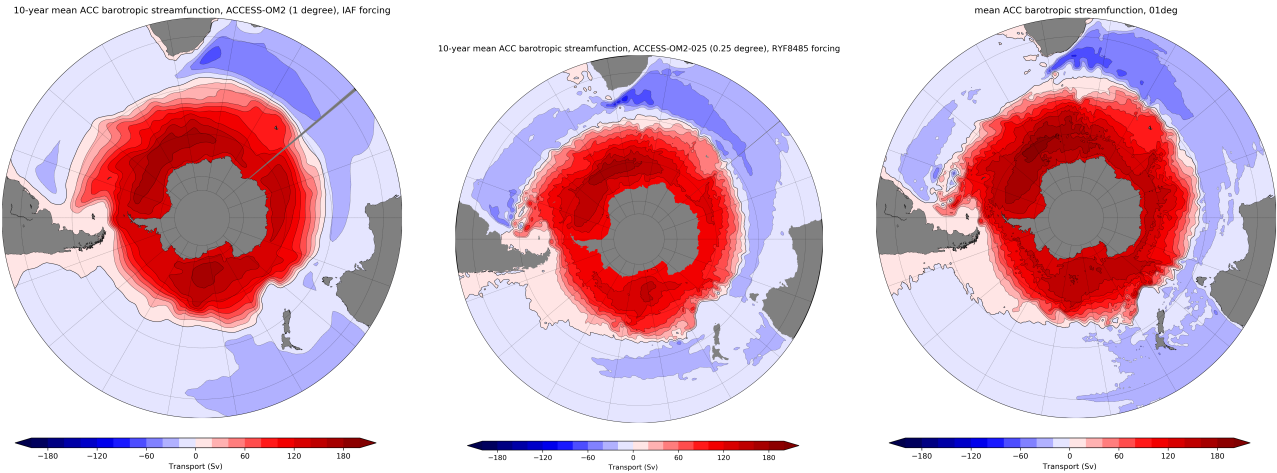


Figure 14: Antarctic Circumpolar Current barotropic streamfunction for ACCESS-OM2 simulations. **TODO:** Compare with Colin de Verdière and Ollitrault (2016) figure 9: <https://journals.ametsoc.org/na101/home/literatum/publisher/ams/journals/content/phoc/2016/15200485-46.1/jpo-d-15-0046.1/20160222/images/large/jpo-d-15-0046.1-f9.jpeg>

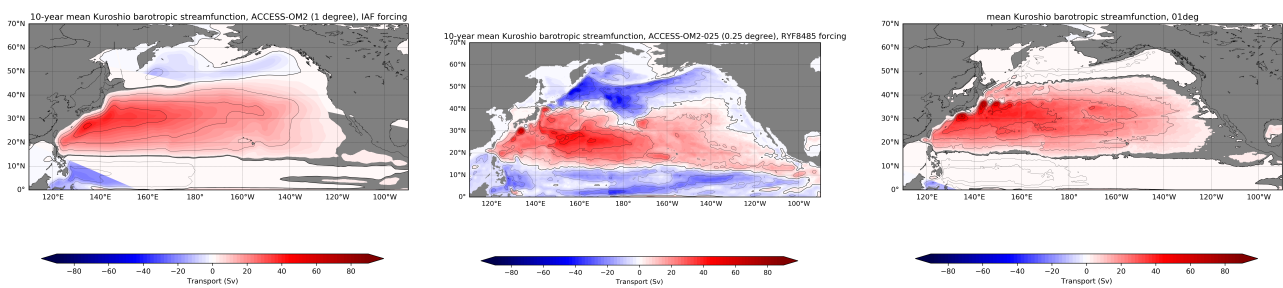


Figure 15: Kuroshio barotropic streamfunction for ACCESS-OM2 simulations. **TODO:** Compare with Colin de Verdière and Ollitrault (2016) figure 7: <https://journals.ametsoc.org/na101/home/literatum/publisher/ams/journals/content/phoc/2016/15200485-46.1/jpo-d-15-0046.1/20160222/images/large/jpo-d-15-0046.1-f7.jpeg>

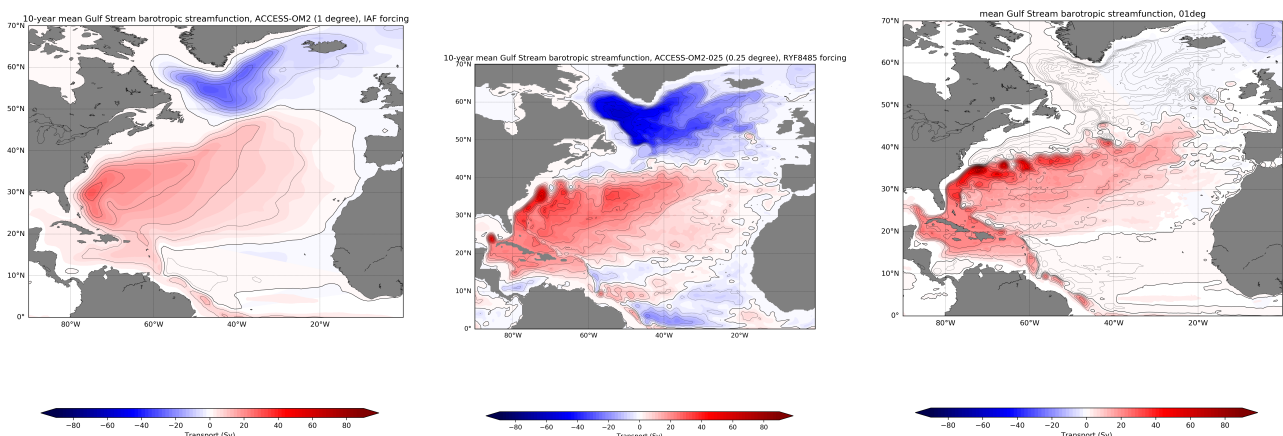


Figure 16: Gulf Stream barotropic streamfunction for ACCESS-OM2 simulations. **TODO:** Compare with Colin de Verdière and Ollitrault (2016) figure 3: <https://journals.ametsoc.org/na101/home/literatum/publisher/ams/journals/content/phoc/2016/15200485-46.1/jpo-d-15-0046.1/20160222/images/large/jpo-d-15-0046.1-f3.jpeg>

4.4 Transports through key straits and boundary currents

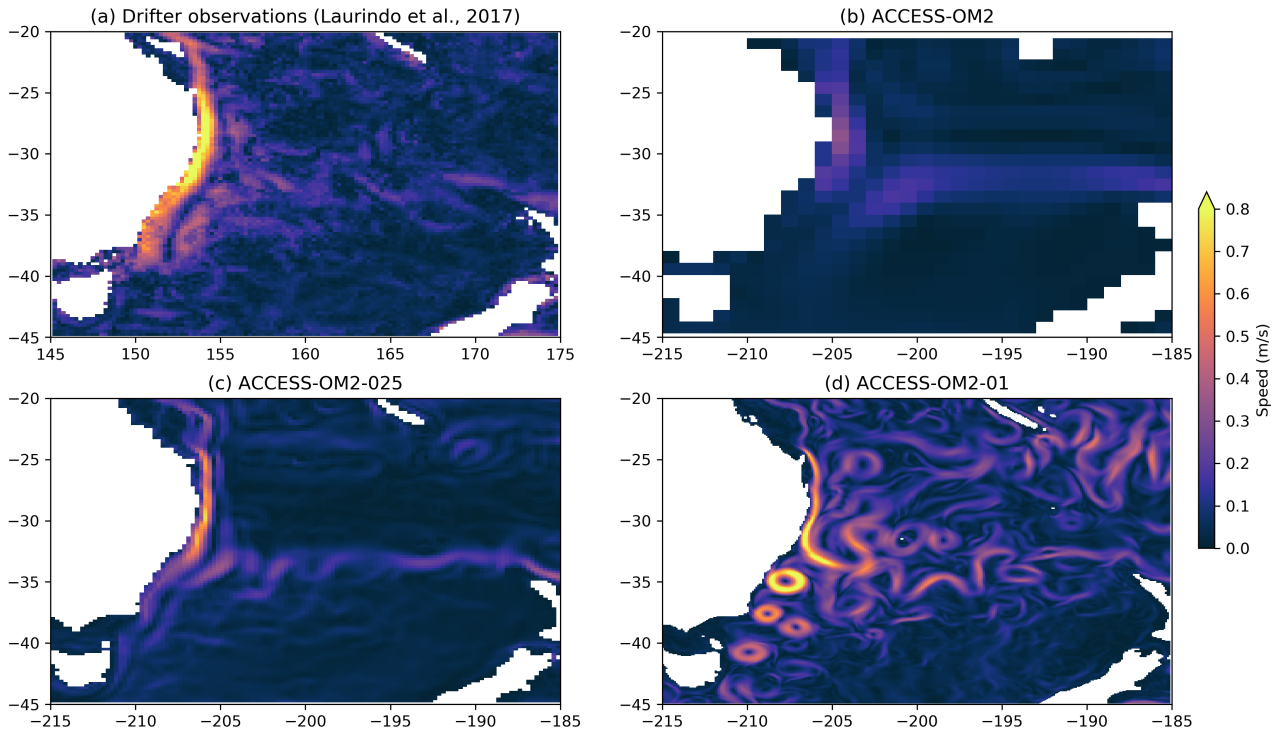


Figure 17: East Australian Current surface speed from (a) observations (1979–2015 mean from drifters at 15 m; Laurindo et al., 2017) and snapshots **FIXME: daily mean at 0.1 deg and annual mean at 0.25 and 1 deg? what date?** from ACCESS-OM2 simulations at (b) 1° resolution; (c) 0.25° resolution and (d) 0.1° resolution.

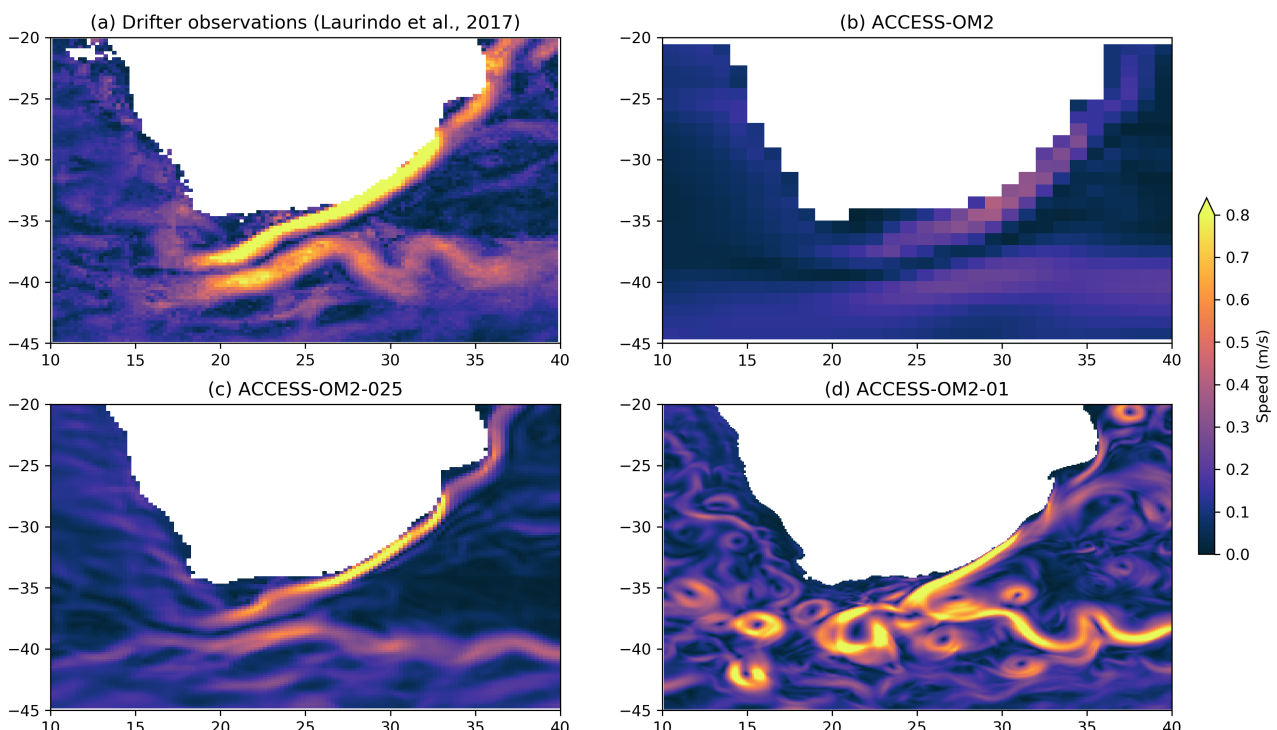


Figure 18: Agulhas Current surface speed from (a) observations (1979–2015 mean from drifters at 15 m; Laurindo et al., 2017) and snapshots **FIXME: daily mean at 0.1 deg and annual mean at 0.25 and 1 deg? what date?** from ACCESS-OM2 simulations at (b) 1° resolution; (c) 0.25° resolution and (d) 0.1° resolution.

4.4 Transports through key straits and boundary currents

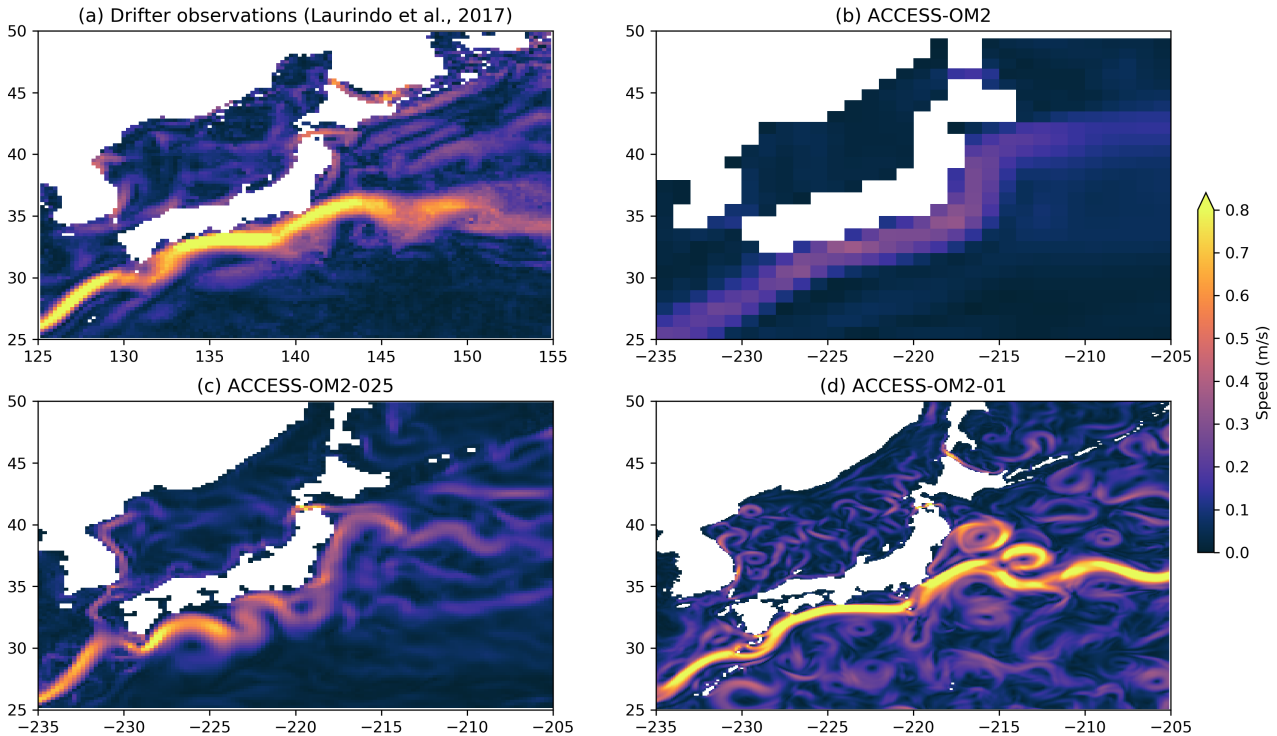


Figure 19: Kuroshio surface speed from (a) observations (1979–2015 mean from drifters at 15 m; Laurindo et al., 2017) and snapshots **FIXME: daily mean at 0.1 deg and annual mean at 0.25 and 1 deg? what date?** from ACCESS-OM2 simulations at (b) 1° resolution; (c) 0.25° resolution and (d) 0.1° resolution.

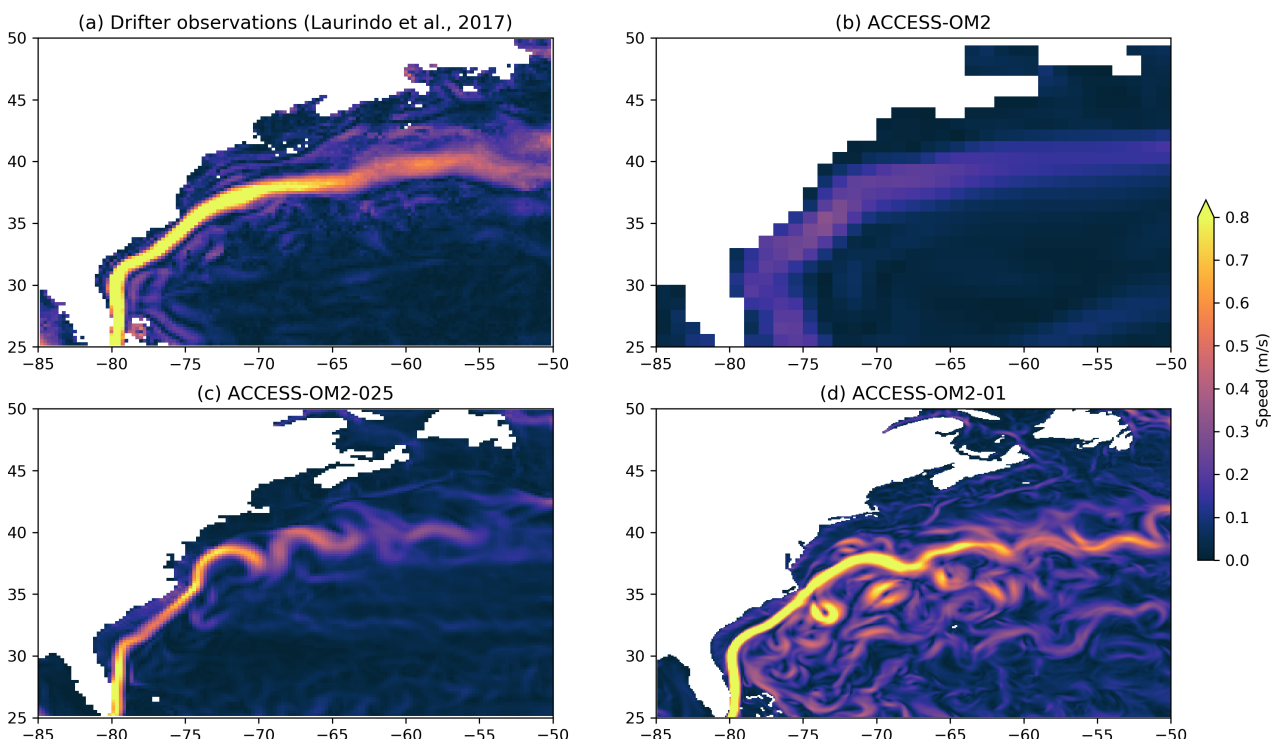


Figure 20: Gulf Stream surface speed from (a) observations (1979–2015 mean from drifters at 15 m; Laurindo et al., 2017) and snapshots **FIXME: daily mean at 0.1 deg and annual mean at 0.25 and 1 deg? what date?** from ACCESS-OM2 simulations at (b) 1° resolution; (c) 0.25° resolution and (d) 0.1° resolution.

4.4 Transports through key straits and boundary currents

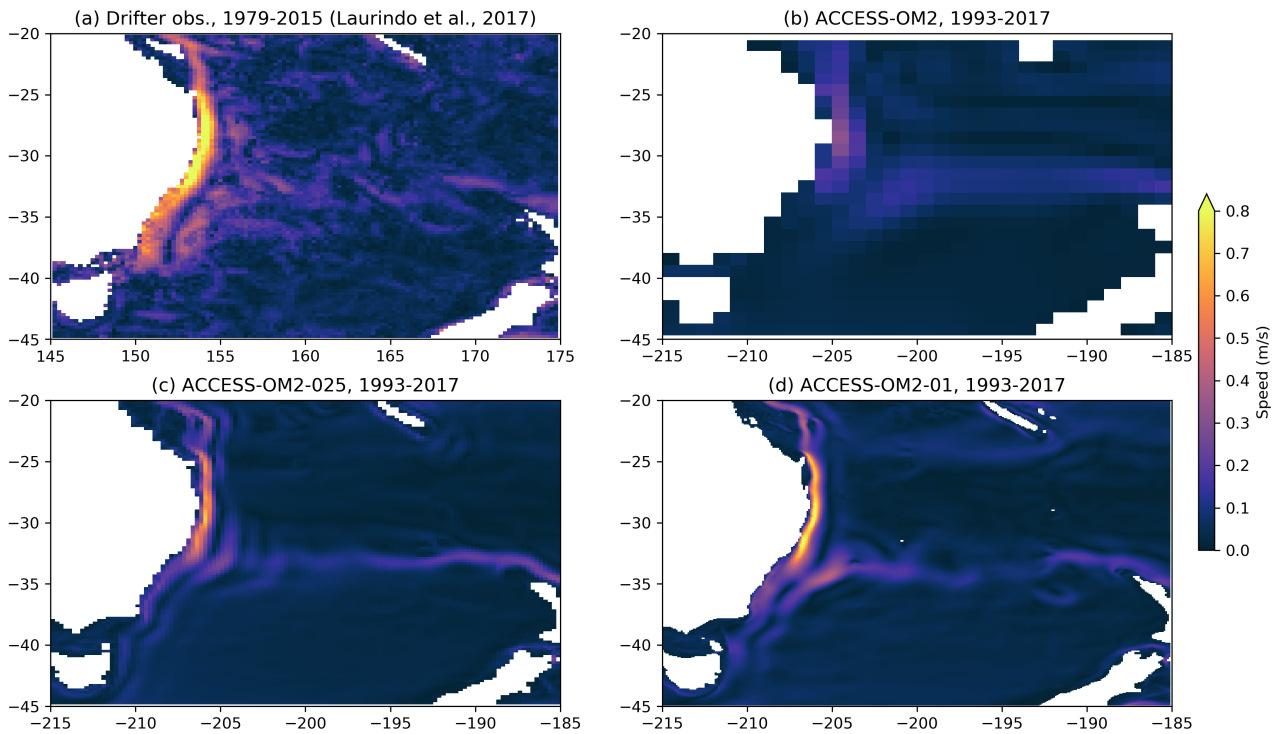


Figure 21: East Australian Current surface speed from (a) observations (1979–2015 mean from drifters at 15 m; Laurindo et al., 2017) and climatology from ACCESS-OM2 simulations at (b) 1° resolution; (c) 0.25° resolution and (d) 0.1° resolution.

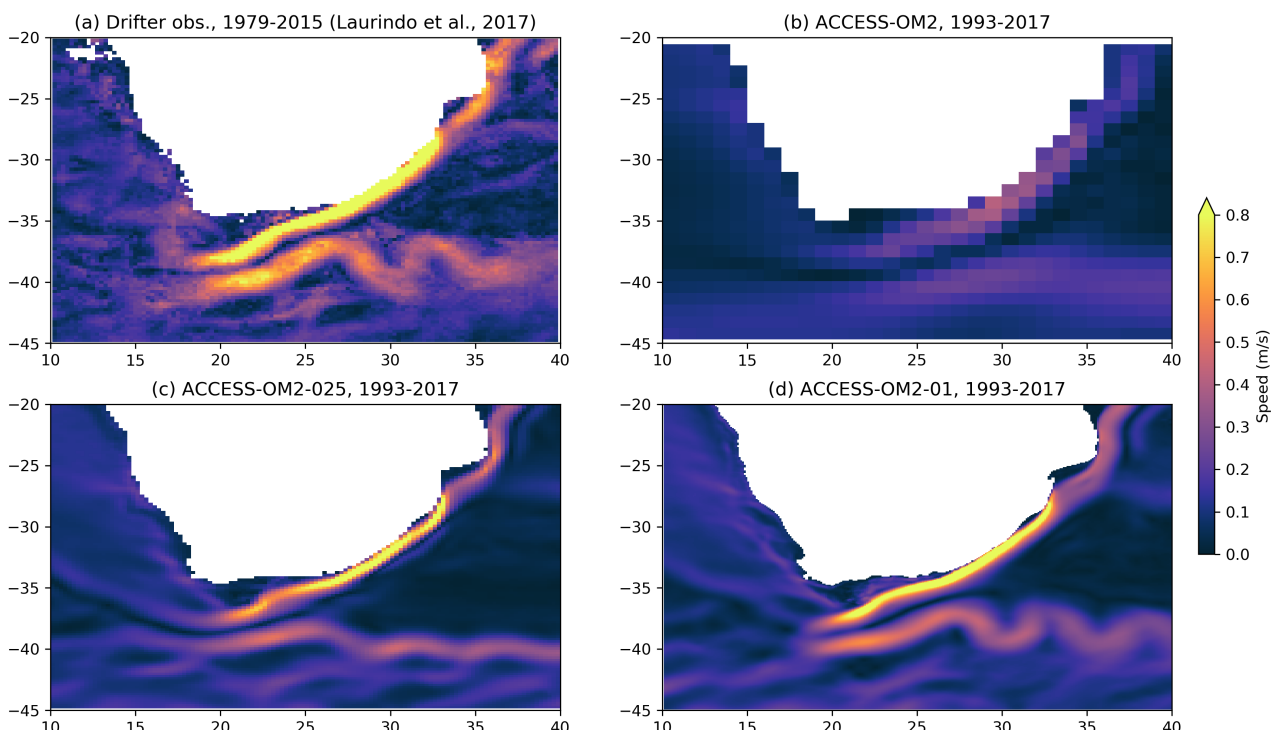


Figure 22: Agulhas Current surface speed from (a) observations (1979–2015 mean from drifters at 15 m; Laurindo et al., 2017) and climatology from ACCESS-OM2 simulations at (b) 1° resolution; (c) 0.25° resolution and (d) 0.1° resolution.

4.4 Transports through key straits and boundary currents

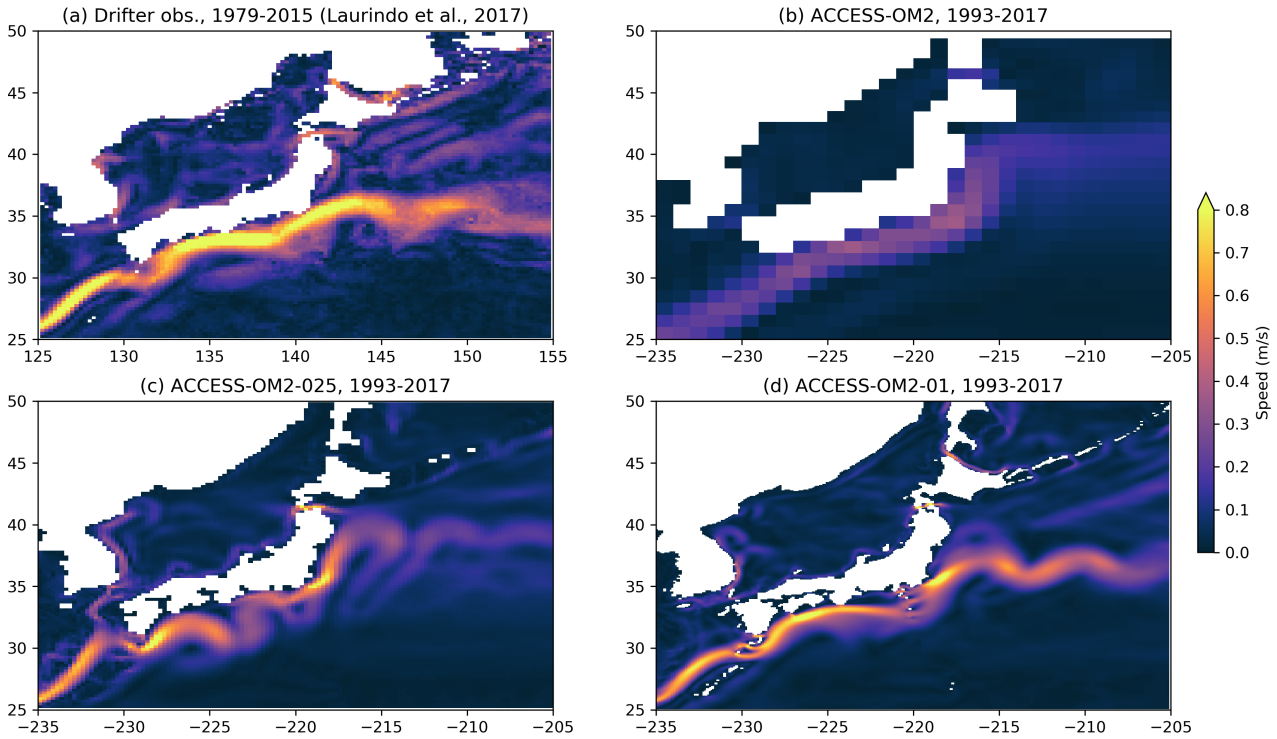


Figure 23: Kuroshio surface speed from (a) observations (1979–2015 mean from drifters at 15 m; Laurindo et al., 2017) and climatology from ACCESS-OM2 simulations at (b) 1° resolution; (c) 0.25° resolution and (d) 0.1° resolution.

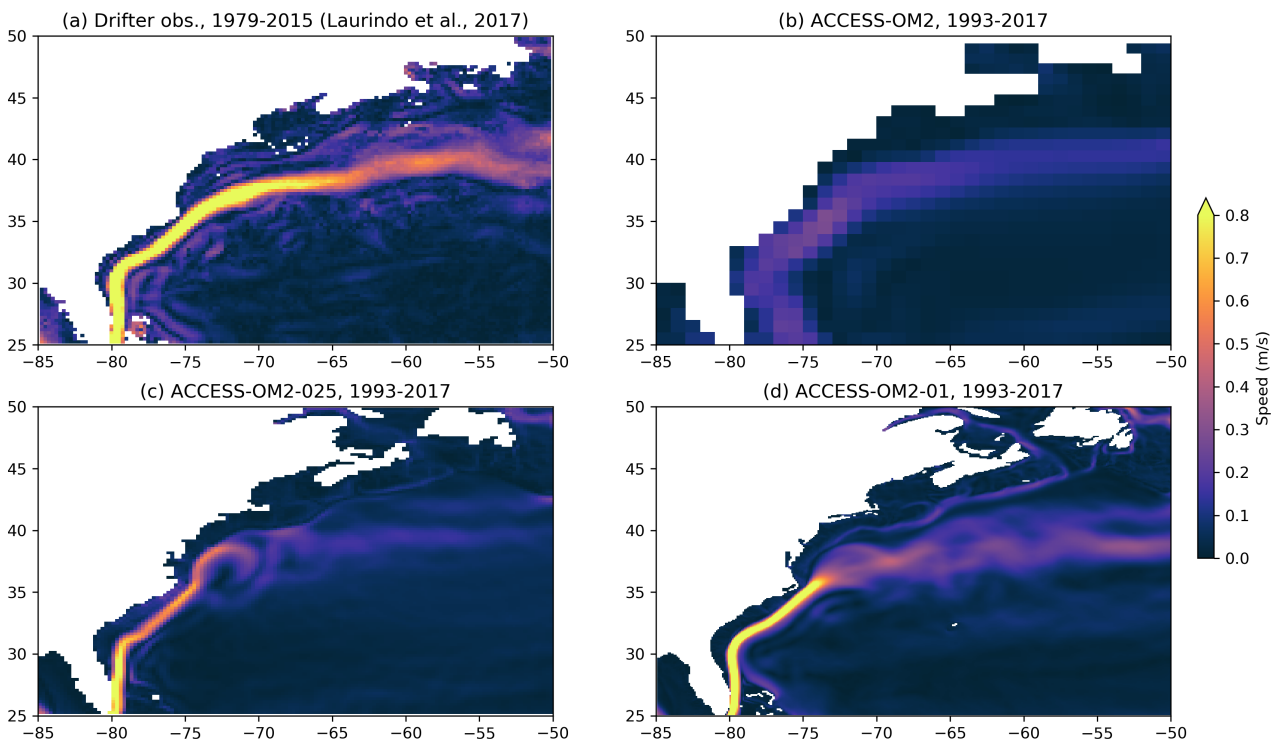


Figure 24: Gulf Stream surface speed from (a) observations (1979–2015 mean from drifters at 15 m; Laurindo et al., 2017) and climatology from ACCESS-OM2 simulations at (b) 1° resolution; (c) 0.25° resolution and (d) 0.1° resolution.

4.4 Transports through key straits and boundary currents

See Griffies et al. (2016, figure J1) for standard CMIP6/OMIP sections.

use zigzag method in tripolar region? - see appendix C4 in Griffies et al. (2016)

TODO: output vertical sections at high spatiotemporal resolution in diag_table



Figure 25: Transports through key straits. **TODO:** update **TODO:** fix Lombok, fix ranges, include 1 deg, label panels (a), (b) etc **FIXME:** meridional transports are wrong - see <https://github.com/COSIMA/ACCESS-OM2-1-025-010deg-report/issues/47>

4.4.1 ITF

TODO: See “Océane Richet - Indonesian Seas model assessment” dir

transports through straits - cf INSTANT array obs and Sprintall et al. (2009); Hautala et al. (2001)

Marsland 12 Apr 2018: ACCESS (1°) used Rayleigh drag to shift transport from westernmost to easternmost strait to match obs. Also cf. Perth-Jakarta line (XBT?)

TODO: check that water mass transformation between inflow and outflow resembles obs — may need enhanced mixing to represent the strong tidal mixing in this region (Koch-Larrouy et al., 2008a,b; Atmadipoera et al., 2009).

4.5 Equatorial current velocity and temperature structure

4.4.2 Drake Passage

CONTRIBUTORS: Andy Hogg

Drake passage transport is about 135 Sv at 0.1° resolution and about 105 Sv 0.25° (see Figure 25),
TODO: keep these up to date significantly below the observed values of 173.3 Sv (Donohue et al., 2016) and 175 Sv (Colin de Verdière and Ollitrault, 2016).

ACC transport is increased by spurious deep convection (Cheon et al., 2014; Martin et al., 2012)—so perhaps the reduced DP transport at 0.1deg is related to reduced spurious deep convection?

4.5 Equatorial current velocity and temperature structure

CONTRIBUTORS: Ryan Holmes

See Figure 26.

cf. TOGA?

4.6 Overturning

The overturning circulation on density surfaces for all three resolutions is shown in Fig. 27. This figure ...

Farneti et al. (2015)

Lumpkin and Speer (2007)

Talley (2013)

4.7 Meridional heat transport

CONTRIBUTORS: Ryan Holmes, Adele Morrison

AMOC: do transect at 26.5N to cf RAPID array <http://www.rapid.ac.uk/rapidmoc/> Smeed et al. (2018)

Could also split AMOC into western and eastern components for comparison on OSNAP (Lozier et al., 2017, 2019; Holliday et al., 2018). Data: <https://www.o-snap.org>

AMOC reviews: Zhang et al. (2019), Frajka-Williams et al. (2019) and Hirschi et al. (2019).

Caesar et al. (2018); Böning et al. (2016); Rahmstorf et al. (2015)

cf. Newsom et al. (2016)? But this is just another model analysis?

Could also compare to reanalysis products, as done in Griffies et al. (2015), Figure 7. Ganachaud and Wunsch (2003) is another obs estimate to compare with.

4.8 Model bias assessments

Minimal model bias important for BOM for data assimilation in oceanMAPS, but is difficult to assess with repeat-year forcing as the mean of RYF is not climatology, so after many repeats of RYF the slowly-adjusting ocean features will match neither climatology nor the state in the repeat year, even if the model itself is unbiased.

cf BRAN

cf Kerry et al. (2016)

4.8 Model bias assessments

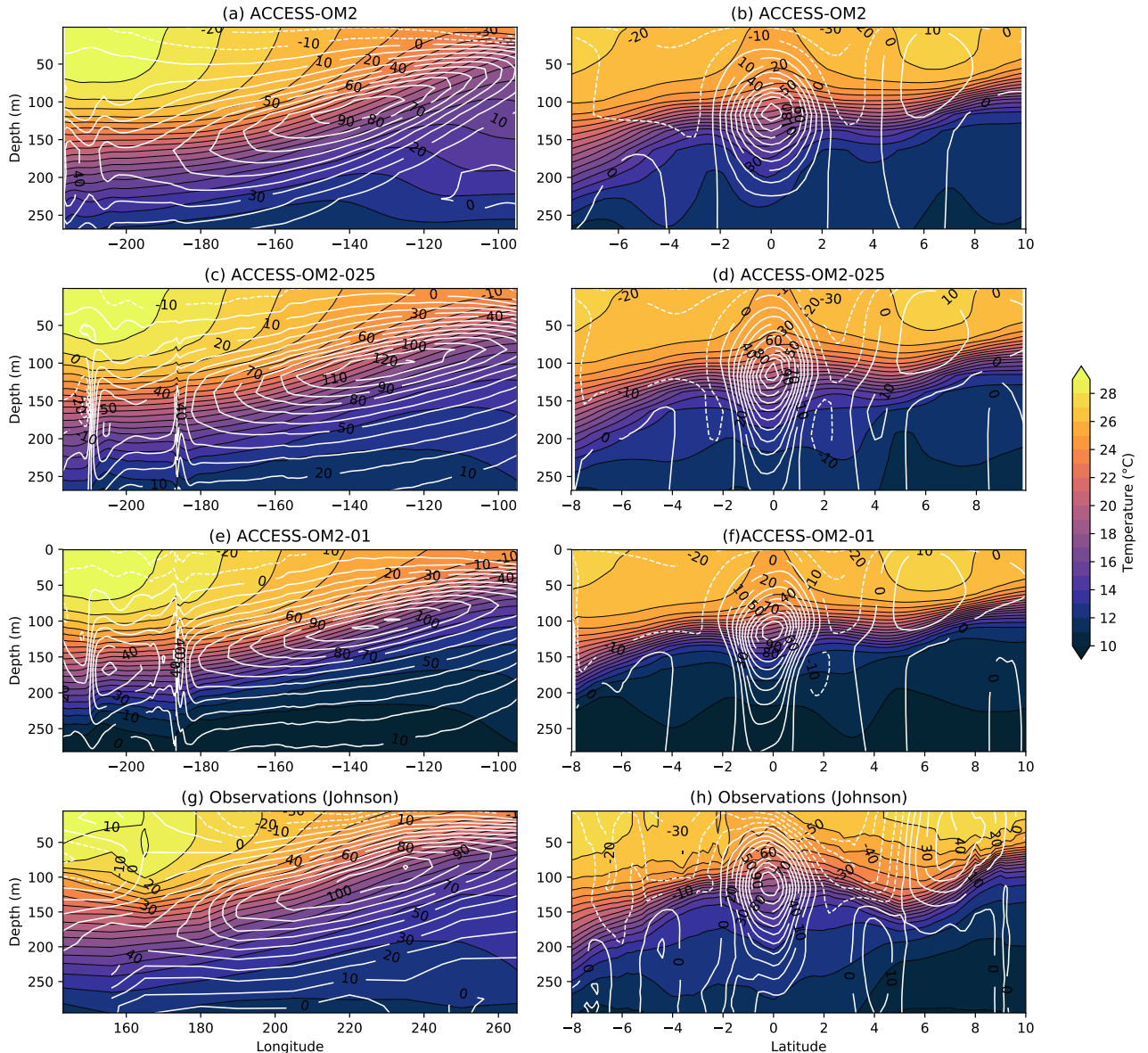


Figure 26: Transects in the upper equatorial Pacific versus longitude at the Equator (left) and versus latitude at 220°E (right) for the model configurations **TODO: averaged over which years?** and observations from **Johnson et al. (2002)** **TODO: averaged over which years?** **TODO: check this is the correct reference.** Colours show temperature in °C and white contours with black labels are eastward velocity isolachs (in cm s^{-1} ; westward contours are dashed).

4.9 Water mass properties and structure

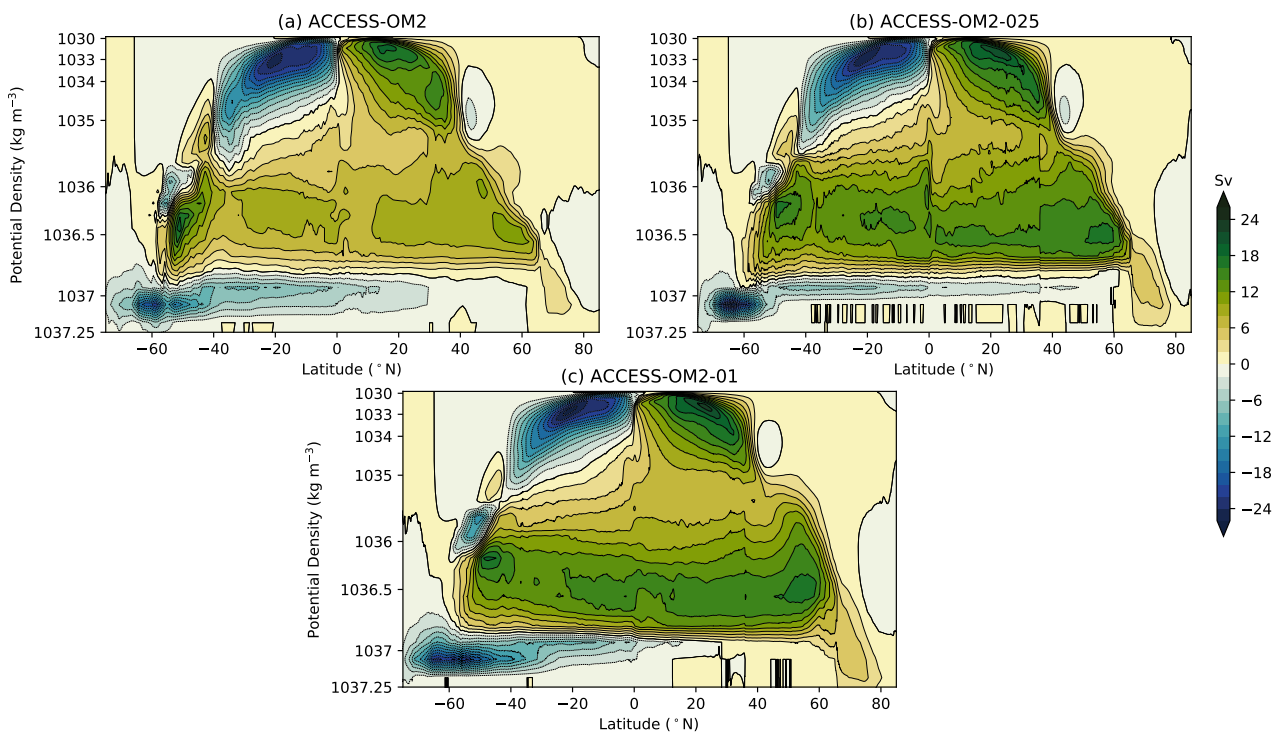


Figure 27: Global overturning circulation on density surfaces (σ_2) for ACCESS-OM2 simulations at (a) 1° resolution; (b) 0.25° resolution and (c) 0.1° resolution.

4.9 Water mass properties and structure

CONTRIBUTORS: Adele Morrison

4.10 Mixed layer depth (MLD)

TODO: cf. MLD obs from Holte et al. (2017); Schmidtko et al. (2013); de Boyer Montégut et al. (2004)? **TODO:** plot MLD and check to see that consistent definitions are used - see notebooks that compare model with IFREMER and MILA_GPV obs The mld diagnostic is mixed layer depth determined by density criteria. It is the depth at which the buoyancy exceeds the surface buoyancy by more than the default buoyancy criterion `buoyancy_crit`= 0.0003 ms^{-2} . Since buoyancy is $g\Delta\sigma/\rho$, this very nearly identical to the $\Delta\sigma = 0.03\text{ kgm}^{-3}$ density criterion used by Sallée et al. (2013) and advocated by Downes et al. (2009); Sallée et al. (2006) and de Boyer Montégut et al. (2004).

CMIP5 models tend to underestimate winter MLD (Sallée et al., 2013).

Full-depth convection in the Antarctic has been observed only once, in the 1974–6 Weddell Polynya (Gordon, 1978). Otherwise, Antarctic MLD is shallower than 1000 m (Schmidtko et al., 2013). All 3 resolutions display regions of anomalously deep (often full-depth) convection. This covers large areas in the eastern Weddell Sea and western Ross Sea every winter and spring in the 1° and 0.25° simulations, but is much reduced in the 0.1° simulation, and confined to a much smaller region in the northwest Weddell Sea, with significant interannual variability.

The behaviour of the two coarser models is typical of CMIP5 models, which produce bottom water by spurious deep-ocean convection rather than down-slope flows (Heuzé et al., 2013, 2015).

Connection to polynyas: see Goosse and Fichefet (2001); Heuzé et al. (2015); Kjellsson et al. (2015), section 4.15.7.

see Uotila et al. (2019)

use Argo data

4.11 Heat conservation, bias and drift

and MEOP southern ocean seal data <http://www.meop.net>?

4.10.1 T/S diagrams

4.10.2 Deep water formation / transformation rates, locations, properties

[Farneti et al. \(2015\)](#) [Abernathay et al. \(2016\)](#) [Downes et al. \(2011\)](#) [Pelichero et al. \(2018\)](#)

4.11 Heat conservation, bias and drift

CONTRIBUTORS: [Chris Chapman](#), [Ryan Holmes](#)

use XBT data from Chris Chapman?

cf FAFMIP? [Gregory et al. \(2016\)](#)

4.11.1 SST bias

WOA13v2 0.25-degree Arctic SST has spurious steps - see <https://github.com/COSIMA/access-om2/issues/103>

new sst obs datasets: see Pilo email 2018-11-05

cf. SSTARS ([Wijffels et al., 2018](#)), available via <https://portalaodn.org.au/>?

Daily 0.25 deg JMA MGDSST Reanalysis and Real Time MGDSST Analysis: 1982 - present https://www.data.jma.go.jp/gmd/goos/data/pub/JMA-product/mgd_sst_glb_D Canadian Meteorological Centre's (CMC) 0.2 degree SST analysis: 1991–2017: <https://podaac.jpl.nasa.gov/dataset/CMC0.2deg-CMC-L4-GLOB-v2.0> Canadian Meteorological Centre's (CMC) 0.1 degree SST analysis: 2016 - present: <https://podaac.jpl.nasa.gov/dataset/CMC0.1deg-CMC-L4-GLOB-v3.0?ids=&values=&search=CMC> For assessment and validation of these analyses, see [Fiedler et al. \(2019\)](#).

4.11.2 lat/depth T sections and bias

4.11.3 Drift: depth/time T hovmollers

4.11.4 zonally averaged surface heat flux terms

4.12 Salt conservation, bias and drift

cf FAFMIP? [Gregory et al. \(2016\)](#)

4.12.1 SSS bias

WOA13v2 0.25-degree Arctic SSS has spurious steps - see <https://github.com/COSIMA/access-om2/issues/103>

4.13 Variability

4.12.2 lat/depth S sections and bias

4.12.3 Drift: depth/time S hovmollers

4.12.4 zonally averaged surface salt/freshwater flux terms

4.12.5 Variation of ocean volume

Over a 60-year forcing cycle the global mean SSH increases by about 3.5 cm and the global mean salinity falls by about 0.0002 psu (figure 28). This is due to ocean-ice mass exchange, as P-E+R is constrained to be zero (section 3.5.2). The 3.5 cm SSH change represents an increase in ocean volume of about $1.26 \times 10^{13} \text{ m}^3$. This is in close agreement with a roughly $1.3 \times 10^{13} \text{ m}^3$ sea ice decline over 40 years (Figure 35).

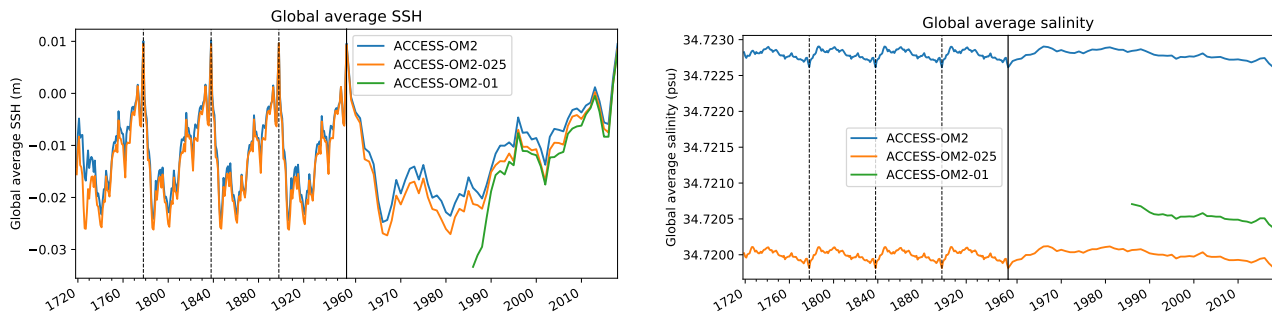


Figure 28: Global mean sea surface height (left) and salinity (right) for the 3 runs.

4.13 Variability

Danabasoglu et al. (2016)

4.13.1 Western boundary current variability

4.13.2 EKE spatial distribution and wavenumber spectrum

EKE near 1000dbar: Ollitrault and Colin de Verdière (2014)

also check EKE spectrum to see if it follows the expected slope - eg Capet et al. (2008)

cf. SSH spectrum obs: Xu and Fu (2011, 2012)

Scott Bachman recommends 2D Laplacian Leith (or his new QG Leith, currently being tested in MOM 6) over Smagorinsky, as Smagorinsky over-damps the fine scales. However Leith is not implemented in MOM5. O'Kane finds good agreement between 0.25 and 0.1 deg despite using Smag biharmonic

See Errico (1985); Durran et al. (2017)

4.14 Sea level

Griffies et al. (2014)

4.15 Sea ice

Year of Polar Prediction (YOPP) data portal: <https://yopp.met.no>, e.g. http://thredds.met.no/thredds/fou-hi/arctic20km.html?dataset=arctic20km_24h_be

discuss linear kinematic features (leads): [Hutchings et al. \(2005\)](#); [Wang et al. \(2016a\)](#); [Wang and Wang \(2009\)](#); [Losch et al. \(2014\)](#); [Hutter et al. \(2018\)](#). These are too fine to be resolved by the large footprint of the SSM/I and SSMIS passive microwave sensors ([Lemieux et al., 2015](#)). But can be detected in ice drift <http://rkwok.jpl.nasa.gov/envisat/index.html> ([Hutter et al., 2018](#)).

See [Uotila et al. \(2013\)](#)

see [Smith et al. \(2015\)](#)

see <https://medium.com/pangeo/polar-deployment-of-pangeo-96865774287c>

see [Schroeter et al. \(2018\)](#); [Barthélemy et al. \(2017\)](#); [Uotila et al. \(2017\)](#); [Schweiger et al. \(2011\)](#)

see [Vaughan et al. \(2013\)](#); [Flato et al. \(2013\)](#); [Dorn et al. \(2018\)](#)

problems comparing models to obs: [Notz et al. \(2013\)](#)

see [Naughten \(2018\)](#); [Naughten et al. \(2018\)](#)

see [NAS \(2017\)](#), [Hobbs et al. \(2016\)](#); [Uotila et al. \(2019\)](#)

special issue: [https://agupubs.onlinelibrary.wiley.com/doi/toc/10.1002/\(ISSN\)2169-9291.NICE1](https://agupubs.onlinelibrary.wiley.com/doi/toc/10.1002/(ISSN)2169-9291.NICE1)

see Kial's RYF sea ice assessment at 1deg

cf. ACCESS-OM ([Uotila et al., 2012, 2013](#))

wavy ice features in 0.25deg — poor EVP convergence? <https://github.com/COSIMA/access-om2/issues/87>

Too much ice south of Svalbard in 0.10deg — **TODO:** check Gulf Stream in 0.1deg – is it carrying heat far enough north?

TODO: put probe points at narrowest point of northern Nares Str between Greenland and Ellesmere - compare ice export to [Kwok et al. \(2010\)](#)

TODO: summary plot of sea ice extent min and max contours for the 3 models and obs in NH and SH

We have quite thick ice in small, isolated locations in some Arctic embayments (up to about 22m **TODO: check**) but at least it's not hundreds of metres as in [Delworth et al. \(2012\)](#).

Reanalyses for possible comparison with model (from Helen Beggs' email 21 Mar 2018):

- Reanalyses of sea ice observations: The OSI-SAF reanalysis is available in 10 km resolution from: <http://osisaf.met.no/p/ice/index.html#conc-reproc> It covers the period from 1978 to 2009 with consistent algorithm processing. PUM and validation reports are available at the website as well. OSI-SAF Daily sea ice concentration analyses are being ingested into the new Decadal OFAM Climate Model by Sakov and Sandery.
- <http://osisaf.met.no>: ice concentration, edge, drift and emissivity on both hemispheres, as well as climate consistent time series
- Bremen/Hamburg University and their AMSR2 based products
- NCEP (Bob Grumbine), <http://polar.ncep.noaa.gov/seacie/> - BoM uses NCEP 1/12° Daily Global Sea Ice Analyses as operational inputs into their SST analyses, used as the boundary condition to the NWP models

<http://psc.apLuw.edu/research/projects/arctic-sea-ice-volume-anomaly/>

TODO: check: are there katabatic winds in JRA55? if not, does this explain our lack of coastal polynyas? see [Zhang et al.](#)

4.15 Sea ice

(2015); Stössel et al. (2011) **TODO:** Alex Fraser suggestion at AUV workshop: check formation rate – is it just thin frazil in the model, so we actually do have coastal polynyas? could also look at category 1 ice thickness

see Ice_Validation_ACCESS-OM2-01.ipynb https://github.com/aeckiss/cosima-cookbook/blob/master/notebooks/Ice_Validation_ACCESS-OM2-01.ipynb uses data from <http://nsidc.org>

see SIMIP Notz et al. (2016)

see Toyota and Kimura (2018) - plastic rheology applies in MIZ

and check convergence Bouillon et al. (2013); Kimmritz et al. (2015); Losch and Danilov (2012); Lemieux and Tremblay (2009)

Wang et al. (2016b)

Downes et al. (2015)

cf Heil et al. (2011) **ISSUE 3**

4.15.1 Seasonal cycle of extent and area

ISSUE 1 ISSUE 2

We adopt the usual definition of sea ice extent as the area in which sea ice concentration exceeds 15%.

See Figures 33 and 34. **FIXME:** land mask area differs between the three configurations (figure 4) and differs from obs, especially in the Canadian Archipelago and River Ob - how to remove this bias in the total extent, area and volume?

Note that there are significant differences between passive microwave observational products (Ivanova et al., 2015; Roach et al., 2018; Meier et al., 2014) and <https://nsidc.org/support/faq/what-difference-between-nasa-team-algorithm-and-fritzner-2018> use both methods: Bootstrap primarily for observations with low SIC, and Bristol for high SIC. Sea ice extent is generally consistent, but sea ice area or concentration distributions differ significantly and this should be taken into account when assessing model performance (Roach et al., 2018). NAS (2017): “ As a general rule of thumb, said Dr. Massom, overall accuracies in ice concentration retrieval ranging from $\pm 5\%$ to $\pm 15\%$ are expected. Errors are largest in summer, over regions of predominantly thin/new ice, and year round in the marginal ice zone (MIZ) (up to $\pm 30\%$) (Brucker et al., 2014; Comiso et al., 2011). ”

NOAA/NSIDC Climate Data Record of Passive Microwave Sea Ice Concentration, Version 3 Meier et al. (2017); Peng et al. (2013), <http://nsidc.org/data/G02202> This has a nominal resolution of 25 km, considerably coarser than both the 0.25° and 0.1° models (Table 6). Leads are too fine to be resolved by the large footprint of the SSM/I and SSMIS passive microwave sensors (Lemieux et al., 2015).

TODO: show March and Sept ice concentration vs. obs obs: 1988–1997 climatology from NOAA/NSIDC Climate Data Record of Passive Microwave Sea Ice Concentration, v3

Sea Ice Index, Version 3 (Fetterer et al., 2017, updated daily, <http://nsidc.org/data/g02135>).

See Figure 35: the growth of Arctic ice volume is due to increasing category 5, presumably due to ridging. We use `kcatbound=0`, so lower bound of ice categories is 0, 0.64, 1.39, 2.47, 4.57m (Hunke et al., 2015, table 2). So by year 9 most of the ice volume (not area) is more than 4.57m thick, including in the summer minimum.

thickness: http://psc.apl.uw.edu/sea_ice_cdr/

We capture the 2016 decline in Antarctic sea ice extent (Meehl et al., 2019; Wang et al., 2019).

4.15.2 Sea ice thickness and volume

TODO: also plot snow thickness timeseries hs

4.15 Sea ice

TODO: maps of summer and winter mean snow thickness

cf. IceSat data 2003–2008 ([Kurtz and Markus, 2012](#))

Compare thickness with cryosat data? - from late 2010 onwards <http://science-pds.cryosat.esa.int> Schröder et al. (2019)

Or GIOMAS (see [Uotila et al., 2013](#))? - though this is output from a data-assimilated model ([Zhang and Rothrock, 2003](#)) at about 1 degree resolution, monthly data from 1/1979 to present http://psc.apl.washington.edu/zhang/Global_seaice/model.html and <http://psc.apl.uw.edu/data/global-sea-ice-giomas-data-sets/> Or [Worby et al. \(2008\)](#)? Or [Kwok and Cunningham \(2008\)](#)? or [Kwok and Rothrock \(2009\)](#)? or [Kwok \(2018\)](#)?

See Petra email 2018-11-26: Ron Kwok's data

or PIOMAS? [Schweiger et al. \(2011\)](#), from <ftp://pscftp.apl.washington.edu/zhang/PIOMAS/data/v2.1/>, used by [Ridley et al. \(2018\)](#) and others

Axel's APL Zice Arctic climate record http://psc.apl.uw.edu/sea_ice_cdr/data_tables.html

TODO: include maps of monthly mean concentration bias relative to passive microwave at the 3 resolutions: Sept and March in NH, Feb and Sept in SH

Sea ice extent — see [Ivanova et al. \(2016\)](#)

4.15.3 Age

4.15.4 Formation rate

ice production rate in coastal polynyas ([Tamura et al., 2008; Tamura and Ohshima, 2011; Tamura et al., 2016; Nihashi and Ohshima, 2015; Ohshima et al., 2016](#)) - see Adele's email 9 Mar 2018 - includes a script and netcdf version. Looks like you can download the data set here: <http://www.lowtem.hokudai.ac.jp/wwwod/polar-seaflux/> what diagnostics give us production in CICE? f_congel gives basal growth – not relevant? meltb, meltl,melts, meltt? frazil?

See [Pelichero et al. \(2018\)](#)

4.15.5 Drift

cf. Kimura ice motion dataset - 60km Petra is getting a 30km dataset

[Giles et al. \(2011\)](#) [Sumata et al. \(2014, 2015b,a\)](#); [Szanyi et al. \(2016\)](#) [Kwok et al. \(2017\)](#)

4.15.6 Ice deformation

cf. [Hutchings et al. \(2011\)](#)

scaling - see [Hutter et al. \(2018\)](#), [Girard et al. \(2009\)](#) and reviews by [Weiss \(2003, 2017\); Weiss and Dansereau \(2017\)](#)

4.15.7 Polynyas

How good are katabatic winds in JRA55? cf. polar WRF?

[Morales Maqueda \(2004\)](#) review polynya observations and dynamics.

[Uotila et al. \(2013\)](#) [Kwok et al. \(2008\)](#)

Polynyas are occasionally seen at 1° in the monthly mean sea ice thickness near Maud Rise but they don't persist from year to year. No open-ocean polynyas are seen in the Weddell or Ross Seas

4.15 Sea ice

at 0.25° in Sept in any year in the final cycle—so occurrence is less than observed, not more. No open-ocean polynyas are seen in Weddell or Ross Seas at 0.1° in September.

[Dufour et al. \(2017\)](#) see quasi-continuous deep convection at 0.25° but no polynyas

Also see section [4.10](#).

4.15 Sea ice

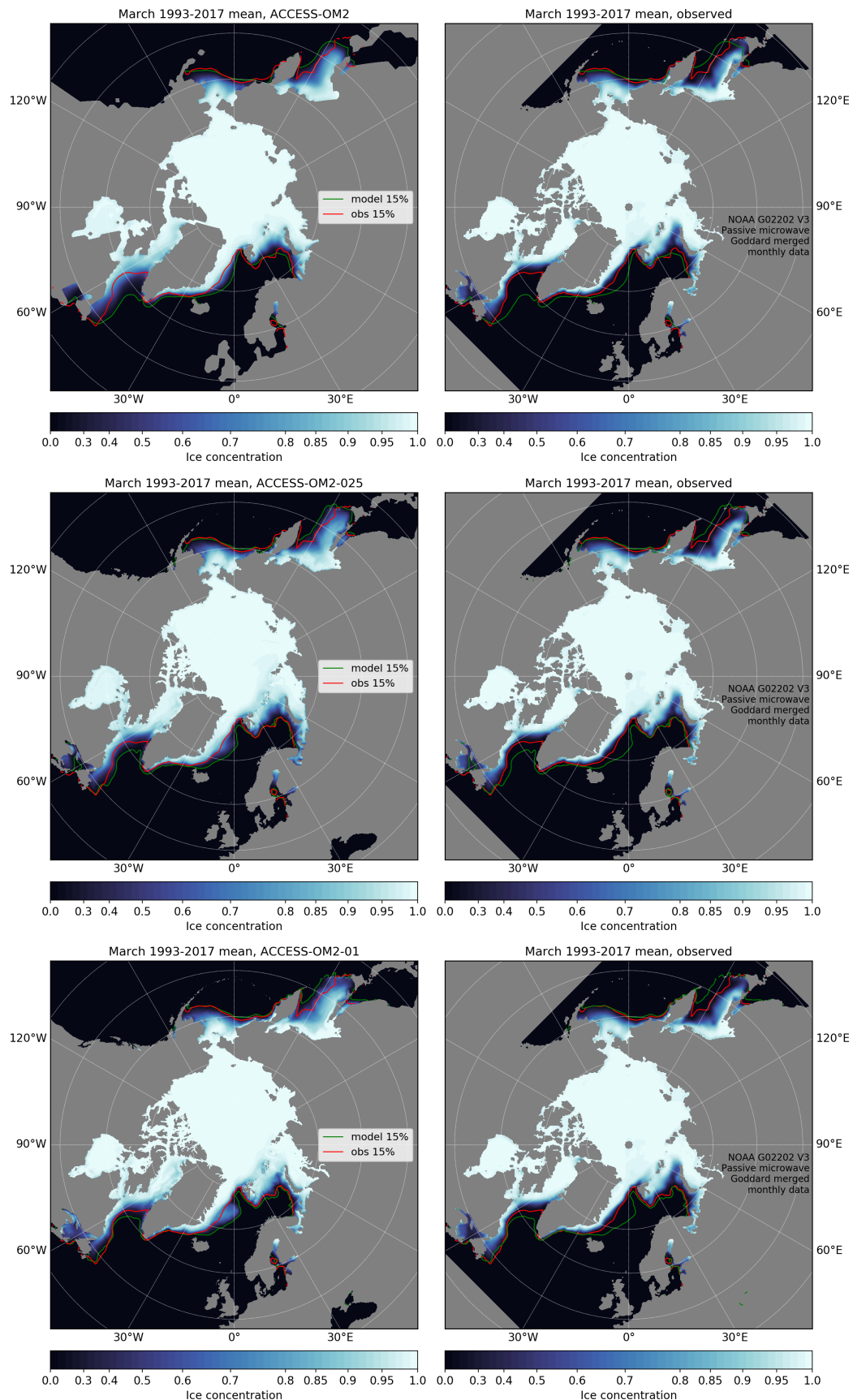


Figure 29: Arctic sea ice concentration from the ACCESS-OM2 suite (left) and passive microwave (right), March mean. Green (red) line is the 15% concentration contour in the model (observations). The scale is nonlinear to highlight differences at high concentrations. **TODO:** make this more compact - no need to repeat obs 3 times

4.15 Sea ice

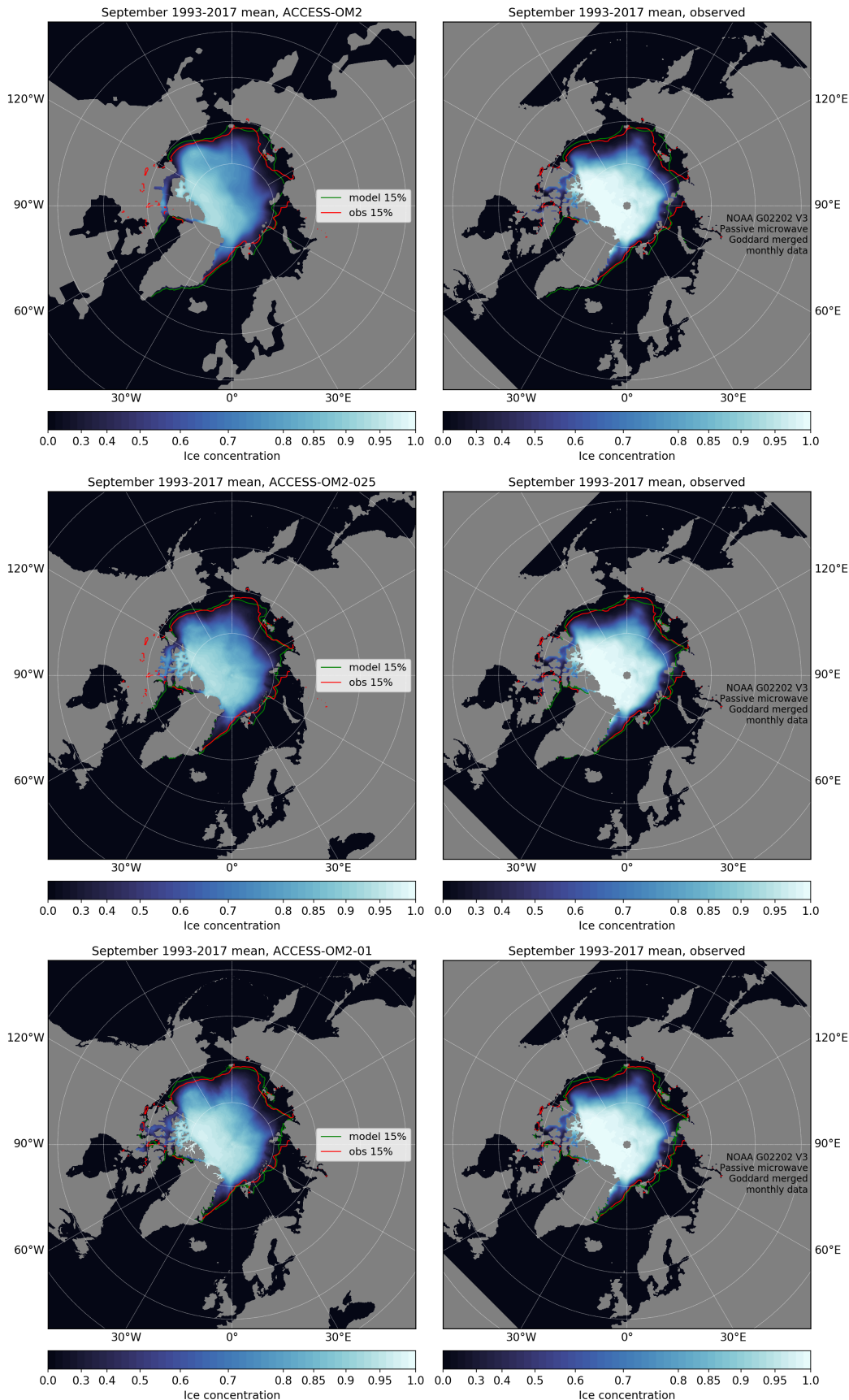


Figure 30: Arctic sea ice concentration from the ACCESS-OM2 suite (left) and passive microwave (right), September mean. Green (red) line is the 15% concentration contour in the model (observations). The scale is nonlinear to highlight differences at high concentrations. **TODO:** make this more compact - no need to repeat obs 3 times

4.15 Sea ice

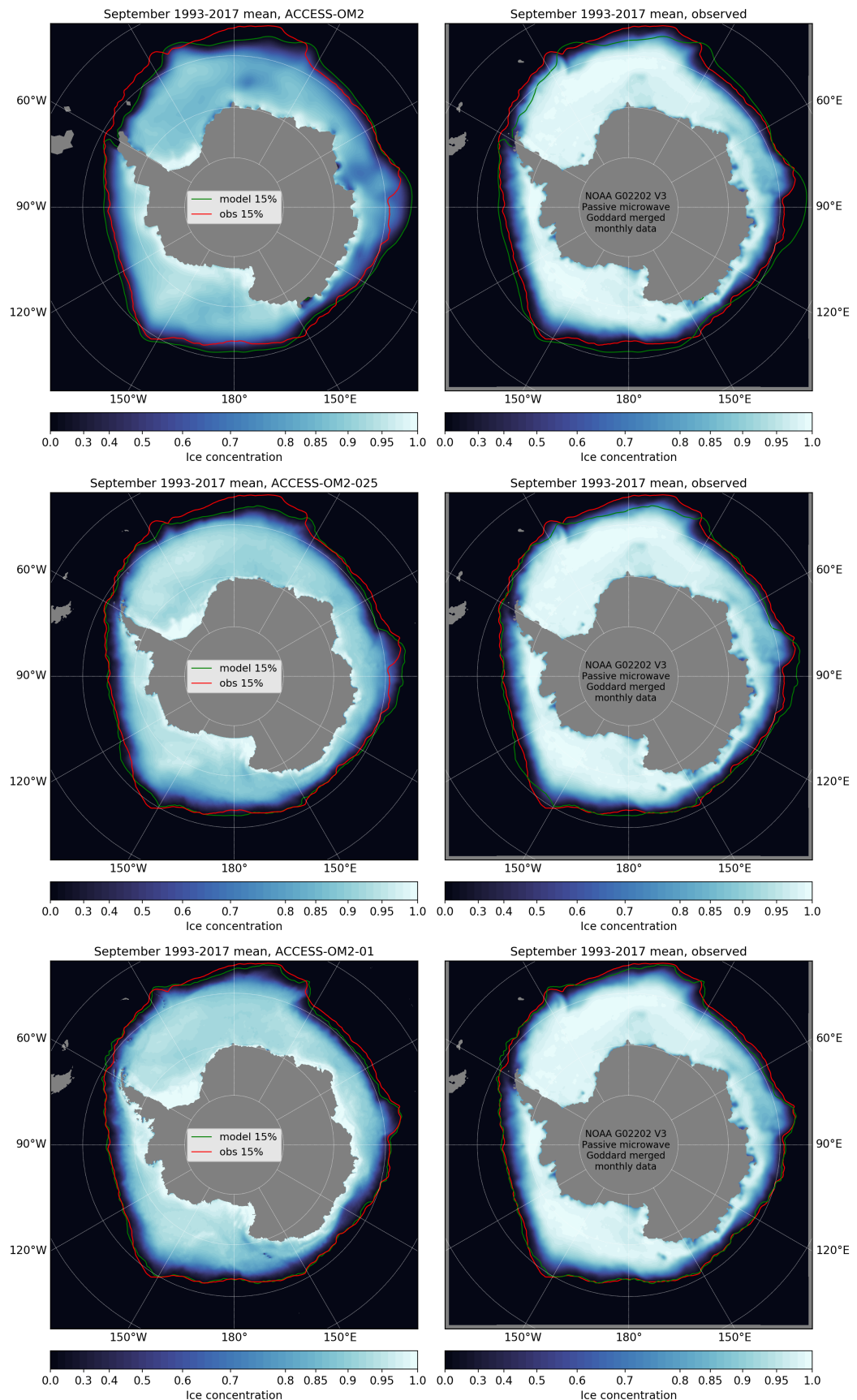


Figure 31: Antarctic sea ice concentration from the ACCESS-OM2 suite (left) and passive microwave (right), September mean. Green (red) line is the 15% concentration contour in the model (observations). The scale is nonlinear to highlight differences at high concentrations. **TODO:** make this more compact - no need to repeat obs 3 times

4.15 Sea ice

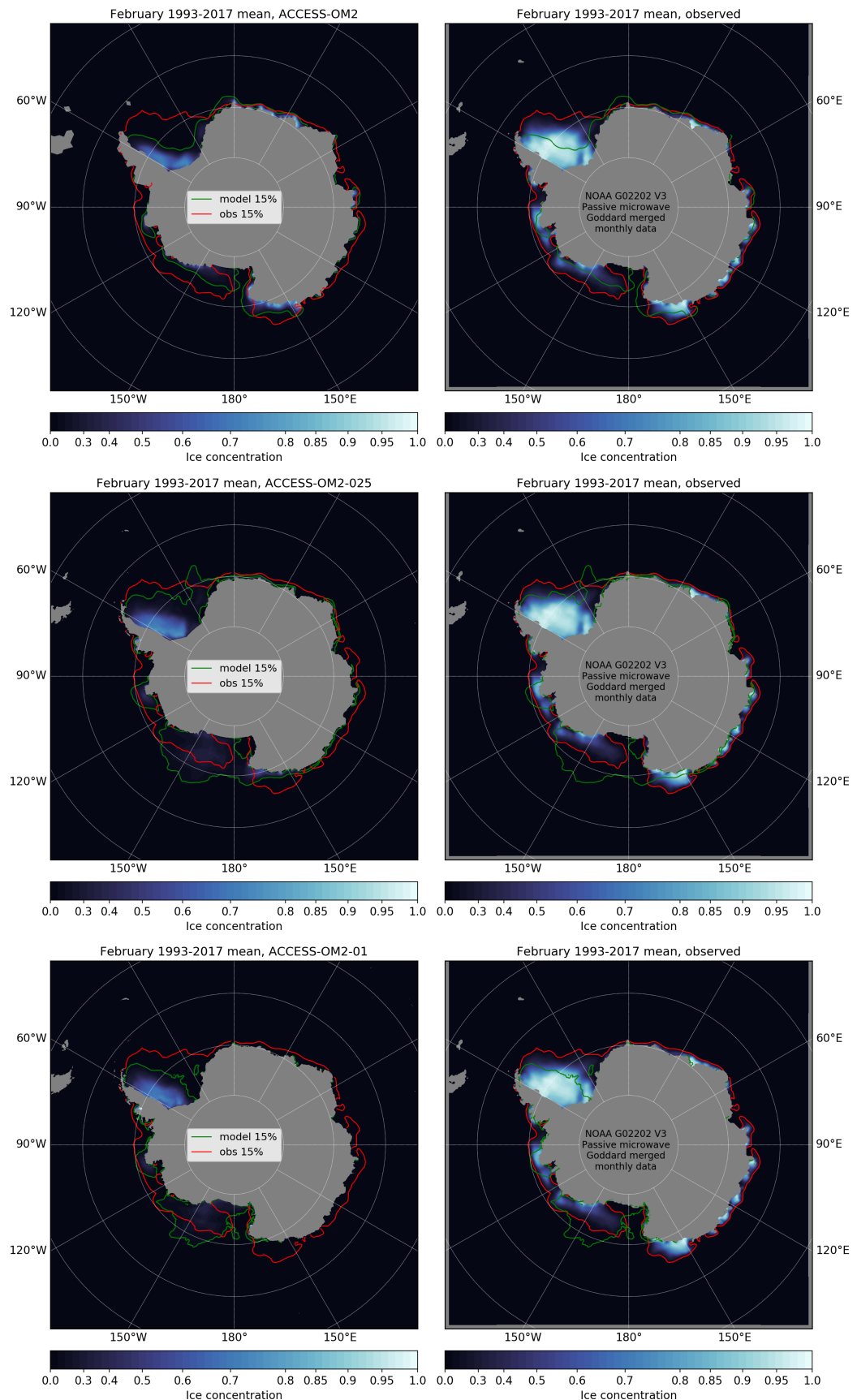


Figure 32: Antarctic sea ice concentration from the ACCESS-OM2 suite (left) and passive microwave (right), February mean. Green (red) line is the 15% concentration contour in the model (observations). The scale is nonlinear to highlight differences at high concentrations. **TODO:** make this more compact - no need to repeat obs 3 times

4.15 Sea ice

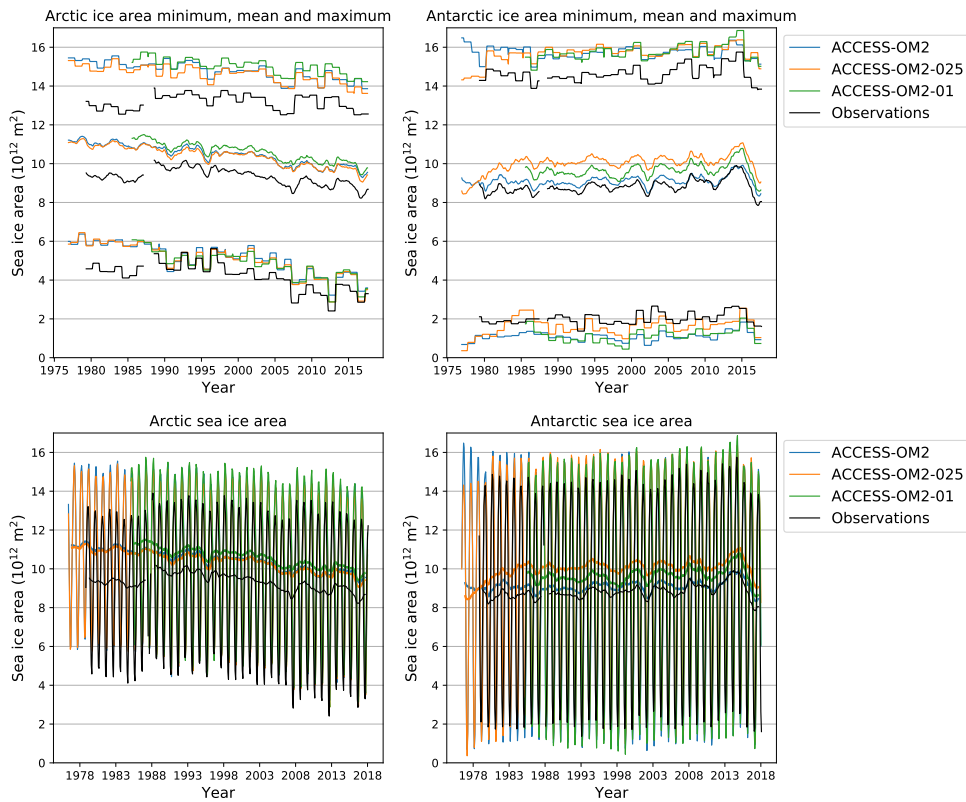


Figure 33: Sea ice area timeseries in the different configurations. Top row: running 12-month minimum, mean and maximum. Bottom row: timeseries (thick lines show the 12-month running mean). **FIXME:** missing obs data (-9999): Dec 1987, Jan 1988

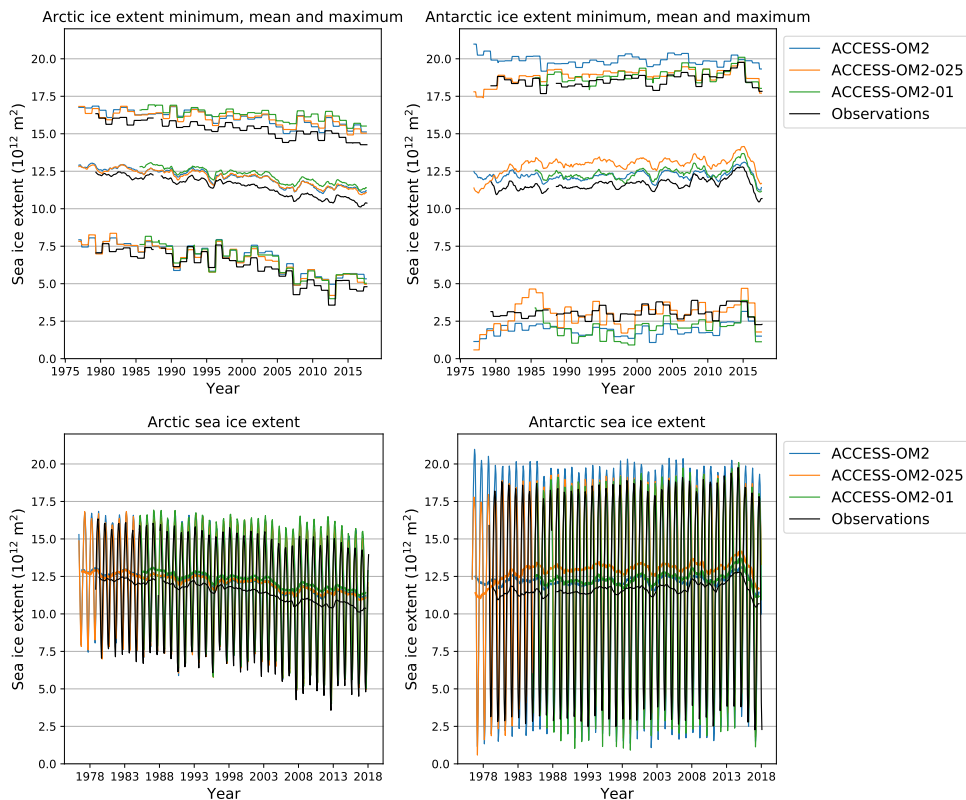


Figure 34: Sea ice extent timeseries in the different configurations. Top row: running 12-month minimum, mean and maximum. Bottom row: timeseries (thick lines show the 12-month running mean). **FIXME:** missing obs data (-9999): Dec 1987, Jan 1988

4.15 Sea ice

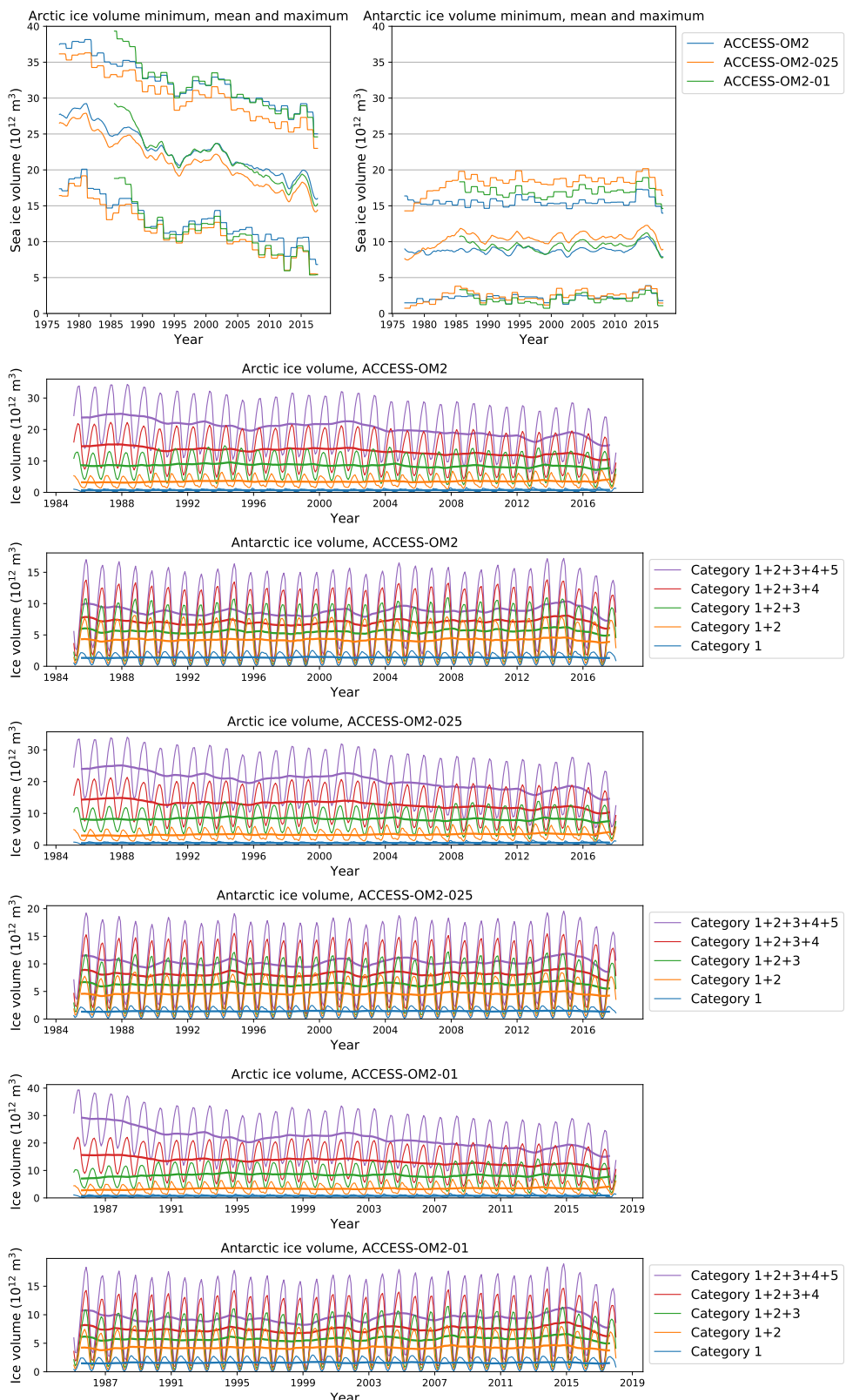


Figure 35: Sea ice volume timeseries in the different configurations. Top row: running 12-month minimum, mean and maximum. Remaining rows: breakdown of ice volume by category (thick lines show the 12-month running mean). Lower bound of ice thickness categories is 0, 0.64, 1.39, 2.47, 4.57m. **TODO:** use a common scale for the category plots in each hemisphere

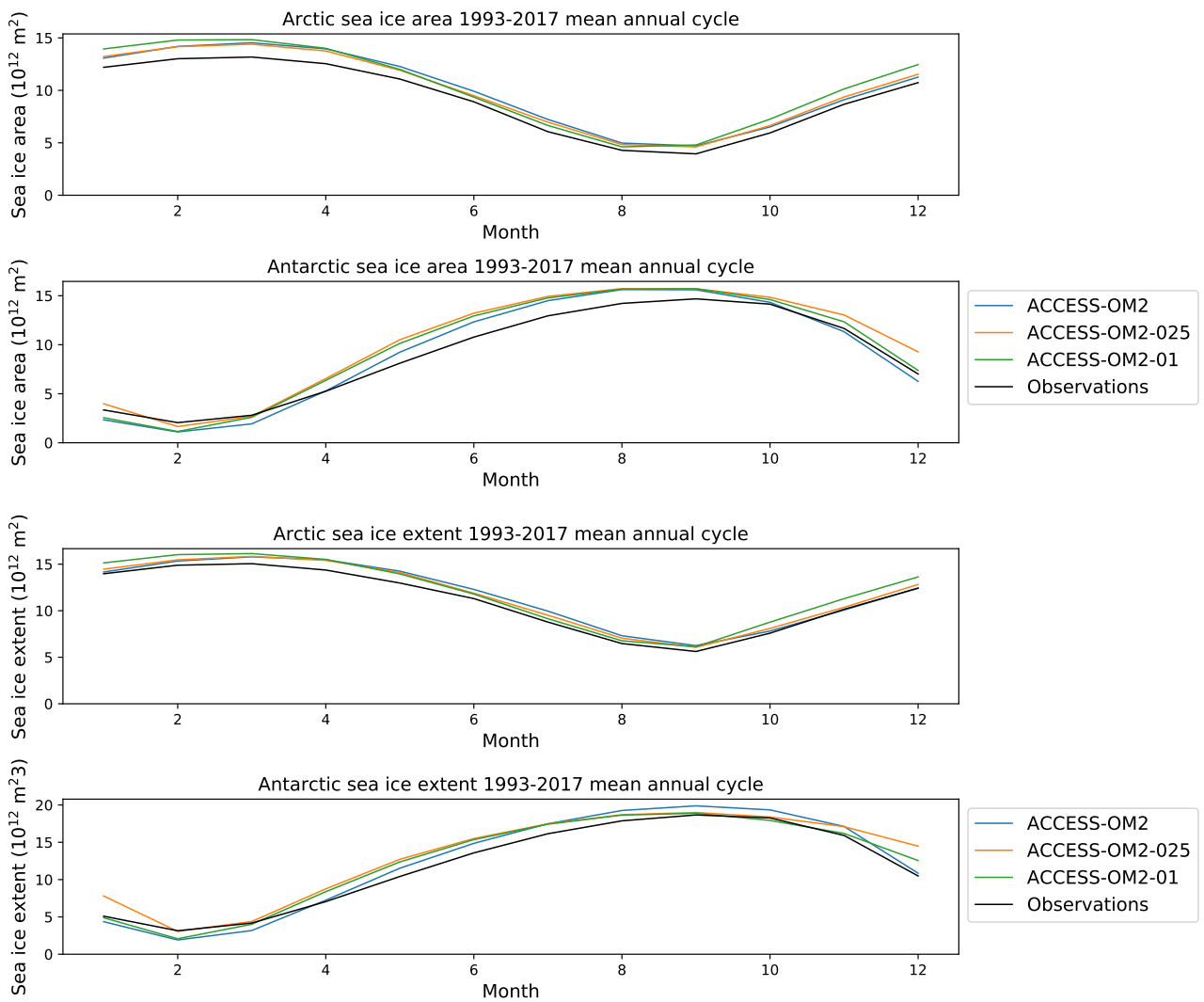


Figure 36: Seasonal cycle of ice area and extent compared to climatology of NOAA/NSIDC G02135 Sea Ice Index v3 (Fetterer et al., 2017, updated daily, <http://nsidc.org/data/g02135>)

4.16 Particularly important regions

4.16 Particularly important regions

Pick locations with detailed obs records for regional studies

4.16.1 ACC

Rintoul (2018)

cf SOSE [Mazloff et al. \(2010\)](#)

transport

EKE [Farneti et al. \(2015\)](#)

4.16.2 Antarctic margins

CONTRIBUTORS: Adele Morrison

dense water formation dense water transport down slope

4.16.3 East Australian Current

Laurindo et al. (2017) Archer et al. (2017a,b, 2018) Wijeratne et al. (2018) Zilberman et al. (2018, 2014)
Feng et al. (2016) Sloyan et al. (2016)

<http://www.clivar.org/clivar-panels/pacific/spice>

4.16.4 Leeuwin Current

Wijeratne et al. (2018) Feng et al. (2016)

4.16.5 North Atlantic

North Atlantic mean state [Danabasoglu et al. \(2014\)](#) and variability [Danabasoglu et al. \(2016\)](#)

4.16.6 Arctic Ocean / Greenland-Iceland-Norway (GIN) Seas

cf. [Behrendt et al. \(2018\)](#) [https://doi.pangaea.de/10.1594/PANGAEA.872931?](https://doi.pangaea.de/10.1594/PANGAEA.872931)

mixed layer depth

water properties

bottom water formation

bottom water transport over sills

[Wang et al. \(2016c\)](#) [Ilicak et al. \(2016\)](#)

4.16.7 Pacific

[Tseng et al. \(2016\)](#)

Kuroshio transport obs: [Johns et al. \(2001\)](#)

4.16 Particularly important regions

4.16.8 Agulhas

transport, structure, variability, leakage

5 Changes made in new version

Namelist changes from the original version are tabulated in Appendix D, and differences between the new namelists are tabulated in Appendix E.

5.1 For all resolutions

- switch to JRA55-do v1.4.0 <https://github.com/COSIMA/access-om2/issues/155>
- automatically sweep and resubmit on specific errors <https://github.com/payu-org/payu/issues/241>
- Update datetime-fortran and json-fortran <https://github.com/COSIMA/libaccessom2/issues/29>
- fixed units for temp: <https://github.com/mom-ocean/MOM5/issues/295>
- stop using -lother=hyperthread <https://github.com/COSIMA/access-om2/issues/191>
- fixed initial condition <https://github.com/COSIMA/access-om2/issues/39>
- use conservative temperature for initial condition: <https://github.com/COSIMA/access-om2/issues/206>
- updated compile scripts for gadi — library versions, compiler flags
- Compile with intel 19 and openMPI4.0.2 <https://github.com/COSIMA/access-om2/issues/127>
- move inputs and executables from /short/public to /g/data/ik11 for transition to gadi
- use new JRA55-do path <https://github.com/COSIMA/access-om2/issues/120> — requires membership of qv56 via <https://my.nci.org.au/mancini/project/> for all users.
- Fix calendar <https://github.com/COSIMA/access-om2/issues/117>
- Use relative wind for ice (set `highfreq=true` in group `forcing_nml`) since this is what use use for the ocean <https://github.com/COSIMA/access-om2/issues/138>
- Tidy up neutral physics namelist: <https://github.com/COSIMA/access-om2/issues/197>
- Set `pottemp_equal_contemp` to false: <https://github.com/COSIMA/access-om2/issues/148>
- Fix neutral density diagnostic levels: now set to `neutralrho_min=1028.0` and `neutralrho_max=1038.0` <https://github.com/COSIMA/access-om2/issues/135>
- Use updated payu (at least 0.11.2) that fixes cice coupling bug: <https://github.com/COSIMA/access-om2/issues/123>
- Set `drhodz_mom4p1=true` for 0.25 degree
- Set `zmax_pen` to 1e6 (the default — see comments in code)
- Set `ncar_boundary_scaling=false` at 0.25 and 0.1deg, since we're not using it anyway
- turn off MOM output/restart compression at 1 deg (since this can be done for both output and restart by payu in collation step): set `deflate_level=-1` <https://github.com/COSIMA/access-om2/issues/168>
- dropped support for CORE and minimal configs (mark as deprecated) <https://github.com/COSIMA/access-om2/issues/183>
- use safer `min_thickness` <https://github.com/mom-ocean/MOM5/issues/307> and <https://github.com/mom-ocean/MOM5/pull/303>
- fix PBS directives for gadi <https://opus.nci.org.au/display/Help/Preparing+for+Gadi>

5.1 For all resolutions

- Fix salt restoring file at 0.1 and 0.25 deg <https://github.com/COSIMA/access-om2/issues/74>
- use mppnccombine-fast at 0.1 and 0.25 deg and <https://github.com/COSIMA/access-om2/issues/154> and <https://github.com/COSIMA/access-om2/issues/168>
- tidy namelists for easy comparison across new configs; con: hard to compare to old configs (need to use nmltab) <https://arccss.slack.com/archives/C6PP0GU9Y/p1589497779266600>
- remove `cdbot` from MOM namelist - it is unused, since `cdbot_law_of_wall=false` (the default) <https://github.com/COSIMA/access-om2/issues/200>
- merge sync_output_to_gdata.sh and RM_SYNCHED_OUTPUT.sh into one script with a --remove-source-files option <https://github.com/COSIMA/access-om2/issues/171>
- delete any ice.log.task_* files that only have a 105-character header and nothing else
- Fixed up Rayleigh damping locations at 1 degree: see section 3.2.7 and <https://github.com/COSIMA/access-om2/issues/156> and https://github.com/COSIMA/1deg_core_nyf/issues/1
- fixed vertical grid issue <https://github.com/COSIMA/access-om2/issues/159>
- Stop using 2nd order conservative remapping until we work out how to avoid negative values: <https://github.com/COSIMA/access-om2/issues/71> and <https://github.com/COSIMA/access-om2/issues/74#issuecomment-454660871>
- Compress CICE output <https://github.com/COSIMA/cice5/issues/26>
- let payu determine the total ncpus <https://github.com/payu-org/payu/issues/97>
- put date in MOM output filenames, and make outputs a consistent length (e.g. monthly at 0.1 deg) <https://github.com/COSIMA/access-om2/issues/185>; also have one file per field
- use Large and Yeager (2009) latitude-dependent ocean albedo (`cst_ocn_albedo=false`) <https://github.com/COSIMA/access-om2/issues/172>. Note that this differs from MOM5's `ocean_albedo_option=3` formula, which depends on zenith angle.
- removed some redundant items from input.nml
- Diagnostics
 - Consistent ocean and ice diag outputs across all resolutions, including monthly outputs of 3d fields in coarse runs
 - Output squared velocity components (for EKE)
 - Output all terms to close heat budget: <https://github.com/COSIMA/access-om2/issues/139> and <https://github.com/COSIMA/access-om2/issues/142>
 - output min SST as well as mean — min is useful for comparison with foundation temperature or night time obs.
 - save max MLD as well as mean
 - Don't duplicate outputs from CICE and MOM (and prefer output from MOM as it is parallel)
 - Daily polynya and ice-production related diagnostics from CICE: `f_frzmlt`, `f_frazil`, `f_congel`
- updated model components to support WOMBAT BGC (<https://github.com/mom-ocean/MOM5/pull/317> and <https://github.com/COSIMA/cice5/pull/47> and <https://github.com/COSIMA/access-om2/pull/199>)
- automatically do run_summary.py

5.2 At 0.1 degree

- New topography at 1 deg and 0.25 deg, now based on GEBCO 2014 and fixing many issues: <https://github.com/COSIMA/access-om2/issues/141> and <https://github.com/COSIMA/access-om2/issues/158> and <https://github.com/mom-ocean/MOM5/issues/172> and <https://github.com/COSIMA/access-om2/issues/210>
- update MOM to fix ty_trans_int_z diagnostic bug: <https://github.com/COSIMA/access-om2/issues/220>
- turned off daily output from CICE as it is a serial bottleneck: <https://github.com/COSIMA/cice5/issues/34>
- update model components to support PIO for CICE <https://github.com/COSIMA/cice5/issues/34>
- update NetCDF version to get compression with parallel I/O (PIO) in CICE <https://github.com/COSIMA/access-om2/issues/166>
- generalised spatiotemporal forcing perturbations <https://github.com/COSIMA/access-om2/wiki/Tutorials#Scaling-the-forcing-fields>

5.2 At 0.1 degree

- Use improved bathymetry that
 - Sets min_thick to the top level thickness in bathymetry, removing terraces in shallow water: <https://github.com/COSIMA/access-om2/issues/99>
 - Removes Severny Island seamounts
 - Fills in very fine bathymetry near tripodes <https://github.com/COSIMA/access-om2/issues/126>
- Fixed misaligned CICE grid <https://github.com/COSIMA/access-om2/issues/190>
- Use conservative temperature <https://github.com/COSIMA/access-om2/issues/97> and omit `pottemp_equal_contemp` so it defaults to false: <https://github.com/COSIMA/access-om2/issues/148>
- fixed 0.1 degree vertical grid issue <https://github.com/COSIMA/access-om2/issues/161>
- Use explicit vertical diffusivity, spatially uniform ($j09_bgmax=j09_bgmin=1 \times 10^{-6} \text{ m}^2\text{s}^{-1}$). See <https://github.com/COSIMA/access-om2/issues/134> see https://github.com/rmholmes/cosima-scripts/blob/master/Equatorial_Pacific_Analysis/Equatorial_Pacific_Thermal_Bias.ipynb

6 TODO for v2.0.0

- check parameter agreement with ACCESS-CM2 at 1deg
- set GM limits to 100-1200m²/s for 1deg to match ACCESS-CM2?
- use Langmuir mixing at 1 deg to match ACCESS-CM2 ?
- increase non-equatorial vertical diffusivity to match ACCESS-CM2?
- remove static fields from CICE output <https://github.com/COSIMA/access-om2/issues/201>

6.1 at 0.1 deg

- fix land masks for 0.1deg <https://github.com/COSIMA/access-om2/issues/198>
- calculate wavenumber spectra to see if we need different viscosity - see <https://github.com/COSIMA/ACCESS-OM2-1-025-010deg-report/blob/master/figures/spectra/spectra.ipynb>
- Try increased lateral viscosity to reduce vorticity noise? Or does non-terraced topography fix this? <https://github.com/COSIMA/access-om2/issues/107>

7 Things to improve for next time

See <https://github.com/COSIMA/access-om2/issues>.

7.1 For all resolutions

- explicit melt ponds in CCSM3, as in ACCESS-CM2 and [Ridley et al. \(2018\)](#)? only really relevant for Arctic
- distributed iceberg discharge (solid runoff) and latent heat — improves retention of Antarctic summer sea ice in ACCESS-CM2j
- Diagnostics
 - Make cice output more like SIMIP ([Notz et al., 2016](#))?
 - Outputs like HighResMIP ([Haarsma et al., 2016](#))?
- fix up access attributes at start of sync_data.sh (access seems to get stuffed up if this times out) <https://climatefluidphysics.slack.com/archives/C0104HQ8K50/p1586838051081000> and <https://climatefluidphysics.slack.com/archives/G010Q6Z28UA/p1589959710003200> **TODO:** see comments in .tex
- when available, check whether normalbw is cheaper than gadi normal (may need to recompile for this) <https://opus.nci.org.au/display/Help/Broadwell+Compute+Nodes>
- Use an updated version of JRA55-do when they've fixed the cyclone sign problem: <https://github.com/COSIMA/access-om2/issues/186>
- Performance: Maybe the -ftz option could be worth trying, in case denormalised floats are hampering performance? or -fpe0?
- Consistent physical parameters: <https://github.com/COSIMA/access-om2/issues/121> and <https://github.com/COSIMA/access-om2/issues/22> - also see emails 26-27 Nov 2018
- Do separate forcing cycles rather than consecutive: <https://github.com/COSIMA/access-om2/issues/149>
- Upgrade OASIS <https://github.com/COSIMA/access-om2/issues/85>
- Use WOA2018 for initial condition and salt restoring? <https://www.nodc.noaa.gov/OC5/woa18/> — like WOA13v2, WOA2018 has discontinuities and noise in Arctic surface salinity <https://github.com/COSIMA/access-om2/issues/103> — but OMIP specifies WOA13v2
- As recommended by [Tsujino et al. \(2018a\)](#), for consistency with JRA55-do, use [Gill \(1982\)](#) bulk formulas instead of [Large and Yeager \(2004, 2009\)](#)? Also see [Brodeau et al. \(2017\)](#).
- Absolute or relative wind? <https://github.com/COSIMA/access-om2/issues/79> and <https://github.com/COSIMA/access-om2/issues/137> Add [Rio et al. \(2014\)](#) climatological mean surface ocean current to JRA55-do as recommended by [Tsujino et al. \(2018a\)](#)? But this suggestion has never been tested and is not widely supported (especially for high resolution) and no groups seem to be doing it — obs data may not be good enough. Also this attempts to deal with the adjustment of JRA55-do to match observed mean winds, but not the effect of ocean eddies in the scatterometer data ingested into the JRA55 reanalysis.
- TEOS-10? - requires conservative temp and absolute salinity; doing it properly requires an additional salt tracer, but nobody does it that way. It isn't more expensive than pre-TEOS-10 - <https://github.com/COSIMA/access-om2/issues/140>.
- Investigate wavy ice features in 0.25deg — poor EVP convergence? <https://github.com/COSIMA/access-om2/issues/87>

7.2 At 1 degree

- increase `ndte`? Hunke said CICE consortium now uses `ndte=240` instead of `120` - better for high resolution - worth doing some tests?
- parallel I/O in MOM? [Yang et al. \(2019\)](#)

7.2 At 1 degree

- disable NCAR boundary scaling of viscosity in tripole? <https://github.com/mom-ocean/MOM5/issues/282#issuecomment-520634586>

7.3 At 0.1 degree

Easy things:

- sort out run performance degradation <https://github.com/COSIMA/access-om2/issues/192>
- Use non-mushy ice thermodynamics for speed (may need to tweak restarts to make freezing point compatible?)
- Include Antarctic glacial ice tongues, e.g. Mertz, Dalton etc? they can produce polynyas in their lee but model can only represent them as peninsulas so will this cause more problems with currents? (and maybe no polynyas, if current separates and recirculates since it can't flow under ice tongue)
- experiment with EAP? [Naughten \(2018\)](#) found it improved things
- is runoff cap needed now we have Russ' ice salinity fix? try larger runoff caps, e.g. to avoid Ob outflow being smeared into the embayment to its west? e.g. see /g/data/hh5/tmp/cosima/access-om2-01/01deg_jra55v13_iaf/output194/ocean/ocean_month.nc
- fix Ob runoff misdirection <https://github.com/COSIMA/access-om2/issues/130>

Harder things:

- Sort out noise in surface vertical tracer diffusion <https://github.com/COSIMA/access-om2/issues/110> - back-port MOM6 KPP fix to MOM5? or use this? <https://github.com/mom-ocean/MOM5/issues/264> and <https://github.com/mom-ocean/MOM5/issues/265> and <https://github.com/mom-ocean/MOM5/issues/267>
- Fix bug at tripole seam <https://github.com/COSIMA/access-om2/issues/86>
- Move tripole further from ocean to increase minimum cell size
- Distributed iceberg freshwater and heat flux, using JRA55-do 1.4.0 solid runoff
- Separate solid and liquid runoff caps for JRA55-do v1.4.0
- Basal melt at depth
- Improve Gulf Stream variability distribution — see [Renault et al. \(2016, 2019a,b\)](#)
- Gulf Stream separation issue: <https://github.com/COSIMA/access-om2/issues/151>

8 Acknowledgments

Model development has been partly funded by ARC Linkage grant LP160100073. Runs were undertaken on the NCI National Facility in Canberra, which is supported by the Australian Commonwealth Government.

A Namelists

These tables show the namelist files used for the final run of each model spinup. Changes to namelists within these spinups are tabulated in Appendix B.

These tables are auto-generated by `namelists/make_tables.py` which uses `nmltab` (<https://github.com/aeckiss/nmltab>). Variables are weblinks to source code searches. Variables that differ between the models are highlighted. Greyed values are ignored.

TODO: generate complete tables that include the default values of parameters not specified in namelists

A.1 ACCESS-OM2 namelist *accessom2.nml*

| Group | Variable | accessom2.nml | ./gadi/g/data/ hh5/tmp/cosima/ access-om2-025/ 025deg_- jra55v13_ifa- gmredi6/ output153/ accessom2.nml | ./gadi/g/data/ hh5/tmp/cosima/ access-om2-01/ 01deg_jra55v13_- iaf/output197/ accessom2.nml |
|-------------------|--------------------|-----------------------|--|--|
| &accessom2_nml | ice_ocean_timestep | 5400 | 1350 | 450 |
| | log_level | 'DEBUG' | 'DEBUG' | 'DEBUG' |
| &date_manager_nml | forcing_end_date | '2018-01-01T00:00:00' | '2018-01-01T00:00:00' | '2018-01-01T00:00:00' |
| | forcing_start_date | '1958-01-01T00:00:00' | '1958-01-01T00:00:00' | '1985-01-01T00:00:00' |
| | restart_period | 5, 0, 0 | 1, 0, 0 | 0, 2, 0 |

A.2 MOM namelist *input.nml*

| Group | Variable | input.nml | ./gadi/g/data/ hh5/tmp/cosima/ access-om2-025/ 025deg_- jra55v13_ifa- gmredi6/ output153/ocean/ input.nml | ./gadi/g/data/ hh5/tmp/cosima/ access-om2-01/ 01deg_jra55v13_- iaf/output197/ ocean/input.nml |
|-----------------|------------------|-----------|--|--|
| &auscom_ice_nml | aice_cutoff | 0.15 | 0.15 | 0.15 |
| | chk_i2o_fields | False | False | False |
| | chk_o2i_fields | False | False | False |
| | do_ice_once | False | False | False |
| | fixmeltt | False | False | False |
| | frazil_factor | 1.0 | 1.0 | 1.0 |
| | iceform_adj_salt | False | False | False |
| | icemlt_factor | 1.0 | 1.0 | 1.0 |

A.2 MOM namelist *input.nml*

| Group (continued) | Variable | input.nml | input.nml | input.nml |
|-------------------------------|----------------------------|---|---|---|
| | kmxic | 5 | 5 | 5 |
| | pop_icediag | True | True | True |
| | redsea_gulfbay_sfxt | False | | |
| | sign_stflx | 1.0 | 1.0 | 1.0 |
| | tmelt | -0.216 | -0.216 | -0.216 |
| | use_ioice | True | True | True |
| &diag_manager_nml | debug_diag_manager | False | True | True |
| | issue_oor_warnings | True | True | True |
| &fms_io_nml | checksum_required | | | False |
| | fileset_write | 'single' | 'single' | 'multi' |
| | threading_read | 'multi' | 'multi' | 'multi' |
| | threading_write | 'single' | 'single' | 'multi' |
| &fms_nml | clock_grain | 'LOOP' | 'LOOP' | 'ROUTINE' |
| | domains_stack_size | 115200 | | 115200 |
| &mom_oasis3_interface_nml | fields_in | 'u_flux', 'v_flux', 'lprec', 'fprec', 'salt_flux', 'mh_flux', 'sw_flux', 'q_flux', 't_flux', 'lw_flux', 'runof', 'p', 'aice', 'wfmelt', 'wfiform' | 'u_flux', 'v_flux', 'lprec', 'fprec', 'salt_flux', 'mh_flux', 'sw_flux', 'q_flux', 't_flux', 'lw_flux', 'runof', 'p', 'aice', 'wfmelt', 'wfiform' | 'u_flux', 'v_flux', 'lprec', 'fprec', 'salt_flux', 'mh_flux', 'sw_flux', 'q_flux', 't_flux', 'lw_flux', 'runof', 'p', 'aice', 'wfmelt', 'wfiform' |
| | fields_out | 'frazil' | 'frazil' | 'frazil' |
| | num_fields_in | 15 | 15 | 15 |
| | num_fields_out | 7 | 7 | 7 |
| | send_after_ocean_update | True | True | True |
| | send_before_ocean_update | False | False | False |
| &monin_obukhov_nml | neutral | True | True | True |
| &mpp_io_nml | deflate_level | 5 | 5 | 5 |
| | shuffle | 1 | 1 | 1 |
| &ocean_adv_vel_diag_nml | diag_step | 4320 | 4320 | 576 |
| | large_cfl_value | 10.0 | 10.0 | 10.0 |
| | max_cfl_value | 100.0 | 100.0 | 100.0 |
| | verbose_cfl | True | True | True |
| &ocean_advection_velocity_nml | max_advection_velocity | 0.5 | 0.5 | 0.3 |
| &ocean_albedo_nml | ocean_albedo_option | 2 | 2 | 2 |
| &ocean_barotropic_nml | barotropic_halo | 10 | 10 | 10 |
| | barotropic_time_stepping_a | True | True | True |
| | barotropic_time_stepping_b | False | False | False |
| | debug_this_module | False | False | False |
| | diag_step | 4320 | 4320 | 576 |
| | eta_max | 8.0 | 8.0 | 8.0 |
| | frac_crit_cell_height | 0.2 | 0.2 | 0.2 |
| | pred_corr_gamma | 0.2 | 0.2 | 0.2 |
| | smooth_eta_diag_laplacian | True | True | True |
| | smooth_eta_t_biharmonic | False | False | False |
| | smooth_eta_t_laplacian | True | True | True |
| | smooth_pbot_t_biharmonic | False | False | False |
| | smooth_pbot_t_laplacian | True | True | True |

A.2 MOM namelist *input.nml*

| Group (continued) | Variable | ./gadi/g/data/ hh5/tmp/cosima/ access-om2/ 1deg_jra55v13_- iaf_spinup1_B1/ output059/ocean/ input.nml | ./gadi/g/data/ hh5/tmp/cosima/ access-om2-025/ 025deg_- jra55v13_iaf_- gmredi6/ output153/ocean/ input.nml | ./gadi/g/data/ hh5/tmp/cosima/ access-om2-01/ 01deg_jra55v13_- iaf/output197/ ocean/input.nml |
|----------------------------|-----------------------------|---|---|--|
| | truncate_eta | False | False | False |
| | use_legacy_barotropic_halos | False | False | False |
| | vel_micom_bih | 0.01 | 0.01 | 0.01 |
| | vel_micom_lap | 0.05 | 0.05 | 0.05 |
| | vel_micom_lap_diag | 0.2 | 0.2 | 0.2 |
| | verbose_truncate | True | True | True |
| | zero_tendency | False | False | False |
| &ocean_bbc_nml | bmf_implicit | True | True | True |
| | cdbot | 0.001 | 0.001 | 0.001 |
| | cdbot_hi | 0.007 | 0.007 | 0.007 |
| | cdbot_roughness_length | False | False | False |
| | cdbot_roughness_uamp | True | True | True |
| | uresidual | 0.05 | 0.05 | 0.05 |
| | use_geothermal_heating | False | False | False |
| &ocean_bih_friction_nml | bih_friction_scheme | 'general' | 'general' | 'general' |
| &ocean_bih_tracer_nml | use_this_module | False | False | False |
| &ocean_bihcst_friction_nml | use_this_module | False | False | False |
| &ocean_bihgen_friction_nml | bottom_5point | True | False | False |
| | eq_lat_micom | 0.0 | 0.0 | 0.0 |
| | eq_vel_micom_aniso | 0.0 | 0.0 | 0.0 |
| | eq_vel_micom_iso | 0.0 | 0.0 | 0.0 |
| | equatorial_zonal | False | False | False |
| | k_smag_aniso | 0.0 | 0.0 | 0.0 |
| | k_smag_iso | 2.0 | 2.0 | 2.0 |
| | ncar_boundary_scaling | True | True | True |
| | ncar_boundary_scaling_read | False | False | False |
| | ncar_rescale_power | 2 | 2 | 2 |
| | ncar_vconst_4 | 2×10^{-8} | 2×10^{-8} | 2×10^{-8} |
| | ncar_vconst_5 | 5 | 5 | 5 |
| | use_this_module | True | True | True |
| | vel_micom_aniso | 0.0 | 0.0 | 0.0 |
| | vel_micom_bottom | 0.01 | 0.0 | 0.0 |
| | vel_micom_iso | 0.04 | 0.0 | 0.0 |
| | visc_crit_scale | 0.25 | 1.0 | 1.0 |
| &ocean_convect_nml | use_this_module | False | False | False |
| &ocean_coriolis_nml | acor | 0.5 | 0.5 | 0.5 |
| | use_this_module | True | True | True |
| &ocean_density_nml | eos_linear | False | False | False |
| | eos_preteos10 | True | True | True |
| | layer_nk | 80 | 80 | 80 |
| | neutralrho_max | 1030.0 | 1030.0 | 1030.0 |
| | neutralrho_min | 1020.0 | 1020.0 | 1020.0 |
| | potrho_max | 1038.0 | 1038.0 | 1038.0 |
| | potrho_min | 1028.0 | 1028.0 | 1028.0 |
| &ocean_domains_nml | max_tracers | 5 | 5 | 5 |
| &ocean_form_drag_nml | use_this_module | False | False | False |
| &ocean_frazil_nml | debug_this_module | False | False | False |
| | frazil_only_in_surface | False | False | False |
| | freezing_temp_preteos10 | True | True | True |
| | freezing_temp_simple | False | False | False |
| | use_this_module | True | True | True |

| Group (continued) | Variable | input.nml | input.nml | input.nml |
|-------------------------------|---------------------------------|------------|------------|------------|
| &ocean_grids_nml | debug_this_module | False | False | False |
| &ocean_increment_eta_nml | use_this_module | False | False | False |
| &ocean_increment_tracer_nml | use_this_module | False | False | False |
| &ocean_increment_velocity_nml | use_this_module | False | False | False |
| &ocean_lap_friction_nml | lap_friction_scheme | 'general' | 'general' | 'general' |
| &ocean_lap_tracer_nml | use_this_module | False | False | False |
| &ocean_lap cst_friction_nml | use_this_module | False | False | False |
| &ocean_lapgen_friction_nml | bottom_5point | True | | |
| | k_smag_aniso | 0.0 | | |
| | k_smag_iso | 0.0 | | |
| | restrict_polar_visc | True | | |
| | restrict_polar_visc_lat | 60.0 | | |
| | restrict_polar_visc_ratio | 0.35 | | |
| | use_this_module | True | False | False |
| | vel_micom_iso | 0.1 | | |
| | viscosity_ncar | False | | |
| | viscosity_ncar_2007 | False | | |
| | viscosity_scale_by_rossby | True | | |
| | viscosity_scale_by_rossby_power | 4.0 | | |
| &ocean_mixdownslope_nml | debug_this_module | False | | |
| | mixdownslope_mask_gfdl | False | | |
| | mixdownslope_npts | 4 | | |
| | read_mixdownslope_mask | False | | |
| | use_this_module | True | False | False |
| &ocean_model_nml | baroclinic_split | 1 | 1 | 1 |
| | barotropic_split | 80 | 80 | 80 |
| | cmip_units | True | True | True |
| | debug | False | False | False |
| | io_layout | 4, 3 | 6, 5 | 5, 5 |
| | layout | 16, 15 | 48, 40 | 80, 75 |
| | surface_height_split | 1 | 1 | 1 |
| | time_tendency | 'twolevel' | 'twolevel' | 'twolevel' |
| | vertical_coordinate | 'zstar' | 'zstar' | 'zstar' |
| &ocean_momentum_source_nml | rayleigh_damp_exp_from_bottom | False | False | False |
| | use_rayleigh_damp_table | True | True | True |
| | use_this_module | True | True | True |
| &ocean_nphysics_nml | debug_this_module | False | False | False |
| | use_nphysicsa | False | False | False |
| | use_nphysicsb | False | False | False |
| | use_nphysicsc | True | True | False |
| | use_this_module | True | True | False |
| &ocean_nphysics_util_nml | agm | 600.0 | 200.0 | 100.0 |
| | agm_closure | True | True | True |
| | agm_closure_baroclinic | True | True | True |
| | agm_closure_buoy_freq | 0.004 | 0.004 | 0.004 |
| | agm_closure_eady_ave_mixed | True | True | |
| | agm_closure_eady_cap | True | True | |
| | agm_closure_eady_smooth_horz | True | True | |
| | agm_closure_eady_smooth_vert | True | True | |
| | agm_closure_eden_gamma | 0.0 | 0.0 | |
| | agm_closure_eden_greatbatch | False | False | |

| Group (continued) | Variable | ./gadi/g/data/ hh5/tmp/cosima/ access-om2/ | ./gadi/g/data/ hh5/tmp/cosima/ access-om2-025/ 025deg_- | ./gadi/g/data/ hh5/tmp/cosima/ access-om2-01/ |
|------------------------------------|---|---|---|--|
| | <i>1deg_jra55v13_- iaf_spinup1_B1/ output059/ocean/ input.nml</i> | <i>1deg_jra55v13_- iaf_spinup1_B1/ output059/ocean/ input.nml</i> | <i>jra55v13_iaf_- gmredi6/ output153/ocean/ input.nml</i> | <i>01deg_jra55v13_- iaf/output197/ ocean/input.nml</i> |
| | <i>agm_closure_grid_scaling</i> | True | True | |
| | <i>agm_closure_length</i> | 50 000.0 | 20 000.0 | 50 000.0 |
| | <i>agm_closure_length_bczone</i> | False | False | False |
| | <i>agm_closure_length_fixed</i> | False | False | False |
| | <i>agm_closure_length_rossby</i> | False | False | False |
| | <i>agm_closure_lower_depth</i> | 2000.0 | 2000.0 | 2000.0 |
| | <i>agm_closure_max</i> | 600.0 | 200.0 | 600.0 |
| | <i>agm_closure_min</i> | 50.0 | 1.0 | 100.0 |
| | <i>agm_closure_scaling</i> | 0.07 | 0.07 | 0.07 |
| | <i>agm_closure_upper_depth</i> | 100.0 | 100.0 | 100.0 |
| | <i>agm_damping_time</i> | 45.0 | 45.0 | |
| | <i>agm_smooth_space</i> | False | False | |
| | <i>agm_smooth_time</i> | False | False | |
| | <i>aredi</i> | 600.0 | 200.0 | 600.0 |
| | <i>aredi_diffusivity_grid_scaling</i> | | True | |
| | <i>aredi_equal_agm</i> | False | False | False |
| | <i>dihodz_mom4p1</i> | True | False | False |
| | <i>drhodz_smooth_horz</i> | False | False | False |
| | <i>drhodz_smooth_vert</i> | False | False | False |
| | <i>nphysics_util_zero_init</i> | True | True | |
| | <i>rossby_radius_max</i> | 100 000.0 | 100 000.0 | 100 000.0 |
| | <i>rossby_radius_min</i> | 15 000.0 | 10 000.0 | 15 000.0 |
| | <i>tracer_mix_micom</i> | False | False | False |
| | <i>vel_micom</i> | 0.0 | 0.0 | 0.0 |
| <i>&ocean_nphysicsa_nml</i> | <i>use_this_module</i> | False | False | False |
| <i>&ocean_nphysicsb_nml</i> | <i>use_this_module</i> | False | False | False |
| <i>&ocean_nphysicsc_nml</i> | <i>bv_freq_smooth_vert</i> | True | True | |
| | <i>bvp_bc_mode</i> | 2 | 2 | |
| | <i>bvp_min_speed</i> | 0.1 | 0.1 | |
| | <i>bvp_speed</i> | 0.0 | 0.0 | |
| | <i>debug_this_module</i> | False | False | |
| | <i>do_gm_skewson</i> | True | True | |
| | <i>do_neutral_diffusion</i> | True | True | |
| | <i>epsln_bv_freq</i> | 1×10^{-12} | 1×10^{-12} | |
| | <i>gm_skewson_bvproblem</i> | True | True | |
| | <i>gm_skewson_modes</i> | False | False | |
| | <i>neutral_eddy_depth</i> | True | True | |
| | <i>neutral_physics_limit</i> | True | True | |
| | <i>number_bc_modes</i> | 2 | 2 | |
| | <i>regularize_psi</i> | False | False | |
| | <i>smax_psi</i> | 0.01 | 0.01 | |
| | <i>smooth_psi</i> | True | True | |
| | <i>tmask_neutral_on</i> | True | True | |
| | <i>turb_blayer_min</i> | 50.0 | 50.0 | |
| | <i>use_this_module</i> | True | True | False |
| <i>&ocean_operators_nml</i> | <i>use_legacy_div_ud</i> | False | False | False |
| <i>&ocean_overexchange_nml</i> | <i>debug_this_module</i> | False | False | False |
| | <i>overexch_npts</i> | 4 | 4 | 4 |
| | <i>overexch_weight_far</i> | False | False | False |
| | <i>overflow_umax</i> | 5.0 | 5.0 | 5.0 |
| | <i>use_this_module</i> | False | False | False |

| Group (continued) | Variable | input.nml | input.nml | input.nml |
|----------------------------|-------------------------------|------------|------------|------------|
| &ocean_overflow_nml | use_this_module | False | False | False |
| &ocean_overflow_ofp_nml | use_this_module | False | False | False |
| &ocean_polar_filter_nml | use_this_module | False | False | False |
| &ocean_pressure_nml | zero_pressure_force | False | False | False |
| &ocean_rivermix_nml | debug_this_module | False | False | False |
| | river_diffuse_salt | True | True | True |
| | river_diffuse_temp | True | True | True |
| | river_diffusion_thickness | 0.0 | 0.0 | 0.0 |
| | river_diffusivity | 0.0 | 0.0 | 0.0 |
| | river_insertion_thickness | 40.0 | 40.0 | 40.0 |
| | use_this_module | True | True | True |
| &ocean_riverspread_nml | debug_this_module | | | False |
| | use_this_module | False | False | False |
| &ocean_rough_nml | rough_scheme | 'beljaars' | 'beljaars' | 'beljaars' |
| &ocean_sbc_nml | avg_sfc_temp_salt_eta | True | True | True |
| | avg_sfc_velocity | True | True | True |
| | calvingspread | False | False | False |
| | do_bitwise_exact_sum | True | False | False |
| | do_flux_correction | False | False | False |
| | land_model_heat_fluxes | False | False | False |
| | max_delta_salinity_restore | -0.5 | 0.5 | 0.5 |
| | max_ice_thickness | 0.0 | 0.0 | 0.0 |
| | ocean_ice_salt_limit | | | 0.006 |
| | read_restore_mask | False | False | False |
| | restore_mask_gfdl | False | False | False |
| | runoff_salinity | 0.0 | 0.0 | 0.0 |
| | runoffsplash | | | False |
| | salt_correction_scale | 0.0 | 0.0 | 0.0 |
| | salt_restore_as_salt_flux | True | True | True |
| | salt_restore_tscale | 21.28 | 21.28 | 10.0 |
| | salt_restore_under_ice | True | True | True |
| | temp_restore_tscale | -10.0 | -10.0 | -10.0 |
| | use_full_patm_for_sea_level | False | False | False |
| | use_waterflux | True | True | True |
| | zero_heat_fluxes | False | False | False |
| | zero_net_salt_correction | False | False | False |
| | zero_net_salt_restore | True | True | True |
| | zero_net_water_correction | False | False | False |
| | zero_net_water_couple_restore | True | True | True |
| | zero_net_water_coupler | True | True | True |
| | zero_net_water_restore | True | True | True |
| | zero_surface_stress | False | False | False |
| | zero_water_fluxes | False | False | False |
| &ocean_shortwave_csiro_nml | use_this_module | False | False | False |
| &ocean_shortwave_gfdl_nml | debug_this_module | False | False | False |
| | enforce_sw_frac | True | True | True |
| | optics_manizza | True | True | True |
| | optics_morel_antoine | False | False | False |
| | read_chl | True | True | True |
| | use_this_module | True | True | True |
| | zmax_pen | 300.0 | 300.0 | 300.0 |

| Group (continued) | Variable | ./gadi/g/data/ hh5/tmp/cosima/ access-om2-025/ 025deg_- jra55v13_ifa- gmredi6/ output153/ocean/ input.nml | ./gadi/g/data/ hh5/tmp/cosima/ access-om2-01/ 01deg_jra55v13_ifa/ output197/ocean/ input.nml | ./gadi/g/data/ hh5/tmp/cosima/ access-om2-01/ 01deg_jra55v13_ifa/ output197/ocean/ input.nml |
|-----------------------------|------------------------------|--|---|---|
| &ocean_shortwave_jerlov_nml | use_this_module | False | False | False |
| &ocean_shortwave_nml | use_shortwave_csiro | False | False | False |
| | use_shortwave_gfdl | True | True | True |
| | use_shortwave_jerlov | False | False | False |
| | use_this_module | True | True | True |
| &ocean_sigma_transport_nml | use_this_module | True | False | False |
| &ocean_sponges_eta_nml | use_this_module | False | False | False |
| &ocean_sponges_tracer_nml | use_this_module | False | False | False |
| &ocean_sponges_velocity_nml | use_this_module | False | False | False |
| &ocean_submesoscale_nml | coefficient_ce | 0.05 | 0.05 | 0.05 |
| | debug_this_module | False | False | False |
| | front_length_const | 5000.0 | 5000.0 | 5000.0 |
| | front_length_deform_radius | True | True | True |
| | limit_psi | True | True | True |
| | limit_psi_velocity_scale | 0.5 | 0.5 | 0.5 |
| | min_kblt | 4 | 4 | 4 |
| | smooth_advect_transport | True | True | True |
| | smooth_advect_transport_num | 2 | 4 | 4 |
| | smooth_hblt | False | False | False |
| | smooth_psi | True | True | True |
| | smooth_psi_num | 2 | 3 | 3 |
| | submeso_advect_flux | False | False | False |
| | submeso_advect_limit | True | True | True |
| | submeso_advect_upwind | True | True | True |
| | submeso_advect_zero_bdy | True | True | True |
| | submeso_diffusion | False | False | False |
| | submeso_diffusion_biharmonic | True | True | True |
| | submeso_diffusion_scale | 10.0 | 10.0 | 10.0 |
| | submeso_skew_flux | True | True | True |
| | use_hblt_equal_mld | True | True | True |
| | use_psi_legacy | False | False | False |
| | use_this_module | True | True | True |
| &ocean_tempsalt_nml | debug_this_module | False | False | False |
| | pottemp_2nd_iteration | True | True | True |
| | pottemp_equal_contemp | True | True | True |
| | s_max | 70.0 | 70.0 | 70.0 |
| | s_max_limit | 42.0 | 42.0 | 42.0 |
| | s_min | 0.0 | 0.0 | 0.0 |
| | s_min_limit | 2.0 | 2.0 | 2.0 |
| | t_max | 55.0 | 55.0 | 55.0 |
| | t_max_limit | 32.0 | 32.0 | 32.0 |
| | t_min | -20.0 | -20.0 | -20.0 |
| | t_min_limit | -5.0 | -5.0 | -5.0 |
| | temperature_variable | 'conservative_temp' | 'conservative_temp' | 'potential_temp' |
| &ocean_thickness_nml | debug_this_module | False | False | False |
| | debug_this_module_detail | False | False | False |
| | rescale_mass_to_get_ht_mod | False | False | False |
| | thickness_method | 'energetic' | 'energetic' | 'energetic' |
| &ocean_tracer_advect_nml | debug_this_module | False | False | False |
| | read_basin_mask | False | False | False |
| &ocean_tracer_diag_nml | diag_step | 4320 | 4320 | 576 |

A.2 MOM namelist *input.nml*

| Group (continued) | Variable | ./gadi/g/data/ hh5/tmp/cosima/ access-om2/025/ 025deg_- jra55v13_ifa- gmredi6/ output153/ocean/ input.nml | ./gadi/g/data/ hh5/tmp/cosima/ access-om2-025/ 025deg_- jra55v13_ifa- gmredi6/ output153/ocean/ input.nml | ./gadi/g/data/ hh5/tmp/cosima/ access-om2-01/ 01deg_jra55v13_ifa/ output197/ocean/ input.nml |
|----------------------------|--------------------------------|--|--|---|
| | do_bitwise_exact_sum | False | False | False |
| | tracer_conserve_days | 30.0 | 30.0 | 30.0 |
| &ocean_tracer_nml | age_tracer_max_init | 0.0 | 0.0 | 0.0 |
| | debug_this_module | False | False | False |
| | frazil_heating_after_vphysics | True | True | True |
| | frazil_heating_before_vphysics | False | False | False |
| | limit_age_tracer | True | True | True |
| | remap_depth_to_s_init | False | False | False |
| | use_tempsalt_check_range | True | True | True |
| | zero_tendency | False | False | False |
| | zero_tracer_source | False | False | False |
| &ocean_velocity_diag_nml | debug_this_module | False | False | False |
| | diag_step | 4320 | 4320 | 576 |
| | energy_diag_step | 4320 | 4320 | 5760 |
| | large_cfl_value | 10.0 | 10.0 | 10.0 |
| | max_cfl_value | 100.0 | 100.0 | 100.0 |
| &ocean_velocity_nml | adams_bashforth_third | True | True | True |
| | max_cgint | 1.0 | 1.0 | 1.0 |
| | truncate_velocity | False | False | False |
| | truncate_velocity_value | 2.0 | 2.0 | 2.0 |
| | truncate_verbose | True | True | True |
| | zero_tendency | False | False | False |
| | zero_tendency_explicit_a | False | False | False |
| | zero_tendency_explicit_b | False | False | False |
| | zero_tendency_implicit | False | False | False |
| &ocean_vert_kpp_iow_nml | use_this_module | False | False | False |
| &ocean_vert_kpp_mom4p1_nml | diff_cbt_iw | 0.0 | 0.0 | 0.0 |
| | double_diffusion | True | True | True |
| | kbl_standard_method | False | False | False |
| | ricr | 0.3 | 0.3 | 0.3 |
| | smooth_blmc | False | False | False |
| | smooth_ri_kmax_eq_kmu | True | True | True |
| | use_this_module | True | True | True |
| | visc_cbu_iw | 0.0 | 0.0 | 0.0 |
| &ocean_vert_mix_nml | aidif | 1.0 | 1.0 | 1.0 |
| | bryan_lewis_diffusivity | False | False | False |
| | bryan_lewis_lat_depend | False | False | False |
| | hwf_diffusivity | False | False | False |
| | hwf_min_diffusivity | 2×10^{-6} | 2×10^{-6} | 2×10^{-6} |
| | hwf_n0_2omega | 20.0 | 20.0 | 20.0 |
| | j09_bgmax | 5×10^{-6} | | |
| | j09_bgmin | 1×10^{-6} | | |
| | j09_diffusivity | True | | |
| | j09_lat | 20.0 | | |
| | use_diff_cbt_table | False | False | False |
| | vert_diff_back_via_max | True | True | True |
| | vert_mix_scheme | 'kpp_mom4p1' | 'kpp_mom4p1' | 'kpp_mom4p1' |
| &ocean_vert_tidal_nml | background_diffusivity | 0.0 | 0.0 | 0.0 |
| | background_viscosity | 0.0001 | 0.0001 | 0.0001 |
| | decay_scale | 500.0 | 500.0 | 500.0 |
| | drag_dissipation_use_cdbot | True | True | True |

A.3 CICE namelists

| Group (continued) | Variable | ./gadi/g/data/ hh5/tmp/cosima/ access-om2/ 1deg_jra55v13_- iaf_spinup1_B1/ output059/ocean/ input.nml | ./gadi/g/data/ hh5/tmp/cosima/ access-om2-025/ 025deg_- jra55v13_iaf_- gmredi6/ output153/ocean/ input.nml | ./gadi/g/data/ hh5/tmp/cosima/ access-om2-01/ 01deg_jra55v13_- iaf/output197/ ocean/input.nml |
|------------------------|----------------------------|---|---|--|
| | drhodz_min | 1×10^{-10} | 1×10^{-10} | 1×10^{-10} |
| | fixed_wave_dissipation | False | False | False |
| | max_wave_diffusivity | 0.01 | 0.01 | 0.01 |
| | mixing_efficiency_n2depend | True | True | True |
| | read_roughness | True | True | True |
| | read_tide_speed | True | True | True |
| | read_wave_dissipation | False | False | False |
| | reading_roughness_amp | True | True | True |
| | reading_roughness_length | False | False | False |
| | roughness_scale | 12 000.0 | 12 000.0 | 12 000.0 |
| | shelf_depth_cutoff | -1000.0 | -1000.0 | -1000.0 |
| | tide_speed_data_on_t_grid | True | True | True |
| | use_drag_dissipation | True | True | True |
| | use_legacy_methods | False | False | False |
| | use_this_module | True | True | True |
| | use_wave_dissipation | True | True | True |
| | wave_energy_flux_max | 0.1 | 0.1 | 0.1 |
| &ocean_xlandinsert_nml | use_this_module | False | False | False |
| &ocean_xlandmix_nml | use_this_module | False | False | False |
| &xgrid_nml | do_alltoall | | | True |
| | do_alltoally | | | True |
| | interp_method | 'second_order' | 'second_order' | 'second_order' |
| | make_exchange_reproduce | False | False | False |
| | nsubset | 16 | 16 | 16 |

A.3 CICE namelists

See https://ncar.github.io/CICE/users_guide/ice_nml_var.html.

A.3.1 cice_in.nml

| Group | Variable | ./gadi/g/data/ hh5/tmp/cosima/ access-om2/ 1deg_jra55v13_- iaf_spinup1_B1/ output059/ice/ cice_in.nml | ./gadi/g/data/ hh5/tmp/cosima/ access-om2-025/ 025deg_- jra55v13_iaf_- gmredi6/ output153/ice/ cice_in.nml | ./gadi/g/data/ hh5/tmp/cosima/ access-om2-01/ 01deg_jra55v13_- iaf/output197/ ice/cice_in.nml |
|-------------|-------------------|---|---|--|
| &domain_nml | distribution_type | 'cartesian' | 'roundrobin' | 'roundrobin' |
| | distribution_wght | 'latitude' | 'latitude' | 'latitude' |
| | ew_boundary_type | 'cyclic' | 'cyclic' | 'cyclic' |
| | maskhalo_bound | True | True | True |
| | maskhalo_dyn | True | True | True |
| | maskhalo_remap | True | True | True |
| | nprocs | 24 | 361 | 1600 |
| | ns_boundary_type | 'tripole' | 'tripole' | 'tripole' |
| | processor_shape | 'slenderX1' | 'square-ice' | 'square-ice' |

| Group (continued) | Variable | ./gadi/g/data/ hh5/tmp/cosima/ access-om2/ 1deg_jra55v13 - iaf_spinup1_B1/ output059/ice/ cice_in.nml | ./gadi/g/data/ hh5/tmp/cosima/ access-om2-025/ 025deg_- jra55v13_iaf - gmredi6/ output153/ice/ cice_in.nml | ./gadi/g/data/ hh5/tmp/cosima/ access-om2-01/ 01deg_jra55v13 - iaf/output197/ ice/cice_in.nml |
|--------------------|------------------|---|---|--|
| &dynamics_nml | advection | 'remap' | 'remap' | 'remap' |
| | cosw | 1.0 | 1.0 | 1.0 |
| | dragio | 0.005 36 | 0.005 36 | 0.005 36 |
| | iceruf | 0.0005 | 0.0005 | 0.0005 |
| | kdyn | 1 | 1 | 1 |
| | krdg_partic | 1 | 1 | 1 |
| | krdg_redist | 1 | 1 | 1 |
| | kstrength | 1 | 1 | 1 |
| | mu_rdg | 3 | 3 | 3 |
| | ndte | 120 | 120 | 120 |
| | revised_evp | False | False | False |
| | sinw | 0.0 | 0.0 | 0.0 |
| &forcing_nml | atm_data_dir | 'unknown_atm - data_dir' | 'unknown_atm - data_dir' | 'unknown_atm - data_dir' |
| | atm_data_format | 'nc' | 'nc' | 'nc' |
| | atm_data_type | 'default' | 'default' | 'default' |
| | atmbndy | 'default' | 'default' | 'default' |
| | calc_strair | True | True | True |
| | calc_tsfc | True | True | True |
| | formdrag | False | False | False |
| | fyear_init | 1 | 1 | 1 |
| | oceannmixed_file | 'unknown - oceannmixed_file' | 'unknown - oceannmixed_file' | 'unknown - oceannmixed_file' |
| | oceannmixed_ice | False | False | False |
| | ocn_data_dir | 'unknown_ocn - data_dir' | 'unknown_ocn - data_dir' | 'unknown_ocn - data_dir' |
| | ocn_data_format | 'nc' | 'nc' | 'nc' |
| | precip_units | 'mks' | 'mks' | 'mks' |
| | restore_ice | False | False | False |
| | restore_sst | False | False | False |
| | sss_data_type | 'default' | 'default' | 'default' |
| | sst_data_type | 'default' | 'default' | 'default' |
| | tfrz_option | 'linear_salt' | 'linear_salt' | 'mushy' |
| | trestore | 0 | 0 | 0 |
| | update_ocn_f | True | True | True |
| | ustar_min | 0.0005 | 0.0005 | 0.0005 |
| | ycycle | 1 | 1 | 1 |
| &grid_nml | grid_file | 'RESTART/grid.nc' | 'RESTART/grid.nc' | 'RESTART/grid.nc' |
| | grid_format | 'nc' | 'nc' | 'nc' |
| | grid_type | 'tripole' | 'tripole' | 'tripole' |
| | kcatbound | 0 | 0 | 0 |
| | kmt_file | 'RESTART/kmt.nc' | 'RESTART/kmt.nc' | 'RESTART/kmt.nc' |
| &icefields_bgc_nml | f_aero | 'x' | 'x' | 'x' |
| | f_bgc_am_ml | 'x' | 'x' | 'x' |
| | f_bgc_am_sk | 'x' | 'x' | 'x' |
| | f_bgc_c_sk | 'x' | 'x' | 'x' |
| | f_bgc_chl_sk | 'x' | 'x' | 'x' |
| | f_bgc_dms_sk | 'x' | 'x' | 'x' |
| | f_bgc_dmssp_ml | 'x' | 'x' | 'x' |
| | f_bgc_dmspd_sk | 'x' | 'x' | 'x' |
| | f_bgc_dmspp_sk | 'x' | 'x' | 'x' |
| | f_bgc_n_sk | 'x' | 'x' | 'x' |

| Group (continued) | Variable | ./gadi/g/data/ hh5/tmp/cosima/ access-om2/025/ 025deg_- jra55v13_ifa- gmredi6/ output153/ice/ cice_in.nml | ./gadi/g/data/ hh5/tmp/cosima/ access-om2-01/ 01deg_jra55v13_ifa/ output197/ice/cice_in.nml |
|------------------------|--------------|--|---|
| | f_bgc_nit_ml | 'x' | 'x' |
| | f_bgc_nit_sk | 'x' | 'x' |
| | f_bgc_sil_ml | 'x' | 'x' |
| | f_bgc_sil_sk | 'x' | 'x' |
| | f_bphi | 'x' | 'x' |
| | f_btin | 'x' | 'x' |
| | f_faero_atm | 'x' | 'x' |
| | f_faero_ocn | 'x' | 'x' |
| | f_fbri | 'm' | 'm' |
| | f_fn | 'x' | 'x' |
| | f_fn_ai | 'x' | 'x' |
| | f_fnh | 'x' | 'x' |
| | f_fnh_ai | 'x' | 'x' |
| | f_fno | 'x' | 'x' |
| | f_fno_ai | 'x' | 'x' |
| | f_fsil | 'x' | 'x' |
| | f_fsil_ai | 'x' | 'x' |
| | f_grownet | 'x' | 'x' |
| | f_hbri | 'm' | 'm' |
| | f_ppnet | 'x' | 'x' |
| &icefields_drag_nml | f_cdn_atm | 'x' | 'x' |
| | f_cdn_ocn | 'x' | 'x' |
| | f_drag | 'x' | 'x' |
| &icefields_mechred_nml | f_alvl | 'm' | 'm' |
| | f_aparticn | 'x' | 'x' |
| | f_araftn | 'x' | 'x' |
| | f_ardg | 'm' | 'm' |
| | f_ardgnd | 'x' | 'x' |
| | f_aredistn | 'x' | 'x' |
| | f_dardg1dt | 'x' | 'x' |
| | f_dardg1ndt | 'x' | 'x' |
| | f_dardg2dt | 'x' | 'x' |
| | f_dardg2ndt | 'x' | 'x' |
| | f_dvirdgdt | 'x' | 'x' |
| | f_dvirdgndt | 'x' | 'x' |
| | f_krdgn | 'x' | 'x' |
| | f_opening | 'x' | 'm' |
| | f_vlvl | 'm' | 'm' |
| | f_vraftn | 'x' | 'x' |
| | f_vrdg | 'm' | 'x' |
| | f_vrdgn | 'x' | 'x' |
| | f_yredistn | 'x' | 'x' |
| &icefields_nml | f_aice | 'm' | 'm' |
| | f_aicen | 'm' | 'md' |
| | f_aisnap | 'x' | 'x' |
| | f_albice | 'm' | 'x' |
| | f_albpnd | 'x' | 'x' |
| | f_albsni | 'm' | 'x' |
| | f_albsno | 'm' | 'x' |
| | f_alidr | 'x' | 'x' |
| | f_alvdr | 'x' | 'x' |
| | f_angle | True | True |

| Group (continued) | Variable | ./gadi/g/data/ hh5/tmp/cosima/ access-om2/025/ 025deg_- jra55v13_iaf_- gmredi6/ output153/ice/ cice_in.nml | ./gadi/g/data/ hh5/tmp/cosima/ access-om2-025/ 025deg_- jra55v13_iaf_- gmredi6/ output153/ice/ cice_in.nml | ./gadi/g/data/ hh5/tmp/cosima/ access-om2-01/ 01deg_jra55v13_- iaf/output197/ ice/cice_in.nml |
|-------------------|----------------|---|---|--|
| | f_anglet | True | True | True |
| | f_bounds | False | False | False |
| | f_congel | 'm' | 'm' | 'm' |
| | f_coszen | 'x' | 'x' | 'x' |
| | f_daidtd | 'm' | 'm' | 'x' |
| | f_daidtt | 'm' | 'm' | 'x' |
| | f_divu | 'm' | 'm' | 'md' |
| | f_dsnow | 'x' | 'x' | 'x' |
| | f_dvidtd | 'm' | 'm' | 'x' |
| | f_dvidtt | 'm' | 'm' | 'x' |
| | f_dxdt | True | True | True |
| | f_dxu | True | True | True |
| | f_dydt | True | True | True |
| | f_dyu | True | True | True |
| | f_evap | 'x' | 'x' | 'x' |
| | f_evap_ai | 'm' | 'm' | 'x' |
| | f_fcondtop_ai | 'm' | 'm' | 'x' |
| | f_fcondtopn_ai | 'm' | 'm' | 'x' |
| | f_fhocn | 'x' | 'x' | 'x' |
| | f_fhocn_ai | 'm' | 'm' | 'x' |
| | f_flat | 'x' | 'x' | 'x' |
| | f_flat_ai | 'm' | 'm' | 'x' |
| | f.flatn_ai | 'm' | 'm' | 'm' |
| | f_flwdn | 'm' | 'm' | 'x' |
| | f_flwup | 'x' | 'x' | 'x' |
| | f_flwup_ai | 'm' | 'm' | 'x' |
| | f_fmeltt_ai | 'x' | 'm' | 'm' |
| | f_fmeltnn_ai | 'm' | 'm' | 'x' |
| | f_frazil | 'm' | 'm' | 'm' |
| | f_fresh | 'x' | 'x' | 'x' |
| | f_fresh_ai | 'm' | 'm' | 'x' |
| | f_frzonset | 'm' | 'm' | 'm' |
| | f_frzmlt | 'm' | 'm' | 'x' |
| | f_fsalt | 'x' | 'x' | 'd' |
| | f_fsalt_ai | 'm' | 'x' | 'd' |
| | f_fsens | 'x' | 'x' | 'x' |
| | f_fsens_ai | 'm' | 'm' | 'x' |
| | f_fsurf_ai | 'x' | 'x' | 'x' |
| | f_fsurfnn_ai | 'm' | 'm' | 'x' |
| | f_fswabs | 'x' | 'x' | 'x' |
| | f_fswabs_ai | 'm' | 'm' | 'x' |
| | f_fswdn | 'm' | 'm' | 'x' |
| | f_fswfac | 'm' | 'm' | 'x' |
| | f_fswthru | 'x' | 'x' | 'x' |
| | f_fswthru_ai | 'm' | 'm' | 'x' |
| | f_fy | 'x' | 'x' | 'x' |
| | f_hi | 'm' | 'm' | 'md' |
| | f_hisnap | 'x' | 'x' | 'x' |
| | f_hs | 'm' | 'm' | 'md' |
| | f_hte | True | True | True |
| | f_htn | True | True | True |
| | f_iage | 'm' | 'm' | 'm' |

| Group (continued) | Variable | ./gadi/g/data/ hh5/tmp/cosima/ access-om2/025/ 025deg_- jra55v13_ifa- gmredi6/ output153/ice/ cice_in.nml | ./gadi/g/data/ hh5/tmp/cosima/ access-om2-025/ 025deg_- jra55v13_ifa- gmredi6/ output153/ice/ cice_in.nml | ./gadi/g/data/ hh5/tmp/cosima/ access-om2-01/ 01deg_jra55v13_ifa/ output197/ice/cice_in.nml |
|---------------------|---------------------|--|--|---|
| | f_icepresent | 'm' | 'm' | 'x' |
| | f_meltb | 'm' | 'm' | 'x' |
| | f_meltl | 'm' | 'm' | 'x' |
| | f_melts | 'm' | 'm' | 'x' |
| | f_meltt | 'm' | 'm' | 'x' |
| | f_mlt_onset | 'm' | 'm' | 'm' |
| | f_ncat | True | True | True |
| | f_qref | 'x' | 'x' | 'x' |
| | f_rain | 'x' | 'x' | 'x' |
| | f_rain_ai | 'm' | 'm' | 'x' |
| | f_shear | 'm' | 'm' | 'md' |
| | f_sice | 'm' | 'm' | 'x' |
| | f_sig1 | 'x' | 'm' | 'md' |
| | f_sig2 | 'x' | 'm' | 'md' |
| | f_sinz | 'x' | 'x' | 'x' |
| | f_snoise | 'm' | 'm' | 'x' |
| | f_snow | 'x' | 'x' | 'x' |
| | f_snow_ai | 'm' | 'm' | 'x' |
| | f_sss | 'm' | 'x' | 'd' |
| | f_sst | 'm' | 'x' | 'd' |
| | f_strainx | 'm' | 'm' | 'md' |
| | f_strainy | 'm' | 'm' | 'md' |
| | f_strcorx | 'm' | 'm' | 'x' |
| | f_strcory | 'm' | 'm' | 'x' |
| | f_strength | 'm' | 'm' | 'm' |
| | f_strintx | 'm' | 'm' | 'x' |
| | f_strinty | 'm' | 'm' | 'x' |
| | f_strocnx | 'm' | 'm' | 'x' |
| | f_strocnyn | 'm' | 'm' | 'x' |
| | f_strltx | 'm' | 'm' | 'x' |
| | f_strlty | 'm' | 'm' | 'x' |
| | f_tair | 'm' | 'm' | 'x' |
| | f_tarea | True | True | True |
| | f_tinz | 'x' | 'x' | 'x' |
| | f_tmask | True | True | True |
| | f_tref | 'x' | 'x' | 'x' |
| | f_trsig | 'm' | 'm' | 'x' |
| | f_tsfc | 'm' | 'm' | 'm' |
| | f_tsnz | 'x' | 'x' | 'x' |
| | f_uarea | True | True | True |
| | f_uocn | 'm' | 'x' | 'd' |
| | f_uvel | 'm' | 'm' | 'md' |
| | f_vgrdb | False | False | False |
| | f_vgrdi | False | False | False |
| | f_vgrds | False | False | False |
| | f_vicen | 'm' | 'm' | 'md' |
| | f_vocn | 'm' | 'x' | 'd' |
| | f_vvel | 'm' | 'm' | 'md' |
| &icefields_pond_nml | f_apeff | 'm' | 'm' | 'x' |
| | f_apeff_ai | 'm' | 'm' | 'x' |
| | f_apeffn | 'x' | 'x' | 'x' |
| | f_apond | 'm' | 'm' | 'x' |

| Group (continued) | Variable | ./gadi/g/data/ hh5/tmp/cosima/ access-om2/ 1deg_jra55v13_- iaf_spinup1_B1/ output059/ice/ cice_in.nml | ./gadi/g/data/ hh5/tmp/cosima/ access-om2-025/ 025deg_- jra55v13_iaf_- gmredi6/ output153/ice/ cice_in.nml | ./gadi/g/data/ hh5/tmp/cosima/ access-om2-01/ 01deg_jra55v13_- iaf/output197/ ice/cice_in.nml |
|-----------------------|-------------------|---|---|--|
| | f_apond_ai | 'm' | 'm' | 'x' |
| | f_apondn | 'x' | 'x' | 'x' |
| | f_hpond | 'm' | 'm' | 'x' |
| | f_hpond_ai | 'm' | 'm' | 'x' |
| | f_hpondn | 'x' | 'x' | 'x' |
| | f_ipond | 'm' | 'm' | 'x' |
| | f_ipond_ai | 'm' | 'm' | 'x' |
| &ponds_nml | dpscale | 0.001 | 0.001 | 0.001 |
| | frzpnnd | 'hlid' | 'hlid' | 'hlid' |
| | hp1 | 0.01 | 0.01 | 0.01 |
| | hs0 | 0.0 | 0.0 | 0.0 |
| | hs1 | 0.03 | 0.03 | 0.03 |
| | pndaspect | 0.8 | 0.8 | 0.8 |
| | rfracmax | 1.0 | 1.0 | 1.0 |
| | rfracmin | 0.15 | 0.15 | 0.15 |
| &setup_nml | days_per_year | 365 | 365 | 365 |
| | dbug | False | False | False |
| | diag_file | 'ice_diag.d' | 'ice_diag.d' | 'ice_diag.d' |
| | diag_type | 'file' | 'file' | 'file' |
| | diagfreq | 960 | 960 | 960 |
| | dt | 3600 | 1800 | 300 |
| | dump_last | True | True | True |
| | dumpfreq | 'y' | 'y' | 'm' |
| | dumpfreq_n | 1 | 1 | 3 |
| | hist_avg | True | True | True |
| | histfreq | 'd', 'm', 'x', 'x', 'x' | 'd', 'm', 'x', 'x', 'x' | 'd', 'm', 'x', 'x', 'x' |
| | histfreq_n | 1, 1, 1, 1, 1 | 1, 1, 1, 1, 1 | 1, 1, 1, 1, 1 |
| | history_dir | '/OUTPUT/' | '/OUTPUT/' | '/OUTPUT/' |
| | history_file | 'iceh' | 'iceh' | 'iceh' |
| | ice_ic | 'default' | 'default' | 'default' |
| | incond_dir | '/OUTPUT/' | '/OUTPUT/' | '/OUTPUT/' |
| | incond_file | 'iceh_ic' | 'iceh_ic' | 'iceh_ic' |
| | istep0 | 2067360 | 341496 | 3906432 |
| | latpnt | 90.0, -65.0 | 90.0, -65.0 | 66.75, 68.0 |
| | lcdf64 | False | True | True |
| | lonpnt | 0.0, -45.0 | 0.0, -45.0 | 72.5, 74.0 |
| | ndtd | 1 | 1 | 3 |
| | npt | 35 040.0 | 2232.0 | 6480 |
| | | '/RESTART/' | '/RESTART/' | '/RESTART/' |
| | pointer_file | ice.restart_file' | ice.restart_file' | ice.restart_file' |
| | print_global | False | False | False |
| | print_points | False | False | False |
| | restart | True | True | True |
| | restart_dir | '/RESTART/' | '/RESTART/' | '/RESTART/' |
| | restart_ext | False | False | False |
| | restart_file | 'iced' | 'iced' | 'iced' |
| | restart_format | 'nc' | 'nc' | 'nc' |
| | runtype | 'continue' | 'continue' | 'continue' |
| | use_leap_years | False | False | False |
| | use_restart_time | True | True | True |
| | write_ic | False | False | False |

A.3 CICE namelists

| Group (continued) | Variable | ./gadi/g/data/ hh5/tmp/cosima/ access-om2/025/ 025deg_- jra55v13_if_ - gmredi6/ output153/ice/ cice_in.nml | ./gadi/g/data/ hh5/tmp/cosima/ access-om2-025/ 025deg_- jra55v13_if_ - gmredi6/ output153/ice/ cice_in.nml | ./gadi/g/data/ hh5/tmp/cosima/ access-om2-01/ 01deg_jra55v13_- iaf/output197/ ice/cice_in.nml |
|-------------------|-------------------|---|---|--|
| | year_init | 1 | 1 | 1 |
| &shortwave_nml | ahmax | 0.1 | 0.1 | 0.1 |
| | albedo_type | 'default' | 'default' | 'default' |
| | albicei | 0.44 | 0.44 | 0.44 |
| | albicev | 0.86 | 0.86 | 0.86 |
| | albsnowi | 0.7 | 0.7 | 0.7 |
| | albsnowv | 0.98 | 0.98 | 0.98 |
| | dalb_mlt | -0.02 | -0.02 | -0.02 |
| | dt_mlt | 1.0 | 1.0 | 1.0 |
| | r_ice | 0.0 | 0.0 | 0.0 |
| | r_pnd | 0.0 | 0.0 | 0.0 |
| | r_snw | 0.0 | 0.0 | 0.0 |
| | rsnw_mlt | 1500.0 | 1500.0 | 1500.0 |
| | shortwave | 'default' | 'default' | 'default' |
| | tocnfrz | -1.8 | -1.8 | -1.8 |
| &thermo_nml | a_rapid_mode | 0.0005 | 0.0005 | 0.0005 |
| | aspect_rapid_mode | 1.0 | 1.0 | 1.0 |
| | chio | 0.004 | 0.004 | 0.004 |
| | conduct | 'bubbly' | 'bubbly' | 'bubbly' |
| | dsdt_slow_mode | -5×10^{-8} | -5×10^{-8} | -5×10^{-8} |
| | kitd | 1 | 1 | 1 |
| | ktherm | 1 | 1 | 2 |
| | phi_c_slow_mode | 0.05 | 0.05 | 0.05 |
| | phi_i_mushy | 0.85 | 0.85 | 0.85 |
| | rac_rapid_mode | 10.0 | 10.0 | 10.0 |
| &tracer_nml | restart_aero | False | False | False |
| | restart_age | False | False | False |
| | restart_fy | False | False | False |
| | restart_lvl | False | False | False |
| | restart_pond Cesm | False | False | False |
| | restart_pond lvl | False | False | False |
| | restart_pond topo | False | False | False |
| | tr_aero | False | False | False |
| | tr_fy | False | False | False |
| | tr_iage | False | False | False |
| | tr_lvl | False | False | False |
| | tr_pond Cesm | False | False | False |
| | tr_pond lvl | False | False | False |
| | tr_pond topo | False | False | False |
| &zbgc_nml | bgc_data_dir | 'unknown_bgc_- data_dir' | 'unknown_bgc_- data_dir' | 'unknown_bgc_- data_dir' |
| | bgc_flux_type | 'Jin2006' | 'Jin2006' | 'Jin2006' |
| | nit_data_type | 'default' | 'default' | 'default' |
| | phi_snow | 0.5 | 0.5 | 0.5 |
| | restart_bgc | False | False | False |
| | restart_hbrine | False | False | False |
| | restore_bgc | False | False | False |
| | sil_data_type | 'default' | 'default' | 'default' |
| | skl_bgc | False | False | False |
| | tr_bgc_am_sk | False | False | False |
| | tr_bgc_c_sk | False | False | False |
| | tr_bgc_chl_sk | False | False | False |

A.3 CICE namelists

| | | | | |
|--------------------------|-----------------|---|---|--|
| Group (continued) | Variable | . /gadi/g/data/ hh5/tmp/cosima/ access-om2/ 1deg_jra55v13_- iaf_spinup1_B1/ output059/ice/ cice_in.nml | . /gadi/g/data/ hh5/tmp/cosima/ access-om2-025/ 025deg_- jra55v13_iaf_- gmredi6/ output153/ice/ cice_in.nml | . /gadi/g/data/ hh5/tmp/cosima/ access-om2-01/ 01deg_jra55v13_- iaf/output197/ ice/cice_in.nml |
| | tr_bgc_dms_sk | False | False | False |
| | tr_bgc_dmspd_sk | False | False | False |
| | tr_bgc_dmspp_sk | False | False | False |
| | tr_bgc_sil_sk | False | False | False |
| | tr_brine | False | False | False |

A.3.2 input_ice.nml

| | | | | |
|---------------|--------------------|---|---|--|
| Group | Variable | . /gadi/g/data/ hh5/tmp/cosima/ access-om2/ 1deg_jra55v13_- iaf_spinup1_B1/ output059/ice/ input_ice.nml | . /gadi/g/data/ hh5/tmp/cosima/ access-om2-025/ 025deg_- jra55v13_iaf_- gmredi6/ output153/ice/ input_ice.nml | . /gadi/g/data/ hh5/tmp/cosima/ access-om2-01/ 01deg_jra55v13_- iaf/output197/ ice/input_ice.nml |
| &coupling_nml | chk_a2i_fields | False | False | False |
| | chk_fzmlt_sst | | False | False |
| | chk_gfdl_roughness | False | False | False |
| | chk_i2a_fields | | False | False |
| | chk_i2o_fields | | False | False |
| | chk_o2i_fields | | False | False |
| | cst_ocn_albedo | True | True | True |
| | gfdl_surface_flux | True | True | True |
| | ice_fwflux | True | True | True |
| | ice_pressure_on | True | True | True |
| | limit_icemelt | False | False | False |
| | meltlimit | -200.0 | -200.0 | -200.0 |
| | ocn_albedo | 0.1 | 0.1 | 0.1 |
| | pop_icediag | True | True | True |
| | precip_factor | 1.0 | 1.0 | 1.0 |
| | rotate_winds | True | True | True |
| | use_ocnslope | False | False | False |
| | use_umask | False | False | False |

A.3.3 input_ice_gfdl.nml

| | | | | |
|------------------|-----------------|--|--|---|
| Group | Variable | . /gadi/g/data/ hh5/tmp/cosima/ access-om2/ 1deg_jra55v13_- iaf_spinup1_B1/ output059/ice/ input_ice_gfdl.nml | . /gadi/g/data/ hh5/tmp/cosima/ access-om2-025/ 025deg_- jra55v13_iaf_- gmredi6/ output153/ice/ input_ice_gfdl.nml | . /gadi/g/data/ hh5/tmp/cosima/ access-om2-01/ 01deg_jra55v13_- iaf/output197/ ice/input_ice_gfdl.nml |
| &ocean_rough_nml | charnock | 0.032 | 0.032 | 0.032 |
| | do_cap40 | False | False | False |

A.4 YATM namelist atm.nml

| | | | | |
|------------------------------|----------------------|---------------------------|---|--|
| | | | ./gadi/g/data/ hh5/tmp/cosima/ access-om2/025/ 025deg_- jra55v13_ifa- gmredi6/ output153/ice/ ice/ | ./gadi/g/data/ hh5/tmp/cosima/ access-om2-01/ 01deg_jra55v13- iaf/output197/ ice/ |
| Group (continued) | Variable | input_ice_gfdl.nml | input_ice_gfdl.nml | input_ice_gfdl.nml |
| | do_highwind | False | False | False |
| | rough_scheme | 'beljaars' | 'beljaars' | 'beljaars' |
| | roughness_heat | 5.8×10^{-5} | 5.8×10^{-5} | 5.8×10^{-5} |
| | roughness_min | 1×10^{-6} | 1×10^{-6} | 1×10^{-6} |
| | roughness_moist | 5.8×10^{-5} | 5.8×10^{-5} | 5.8×10^{-5} |
| | roughness_mom | 5.8×10^{-5} | 5.8×10^{-5} | 5.8×10^{-5} |
| | zcoh1 | 0.0 | 0.0 | 0.0 |
| | zcoq1 | 0.0 | 0.0 | 0.0 |
| &surface_flux_nml | alt_gustiness | False | False | False |
| | gust_const | 1.0 | 1.0 | 1.0 |
| | gust_min | 0.0 | 0.0 | 0.0 |
| | ncar_ocean_flux | True | True | True |
| | ncar_ocean_flux_orig | False | False | False |
| | no_neg_q | False | False | False |
| | old_dtaudv | False | False | False |
| | raoult_sat_vap | False | False | False |
| | use_mixing_ratio | False | False | False |
| | use_virtual_temp | True | True | True |

A.3.4 input_ice_monin.nml

| | | | | |
|-------------------------------|-----------------|------|---|--|
| | | | ./gadi/g/data/ hh5/tmp/cosima/ access-om2/025/ 025deg_- jra55v13_ifa- gmredi6/ output153/ice/ ice/input_ice_- monin.nml | ./gadi/g/data/ hh5/tmp/cosima/ access-om2-01/ 01deg_jra55v13- iaf/output197/ ice/input_ice_- monin.nml |
| Group | Variable | | | |
| &monin_obukhov_nml | neutral | True | True | True |

A.4 YATM namelist atm.nml

| | | | | |
|------------------------|---------------------------|--|---|--|
| | | | ./gadi/g/data/ hh5/tmp/cosima/ access-om2/025/ 025deg_- jra55v13_ifa- gmredi6/ output153/ice/ atmosphere/ atm.nml | ./gadi/g/data/ hh5/tmp/cosima/ access-om2-01/ 01deg_jra55v13- iaf/output197/ atmosphere/ atm.nml |
| Group | Variable | | | |
| &runoff_nml | num_runoff_caps | | | 4 |
| | | 'INPUT/ rmp_jrar_to_cict_- CONSERV.nc' | 'INPUT/ rmp_jrar_to_cict_- CONSERV.nc' | 'INPUT/ rmp_jrar_to_cict_- CONSERV.nc' |
| | remap_weights_file | | | |

B.1 ACCESS-OM2 namelist `accessom2.nml`

| Group (continued) | Variable | atm.nml | atm.nml | atm.nml |
|-------------------|-----------------------------|---------|--|---------|
| | <code>runoff_caps</code> | | 0.03, 0.001, 0.003, 0.003 | |
| | <code>runoff_caps_ie</code> | | 1000000, 3530, 240, 560 | |
| | <code>runoff_caps_is</code> | | 0, 3470, 180, 300 1000000, 2650, 99999, 2470 | |
| | <code>runoff_caps_je</code> | | 0, 2270, 2670, 2260 | |
| | <code>runoff_caps_js</code> | | | |

B Namelist changes within runs

These are auto-generated by `namelists/make_tables.py` which uses `nmltab` (<https://github.com/ae kiss/nmltab>). Variables are weblinks to source code searches. Only differences are shown, and consecutive identical namelists in a run are omitted. Differences in timestep counters are ignored. Tables are omitted if there are no differences at all.

B.1 ACCESS-OM2 namelist `accessom2.nml`

| Group | Vari-able | ./gadi/g/data/ |
|---|-----------|---------------------------------|---------------------------------|---------------------------------|---------------------------------|---------------------------------|---------------------------------|---------------------------------|
| | | hh5/tmp/cosima/ |
| | | access-om2-025/ |
| | | 025deg_- |
| | | jra55v13_iaf_- |
| | | gmredi6/ |
| | | output000/ | output022/ | output078/ | output082/ | output085/ | output086/ | output086/ |
| | | accessom2.nml |
| &acc nml ice_- oce time | | 1800 | 1350 | 1800 | 1350 | 1200 | 1350 | |
| | | | | | | | | |
| &da man ager nml resta pe- riod | | 2, 0, 0 | 2, 0, 0 | 2, 0, 0 | 2, 0, 0 | 2, 0, 0 | 2, 0, 0 | |
| | | | | | | | | |

B.3 CICE namelists

| | | | | | | | |
|------------------------|--|--|--|--|--|--|--|
| | ./gadi/g/data/ hh5/tmp/cosima/ access-om2-01/ 01deg_jra55v13_- iaf/output001/ accessom2.nml | ./gadi/g/data/ hh5/tmp/cosima/ access-om2-01/ 01deg_jra55v13_- iaf/output005/ accessom2.nml | ./gadi/g/data/ hh5/tmp/cosima/ access-om2-01/ 01deg_jra55v13_- iaf/output021/ accessom2.nml | ./gadi/g/data/ hh5/tmp/cosima/ access-om2-01/ 01deg_jra55v13_- iaf/output022/ accessom2.nml | ./gadi/g/data/ hh5/tmp/cosima/ access-om2-01/ 01deg_jra55v13_- iaf/output023/ accessom2.nml | ./gadi/g/data/ hh5/tmp/cosima/ access-om2-01/ 01deg_jra55v13_- iaf/output029/ accessom2.nml | ./gadi/g/data/ hh5/tmp/cosima/ access-om2-01/ 01deg_jra55v13_- iaf/output029/ accessom2.nml |
| Group Vari- able | &acc nml ice_- ocea time | 540 | 450 | 300 | 450 | 450 | 400 |
| | &da man ager nml resta pe- riod | 0, 3, 0 | 0, 2, 0 | 0, 1, 0 | 0, 1, 0 | 0, 2, 0 | 0, 2, 0 |

B.2 MOM namelist input.nml

B.3 CICE namelists

B.3.1 cice_in.nml

Changes to `istep0` are ignored.

| | | |
|------------|---|---|
| | ./gadi/g/data/ hh5/tmp/cosima/ access-om2/ 1deg_jra55v13_- iaf_spinup1_B1/ output000/ice/ cice_in.nml | ./gadi/g/data/ hh5/tmp/cosima/ access-om2/ 1deg_jra55v13_- iaf_spinup1_B1/ output001/ice/ cice_in.nml |
| Group | Variable | Variable |
| &setup_nml | restart | False |
| | runttype | 'initial' |
| | | 'continue' |

| | | |
|------------|---|---|
| | ./gadi/g/data/ hh5/tmp/cosima/ access-om2-025/ 025deg_- jra55v13_iaf_- gmredi6/ output000/ice/ cice_in.nml | ./gadi/g/data/ hh5/tmp/cosima/ access-om2-025/ 025deg_- jra55v13_iaf_- gmredi6/ output001/ice/ cice_in.nml |
| Group | Variable | Variable |
| &setup_nml | restart | False |
| | runttype | 'initial' |
| | | 'continue' |

B.4 YATM namelist atm.nml

| Group | Variable | ./gadi/g/data/ hh5/tmp/cosima/ access-om2-01/ 01deg_jra55v13_- iaf/output001/ ice/cice_in.nml | ./gadi/g/data/ hh5/tmp/cosima/ access-om2-01/ 01deg_jra55v13_- iaf/output002/ ice/cice_in.nml | ./gadi/g/data/ hh5/tmp/cosima/ access-om2-01/ 01deg_jra55v13_- iaf/output010/ ice/cice_in.nml | ./gadi/g/data/ hh5/tmp/cosima/ access-om2-01/ 01deg_jra55v13_- iaf/output115/ ice/cice_in.nml |
|----------------|-------------------|--|--|--|--|
| &domain_nml | distribution_type | 'cartesian' | 'cartesian' | 'cartesian' | 'roundrobin' |
| | nprocs | 2000 | 2000 | 2000 | 1600 |
| &icefields_nml | f_aicen | 'd' | 'd' | 'md' | 'md' |
| | f_hs | 'm' | 'm' | 'md' | 'md' |
| | f_vicen | 'm' | 'm' | 'md' | 'md' |
| &setup_nml | use_restart_time | False | True | True | True |

B.3.2 input_ice.nml

B.3.3 input_ice_gfdl.nml

B.3.4 input_ice_monin.nml

B.4 YATM namelist atm.nml

C Namelist differences from profiling runs

These are auto-generated by namelists/make_tables.py which uses nmllib (<https://github.com/aeckiss/nmllib>). Variables are weblinks to source code searches. Only differences are shown, and duplicate identical profiling namelists are omitted. Differences in timestep counters are ignored. Tables are omitted if there are no differences at all.

*deg runs were used for MOM5 profiling, and *cice runs were used for CICE5 profiling.

C.1 ACCESS-OM2 namelist accessom2.nml

C.2 MOM namelist *input.nml*

| | | | |
|-------------------|----------------------|---------|-----------------|
| Group | | | |
| &accessom2_nml | enable_simple_timers | True | |
| &date_manager_nml | restart_period | 0, 2, 0 | 0, 2, 0 5, 0, 0 |

| | | | |
|-------------------|--------------------|--------------|---------|
| Group | | | |
| &accessom2_nml | ice_ocean_timestep | 1800 | 1350 |
| &date_manager_nml | restart_period | 0, 0, 864000 | 1, 0, 0 |

| | | | |
|-------------------|--------------------|-------------|---------|
| Group | | | |
| &accessom2_nml | ice_ocean_timestep | 400 | 450 |
| &date_manager_nml | restart_period | 0, 0, 86400 | 0, 2, 0 |

C.2 MOM namelist *input.nml*

C.2 MOM namelist input.nml

| Group | ./gadi/g/data/ hh5/tmp/cosima/ rajin-short- public/mxw900/ home/mxw157/ om2bench/1deg/ 1deg_216p/ ocean/input.nml | ./gadi/g/data/ hh5/tmp/cosima/ rajin-short- public/mxw900/ home/mxw157/ om2bench/1deg/ 1deg_60p/ocean/ input.nml | ./gadi/g/data/ hh5/tmp/cosima/ rajin-short- public/mxw900/ home/mxw157/ om2bench/1deg/ 1deg_407p/ ocean/input.nml | ./gadi/g/data/ hh5/tmp/cosima/ rajin-short- public/mxw900/ home/mxw157/ om2bench/1deg/ 1deg_116p/ ocean/input.nml | ./gadi/g/data/ hh5/tmp/cosima/ rajin-short- public/mxw900/ home/mxw157/ om2bench/1deg/ 1deg_784p/ ocean/input.nml | ./gadi/g/data/ hh5/tmp/cosima/ access-om2/ public/mxw900/ home/mxw157/ 1deg_jra55v13_- iaf_spinup1_B1/ output059/ocean/ input.nml |
|--|--|---|--|--|--|---|
| Vari- able | | | | | | |
| &au: ice_ nml red- sea_ gulf- bay_ sfix | True | True | True | True | True | False |
| &fm io_- nml chec sum_ re- quire | False | False | False | False | False | |
| &fm nml do- mair stack size | 115200 | 115200 | 152000 | 115200 | 152000 | 115200 |
| &oci mod nml io_- lay- out | 4, 3 | 3, 2 | 6, 4 | 3, 2 | 8, 6 | 4, 3 |
| lay- out | 16, 15 | 6, 10 | 24, 20 | 12, 10 | 32, 30 | 16, 15 |
| &oci sbc_- nml max_ delta: salin ity_- re- store | 0.5 | 0.5 | 0.5 | 0.5 | 0.5 | -0.5 |
| salt_- re- store tscl | 60.0 | 60.0 | 60.0 | 60.0 | 60.0 | 21.28 |

C.2 MOM namelist input.nml

| | | | | | | | |
|----------------|---|--|---|--|--|---|---|
| | ./gadi/g/data/ hh5/tmp/cosima/ rajin-short- public/mxw900/ home/mxw157/ om2bench/ 025deg/025deg - 213p/ocean/ input.nml | ./gadi/g/data/ hh5/tmp/cosima/ rajin-short- public/mxw900/ home/mxw157/ om2bench/ 025deg/025deg - 5425p/ocean/ input.nml | ./gadi/g/data/ hh5/tmp/cosima/ rajin-short- public/mxw900/ home/mxw157/ om2bench/ 025deg/025deg - 395p/ocean/ input.nml | ./gadi/g/data/ hh5/tmp/cosima/ rajin-short- public/mxw900/ home/mxw157/ om2bench/ 025deg/025deg - 1455p/ocean/ input.nml | ./gadi/g/data/ hh5/tmp/cosima/ rajin-short- public/mxw900/ home/mxw157/ om2bench/ 025deg/025deg - 2801p/ocean/ input.nml | ./gadi/g/data/ hh5/tmp/cosima/ rajin-short- public/mxw900/ home/mxw157/ om2bench/ 025deg/025deg - 761p/ocean/ input.nml | ./gadi/g/data/ hh5/tmp/cosima/ rajin-short- public/mxw900/ home/mxw157/ om2bench/ 025deg/025deg - 10634p/ input.nml |
| Group Variable | &fm io_nml check sum require | False | False | False | False | False | False |
| | &oci mod nml io_lay- out | 4, 5 | 12, 10 | 4, 5 | 6, 5 | 8, 6 | 4, 5 |
| | lay- out | 16, 15 | 96, 80 | 24, 20 | 48, 40 | 64, 60 | 32, 30 |
| | &oci sbc_nml salt_ re- store tscl | 60.0 | 60.0 | 60.0 | 60.0 | 60.0 | 60.0 |
| | | | | | | | 1 |
| | ./gadi/g/data/ hh5/tmp/cosima/ rajin-short- public/mxw900/ home/mxw157/ om2bench/01deg/ 01deg_8489p/ ocean/input.nml | ./gadi/g/data/ hh5/tmp/cosima/ rajin-short- public/mxw900/ home/mxw157/ om2bench/01deg/ 01deg_2245p/ ocean/input.nml | ./gadi/g/data/ hh5/tmp/cosima/ rajin-short- public/mxw900/ home/mxw157/ om2bench/01deg/ 01deg_4358p/ ocean/input.nml | ./gadi/g/data/ hh5/tmp/cosima/ rajin-short- public/mxw900/ home/mxw157/ om2bench/01deg/ 01deg_16577p/ ocean/input.nml | ./gadi/g/data/ hh5/tmp/cosima/ rajin-short- public/mxw900/ home/mxw157/ om2bench/01deg/ 01deg_619p/ ocean/input.nml | ./gadi/g/data/ hh5/tmp/cosima/ rajin-short- public/mxw900/ home/mxw157/ om2bench/01deg/ 01deg_1180p/ ocean/input.nml | ./gadi/g/data/ hh5/tmp/cosima/ rajin-short- public/mxw900/ home/mxw157/ om2bench/ 01deg_3/ ocean/input.nml |
| Group Variable | &oci mod nml io_lay- out | 25, 16 | 6, 5 | 5, 5 | 16, 15 | 5, 5 | 3, 5 |
| | lay- out | 125, 96 | 60, 50 | 80, 75 | 160, 150 | 30, 25 | 30, 50 |
| | | | | | | | 2 |

C.3 CICE namelists

C.3.1 cice_in.nml

Changes to `istep0` are ignored.

| Group Vari- able | <code>./gadi/g/data/ hh5/tmp/cosima/ rajin-short- public/mxw900/ home/mxw157/ om2bench/1cice/ 1cice_24p/ice/ cice_in.nml</code> | <code>./gadi/g/data/ hh5/tmp/cosima/ rajin-short- public/mxw900/ home/mxw157/ om2bench/1cice/ 1cice_180p/ice/ cice_in.nml</code> | <code>./gadi/g/data/ hh5/tmp/cosima/ rajin-short- public/mxw900/ home/mxw157/ om2bench/1cice/ 1cice_45p/ice/ cice_in.nml</code> | <code>./gadi/g/data/ hh5/tmp/cosima/ rajin-short- public/mxw900/ home/mxw157/ om2bench/1cice/ 1cice_90p/ice/ cice_in.nml</code> | <code>./gadi/g/data/ hh5/tmp/cosima/ rajin-short- public/mxw900/ home/mxw157/ om2bench/1cice/ 1cice_12p/ice/ cice_in.nml</code> | <code>./gadi/g/data/ hh5/tmp/cosima/ rajin-short- public/mxw900/ home/mxw157/ om2bench/1cice/ 1cice_6p/ice/ cice_in.nml</code> | <code>./gadi/g/data/ hh5/tmp/cosima/ rajin-short- public/mxw900/ home/mxw157/ om2bench/1cice/ 1cice_36p/ice</code> |
|---|---|--|---|---|---|--|--|
| <code>&do nml npro</code> | 24 | 180 | 45 | 90 | 12 | 6 | |
| <code>&dyi nml cosw</code> | 0.96 | 0.96 | 0.96 | 0.96 | 0.96 | 0.96 | |
| <code>sinw</code> | 0.28 | 0.28 | 0.28 | 0.28 | 0.28 | 0.28 | |
| <code>&set nml di- agfre</code> | 24 | 24 | 24 | 24 | 24 | 24 | |
| <code>resta</code> | False | False | False | False | False | False | |
| <code>runt</code> | 'initial' | 'initial' | 'initial' | 'initial' | 'initial' | 'initial' | |

| Group Vari- able | <code>./gadi/g/data/ hh5/tmp/cosima/ rajin-short- public/mxw900/ home/mxw157/ om2bench/ 025cice/025cice - 1206p/ice/ cice_in.nml</code> | <code>./gadi/g/data/ hh5/tmp/cosima/ rajin-short- public/mxw900/ home/mxw157/ om2bench/ 025cice/025cice - 190p/ice/ cice_in.nml</code> | <code>./gadi/g/data/ hh5/tmp/cosima/ rajin-short- public/mxw900/ home/mxw157/ om2bench/ 025cice/025cice - 99p/ice/ cice_in.nml</code> | <code>./gadi/g/data/ hh5/tmp/cosima/ rajin-short- public/mxw900/ home/mxw157/ om2bench/ 025cice/025cice - 361p/ice/ cice_in.nml</code> | <code>./gadi/g/data/ hh5/tmp/cosima/ rajin-short- public/mxw900/ home/mxw157/ om2bench/ 025cice/025cice - 2212p/ice/ cice_in.nml</code> | <code>./gadi/g/data/ hh5/tmp/cosima/ rajin-short- public/mxw900/ home/mxw157/ om2bench/ 025cice/025cice - 697p/ice/ cice_in.nml</code> | <code>./gadi/g/data/ hh5/tmp/cosima/ rajin-short- public/mxw900/ home/mxw157/ om2bench/ jra5v1 gr output1 cice</code> |
|---|---|--|---|--|---|--|---|
| <code>&do nml dis- tri- bu- tion_ type</code> | 'sectrobin' | 'sectrobin' | 'sectrobin' | 'sectrobin' | 'sectrobin' | 'sectrobin' | 'rou |
| <code>npro</code> | 1206 | 190 | 99 | 361 | 2212 | 697 | |

C.3 CICE namelists

| | ./gadi/g/data/ hh5/tmp/cosima/ rajin-short- public/mxw900/ home/mxw157/ om2bench/ 025cice/025cice_- 1206p/ice/ cice_in.nml | ./gadi/g/data/ hh5/tmp/cosima/ rajin-short- public/mxw900/ home/mxw157/ om2bench/ 025cice/025cice_- 190p/ice/ cice_in.nml | ./gadi/g/data/ hh5/tmp/cosima/ rajin-short- public/mxw900/ home/mxw157/ om2bench/ 025cice/025cice_- 99p/ice/ cice_in.nml | ./gadi/g/data/ hh5/tmp/cosima/ rajin-short- public/mxw900/ home/mxw157/ om2bench/ 025cice/025cice_- 361p/ice/ cice_in.nml | ./gadi/g/data/ hh5/tmp/cosima/ rajin-short- public/mxw900/ home/mxw157/ om2bench/ 025cice/025cice_- 2212p/ice/ cice_in.nml | ./gadi/g/data/ hh5/tmp/cosima/ rajin-short- public/mxw900/ home/mxw157/ om2bench/ 025cice/025cice_- 697p/ice/ cice_in.nml | ./gadi/g/data/ hh5/tmp/cosima/ rajin-short- public/mxw900/ home/mxw157/ om2bench/ 025cice/025cice_- jra55v1 gr output1 cice |
|--------------------------------|--|---|--|---|--|---|---|
| Group (con- tin- ued) | | | | | | | |
| Vari- able | | | | | | | |
| &ice | 'x' | 'x' | 'x' | 'x' | 'x' | 'x' | 'x' |
| mecl | | | | | | | |
| nml | | | | | | | |
| f_- oper- ing | | | | | | | |
| &ice | 'x' | 'x' | 'x' | 'x' | 'x' | 'x' | 'x' |
| nml | | | | | | | |
| f_- fmel | | | | | | | |
| ai | | | | | | | |
| f_- fsalt | 'm' | 'm' | 'm' | 'm' | 'm' | 'm' | 'm' |
| ai | | | | | | | |
| f_- sig1 | 'x' | 'x' | 'x' | 'x' | 'x' | 'x' | 'x' |
| f_- sig2 | 'x' | 'x' | 'x' | 'x' | 'x' | 'x' | 'x' |
| f_- sss | 'm' | 'm' | 'm' | 'm' | 'm' | 'm' | 'm' |
| f_- sst | 'm' | 'm' | 'm' | 'm' | 'm' | 'm' | 'm' |
| f_- uocn | 'm' | 'm' | 'm' | 'm' | 'm' | 'm' | 'm' |
| f_- vocn | 'm' | 'm' | 'm' | 'm' | 'm' | 'm' | 'm' |
| &set | False | False | False | False | False | False | False |
| nml | | | | | | | |
| resta | | | | | | | |
| runt | 'initial' | 'initial' | 'initial' | 'initial' | 'initial' | 'initial' | 'initial' |

C.4 YATM namelist atm.nml

| Group Vari- able | ./gadi/g/data/ hh5/tmp/cosima/ rajin-short- public/mxw900/ home/mxw157/ om2bench/ 01cice/01cice_- 11935p/ice/ cice_in.nml | ./gadi/g/data/ hh5/tmp/cosima/ rajin-short- public/mxw900/ home/mxw157/ om2bench/ 01cice/01cice_- 428p/ice/ cice_in.nml | ./gadi/g/data/ hh5/tmp/cosima/ rajin-short- public/mxw900/ home/mxw157/ om2bench/ 01cice/01cice_- 1600p/ice/ cice_in.nml | ./gadi/g/data/ hh5/tmp/cosima/ rajin-short- public/mxw900/ home/mxw157/ om2bench/ 01cice/01cice_- 828p/ice/ cice_in.nml | ./gadi/g/data/ hh5/tmp/cosima/ rajin-short- public/mxw900/ home/mxw157/ om2bench/ 01cice/01cice_- 3116p/ice/ cice_in.nml | ./gadi/g/data/ hh5/tmp/cosima/ rajin-short- public/mxw900/ home/mxw157/ om2bench/ 01cice/01cice_- 6077p/ice/ cice_in.nml | ./gadi/ hh5/tmp/ access- 01deg_jra5 iaf/outp ice/cice |
|--|---|---|--|---|--|--|--|
| &do nml dis- tri- bu- tion_ type | 'sectrobin' | 'sectrobin' | 'sectrobin' | 'sectrobin' | 'sectrobin' | 'sectrobin' | 'rou |
| npro | 11935 | 428 | 1600 | 828 | 3116 | 6077 | |
| &set nml resta | False | False | False | False | False | False | |
| runt) | 'initial' | 'initial' | 'initial' | 'initial' | 'initial' | 'initial' | 'co |

C.3.2 input_ice.nml

C.3.3 input_ice_gfdl.nml

C.3.4 input_ice_monin.nml

C.4 YATM namelist atm.nml

D Namelist differences between old and new configs

These are auto-generated by namelists/make_tables.py which uses nmltab (<https://github.com/aeckiss/nmltab>). Variables are weblinks to source code searches. Only differences are shown, and duplicate identical profiling

D.1 ACCESS-OM2 namelist `accessom2.nml`

namelists are omitted. Differences in timestep counters are ignored. Tables are omitted if there are no differences at all.

D.1 ACCESS-OM2 namelist `accessom2.nml`

| Group | Variable | ./gadi/g/ data/ hh5/tmp/ cosima/ access- om2/ 1deg_- jra55v13_- iaf_- spinup1_- B1/ output059/ accessom2.nml | github.com/ COSIMA/ 1deg_- jra55_iaf/ accessom2.nml | github.com/ COSIMA/ 1deg_- jra55_rjf/ accessom2.nml |
|-------------------|--------------------|--|---|---|
| &date_manager_nml | forcing_end_date | '2018-01- 01T00:00:0(| '2019-01- 01T00:00:0(| '1901-01- 01T00:00:00' |
| | forcing_start_date | '1958-01- 01T00:00:0(| '1958-01- 01T00:00:0(| '1900-01- 01T00:00:00' |

| Group | Variable | ./gadi/g/ data/ hh5/tmp/ cosima/ access- om2- 025/ 025deg_- jra55v13_- iaf_gm- redi6/ output153/ accessom2.nml | github.com/ COSIMA/ 025deg_- jra55_iaf/ accessom2.nml | github.com/ COSIMA/ 025deg_- jra55_rjf/ accessom2.nml |
|-------------------|--------------------|--|---|---|
| &date_manager_nml | forcing_end_date | '2018-01- 01T00:00:0(| '2019-01- 01T00:00:0(| '1901-01- 01T00:00:00' |
| | forcing_start_date | '1958-01- 01T00:00:0(| '1958-01- 01T00:00:0(| '1900-01- 01T00:00:00' |
| | restart_period | 1, 0, 0 | 2, 0, 0 | 2, 0, 0 |

D.2 MOM namelist *input.nml*

| Group | Variable | ./gadi/g/ data/ hh5/tmp/ cosima/ access- om2-01/ 01deg_- jra55v13_- iaf/ output197/ &accessom2_nml | ./gadi/g/ data/ hh5/tmp/ cosima/ access- om2-01/ 01deg_- jra55v13_- ryf9091/ output675/ &accessom2_nml | github.com/ COSIMA/ 01deg_- 01deg_- &accessom2_nml | github.com/ COSIMA/ 01deg_- 01deg_- &accessom2_nml |
|-------------------|--------------------|--|--|--|--|
| &date_manager_nml | ice_ocean_timestep | 450 | 540 | 300 | 300 |
| | forcing_end_date | '2018-01-01T00:00:00' | '1901-01-01T00:00:00' | '2019-01-01T00:00:00' | '1901-01-01T00:00:00' |
| | forcing_start_date | '1985-01-01T00:00:00' | '1900-01-01T00:00:00' | '1958-01-01T00:00:00' | '1900-01-01T00:00:00' |
| | restart_period | 0, 2, 0 | 0, 3, 0 | 0, 3, 0 | 0, 3, 0 |

D.2 MOM namelist input.nml

| Group | Variable | max_axes | 400 | 400 | |
|---------------------------|---------------------|--|---|---|--|
| &diag_manager_nml | max_files | 200 | 200 | | |
| | max_num_axis_sets | 200 | 200 | | |
| | | 'u_flux', 'v_flux', 'u_flux', 'lprec', 'v_flux', 'fprec', 'lprec', 'salt_flux', 'fprec', 'salt_flux', 'mh_flux', 'sw_flux', 'mh_flux', 'sw_flux', 'q_flux', 'sw_flux', 't_flux', 'q_flux', 'lw_flux', 't_flux', 'runof', 'p', 'lw_flux', 'runof', 'p', 'aice', 'runof', 'p', 'aice', 'wfimelt', 'aice', 'wfimelt', 'wfiform', 'wfiform', 'licefw', 'wfiform', 'licefw', 'licehf' | 'u_flux', 'v_flux', 'u_flux', 'lprec', 'v_flux', 'fprec', 'lprec', 'salt_flux', 'fprec', 'salt_flux', 'mh_flux', 'sw_flux', 'mh_flux', 'sw_flux', 'q_flux', 't_flux', 'q_flux', 'lw_flux', 't_flux', 'runof', 'p', 'aice', 'runof', 'p', 'aice', 'wfimelt', 'aice', 'wfimelt', 'wfiform', 'wfiform', 'licefw', 'wfiform', 'licefw', 'licehf' | 'u_flux', 'v_flux', 'u_flux', 'lprec', 'v_flux', 'fprec', 'lprec', 'salt_flux', 'fprec', 'salt_flux', 'mh_flux', 'sw_flux', 'mh_flux', 'sw_flux', 'q_flux', 't_flux', 'q_flux', 'lw_flux', 't_flux', 'runof', 'p', 'aice', 'runof', 'p', 'aice', 'wfimelt', 'aice', 'wfimelt', 'wfiform', 'wfiform', 'licefw', 'wfiform', 'licefw', 'licehf' | |
| &mom_oasis3_interface_nml | fields_in | | | | |
| | num_fields_in | 15 | 17 | 17 | |
| &monin_obukhov_nml | neutral | True | | | |
| &mpp_io_nml | deflate_level | 5 | -1 | -1 | |
| &ocean_albedo_nml | ocean_albedo_option | 2 | | | |

| Group | Variable | Value | Description | Description | Description |
|----------------------------|-----------------------------|--------|--|--|--|
| &diag_manager_nml | debug_diag_manager | True | False | False | ./gadi/g/ data/ hh5/tmp/ cosima/ access- om2- 025/ 025deg_- jra55v13_- |
| | max_axes | | 400 | 400 | github.com/ COSIMA/ COSIMA/ |
| | max_files | | 200 | 200 | 025deg_- |
| | max_num_axis_sets | | 200 | 200 | output153/ jra55_if/ jra55_rf/ ocean/ ocean/ ocean/ input.nml input.nml input.nml |
| &mom_oasis3_interface_nml | fields_in | | 'u_flux', 'v_flux', 'u_flux', 'v_flux', 'lprec', 'fprec', 'salt_flex', 'mh_flux', 'salt_flex', 'sw_flux', 'mh_flux', 'q_flux', 'sw_flux', 't_flux', 'q_flux', 'lw_flux', 't_flux', 'runof', 'p', 'lw_flux', 'runof', 'p', 'runof', 'p', 'aice', 'wfilmet', 'aice', 'wfilmet', 'wfilmet', 'wfilmet', 'licefw', 'wfilmet', 'liceht' | 'u_flux', 'v_flux', 'lprec', 'fprec', 'salt_flex', 'mh_flux', 'sw_flux', 'q_flux', 't_flux', 'lw_flux', 't_flux', 'runof', 'p', 'aice', 'wfilmet', 'wfilmet', 'wfilmet', 'wfilmet', 'licefw', 'wfilmet', 'liceht' | 'u_flux', 'v_flux', 'lprec', 'fprec', 'salt_flex', 'mh_flux', 'sw_flux', 'q_flux', 't_flux', 'lw_flux', 't_flux', 'runof', 'p', 'aice', 'wfilmet', 'wfilmet', 'wfilmet', 'wfilmet', 'licefw', 'wfilmet', 'liceht' |
| | num_fields_in | 15 | 17 | 17 | |
| &monin_obukhov_nml | neutral | True | | | |
| &ocean_albedo_nml | ocean_albedo_option | 2 | | | |
| &ocean_barotropic_nml | debug_this_module | False | | | |
| &ocean_bbc_nml | cdbot | 0.001 | | | |
| | cdbot_roughness_length | | False | | |
| | use_geothermal_heating | | False | | |
| &ocean_bihgen_friction_nml | ncar_boundary_scaling | True | False | False | |
| &ocean_density_nml | neutralrho_max | 1030.0 | 1038.0 | 1038.0 | |
| | neutralrho_min | 1020.0 | 1028.0 | 1028.0 | |
| &ocean_frazil_nml | debug_this_module | False | | | |
| &ocean_grids_nml | debug_this_module | False | | | |
| &ocean_nphysics_nml | debug_this_module | False | | | |
| &ocean_nphysics_util_nml | agm | 200.0 | | | |
| | agm_closure_eden_gamma | 0.0 | | | |
| | agm_closure_eden_greatbatch | False | | | |
| | agm_closure_length_bczone | False | | | |
| | agm_closure_length_fixed | False | | | |
| | agm_closure_length_rossby | False | | | |
| | agm_damping_time | 45.0 | | | |
| | agm_smooth_space | False | | | |
| | agm_smooth_time | False | | | |
| | drhodz_mom4p1 | False | True | True | |
| | drhodz_smooth_horz | | False | | |

D.2 MOM namelist *input.nml*

| Group (continued) | Variable | ./gadi/g/ data/ hh5/tmp/ cosima/ access- om2- 025/ 025deg_- jra55v13_- iaf_gm- redi6/ output153/ ocean/ input.nml | github.com/ COSIMA/ 025deg_- jra55_iaf/ ocean/ input.nml | github.com/ COSIMA/ 025deg_- jra55_rf/ ocean/ input.nml |
|---------------------------|-----------------------|--|---|--|
| | drhodz_smooth_vert | False | | |
| | rossby_radius_max | 100 000.0 | | |
| | rossby_radius_min | 10 000.0 | | |
| | tracer_mix_micom | False | | |
| | vel_micom | 0.0 | | |
| &ocean_nphysicsc_nml | debug_this_module | False | | |
| &ocean_operators_nml | use_legacy_div_ud | False | | |
| &ocean_overexchange_nml | debug_this_module | False | | |
| | overexch_npts | 4 | | |
| | overexch_weight_far | False | | |
| | overflow_umax | 5.0 | | |
| &ocean_polar_filter_nml | use_this_module | False | | |
| &ocean_pressure_nml | zero_pressure_force | False | | |
| &ocean_rivermix_nml | debug_this_module | False | | |
| &ocean_sbc_nml | ocean_ice_salt_limit | | 0.006 | 0.006 |
| &ocean_shortwave_gfdl_nml | debug_this_module | False | | |
| | zmax_pen | 300.0 | 1 000 000.0 | 1 000 000.0 |
| &ocean_submesoscale_nml | debug_this_module | False | | |
| &ocean_tempsalt_nml | debug_this_module | False | | |
| | pottemp_equal_contemp | True | | |
| &ocean_thickness_nml | debug_this_module | False | | |
| &ocean_topog_nml | min_thickness | | 0.001 | 0.001 |
| &ocean_tracer_advect_nml | debug_this_module | False | | |
| &ocean_tracer_nml | debug_this_module | False | | |
| &ocean_velocity_diag_nml | debug_this_module | False | | |
| &ocean_vert_kpp_iow_nml | use_this_module | False | | |

| Group | Variable | ./gadi/g/ data/ hh5/tmp/ cosima/ access- om2-01/ 01deg_- jra55v13_- iaf/ output197/ ocean/ input.nml | ./gadi/g/ data/ hh5/tmp/ cosima/ access- om2-01/ 01deg_- jra55v13_- iaf/ ryf9091/ output675/ ocean/ input.nml | github.com/ COSIMA/ 01deg_- jra55_iaf/ ryf9091/ jra55_iwf/ ocean/ input.nml | github.com/ COSIMA/ 01deg_- jra55_rf/ jra55_iwf/ ocean/ input.nml |
|-------------------|--------------------|---|---|--|---|
| &diag_manager_nml | debug_diag_manager | True | False | False | False |
| | max_axes | | 400 | 400 | |
| | max_files | | 200 | 200 | |
| | max_num_axis_sets | | 200 | 200 | |

| Group (continued) | Variable | ./gadi/g/ data/ hh5/tmp/ cosima/ access- om2-01/ 01deg_- jra55v13_- iaf/ output197/ ocean/ input.nml | ./gadi/g/ data/ hh5/tmp/ cosima/ access- om2-01/ 01deg_- jra55v13_- iaf/ output675/ ocean/ input.nml | github.com/ COSIMA/ 01deg_- jra55_iaf/ ocean/ input.nml | github.com/ COSIMA/ 01deg_- jra55_rf/ ocean/ input.nml |
|-------------------------------|---------------------------|---|---|---|---|
| | | 'u_flux', 'v_flux', 'lprec', 'fprec', 'salt_flux', 'mh_flux', 'sw_flux', 'q_flux', 't_flux', 'lw_flux', 'runof', 'p', 'aice', 'wfmelt', 'wform', 'wfmelt', 'wform', 'licefw', 'liceht' | 'u_flux', 'v_flux', 'lprec', 'fprec', 'salt_flux', 'mh_flux', 'sw_flux', 'q_flux', 't_flux', 'lw_flux', 'runof', 'p', 'aice', 'wfmelt', 'wform', 'wfmelt', 'wform', 'licefw', 'liceht' | 'u_flux', 'v_flux', 'lprec', 'fprec', 'salt_flux', 'mh_flux', 'sw_flux', 'q_flux', 't_flux', 'lw_flux', 'runof', 'p', 'aice', 'wfmelt', 'wform', 'wfmelt', 'wform', 'licefw', 'liceht' | 'u_flux', 'v_flux', 'lprec', 'fprec', 'salt_flux', 'mh_flux', 'sw_flux', 'q_flux', 't_flux', 'lw_flux', 'runof', 'p', 'aice', 'wfmelt', 'wform', 'wfmelt', 'wform', 'licefw', 'liceht' |
| &mom_oasis3_interface_nml | fields_in | | | 15 | 15 |
| | num_fields_in | | | 15 | 17 |
| &monin_obukhov_nml | neutral | | | True | True |
| &ocean_advection_velocity_nml | max_advection_velocity | | | 0.3 | 0.2 |
| &ocean_albedo_nml | ocean_albedo_option | | | 2 | 2 |
| &ocean_barotropic_nml | debug_this_module | | | False | False |
| &ocean_bbc_nml | cdbot | | | 0.001 | 0.001 |
| | cdbot_roughness_length | | | False | False |
| | use_geothermal_heating | | | False | False |
| &ocean_bihgen_friction_nml | ncar_boundary_scaling | | | True | True |
| &ocean_density_nml | neutralrho_max | | | 1030.0 | 1038.0 |
| | neutralrho_min | | | 1020.0 | 1028.0 |
| &ocean_frazil_nml | debug_this_module | | | False | False |
| &ocean_grids_nml | debug_this_module | | | False | False |
| &ocean_nphysics_nml | debug_this_module | | | False | False |
| &ocean_nphysics_util_nml | agm | | | 100.0 | 100.0 |
| | agm_closure | | | True | True |
| | agm_closure_baroclinic | | | True | True |
| | agm_closure_buoy_freq | | | 0.004 | 0.004 |
| | agm_closure_length | | | 50 000.0 | 50 000.0 |
| | agm_closure_length_bczone | | | False | False |
| | agm_closure_length_fixed | | | False | False |
| | agm_closure_length_rossby | | | False | False |
| | agm_closure_lower_depth | | | 2000.0 | 2000.0 |
| | agm_closure_max | | | 600.0 | 600.0 |
| | agm_closure_min | | | 100.0 | 100.0 |
| | agm_closure_scaling | | | 0.07 | 0.07 |
| | agm_closure_upper_depth | | | 100.0 | 100.0 |
| | aredi | | | 600.0 | 600.0 |
| | aredi_equal_agm | | | False | False |
| | drhodz_mom4p1 | | | False | False |
| | drhodz_smooth_horz | | | False | False |

D.3 CICE namelists

| | | | | | |
|---------------------------|-----------------|---|---|---|---|
| | | ./gadi/g/ data/ hh5/tmp/ cosima/ access- om2-01/ 01deg_- jra55v13_- iaf/ output197/ ocean/ input.nml | ./gadi/g/ data/ hh5/tmp/ cosima/ access- om2-01/ 01deg_- jra55v13_- ryf9091/ output675/ ocean/ input.nml | github.com/ COSIMA/ 01deg_- jra55_if/ ocean/ input.nml | github.com/ COSIMA/ 01deg_- jra55_rf/ ocean/ input.nml |
| Group (continued) | Variable | drhodz_smooth_vert | False | False | |
| | | rossby_radius_max | 100 000.0 | 100 000.0 | |
| | | rossby_radius_min | 15 000.0 | 15 000.0 | |
| | | tracer_mix_micom | False | False | |
| | | vel_micom | 0.0 | 0.0 | |
| &ocean_operators_nml | | use_legacy_div_ud | False | False | |
| &ocean_overexchange_nml | | debug_this_module | False | False | |
| | | overexch_npts | 4 | 4 | |
| | | overexch_weight_far | False | False | |
| | | overflow_umax | 5.0 | 5.0 | |
| &ocean_polar_filter_nml | | use_this_module | False | False | |
| &ocean_pressure_nml | | zero_pressure_force | False | False | |
| &ocean_rivermix_nml | | debug_this_module | False | False | |
| &ocean_riverspread_nml | | debug_this_module | False | False | |
| &ocean_shortwave_gfdl_nml | | debug_this_module | False | False | |
| | | zmax_pen | 300.0 | 300.0 | 1 000 000.0 1 000 000.0 |
| &ocean_submesoscale_nml | | debug_this_module | False | False | |
| &ocean_tempsalt_nml | | debug_this_module | False | False | |
| | | pottemp_equal_contemp | True | 'potential_- temperature_variable | 'conservative 'temp' 'temp' |
| | | debug_this_module | False | 'temp' | 'temp' |
| &ocean_thickness_nml | | min_thickness | 1.0 | 0.001 | 0.001 |
| &ocean_topog_nml | | debug_this_module | False | False | |
| &ocean_tracer_advect_nml | | debug_this_module | False | False | |
| &ocean_tracer_nml | | debug_this_module | False | False | |
| &ocean_velocity_diag_nml | | debug_this_module | False | False | |
| &ocean_vert_kpp_iow_nml | | use_this_module | False | False | |
| &ocean_vert_mix_nml | | j09_bgmax | 1×10^{-6} | 1×10^{-6} | 1×10^{-6} |
| | | j09_bgmin | 1×10^{-6} | 1×10^{-6} | 1×10^{-6} |
| | | j09_diffusivity | True | True | True |
| | | j09_lat | 20.0 | 20.0 | 20.0 |

D.3 CICE namelists

D.3.1 cice_in.nml

| | | | | |
|------------------------|----------------|-----------------------|--|-------------|
| | | | ./gadi/g/ data/ hh5/tmp/ cosima/ access- om2/ 1deg_- jra55v13_- | |
| | | iaf_- | github.com/ | github.com/ |
| | | spinup1_- | COSIMA/ | COSIMA/ |
| | | B1/ | 1deg_- | 1deg_- |
| | | output059/ | jra55_iaf/ | jra55_rvf/ |
| | | ice/cice_- | ice/cice_- | ice/cice_- |
| | | in.nml | in.nml | in.nml |
| Group | | Variable | | |
| &forcing_nml | | highfreq | True | True |
| &icefields_bgc_nml | | f_fbri | 'm' | 'x' |
| | | f_hbri | 'm' | 'x' |
| &icefields_mechred_nml | | f_opening | 'x' | 'm' |
| &icefields_nml | | f_aice | 'm' | 'md' |
| | | f_congel | 'm' | 'md' |
| | | f_dvidtd | 'm' | 'md' |
| | | f_dvidtt | 'm' | 'md' |
| | | f_fmeltt_ai | 'x' | 'm' |
| | | f_frazil | 'm' | 'md' |
| | | f_frz_onset | 'm' | 'x' |
| | | f_frzmlt | 'm' | 'md' |
| | | f_fsalt | 'x' | 'm' |
| | | f_hi | 'm' | 'md' |
| | | f_hs | 'm' | 'md' |
| | | f_mlt_onset | 'm' | 'x' |
| | | f_snoise | 'm' | 'md' |
| | | f_sss | 'm' | 'x' |
| | | f_sst | 'm' | 'x' |
| | | f_uocn | 'm' | 'x' |
| | | f_uvel | 'm' | 'md' |
| | | f_vocn | 'm' | 'x' |
| | | f_vvel | 'm' | 'md' |
| &icefields_pond_nml | | f_apeff | 'm' | 'x' |
| | | f_apeff_ai | 'm' | 'x' |
| | | f_apond | 'm' | 'x' |
| | | f_apond_ai | 'm' | 'x' |
| | | f_hp pond | 'm' | 'x' |
| | | f_hp pond_ai | 'm' | 'x' |
| | | f_ipond | 'm' | 'x' |
| | | f_ipond_ai | 'm' | 'x' |
| &setup_nml | | history_chunksize_x | 180 | 180 |
| | | history_chunksize_y | 150 | 150 |
| | | history_deflate_level | 1 | 1 |
| | istep0 | 2067360 | 0 | 0 |
| | Lcdf64 | False | | |
| | restart | True | False | False |
| | restart_format | 'nc' | | |
| | runtype | 'continue' | 'initial' | 'initial' |

| | | | | |
|---------------------|-----------------------|------------|-----------|-----------|
| | | | | |
| Group | Variable | | | |
| &forcing_nml | highfreq | | True | True |
| &icefields_bgc_nml | f_fbri | 'm' | 'x' | 'x' |
| | f_hbri | 'm' | 'x' | 'x' |
| &icefields_nml | f_aice | 'm' | 'md' | 'md' |
| | f_congel | 'm' | 'md' | 'md' |
| | f_dvidtd | 'm' | 'md' | 'md' |
| | f_dvidtt | 'm' | 'md' | 'md' |
| | f_frazil | 'm' | 'md' | 'md' |
| | f_frz_onset | 'm' | 'x' | 'x' |
| | f_frzmlt | 'm' | 'md' | 'md' |
| | f_fsalt | 'x' | 'm' | 'm' |
| | f_fsalt_ai | 'x' | 'm' | 'm' |
| | f_hi | 'm' | 'md' | 'md' |
| | f_hs | 'm' | 'md' | 'md' |
| | f_mlt_onset | 'm' | 'x' | 'x' |
| | f_sig1 | 'm' | 'x' | 'x' |
| | f_sig2 | 'm' | 'x' | 'x' |
| | f_snoise | 'm' | 'md' | 'md' |
| | f_uvel | 'm' | 'md' | 'md' |
| | f_vvel | 'm' | 'md' | 'md' |
| &icefields_pond_nml | f_apeff | 'm' | 'x' | 'x' |
| | f_apeff_ai | 'm' | 'x' | 'x' |
| | f_apond | 'm' | 'x' | 'x' |
| | f_apond_ai | 'm' | 'x' | 'x' |
| | f_hp pond | 'm' | 'x' | 'x' |
| | f_hp pond_ai | 'm' | 'x' | 'x' |
| | f_ipond | 'm' | 'x' | 'x' |
| | f_ipond_ai | 'm' | 'x' | 'x' |
| &setup_nml | history_chunksize_x | | 720 | 720 |
| | history_chunksize_y | | 540 | 540 |
| | history_deflate_level | | 1 | 1 |
| | istep0 | 341496 | 0 | 0 |
| | lcdf64 | True | | |
| | restart | True | False | False |
| | restart_format | 'nc' | | |
| | runttype | 'continue' | 'initial' | 'initial' |

| | | | | | |
|----------------|-----------------------|--|--|---|---|
| | | ./gadi/g/ data/ hh5/tmp/ cosima/ access- om2-01/ 01deg_- jra55v13_- iaf/ output197/ ice/cice_- in.nml | ./gadi/g/ data/ hh5/tmp/ cosima/ access- om2-01/ 01deg_- jra55v13_- ryf9091/ output675/ ice/cice_- in.nml | github.com/ COSIMA/ 01deg_- jra55_iaf/ ice/cice_- in.nml | github.com/ COSIMA/ 01deg_- jra55_ryf/ ice/cice_- in.nml |
| Group | Variable | | | | |
| &domain_nml | distribution_type | 'roundrobin' | 'sectrobin' | 'sectrobin' | 'sectrobin' |
| | nprocs | 1600 | 799 | 722 | 722 |
| &forcing_nml | highfreq | | True | True | True |
| &icefields_nml | f_aice | 'md' | 'm' | 'md' | 'md' |
| | f_aicen | 'md' | 'm' | 'm' | 'm' |
| | f_congel | 'm' | 'm' | 'md' | 'md' |
| | f_daidtd | 'x' | 'x' | 'm' | 'm' |
| | f_daidtt | 'x' | 'x' | 'm' | 'm' |
| | f_divu | 'md' | 'm' | 'm' | 'm' |
| | f_dvidtd | 'x' | 'x' | 'md' | 'md' |
| | f_dvidtt | 'x' | 'x' | 'md' | 'md' |
| | f_frazil | 'm' | 'm' | 'md' | 'md' |
| | f_frz_onset | 'm' | 'm' | 'x' | 'x' |
| | f_frzmlt | 'x' | 'x' | 'md' | 'md' |
| | f_fsalt | 'd' | 'm' | 'm' | 'm' |
| | f_fsalt_ai | 'd' | 'm' | 'm' | 'm' |
| | f_hi | 'md' | 'm' | 'md' | 'md' |
| | f_hs | 'md' | 'm' | 'md' | 'md' |
| | f_mlt_onset | 'm' | 'm' | 'x' | 'x' |
| | f_shear | 'md' | 'm' | 'm' | 'm' |
| | f_sig1 | 'md' | 'm' | 'x' | 'x' |
| | f_sig2 | 'md' | 'm' | 'x' | 'x' |
| | f_snoise | 'x' | 'x' | 'md' | 'md' |
| | f_sss | 'd' | 'm' | 'x' | 'x' |
| | f_sst | 'd' | 'm' | 'x' | 'x' |
| | f_strairx | 'md' | 'm' | 'm' | 'm' |
| | f_strairy | 'md' | 'm' | 'm' | 'm' |
| | f_uocn | 'd' | 'm' | 'x' | 'x' |
| | f_uvel | 'md' | 'm' | 'md' | 'md' |
| | f_vicen | 'md' | 'm' | 'm' | 'm' |
| | f_vocn | 'd' | 'm' | 'x' | 'x' |
| | f_vvel | 'md' | 'm' | 'md' | 'md' |
| &setup_nml | history_chunksize_x | | | 360 | 360 |
| | history_chunksize_y | | | 270 | 270 |
| | history_deflate_level | | 1 | 1 | 1 |
| | istep0 | 3906432 | 4374000 | 0 | 0 |
| | latpt | 66.75, 68.0 | 66.75, 68.0 | 90.0, -65.0 | 90.0, -65.0 |
| | lcdf64 | True | | 0.0, | 0.0, |
| | lonpt | 72.5, 74.0 | 72.5, 74.0 | -45.0 | -45.0 |
| | ndtd | 3 | 2 | 2 | 2 |
| | restart | True | True | False | False |
| | restart_format | 'nc' | 'nc' | | |
| | runttype | 'continue' | 'continue' | 'initial' | 'initial' |

D.3.2 input_ice.nml

| Group | Variable | | | |
|---------------|-----------------|------|---|---|
| &coupling_nml | chk_frzmlt_sst | | False | False |
| | chk_i2a_fields | | False | False |
| | chk_i2o_fields | | False | False |
| | chk_o2i_fields | | False | False |
| | cst_ocn_albedo | True | False | False |
| | fields_from_atm | | 'swfld_i', 'lwfld_i', 'rain_i', 'snow_i', 'press_i', 'runof_i', 'tair_i', 'qair_i', 'uwnd_i', 'vwnd_i', 'lcalvf_i' | 'swfld_i', 'lwfld_i', 'rain_i', 'snow_i', 'press_i', 'runof_i', 'tair_i', 'qair_i', 'uwnd_i', 'vwnd_i', 'lcalvf_i' |
| | fields_from_ocn | | 'sst_i', 'sss_i', 'ssu_i', 'ssv_i', 'sslx_i', 'ssly_i', 'pfmice_i' | 'sst_i', 'sss_i', 'ssu_i', 'ssv_i', 'sslx_i', 'ssly_i', 'pfmice_i' |
| | fields_to_ocn | | 'strsu_io', 'strsv_io', 'rain_io', 'snow_io', 'stflx_io', 'htflx_io', 'swflx_io', 'qflux_io', 'shflx_io', 'lwflx_io', 'runof_io', 'press_io', 'aice_io', 'melt_io', 'form_io', 'licefw_io', 'licefh_io' | 'strsu_io', 'strsv_io', 'rain_io', 'snow_io', 'stflx_io', 'htflx_io', 'swflx_io', 'qflux_io', 'shflx_io', 'lwflx_io', 'runof_io', 'press_io', 'aice_io', 'melt_io', 'form_io', 'licefw_io', 'licefh_io' |

| Group | Variable | cst_ocn_albedo | True | False | False |
|---------------|-----------------|----------------|------|---|---|
| &coupling_nml | | | | 'swfld_i', 'lwfld_i', 'rain_i', 'snow_i', 'press_i', 'runof_i', 'tair_i', 'qair_i', 'uwnd_i', 'vwnd_i', 'lcalvf_i' | 'swfld_i', 'lwfld_i', 'rain_i', 'snow_i', 'press_i', 'runof_i', 'tair_i', 'qair_i', 'uwnd_i', 'vwnd_i', 'lcalvf_i' |
| | fields_from_atm | | | 'sst_i', 'sss_i', 'ssu_i', 'ssv_i', 'sslx_i', 'ssly_i', | 'sst_i', 'sss_i', 'ssu_i', 'ssv_i', 'sslx_i', 'ssly_i', |
| | fields_from_ocn | | | 'pfmice_i' 'strsu_io', 'strsv_io', 'rain_io', 'snow_io', 'stflx_io', 'htflx_io', 'swflx_io', 'qflux_io', 'shflx_io', 'lwflx_io', 'runof_io', 'press_io', 'aice_io', 'melt_io', 'form_io', 'licefw_io', 'licefh_io' | 'pfmice_i' 'strsu_io', 'strsv_io', 'rain_io', 'snow_io', 'stflx_io', 'htflx_io', 'swflx_io', 'qflux_io', 'shflx_io', 'lwflx_io', 'runof_io', 'press_io', 'aice_io', 'melt_io', 'form_io', 'licefw_io', 'licefh_io' |
| | fields_to_ocn | | | | |

| Group | Variable | cst_ocn_albedo | True | True | False | False |
|---------------|-----------------|----------------|------|------|---|---|
| &coupling_nml | | | | | 'swfld_i', 'lwfld_i', 'rain_i', 'snow_i', 'press_i', 'runof_i', 'tair_i', 'qair_i', 'uwnd_i', 'vwnd_i', 'lcalvf_i' | 'swfld_i', 'lwfld_i', 'rain_i', 'snow_i', 'press_i', 'runof_i', 'tair_i', 'qair_i', 'uwnd_i', 'vwnd_i', 'lcalvf_i' |
| | fields_from_atm | | | | 'sst_i', 'sss_i', 'ssu_i', 'ssv_i', 'sslx_i', 'ssly_i', 'pfmice_i' | 'sst_i', 'sss_i', 'ssu_i', 'ssv_i', 'sslx_i', 'ssly_i', 'pfmice_i' |
| | fields_from_ocn | | | | 'strsu_io', 'strsv_io', 'rain_io', 'snow_io', 'stflx_io', 'htflx_io', 'swflx_io', 'qflux_io', 'shflx_io', 'lwflx_io', 'runof_io', 'press_io', 'aice_io', 'melt_io', 'form_io', 'licefw_io', 'licefh_io' | 'strsu_io', 'strsv_io', 'rain_io', 'snow_io', 'stflx_io', 'htflx_io', 'swflx_io', 'qflux_io', 'shflx_io', 'lwflx_io', 'runof_io', 'press_io', 'aice_io', 'melt_io', 'form_io', 'licefw_io', 'licefh_io' |
| | fields_to_ocn | | | | | |

D.3.3 input_ice_gfdl.nml

D.3.4 input_ice_monin.nml

D.4 YATM namelist atm.nml

| Group | Variable | atm.nml | atm.nml | atm.nml | atm.nml |
|-------------|----------------|----------|----------|----------|----------|
| | | 0.03, | 0.03, | 0.03, | 0.03, |
| | | 0.001, | 0.003, | 0.003, | 0.003, |
| | | 0.003, | 0.003, | 0.003, | 0.003, |
| | | 0.003 | 0.003 | 0.003 | 0.003 |
| &runoff_nml | runoff_caps | 0, 3470, | 0, 3420, | 0, 3420, | 0, 3420, |
| | | 180, 300 | 180, 300 | 180, 300 | 180, 300 |
| | runoff_caps_is | 1000000, | 1000000, | 1000000, | 1000000, |
| | | 2650, | 2680, | 2680, | 2680, |
| | | 99999, | 99999, | 99999, | 99999, |
| | runoff_caps_je | 2470 | 2470 | 2470 | 2470 |

E Namelist differences between new configs

These are auto-generated by namelists/make_tables.py which uses nmltab (<https://github.com/ae kiss/nm lt ab>). Variables are weblinks to source code searches. Only differences are shown, and duplicate identical profiling namelists are omitted. Differences in timestep counters are ignored. Tables are omitted if there are no differences at all.

E.1 ACCESS-OM2 namelist accessom2.nml

| Group | Variable | accessom2.nml | accessom2.nml | accessom2.nml | accessom2.nml | accessom2.nml | accessom2.nml |
|-------------------|--------------------|---------------|---------------|---------------|---------------|---------------|---------------|
| &accessom2_nml | ice_ocean_timestep | 300 | 300 | 1350 | 1350 | 5400 | 5400 |
| | | '2019-01-01- | '1901-01- | '2019-01- | '1901-01- | '2019-01- | '1901-01- |
| &date_manager_nml | forcing_end_date | 01T00:00:I | 01T00:00:I | 01T00:00:I | 01T00:00:I | 01T00:00:I | 01T00:00:00 |

E.2 MOM namelist input.nml

| Group (continued) | Variable | accessom2.namessom2.namessom2.namessom2.namessom2.namessom2.namessom2.namessom2.namessom2.nml | github.com/github.com/github.com/github.com/github.com/COSIMA/01deg_-jra55_-iaf/rwf/01-01-01-01-01-01- | github.com/github.com/github.com/github.com/github.com/COSIMA/01deg_-jra55_-iaf/rwf/01-01-01-01-01-01- | github.com/github.com/github.com/github.com/github.com/COSIMA/025deg_-jra55_-iaf/rwf/01-01-01-01-01-01- | github.com/github.com/github.com/github.com/github.com/COSIMA/025deg_-jra55_-iaf/rwf/01-01-01-01-01-01- | github.com/github.com/github.com/github.com/github.com/COSIMA/1deg_-jra55_-iaf/rwf/01-01-01-01-01-01- | github.com/github.com/github.com/github.com/github.com/COSIMA/1deg_-jra55_-iaf/rwf/01-01-01-01-01-01- |
|-------------------|---------------------|---|--|--|---|---|---|---|
| | '1958-01-01T00:00:I | '1900-01-01T00:00:I | '1958-01-01T00:00:I | '1900-01-01T00:00:I | '1958-01-01T00:00:I | '1900-01-01T00:00:I | '1958-01-01T00:00:I | '1900-01-01T00:00:I |
| | forcing_start_date | restart_period | 0, 3, 0 | 0, 3, 0 | 2, 0, 0 | 2, 0, 0 | 5, 0, 0 | 5, 0, 0 |

E.2 MOM namelist input.nml

| Group | Variable | input.nml |
|-------------------------------|---------------------------------|-----------|-----------|-----------|-----------|-----------|-----------|-----------|
| &auscom_ice_nml | redsea_gulfbay_sfix | | | | | | False | False |
| &fms_io_nml | checksum_required | False | False | | | | | |
| | fileset_write | 'multi' | 'multi' | 'single' | 'single' | 'single' | 'single' | |
| | threading_write | 'multi' | 'multi' | 'single' | 'single' | 'single' | 'single' | |
| &fms_nml | clock_grain | 'ROUTINE' | 'ROUTINE' | 'LOOP' | 'LOOP' | 'LOOP' | 'LOOP' | |
| | domains_stack_size | 115200 | 115200 | | | 115200 | 115200 | |
| &mpp_io_nml | deflate_level | 5 | 5 | 5 | 5 | -1 | -1 | |
| &ocean_adv_vel_diag_nml | diag_step | 576 | 576 | 4320 | 4320 | 4320 | 4320 | |
| &ocean_advection_velocity_nml | max_advection_velocity | 0.3 | 0.3 | 0.5 | 0.5 | 0.5 | 0.5 | |
| &ocean_barotropic_nml | diag_step | 576 | 576 | 4320 | 4320 | 4320 | 4320 | |
| &ocean_bihgen_friction_nml | bottom_5point | False | False | False | False | True | True | |
| | ncar_boundary_scaling | False | False | False | False | True | True | |
| | vel_micom_bottom | 0.0 | 0.0 | 0.0 | 0.0 | 0.01 | 0.01 | |
| | vel_micom_iso | 0.0 | 0.0 | 0.0 | 0.0 | 0.04 | 0.04 | |
| | visc_crit_scale | 1.0 | 1.0 | 1.0 | 1.0 | 0.25 | 0.25 | |
| &ocean_lapgen_friction_nml | bottom_5point | | | | | True | True | |
| | k_smag_aniso | | | | | 0.0 | 0.0 | |
| | k_smag_iso | | | | | 0.0 | 0.0 | |
| | restrict_polar_visc | | | | | True | True | |
| | restrict_polar_visc_lat | | | | | 60.0 | 60.0 | |
| | restrict_polar_visc_ratio | | | | | 0.35 | 0.35 | |
| | use_this_module | False | False | False | False | True | True | |
| | vel_micom_iso | | | | | 0.1 | 0.1 | |
| | viscosity_ncar | | | | | False | False | |
| | viscosity_ncar_2007 | | | | | False | False | |
| | viscosity_scale_by_rossby | | | | | True | True | |
| | viscosity_scale_by_rossby_power | | | | | 4.0 | 4.0 | |
| &ocean_mixdownslope_nml | mixdownslope_mask_gfdl | | | | | False | False | |
| | mixdownslope_npts | | | | | 4 | 4 | |
| | read_mixdownslope_mask | | | | | False | False | |
| | use_this_module | False | False | False | False | True | True | |
| &ocean_model_nml | io_layout | 5, 5 | 5, 5 | 6, 5 | 6, 5 | 4, 3 | 4, 3 | |
| | layout | 80, 75 | 80, 75 | 48, 40 | 48, 40 | 16, 15 | 16, 15 | |
| &ocean_nphysics_nml | use_nphysicsc | False | False | True | True | True | True | |
| | use_this_module | False | False | True | True | True | True | |
| &ocean_nphysics_util_nml | agm_closure | | | True | True | True | True | |
| | agm_closure_baroclinic | | | True | True | True | True | |

E.2 MOM namelist input.nml

| Group (continued) | Variable | COSIMA/ 01deg_- jra55_- iaf/ ocean/ input.nml | COSIMA/ 01deg_- jra55_- ryf/ ocean/ input.nml | COSIMA/ 025deg_- jra55_- iaf/ ocean/ input.nml | COSIMA/ 025deg_- jra55_- ryf/ ocean/ input.nml | COSIMA/ 1deg_- jra55_- iaf/ ocean/ input.nml | COSIMA/ 1deg_- jra55_- ryf/ ocean/ input.nml |
|----------------------------|--------------------------------|--|--|---|---|---|---|
| | agm_closure_buoy_freq | | | 0.004 | 0.004 | 0.004 | 0.004 |
| | agm_closure_eady_ave_mixed | | | True | True | True | True |
| | agm_closure_eady_cap | | | True | True | True | True |
| | agm_closure_eady_smooth_horz | | | True | True | True | True |
| | agm_closure_eady_smooth_vert | | | True | True | True | True |
| | agm_closure_grid_scaling | | | True | True | True | True |
| | agm_closure_length | 20 000.0 | 20 000.0 | 50 000.0 | 50 000.0 | | |
| | agm_closure_lower_depth | 2000.0 | 2000.0 | 2000.0 | 2000.0 | | |
| | agm_closure_max | 200.0 | 200.0 | 600.0 | 600.0 | | |
| | agm_closure_min | 1.0 | 1.0 | 50.0 | 50.0 | | |
| | agm_closure_scaling | 0.07 | 0.07 | 0.07 | 0.07 | | |
| | agm_closure_upper_depth | 100.0 | 100.0 | 100.0 | 100.0 | | |
| | aredi | 200.0 | 200.0 | 600.0 | 600.0 | | |
| | aredi_diffusivity_grid_scaling | True | True | | | | |
| | aredi_equal_agm | False | False | False | False | | |
| | drhodz_mom4p1 | True | True | True | True | | |
| | nphysics_util_zero_init | True | True | True | True | | |
| &ocean_nphysicsc_nml | bv_freq_smooth_vert | True | True | True | True | | |
| | bvp_bc_mode | 2 | 2 | 2 | 2 | | |
| | bvp_min_speed | 0.1 | 0.1 | 0.1 | 0.1 | | |
| | bvp_speed | 0.0 | 0.0 | 0.0 | 0.0 | | |
| | do_gm_skewson | True | True | True | True | | |
| | do_neutral_diffusion | True | True | True | True | | |
| | epsln_by_freq | 1×10^{-12} | 1×10^{-12} | 1×10^{-12} | 1×10^{-12} | | |
| | gm_skewson_bvproblem | True | True | True | True | | |
| | gm_skewson_modes | False | False | False | False | | |
| | neutral_eddy_depth | True | True | True | True | | |
| | neutral_physics_limit | True | True | True | True | | |
| | number_bc_modes | 2 | 2 | 2 | 2 | | |
| | regularize_psi | False | False | False | False | | |
| | smax_psi | 0.01 | 0.01 | 0.01 | 0.01 | | |
| | smooth_psi | True | True | True | True | | |
| | tmask_neutral_on | True | True | True | True | | |
| | turb_blayer_min | 50.0 | 50.0 | 50.0 | 50.0 | | |
| | use_this_module | False | False | True | True | True | True |
| &ocean_sbc_nml | do_bitwise_exact_sum | False | False | False | False | True | True |
| | max_delta_salinity_restore | 0.5 | 0.5 | 0.5 | 0.5 | -0.5 | -0.5 |
| | ocean_ice_salt_limit | 0.006 | 0.006 | 0.006 | 0.006 | | |
| | runoffspread | False | False | | | | |
| | salt_restore_tscale | 10.0 | 10.0 | 21.28 | 21.28 | 21.28 | 21.28 |
| &ocean_sigma_transport_nml | use_this_module | False | False | False | False | True | True |
| &ocean_submesoscale_nml | smooth_advect_transport_num | 4 | 4 | 4 | 4 | 2 | 2 |
| | smooth_psi_num | 3 | 3 | 3 | 3 | 2 | 2 |
| &ocean_tracer_diag_nml | diag_step | 576 | 576 | 4320 | 4320 | 4320 | 4320 |
| &ocean_velocity_diag_nml | diag_step | 576 | 576 | 4320 | 4320 | 4320 | 4320 |
| | energy_diag_step | 5760 | 5760 | 4320 | 4320 | 4320 | 4320 |
| &ocean_vert_mix_nml | j09_bgmax | 1×10^{-6} | 1×10^{-6} | | | 5×10^{-6} | 5×10^{-6} |
| | j09_bgmin | 1×10^{-6} | 1×10^{-6} | | | 1×10^{-6} | 1×10^{-6} |
| | j09_diffusivity | True | True | | | True | True |

E.3 CICE namelists

| Group (continued) | Variable | j09_lat | 20.0 | 20.0 | 20.0 | 20.0 |
|-------------------|--------------|---------|------|------|------|------|
| &xgrid_nml | do_alltoall | True | True | | | |
| | do_alltoally | True | True | | | |

E.3 CICE namelists

E.3.1 cice_in.nml

| Group | Variable | cice_in.nml | cice_in.nml | cice_in.nml | cice_in.nml | cice_in.nml | cice_in.nml |
|------------------------|-------------------|--------------|--------------|--------------|--------------|-------------|-------------|
| &domain_nml | distribution_type | 'sectrobin' | 'sectrobin' | 'roundrobin' | 'roundrobin' | 'cartesian' | 'cartesian' |
| | nprocs | 722 | 722 | 361 | 361 | 24 | 24 |
| | processor_shape | 'square-ice' | 'square-ice' | 'square-ice' | 'square-ice' | 'slenderX1' | 'slenderX1' |
| &forcing_nml | tfrz_option | 'mushy' | 'mushy' | 'salt' | 'salt' | 'salt' | 'salt' |
| &icefields_mechred_nml | f_vlvl | 'x' | 'x' | 'm' | 'm' | 'm' | 'm' |
| | f_vrdg | 'x' | 'x' | 'm' | 'm' | 'm' | 'm' |
| &icefields_nml | f_albice | 'x' | 'x' | 'm' | 'm' | 'm' | 'm' |
| | f_albsni | 'x' | 'x' | 'm' | 'm' | 'm' | 'm' |
| | f_albsno | 'x' | 'x' | 'm' | 'm' | 'm' | 'm' |
| | f_evap_ai | 'x' | 'x' | 'm' | 'm' | 'm' | 'm' |
| | f_fcondtop_ai | 'x' | 'x' | 'm' | 'm' | 'm' | 'm' |
| | f_fcondtopn_ai | 'x' | 'x' | 'm' | 'm' | 'm' | 'm' |
| | f_fhocn_ai | 'x' | 'x' | 'm' | 'm' | 'm' | 'm' |
| | f_flat_ai | 'x' | 'x' | 'm' | 'm' | 'm' | 'm' |
| | f_flwdn | 'x' | 'x' | 'm' | 'm' | 'm' | 'm' |
| | f_flwup_ai | 'x' | 'x' | 'm' | 'm' | 'm' | 'm' |
| | f_fmelttn_ai | 'x' | 'x' | 'm' | 'm' | 'm' | 'm' |
| | f_fresh_ai | 'x' | 'x' | 'm' | 'm' | 'm' | 'm' |
| | f_fsens_ai | 'x' | 'x' | 'm' | 'm' | 'm' | 'm' |
| | f_fsurfai | 'x' | 'x' | 'm' | 'm' | 'm' | 'm' |
| | f_fswabs_ai | 'x' | 'x' | 'm' | 'm' | 'm' | 'm' |
| | f_fswdn | 'x' | 'x' | 'm' | 'm' | 'm' | 'm' |
| | f_fswfac | 'x' | 'x' | 'm' | 'm' | 'm' | 'm' |
| | f_fswthru_ai | 'x' | 'x' | 'm' | 'm' | 'm' | 'm' |
| | f_icepresent | 'x' | 'x' | 'm' | 'm' | 'm' | 'm' |
| | f_meltb | 'x' | 'x' | 'm' | 'm' | 'm' | 'm' |
| | f_meltl | 'x' | 'x' | 'm' | 'm' | 'm' | 'm' |
| | f_melts | 'x' | 'x' | 'm' | 'm' | 'm' | 'm' |
| | f_meltt | 'x' | 'x' | 'm' | 'm' | 'm' | 'm' |
| | f_rain_ai | 'x' | 'x' | 'm' | 'm' | 'm' | 'm' |
| | f_sice | 'x' | 'x' | 'm' | 'm' | 'm' | 'm' |
| | f_snow_ai | 'x' | 'x' | 'm' | 'm' | 'm' | 'm' |
| | f_strcorx | 'x' | 'x' | 'm' | 'm' | 'm' | 'm' |

E.4 YATM namelist atm.nml

| Group (continued) | Variable | COSIMA/ 01deg_- jra55_- iaf/ice/ cice_- in.nml | COSIMA/ 01deg_- jra55_- ryf/ice/ cice_- in.nml | COSIMA/ 025deg_- jra55_- iaf/ice/ cice_- in.nml | COSIMA/ 025deg_- jra55_- ryf/ice/ cice_- in.nml | COSIMA/ 1deg_- jra55_- iaf/ice/ cice_- in.nml | COSIMA/ 1deg_- jra55_- ryf/ice/ cice_- in.nml |
|-------------------|---------------------|---|---|--|--|--|--|
| | f_strcory | 'x' | 'x' | 'm' | 'm' | 'm' | 'm' |
| | f_strintx | 'x' | 'x' | 'm' | 'm' | 'm' | 'm' |
| | f_strinty | 'x' | 'x' | 'm' | 'm' | 'm' | 'm' |
| | f_strocnx | 'x' | 'x' | 'm' | 'm' | 'm' | 'm' |
| | f_strocnyn | 'x' | 'x' | 'm' | 'm' | 'm' | 'm' |
| | f_strlttx | 'x' | 'x' | 'm' | 'm' | 'm' | 'm' |
| | f_strlty | 'x' | 'x' | 'm' | 'm' | 'm' | 'm' |
| | f_tair | 'x' | 'x' | 'm' | 'm' | 'm' | 'm' |
| | f_trsig | 'x' | 'x' | 'm' | 'm' | 'm' | 'm' |
| &setup_nml | dt | 300 | 300 | 1800 | 1800 | 3600 | 3600 |
| | dumpfreq | 'm' | 'm' | 'y' | 'y' | 'y' | 'y' |
| | dumpfreq_n | 3 | 3 | 1 | 1 | 1 | 1 |
| | history_chunksize_x | 360 | 360 | 720 | 720 | 180 | 180 |
| | history_chunksize_y | 270 | 270 | 540 | 540 | 150 | 150 |
| | ndtd | 2 | 2 | 1 | 1 | 1 | 1 |
| | npt | 6480 | 6480 | 2232 | 2232 | 35040 | 35040 |
| &thermo_nml | ktherm | 2 | 2 | 1 | 1 | 1 | 1 |

E.3.2 input_ice.nml

E.3.3 input_ice_gfdl.nml

E.3.4 input_ice_monin.nml

| Group | Variable | COSIMA/ 01deg_- jra55_- iaf/ atmosphere atm.nml | COSIMA/ 01deg_- jra55_- ryf/ atmosphere atm.nml | COSIMA/ 025deg_- jra55_- iaf/ atmosphere atm.nml | COSIMA/ 025deg_- jra55_- ryf/ atmosphere atm.nml | COSIMA/ 1deg_- jra55_- iaf/ atmosphere atm.nml | COSIMA/ 1deg_- jra55_- ryf/ atmosphere atm.nml |
|-------------|-----------------|--|--|---|---|---|---|
| &runoff_nml | num_runoff_caps | 4 | 4 | | | | |
| | | 0.03, | 0.03, | | | | |
| | | 0.003, | 0.003, | | | | |
| | | 0.003, | 0.003, | | | | |
| | runoff_caps | 0.003 | 0.003 | | | | |
| | | 1000000, | 1000000, | | | | |
| | | 3530, | 3530, | | | | |
| | runoff_caps_ie | 240, 560 | 240, 560 | | | | |
| | | 0, 3420, | 0, 3420, | | | | |
| | runoff_caps_is | 180, 300 | 180, 300 | | | | |

| Group (continued) | Variable | atm.nml | atm.nml | atm.nml | atm.nml | atm.nml | atm.nml |
|-------------------|----------------|----------|----------|---------|---------|---------|---------|
| | | 1000000, | 1000000, | | | | |
| | | 2680, | 2680, | | | | |
| | | 99999, | 99999, | | | | |
| | runoff_caps_je | 2470 | 2470 | | | | |
| | | 0, 2270, | 0, 2270, | | | | |
| | | 2670, | 2670, | | | | |
| | runoff_caps_js | 2260 | 2260 | | | | |

F Namelist differences from ACCESS, ACCESS-CM2, ACCESS-ESM, OFAM3

F.1 ACCESS-OM2-01 MOM compared to OFAM3

input.ofam3_spinup03 is the namelist that was used for the spinup that was the version after “ofam3_spinup01” which was referred to the in Oke et al. (2013). The main difference between these experiments was that spinup01 was forced with ERA fluxes directly, whereas spinup03 used ERA atmosphere fields with bulk formulas.

input.ofam2017.nml is the most recent spinup namelist with several differences.

Only differences are shown.

| Group | Variable | OFAM3/ input.ofam3_‑ spinup03.nml | OFAM3/ input.ofam2017.nml | ./gadif/g/data/ hh5/tmp/cosima/ access-om2-01/ 01deg_jra55v13_‑ iaf/output197/ ocean/input.nml |
|-----------------|------------------|---|------------------------------|---|
| &auscom_ice_nml | aice_cutoff | | | 0.15 |
| | chk_i2o_fields | | | False |
| | chk_o2i_fields | | | False |
| | do_ice_once | | | False |
| | fixmeltt | | | False |
| | frazil_factor | | | 1.0 |
| | iceform_adj_salt | | | False |
| | icemlt_factor | | | 1.0 |
| | kmxice | | | 5 |
| | pop_icediag | | | True |
| | sign_stflx | | | 1.0 |
| | tmelt | | | -0.216 |
| | use_ioaice | | | True |
| &coupler_nml | atmos_npes | 0 | 0 | |
| | calendar | 'gregorian' | 'gregorian' | |
| | check_stocks | -1 | -1 | |
| | current_date | 1993, 1, 1, 0, 0, 0 | 1990, 1, 1, 0, 0, 0 | |
| | days | 6 | 0 | |
| | do_atmos | False | False | |
| | do_ice | True | True | |
| | do_land | False | False | |
| | do_ocean | True | True | |
| | dt_atmos | 10800 | 10800 | |
| | dt_cpld | 10800 | 10800 | |

F.1 ACCESS-OM2-01 MOM compared to OFAM3

| Group (continued) | Variable | OFAM3/ input.ofam3_ - spinup03.nml | OFAM3/ input.ofam2017.nml | ./gadi/g/data/ hh5/tmp/cosima/ access-om2-01/ 01deg_jra55v13_- iaf/output197/ ocean/input.nml |
|-------------------------------|---------------------------------|--|------------------------------|--|
| | hours | 0 | 0 | |
| | minutes | 0 | 0 | |
| | months | 0 | 1 | |
| | ocean_npes | 0 | 0 | |
| | seconds | 0 | 0 | |
| | use_lag_fluxes | | | False |
| &diag_manager_nml | debug_diag_manager | | | True |
| | issue_oor_warnings | | False | True |
| | max_axes | 100 | | |
| &flux_exchange_nml | do_area_weighted_flux | False | False | |
| | do_runoff | False | False | |
| &fms_io_nml | checksum_required | | False | False |
| &fms_nml | clock_grain | 'LOOP' | 'LOOP' | 'ROUTINE' |
| | domains_stack_size | | | 115200 |
| &ice_model_nml | io_layout | 32, 16 | 2, 10 | |
| | layout | 32, 32 | 48, 30 | |
| | nsteps_adv | 0 | 0 | |
| | nsteps_dyn | 0 | 0 | |
| | spec_ice | | False | |
| &mom_oasis3_interface_nml | fields_in | | | 'u_flux', 'v_flux', 'lprec', 'fprec', 'salt_flx', 'mh_flux', 'sw_flux', 'q_flux', 't_flux', 'lw_flux', 'runof', 'p', 'aice', 'wfimelt', 'wfiform' 't_surf', 's_surf', 'u_surf', 'v_surf', 'dssldx', 'dssldy', 'frazil' |
| | fields_out | | | 15 |
| | num_fields_in | | | 7 |
| | num_fields_out | | | |
| | send_after_ocean_update | | | True |
| | send_before_ocean_update | | | False |
| &monin_obukhov_nml | neutral | True | False | True |
| &mpp_io_nml | deflate_level | | | 5 |
| | shuffle | | | 1 |
| &ocean_adv_vel_diag_nml | diag_step | 144 | 144 | 576 |
| | verbose_cfl | False | False | True |
| &ocean_advection_velocity_nml | max_advection_velocity | 0.5 | 0.5 | 0.3 |
| &ocean_barotropic_nml | barotropic_halo | | | 10 |
| | barotropic_leap_frog | False | | |
| | barotropic_pred_corr | True | | |
| | barotropic_time_stepping_a | | True | True |
| | barotropic_time_stepping_b | | False | False |
| | barotropic_time_stepping_mom4p0 | True | | |
| | barotropic_time_stepping_mom4p1 | False | | |
| | diag_step | 144 | 144 | 576 |
| | eta_max | 9.0 | 2.5 | 8.0 |
| | frac_crit_cell_height | 0.25 | 0.25 | 0.2 |
| | pbot_offset | 1×10^{-12} | 1×10^{-12} | |
| | smooth_eta_diag_laplacian | | | True |
| | smooth_pbot_t_biharmonic | | | False |

F.1 ACCESS-OM2-01 MOM compared to OFAM3

| Group (continued) | Variable | OFAM3/ input.ofam3 - spinup03.nml | OFAM3/ input.ofam2017.nml | ./gadi/g/data/ hh5/tmp/cosima/ access-om2-01/ 01deg_jra55v13 - iaf/output197/ ocean/input.nml |
|-----------------------------|-----------------------------|---|------------------------------|--|
| | smooth_pbot_t_laplacian | | | True |
| | use_legacy_barotropic_halos | | | False |
| | vel_micom_lap_diag | | | 0.2 |
| | verbose_truncate | False | False | True |
| &ocean_bbc_nml | bmf_implicit | | | True |
| | cdbot | 0.0015 | 0.0015 | 0.001 |
| | cdbot_hi | | | 0.007 |
| | cdbot_roughness_length | | | False |
| | cdbot_roughness_uamp | | | True |
| | use_geothermal_heating | | | False |
| &ocean_bbc_ofam_nml | read_tide_speed | False | False | |
| | uresidual2_max | 1.0 | 1.0 | |
| &ocean_bihgen_friction_nml | eq_lat_micom | | | 0.0 |
| | eq_vel_micom_aniso | | | 0.0 |
| | eq_vel_micom_iso | | | 0.0 |
| | equatorial_zonal | | | False |
| | k_smag_aniso | 3.0 | 3.0 | 0.0 |
| | k_smag_iso | 3.0 | 3.0 | 2.0 |
| | ncar_boundary_scaling | | | True |
| | ncar_boundary_scaling_read | | | False |
| | ncar_rescale_power | | | 2 |
| | ncar_vconst_4 | | | 2×10^{-8} |
| | ncar_vconst_5 | | | 5 |
| | use_this_module | True | True | True |
| | vel_micom_aniso | 0.005 | 0.005 | 0.0 |
| | vel_micom_bottom | 0.01 | 0.01 | 0.0 |
| | vel_micom_iso | 0.005 | 0.005 | 0.0 |
| | visc_crit_scale | | | 1.0 |
| &ocean_convect_nml | convect_full_scalar | True | True | |
| | convect_full_vector | False | False | |
| | convect_ncon | False | False | |
| | use_this_module | False | False | False |
| &ocean_coriolis_nml | acor | 1.0 | 1.0 | 0.5 |
| | use_this_module | True | True | True |
| &ocean_density_nml | eos_linear | | False | False |
| | eos_preteos10 | | True | True |
| | layer_nk | | | 80 |
| | linear eos | False | | |
| | neutralrho_max | | | 1030.0 |
| | neutralrho_min | | | 1020.0 |
| | potrho_max | | | 1038.0 |
| | potrho_min | | | 1028.0 |
| &ocean_domains_nml | max_tracers | | | 5 |
| &ocean_frazil_nml | debug_this_module | | | False |
| | frazil_only_in_surface | | | False |
| | freezing_temp_preteos10 | | | True |
| | freezing_temp_simple | | | False |
| | use_this_module | False | False | True |
| &ocean_increment_eta_nml | days_to_increment | 0 | 0 | |
| | fraction_increment | 1.0 | 1.0 | |
| | secs_to_increment | 3600 | 3600 | |
| | use_this_module | False | False | False |
| &ocean_increment_tracer_nml | days_to_increment | 0 | 0 | |

F.1 ACCESS-OM2-01 MOM compared to OFAM3

| Group (continued) | Variable | OFAM3/ input.ofam3 - spinup03.nml | OFAM3/ input.ofam2017.nml | ./gadi/g/data/ hh5/tmp/cosima/ access-om2-01/ 01deg_jra55v13 - iaf/output197/ ocean/input.nml |
|-------------------------------|-------------------------------|---|------------------------------|--|
| | fraction_increment | 1.0 | 1.0 | |
| | secs_to_increment | 3600 | 3600 | |
| | use_this_module | False | False | False |
| &ocean_increment_velocity_nml | days_to_increment | 0 | 0 | |
| | fraction_increment | 1.0 | 1.0 | |
| | secs_to_increment | 3600 | 3600 | |
| | use_this_module | False | False | False |
| &ocean_lap_friction_nml | lap_friction_scheme | 'const' | 'const' | 'general' |
| &ocean_mixdownslope_nml | debug_this_module | False | False | |
| | use_this_module | False | False | False |
| &ocean_model_nml | barotropic_split | 60 | 75 | 80 |
| | cmip_units | | | True |
| | dt_ocean | 450 | 600 | |
| | impose_init_from_restart | | False | |
| | io_layout | 32, 16 | 2, 10 | 5, 5 |
| | layout | 32, 32 | 48, 30 | 80, 75 |
| &ocean_momentum_source_nml | rayleigh_damp_exp_from_bottom | True | True | False |
| | rayleigh_damp_exp_scale | 1000.0 | 1000.0 | |
| | rayleigh_damp_exp_time | 86 400.0 | 86 400.0 | |
| | use_rayleigh_damp_table | | | True |
| | use_this_module | False | False | True |
| &ocean_nphysics_mom4p0_nml | debug_this_module | True | True | |
| | use_this_module | False | False | |
| &ocean_nphysics_mom4p1_nml | use_this_module | False | False | |
| &ocean_nphysics_nml | use_nphysicsa | | | False |
| | use_nphysicsb | | | False |
| | use_nphysicsc | | | False |
| | use_this_module | False | False | False |
| &ocean_nphysics_util_nml | agm | | | 100.0 |
| | agm_closure | | | True |
| | agm_closure_baroclinic | | | True |
| | agm_closure_buoy_freq | | | 0.004 |
| | agm_closure_length | | | 50 000.0 |
| | agm_closure_length_bczone | | | False |
| | agm_closure_length_fixed | | | False |
| | agm_closure_length_rossby | | | False |
| | agm_closure_lower_depth | | | 2000.0 |
| | agm_closure_max | | | 600.0 |
| | agm_closure_min | | | 100.0 |
| | agm_closure_scaling | | | 0.07 |
| | agm_closure_upper_depth | | | 100.0 |
| | aredi | | | 600.0 |
| | aredi_equal_agm | | | False |
| | drhodz_mom4p1 | | | False |
| | drhodz_smooth_horz | | | False |
| | drhodz_smooth_vert | | | False |
| | rossby_radius_max | | | 100 000.0 |
| | rossby_radius_min | | | 15 000.0 |
| | tracer_mix_micom | | | False |
| | vel_micom | | | 0.0 |
| &ocean_nphysicsa_nml | use_this_module | | | False |
| &ocean_nphysicsb_nml | use_this_module | | | False |
| &ocean_nphysicsc_nml | use_this_module | | | False |

F.1 ACCESS-OM2-01 MOM compared to OFAM3

| Group (continued) | Variable | OFAM3/ input.ofam3 - spinup03.nml | OFAM3/ input.ofam2017.nml | ./gadi/g/data/ hh5/tmp/cosima/ access-om2-01/ 01deg_jra55v13 - iaf/output197/ ocean/input.nml |
|----------------------------|-------------------------------|---|------------------------------|--|
| &ocean_ofam_diag_nml | debug_this_module | False | False | |
| | do_eta_tendency | False | False | |
| &ocean_operators_nml | use_legacy_div_ud | | | False |
| &ocean_overexchange_nml | debug_this_module | | | False |
| | overexch_npts | | | 4 |
| | overexch_weight_far | | | False |
| | overflow_umax | | | 5.0 |
| | use_this_module | False | False | False |
| &ocean_overflow_nml | debug_this_module | False | False | |
| | use_this_module | False | False | False |
| &ocean_overflow_ofp_nml | use_this_module | | | False |
| &ocean_pressure_nml | zero_pressure_force | | | False |
| &ocean_rivermix_nml | river_diffuse_salt | False | False | True |
| | river_diffuse_temp | False | False | True |
| | river_insertion_thickness | 15.0 | 15.0 | 40.0 |
| | use_this_module | True | True | True |
| &ocean_riverspread_nml | debug_this_module | | | False |
| | use_this_module | True | True | False |
| &ocean_rough_nml | rough_scheme | | 'beljaars' | 'beljaars' |
| &ocean_sbc_nml | avg_sfc_temp_salt_eta | | | True |
| | avg_sfc_velocity | | | True |
| | calvingspread | | | False |
| | do_bitwise_exact_sum | | False | False |
| | do_flux_correction | | | False |
| | land_model_heat_fluxes | | | False |
| | max_delta_salinity_restore | | | 0.5 |
| | max_ice_thickness | | | 0.0 |
| | ocean_ice_salt_limit | | | 0.006 |
| | restore_mask_gfdl | | | False |
| | runoff_salinity | | | 0.0 |
| | runoffspread | | | False |
| | salt_correction_scale | | | 0.0 |
| | salt_restore_tscale | 180.0 | 14.0 | 10.0 |
| | salt_restore_under_ice | | | True |
| | use_full_patm_for_sea_level | | | False |
| | zero_heat_fluxes | | | False |
| | zero_net_salt_correction | | | False |
| | zero_net_salt_restore | | | True |
| | zero_net_water_correction | | | False |
| | zero_net_water_couple_restore | | | True |
| | zero_net_water_coupler | | True | True |
| | zero_net_water_restore | | | True |
| | zero_surface_stress | | | False |
| | zero_water_fluxes | | | False |
| &ocean_sbc_ofam_nml | do_override_stress_ofam | | False | |
| | restore_mask_ofam | False | False | |
| | river_temp_ofam | False | False | |
| &ocean_shortwave_csiro_nml | read_depth | True | True | |
| | use_this_module | True | False | False |
| | zmax_pen | 6000.0 | 6000.0 | |
| &ocean_shortwave_gfdl_nml | optics_manizza | | True | True |
| | optics_morel_antoine | | False | False |
| | use_this_module | False | True | True |

F.1 ACCESS-OM2-01 MOM compared to OFAM3

| Group (continued) | Variable | OFAM3/ input.ofam3 - spinup03.nml | OFAM3/ input.ofam2017.nml | ./gadi/g/data/ hh5/tmp/cosima/ access-om2-01/ 01deg_jra55v13 - iaf/output197/ ocean/input.nml |
|----------------------------------|-----------------------------|---|------------------------------|--|
| | zmax_pen | 100.0 | 6000.0 | 300.0 |
| &ocean_shortwave_jerlov_nml | use_this_module | | | False |
| &ocean_shortwave_nml | use_shortwave_csiro | True | False | False |
| | use_shortwave_gfdl | False | True | True |
| | use_shortwave_jerlov | | | False |
| | use_this_module | True | True | True |
| &ocean_sponges_eta_ofam_nml | athresh | 0.5 | 0.5 | |
| | days_to_restore | -1 | -1 | |
| | lambda | 0.0083 | 0.0083 | |
| | npower | 1.0 | 1.0 | |
| | secs_to_restore | 0 | 0 | |
| | taumin | 1200 | 1200 | |
| | use_adaptive_restore | False | False | |
| | use_hard_thump | False | False | |
| | use_normalising | True | True | |
| &ocean_sponges_tracer_nml | damp_coeff_3d | True | True | |
| | use_this_module | True | True | False |
| &ocean_sponges_tracer_ofam_nml | athresh | 0.5 | 0.5 | |
| | days_to_restore | -1 | -1 | |
| | lambda | 0.0083 | 0.0083 | |
| | limit_salt | | True | |
| | limit_salt_min | | 0.25 | |
| | limit_temp | | True | |
| | limit_temp_restore | | 1800.0 | |
| | npower | 1.0 | 1.0 | |
| | secs_to_restore | 0 | 0 | |
| | taumin | 1200 | 1200 | |
| | use_adaptive_restore | False | False | |
| | use_hard_thump | False | False | |
| | use_normalising | True | True | |
| &ocean_sponges_velocity_nml | damp_coeff_3d | False | False | |
| | use_this_module | False | False | False |
| &ocean_sponges_velocity_ofam_nml | athresh | 0.5 | 0.5 | |
| | days_to_restore | -1 | -1 | |
| | lambda | 0.0083 | 0.0083 | |
| | npower | 1.0 | 1.0 | |
| | secs_to_restore | 0 | 0 | |
| | taumin | 1200 | 1200 | |
| | use_adaptive_restore | True | True | |
| | use_hard_thump | False | False | |
| | use_normalising | True | True | |
| &ocean_submesoscale_nml | coefficient_ce | | | 0.05 |
| | debug_this_module | | | False |
| | front_length_const | | | 5000.0 |
| | front_length_deform_radius | | | True |
| | limit_psi | | | True |
| | limit_psi_velocity_scale | | | 0.5 |
| | min_kblt | | | 4 |
| | smooth_advect_transport | | | True |
| | smooth_advect_transport_num | | | 4 |
| | smooth_hblt | | | False |
| | smooth_psi | | | True |
| | smooth_psi_num | | | 3 |
| | submeso_advect_flux | | | False |

F.1 ACCESS-OM2-01 MOM compared to OFAM3

| Group (continued) | Variable | OFAM3/ input.ofam3 - spinup03.nml | OFAM3/ input.ofam2017.nml | ./gadi/g/data/ hh5/tmp/cosima/ access-om2-01/ 01deg_jra55v13 - iaf/output197/ ocean/input.nml |
|--------------------------|--------------------------------|---|------------------------------|--|
| | submeso_advect_limit | | | True |
| | submeso_advect_upwind | | | True |
| | submeso_advect_zero_bdy | | | True |
| | submeso_diffusion | | | False |
| | submeso_diffusion_biharmonic | | | True |
| | submeso_diffusion_scale | | | 10.0 |
| | submeso_skew_flux | | | True |
| | use_hblt_equal_mld | | | True |
| | use_psi_legacy | | | False |
| | use_this_module | False | False | True |
| &ocean_tempsalt_nml | debug_this_module | | | False |
| | pottemp_equal_contemp | | | True |
| | reinit_ts_with_ideal | False | False | |
| | s_max | 55.0 | 55.0 | 70.0 |
| | s_min_limit | 5.0 | 5.0 | 2.0 |
| | t_min | -5.0 | -5.0 | -20.0 |
| | t_min_limit | -1.5 | -1.5 | -5.0 |
| &ocean_thickness_nml | debug_this_module | | | False |
| | debug_this_module_detail | | | False |
| | rescale_mass_to_get_ht_mod | | | False |
| | update_dzwu_k0 | True | True | |
| &ocean_tracer_advect_nml | advect_sweby_all | True | True | |
| | read_basin_mask | | | False |
| | zero_tracer_advect_horz | False | False | |
| | zero_tracer_advect_vert | False | False | |
| &ocean_tracer_diag_nml | diag_step | 144 | 144 | 576 |
| | tracer_conserve_days | 3.0 | 3.0 | 30.0 |
| &ocean_tracer_nml | age_tracer_max_init | | | 0.0 |
| | compute_tmask_limit_on | False | False | |
| | frazil_heating_before_vphysics | | | False |
| | limit_age_tracer | | | True |
| | remap_depth_to_s_init | | | False |
| | use_tempsalt_check_range | | | True |
| | zero_tracer_source | | | False |
| &ocean_velocity_diag_nml | diag_step | 144 | 144 | 576 |
| | energy_diag_step | 960 | 288 | 5760 |
| &ocean_velocity_nml | max_cgint | | | 1.0 |
| | truncate_velocity_value | 0.2 | 0.2 | 2.0 |
| | truncate_verbose | | | True |
| | zero_tendency_explicit_a | | | False |
| | zero_tendency_explicit_b | | | False |
| | zero_tendency_implicit | | | False |
| &ocean_vert_chen_nml | debug_this_module | False | False | |
| | diff_cbt_iw | 1×10^{-5} | 0.0 | |
| | diff_cbt_limit | 0.005 | 0.005 | |
| | diff_con_limit | 0.1 | 0.1 | |
| | use_this_module | False | False | |
| | visc_cbu_iw | 0.0001 | 0.0 | |
| | visc_cbu_limit | 0.005 | 0.005 | |
| | visc_con_limit | 0.1 | 0.01 | |
| &ocean_vert_const_nml | use_this_module | False | False | |
| &ocean_vert_gotm_nml | advection_gotm_method | | 'upwind' | |
| | correct_adv_errors | | True | |

F.1 ACCESS-OM2-01 MOM compared to OFAM3

| Group (continued) | Variable | OFAM3/ input.ofam3_ - spinup03.nml | OFAM3/ input.ofam2017.nml | ./gadi/g/data/ hh5/tmp/cosima/ access-om2-01/ 01deg_jra55v13_- iaf/output197/ ocean/input.nml |
|----------------------------|---------------------------------|--|------------------------------|--|
| | debug_this_module | | False | |
| | diff_cbt_min | | 0.0001 | |
| | do_advection_gotm | | True | |
| | do_turbulence_gotm | | True | |
| | min_diss | | 1×10^{-10} | |
| | min_tke | | 1×10^{-6} | |
| | use_this_module | False | True | |
| | visc_cbu_min | | 1×10^{-5} | |
| | write_a_restart | | True | |
| | z0b | | 0.002 | |
| | z0s | | 0.2 | |
| &ocean_vert_kpp_iow_nml | use_this_module | | False | |
| &ocean_vert_kpp_mom4p1_nml | diff_cbt_iw | | 0.0 | |
| | double_diffusion | | True | |
| | tbl_standard_method | | False | False |
| | ricr | | 0.3 | |
| | smooth_blmc | | | False |
| | smooth_ri_kmax_eq_kmu | | True | True |
| | use_this_module | | True | True |
| | visc_cbu_iw | | | 0.0 |
| &ocean_vert_kpp_nml | tbl_standard_method | False | | |
| | smooth_ri_kmax_eq_kmu | True | | |
| | use_this_module | True | | |
| &ocean_vert_mix_nml | bryan_lewis_lat_depend | | | False |
| | hwf_diffusivity | | | False |
| | hwf_min_diffusivity | | | 2×10^{-6} |
| | hwf_n0_2omega | | | 20.0 |
| | use_diff_cbt_table | | | False |
| | vert_diff_back_via_max | | | True |
| | vert_mix_scheme | 'kpp' | 'gotm' | 'kpp_mom4p1' |
| &ocean_vert_tidal_nml | background_viscosity | 0.0 | 0.0 | 0.0001 |
| | decay_scale | | | 500.0 |
| | drag_dissipation_use_cdbot | | | True |
| | fixed_wave_dissipation | | | False |
| | max_wave_diffusivity | | | 0.01 |
| | mixing_efficiency_n2depend | | | True |
| | read_roughness | | False | True |
| | read_wave_dissipation | | | False |
| | reading_roughness_amp | | | True |
| | reading_roughness_length | | | False |
| | roughness_scale | | | 12 000.0 |
| | shelf_depth_cutoff | | | -1000.0 |
| | tide_speed_data_on_t_grid | | | True |
| | use_legacy_methods | | | False |
| | use_this_module | True | True | True |
| | use_wave_dissipation | False | False | True |
| | wave_energy_flux_max | | | 0.1 |
| &ocean_xlandinsert_nml | use_this_module | False | False | False |
| | verbose_init | True | True | |
| &ocean_xlandmix_nml | use_this_module | False | False | False |
| | verbose_init | True | True | |
| &sat_vapor_pres_nml | construct_table_wrt_liq_and_ice | True | True | |
| | show_all_bad_values | True | True | |

F.2 ACCESS-OM2-01 MOM compared to MOM-SIS-01 and GFDL

| Group (continued) | Variable | OFAM3/ input.ofam3 - spinup03.nml | OFAM3/ input.ofam2017.nml | ./gadi/g/data/ hh5/tmp/cosima/ access-om2-01/ 01deg_jra55v13 - iaf/output197/ ocean/input.nml |
|-------------------|-----------------|---|------------------------------|--|
| &surface_flux_nml | ncar_ocean_flux | False | | |
| | raoult_sat_vap | True | | |
| &xgrid_nml | do_alltoall | | True | True |
| | do_alltoallv | | True | True |
| | nsubset | | | 16 |

F.2 ACCESS-OM2-01 MOM compared to MOM-SIS-01 and GFDL

F.3 ACCESS-OM2-01 CICE compared to RASM and NCAR

ice_in_RASM **TODO:** get permission

ncar_ice_in **TODO:** get permission

F.4 ACCESS-OM2 MOM and CICE compared to ACCESS, ACCESS-CM2, ACCESS-ESM

Only differences are shown. See https://www.dropbox.com/s/lktfwl3da0jpzp6/Fabio2018_Namelist_meeting_final.pdf?dl=0.

F.4.1 MOM namelist input.nml

| Group | Variable | ACCESS-CM2/ input.nml | ./gadi/g/data/ hh5/tmp/cosima/ access-om2/ 1deg_jra55v13 - iaf_spinup1_B1/ output059/ocean/ input.nml |
|-----------------------------|---------------------|--------------------------|---|
| &auscom_ice_nml | dt_cpl | 1800 | |
| | ige | 345 | |
| | igs | 328 | |
| | ire1 | 324 | |
| | ire2 | 335 | |
| | irs1 | 314 | |
| | irs2 | 325 | |
| | jge | 198 | |
| | jgs | 189 | |
| | jre1 | 196 | |
| | jre2 | 180 | |
| | jrs1 | 169 | |
| | jrs2 | 169 | |
| | kmxice | 15 | 5 |
| | redsea_gulfbay_sfix | True | False |
| | sfix_hours | 24 | |
| &bg_diff_lat_dependence_nml | bg_diff_eq | 1×10^{-6} | |
| | lat_low_bgdiff | 20.0 | |
| &diag_manager_nml | debug_diag_manager | | False |
| | issue_oor_warnings | | True |
| &fms_nml | domains_stack_size | | 115200 |

| Group (continued) | Variable | ACCESS-CM2/ input.nml | ./gadi/g/data/ hh5/tmp/cosima/ access-om2/ 1deg_jra55v13_- iaf_spinup1_B1/ output059/ocean/ input.nml |
|----------------------------|-----------------------------|--|--|
| &mom_oasis3_interface_nml | fields_in | 'u_flux', 'v_flux', 'lprec', 'fprec', 'salt_flux', 'mh_flux', 'sw_flux', 'q_flux', 't_flux', 'lw_flux', 'runof', 'p', 'aice', 'wfimelt', 'wfiform', 'co2_io', 'wnd_io', 'licefw', 'liceht' 't_surf', 's_surf', 'u_surf', 'v_surf', 'dssldx', 'dssldy', 'frazil', 'co2_o', 'co2fx_o' | 'u_flux', 'v_flux', 'lprec', 'fprec', 'salt_flux', 'mh_flux', 'sw_flux', 'q_flux', 't_flux', 'lw_flux', 'runof', 'p', 'aice', 'wfimelt', 'wfiform' |
| | fields_out | 19 | 15 |
| | num_fields_in | 9 | 7 |
| | num_fields_out | | |
| | send_after_ocean_update | False | True |
| | send_before_ocean_update | True | False |
| &monin_obukhov_nml | neutral | | True |
| &mpp_io_nml | deflate_level | 5 | |
| | shuffle | 1 | |
| &ocean_adv_vel_diag_nml | diag_step | 120 | 4320 |
| | verbose_cfl | False | True |
| &ocean_albedo_nml | ocean_albedo_option | 2 | |
| &ocean_barotropic_nml | barotropic_halo | 10 | |
| | diag_step | 120 | 4320 |
| | smooth_eta_t_biharmonic | True | False |
| | smooth_eta_t_laplacian | False | True |
| | smooth_pbot_t_biharmonic | True | False |
| | smooth_pbot_t_laplacian | False | True |
| | use_legacy_barotropic_halos | | False |
| | zero_tendency | | False |
| &ocean_bbc_nml | bmf_implicit | | True |
| | cdbot_hi | | 0.007 |
| | cdbot_law_of_wall | False | |
| | cdbot_roughness_length | | False |
| | cdbot_roughness_uamp | | True |
| | uresidual | | 0.05 |
| &ocean_bbc_ofam_nml | read_tide_speed | False | |
| | uresidual2_max | 1.0 | |
| &ocean_bihgen_friction_nml | ncar_boundary_scaling_read | | False |
| | use_this_module | True | True |
| &ocean_convect_nml | convect_full_scalar | True | |
| | convect_full_vector | False | |
| | use_this_module | False | False |
| &ocean_domains_nml | max_tracers | 20 | 5 |
| &ocean_form_drag_nml | cprime_aiki | 0.6 | |
| | use_this_module | False | False |
| &ocean_frazil_nml | debug_this_module | | False |
| | frazil_only_in_surface | True | False |
| | freezing_temp_preteos10 | | True |
| | freezing_temp_simple | True | False |

| Group (continued) | Variable | ACCESS-CM2/ input.nml | ./gadi/g/data/ hh5/tmp/cosima/ access-om2/ 1deg_jra55v13_- iaf_spinup1_B1/ output059/ocean/ input.nml |
|-------------------------------|-------------------------------|--------------------------|---|
| | use_this_module | True | True |
| &ocean_grids_nml | debug_this_module | True | False |
| | read_rho0_profile | False | |
| &ocean_increment_eta_nml | days_to_increment | 0 | |
| | fraction_increment | 1.0 | |
| | secs_to_increment | 3600 | |
| | use_this_module | False | False |
| &ocean_increment_tracer_nml | days_to_increment | 0 | |
| | fraction_increment | 1.0 | |
| | secs_to_increment | 3600 | |
| | use_this_module | False | False |
| &ocean_increment_velocity_nml | days_to_increment | 0 | |
| | fraction_increment | 1.0 | |
| | secs_to_increment | 3600 | |
| | use_this_module | False | False |
| &ocean_lapgen_friction_nml | ncar_only_equatorial | True | |
| | use_this_module | True | True |
| | vconst_1 | 8 000 000.0 | |
| | vconst_2 | 0.0 | |
| | vconst_3 | 0.8 | |
| | vconst_4 | 5×10^{-9} | |
| | vconst_5 | 3 | |
| | vconst_6 | 300 000 000.0 | |
| | vconst_7 | 100.0 | |
| | viscosity_ncar | True | False |
| | viscosity_ncar_2000 | False | |
| | viscosity_ncar_2007 | True | False |
| &ocean_model_nml | barotropic_split | 100 | 80 |
| | do_wave | True | |
| | dt_ocean | 1800 | |
| | io_layout | | 4, 3 |
| | layout | 8, 14 | 16, 15 |
| &ocean_momentum_source_nml | rayleigh_damp_exp_from_bottom | | False |
| | use_this_module | True | True |
| &ocean_nphysics_util_nml | agm_closure_max | 1200.0 | 600.0 |
| | agm_closure_min | 100.0 | 50.0 |
| | aredi | 300.0 | 600.0 |
| | smax | 0.002 | |
| | swidth | 0.0002 | |
| &ocean_nphysicsa_nml | debug_this_module | False | |
| | neutral_linear_gm_taper | True | |
| | neutral_physics_limit | True | |
| | neutral_physics_simple | 'false' | |
| | neutral_sine_taper | True | |
| | tmask_neutral_on | True | |
| | use_this_module | False | False |
| &ocean_operators_nml | use_legacy_div_ud | | False |
| &ocean_overexchange_nml | overexch_check_extrema | False | |
| | use_this_module | False | False |
| &ocean_overflow_nml | debug_this_module | False | |
| | use_this_module | False | False |
| &ocean_overflow_ofp_nml | use_this_module | | False |

| Group (continued) | Variable | ACCESS-CM2/ input.nml | ./gadi/g/data/ hh5/tmp/cosima/ access-om2/ 1deg_jra55v13_- iaf_spinup1_B1/ output059/ocean/ input.nml |
|----------------------------|-------------------------------|--------------------------|---|
| &ocean_pressure_nml | zero_pressure_force | | False |
| &ocean_rivermix_nml | river_diffuse_salt | False | True |
| | river_diffuse_temp | False | True |
| | use_this_module | True | True |
| &ocean_riverspread_nml | use_this_module | True | False |
| &ocean_rough_nml | rough_scheme | | 'beljaars' |
| &ocean_sbc_nml | calvingspread | | False |
| | do_bitwise_exact_sum | | True |
| | do_flux_correction | | False |
| | ice_salt_concentration | 0.004 | |
| | land_model_heat_fluxes | | False |
| | max_delta_salinity_restore | 0.5 | -0.5 |
| | max_ice_thickness | 8.0 | 0.0 |
| | salt_correction_scale | | 0.0 |
| | salt_restore_tscale | -1.0 | 21.28 |
| | salt_restore_under_ice | False | True |
| | temp_restore_tscale | -1.0 | -10.0 |
| | use_full_patm_for_sea_level | | False |
| | waterflux_tavg | False | |
| | zero_net_salt_correction | | False |
| | zero_net_salt_restore | False | True |
| | zero_net_water_correction | | False |
| | zero_net_water_couple_restore | False | True |
| | zero_net_water_coupler | False | True |
| | zero_net_water_restore | False | True |
| &ocean_sbc_ofam_nml | restore_mask_ofam | False | |
| | river_temp_ofam | False | |
| &ocean_shortwave_csiro_nml | read_depth | True | |
| | use_this_module | False | False |
| | zmax_pen | 7000 | |
| &ocean_shortwave_gfdl_nml | use_this_module | True | True |
| | zmax_pen | 7000.0 | 300.0 |
| &ocean_sigma_transport_nml | sigma_advection_on | False | |
| | sigma_advection_sgs_only | False | |
| | sigma_diffusion_on | True | |
| | sigma_diffusivity_ratio | 1×10^{-6} | |
| | sigma_just_in_bottom_cell | True | |
| | sigma_umax | 0.01 | |
| | smooth_sigma_thickness | True | |
| | smooth_sigma_velocity | True | |
| | smooth_yelmicom | 0.2 | |
| | thickness_sigma_layer | 100.0 | |
| | thickness_sigma_max | 100.0 | |
| | thickness_sigma_min | 100.0 | |
| | tmask_sigma_on | False | |
| | tracer_mix_micom | True | |
| | use_this_module | True | True |
| | vel_micom | 0.05 | |
| &ocean_solo_nml | calendar | 'gregorian' | |
| | date_init | 301, 1, 1, 0, 0, 0 | |
| | days | 30 | |
| | dt_cpld | 1800 | |

| Group (continued) | Variable | ACCESS-CM2/ input.nml | ./gadi/g/data/ hh5/tmp/cosima/ access-om2/ 1deg_jra55v13_- iaf_spinup1_B1/ output059/ocean/ input.nml |
|---------------------------|------------------------------|--------------------------|---|
| | hours | 0 | |
| | minutes | 0 | |
| | months | 0 | |
| | seconds | 0 | |
| | years | 0 | |
| &ocean_sponges_tracer_nml | damp_coeff_3d | False | |
| | use_this_module | False | False |
| &ocean_submesoscale_nml | coefficient_ce | 0.05 | |
| | smooth_advect_transport | True | |
| | smooth_advect_transport_num | 2 | |
| | smooth_psi | True | |
| | smooth_psi_num | 2 | |
| | submeso_advect_flux | False | |
| | submeso_advect_limit | True | |
| | submeso_advect_upwind | True | |
| | submeso_advect_zero_bdy | True | |
| | submeso_diffusion | False | |
| | submeso_diffusion_biharmonic | True | |
| | submeso_diffusion_scale | 10.0 | |
| | submeso_limit_flux | True | |
| | submeso_skew_flux | True | |
| | use_psi_legacy | False | |
| | use_this_module | True | True |
| &ocean_tempsalt_nml | debug_this_module | False | |
| | pottemp_equal_contemp | False | True |
| | s_max | 55.0 | 70.0 |
| | s_min | -1.0 | 0.0 |
| | s_min_limit | 0.0 | 2.0 |
| | t_min | -5.0 | -20.0 |
| | t_min_limit | -2.0 | -5.0 |
| &ocean_thickness_nml | initialize_zero_eta | False | |
| | read_rescale_rho0_mask | False | |
| | rescale_mass_to_get_ht_mod | | False |
| | rescale_rho0_basin_label | 7.0 | |
| | rescale_rho0_mask_gfdl | False | |
| | rescale_rho0_value | 0.75 | |
| | thickness_dzt_min | 1.0 | |
| | thickness_dzt_min_init | 2.0 | |
| &ocean_topog_nml | min_thickness | 25.0 | |
| &ocean_tracer_advect_nml | advect_sweby_all | True | |
| | read_basin_mask | | False |
| &ocean_tracer_diag_nml | diag_step | 120 | 4320 |
| | tracer_conserve_days | 1.0 | 30.0 |
| &ocean_tracer_nml | debug_this_module | True | False |
| | use_tempsalt_check_range | | True |
| &ocean_velocity_diag_nml | diag_step | 120 | 4320 |
| | energy_diag_step | 120 | 4320 |
| &ocean_velocity_nml | truncate_verbose | False | True |
| | zero_tendency_explicit_a | | False |
| | zero_tendency_explicit_b | | False |
| | zero_tendency_implicit | | False |
| &ocean_vert_gotm_nml | advection_gotm_method | 'sweby' | |

| Group (continued) | Variable | ACCESS-CM2/ input.nml | ./gadi/g/data/ hh5/tmp/cosima/ access-om2/ 1deg_jra55v13_- iaf_spinup1_B1/ output059/ocean/ input.nml |
|----------------------------|-----------------------------|--------------------------|---|
| | correct_adv_errors | True | |
| | debug_this_module | False | |
| | diff_cbt_min | 0.0001 | |
| | do_advection_gotm | False | |
| | do_turbulence_gotm | True | |
| | min_diss | 1×10^{-10} | |
| | min_tke | 1×10^{-6} | |
| | use_this_module | False | |
| | visc_cbu_min | 1×10^{-5} | |
| | write_a_restart | True | |
| | z0b | 0.002 | |
| | z0s | 0.2 | |
| &ocean_vert_kpp_iow_nml | use_this_module | | False |
| &ocean_vert_kpp_mom4p1_nml | diff_con_limit | 0.1 | |
| | do_langmuir | True | |
| | kbl_standard_method | True | False |
| | smooth_blmc | True | False |
| | smooth_ri_kmax_eq_kmu | | True |
| | use_this_module | True | True |
| | visc_con_limit | 0.1 | |
| &ocean_vert_mix_nml | afkph_00 | 0.65 | |
| | afkph_90 | 0.75 | |
| | bryan_lewis_lat_depend | True | False |
| | bryan_lewis_lat_transition | 35.0 | |
| | dfkph_00 | 1.15 | |
| | dfkph_90 | 0.95 | |
| | hwf_diffusivity | | False |
| | hwf_min_diffusivity | | 2×10^{-6} |
| | hwf_n0_2omega | | 20.0 |
| | j09_bgmax | | 5×10^{-6} |
| | j09_bgmin | | 1×10^{-6} |
| | j09_diffusivity | | True |
| | j09_lat | | 20.0 |
| | linear_taper_diff_cbt_table | | False |
| | sfkph_00 | 4.5×10^{-5} | |
| | sfkph_90 | 4.5×10^{-5} | |
| | zfkph_00 | 250 000.0 | |
| | zfkph_90 | 250 000.0 | |
| &ocean_vert_tidal_nml | background_diffusivity | 5×10^{-6} | 0.0 |
| | decay_scale | 300.0 | 500.0 |
| | drag_dissipation_use_cdbot | | True |
| | drhodz_min | 1×10^{-12} | 1×10^{-10} |
| | max_drag_diffusivity | 0.005 | |
| | roughness_scale | 20 000.0 | 12 000.0 |
| | shelf_depth_cutoff | 160.0 | -1000.0 |
| | use_legacy_methods | | False |
| | use_this_module | True | True |
| &ocean_xlandinsert_nml | use_this_module | False | False |
| | verbose_init | True | |
| &ocean_xlandmix_nml | use_this_module | False | False |
| | verbose_init | True | |
| | xlandmix_kmt | True | |

| Group (continued) | Variable | ACCESS-CM2/ input.nml | ./gadi/g/data/ hh5/tmp/cosima/ access-om2/ 1deg_jra55v13_- iaf_spinup1_B1/ output059/ocean/ input.nml |
|-------------------|-------------------------|--------------------------|---|
| &xgrid_nml | interp_method | 'second_order' | |
| | make_exchange_reproduce | False | |
| | nsubset | 16 | |

F.4.2 CICE namelist cice_in.nml

| Group | Variable | ACCESS-CM2/ cice_in.nml | ./gadi/g/data/ hh5/tmp/cosima/ access-om2/ 1deg_jra55v13_- iaf_spinup1_B1/ output059/ice/ cice_in.nml |
|--------------------|-------------------|----------------------------|---|
| &domain_nml | distribution_wght | 'block' | 'latitude' |
| | maskhalo_bound | False | True |
| | maskhalo_dyn | False | True |
| | maskhalo_remap | False | True |
| | nprocs | 16 | 24 |
| | processor_shape | 'square-pop' | 'slenderX1' |
| &dynamics_nml | cosw | 1.0 | |
| | dragio | 0.005 36 | |
| | iceruf | 0.0005 | |
| | sinw | 0.0 | |
| &forcing_nml | calc_strair | False | True |
| | calc_tsfc | False | True |
| | cap_fluxes | True | |
| | fyear_init | 1997 | 1 |
| | tfrz_option | | 'linear_salt' |
| &grid_nml | grid_file | 'INPUT/grid.nc' | 'RESTART/grid.nc' |
| | kcatbound | 1 | 0 |
| | kmt_file | 'INPUT/kmt.nc' | 'RESTART/kmt.nc' |
| &icefields_bgc_nml | f_aero | | 'x' |
| | f_bgc_am_ml | | 'x' |
| | f_bgc_am_sk | | 'x' |
| | f_bgc_c_sk | | 'x' |
| | f_bgc_chl_sk | | 'x' |
| | f_bgc_dms_sk | | 'x' |
| | f_bgc_dmsp_ml | | 'x' |
| | f_bgc_dmspd_sk | | 'x' |
| | f_bgc_dmspp_sk | | 'x' |
| | f_bgc_n_sk | | 'x' |
| | f_bgc_nit_ml | | 'x' |
| | f_bgc_nit_sk | | 'x' |
| | f_bgc_sil_ml | | 'x' |
| | f_bgc_sil_sk | | 'x' |
| | f_bpphi | | 'x' |
| | f_btin | | 'x' |
| | f_faero_atm | | 'x' |
| | f_faero_ocn | | 'x' |
| | f_fbri | | 'm' |
| | f_fn | | 'x' |

| Group (continued) | Variable | ACCESS-CM2/ cice_in.nml | ./gadi/g/data/ hh5/tmp/cosima/ access-om2/ 1deg_jra55v13_- iaf_spinup1_B1/ output059/ice/ cice_in.nml |
|------------------------|----------------|----------------------------|---|
| | f_fn_ai | | 'x' |
| | f_fnh | | 'x' |
| | f_fnh_ai | | 'x' |
| | f_fno | | 'x' |
| | f_fno_ai | | 'x' |
| | f_fsil | | 'x' |
| | f_fsil_ai | | 'x' |
| | f_grownet | | 'x' |
| | f_hbri | | 'm' |
| | f_ppnet | | 'x' |
| &icefields_drag_nml | f_cdn_atm | | 'x' |
| | f_cdn_ocn | | 'x' |
| | f_drag | | 'x' |
| &icefields_mechred_nml | f_alvl | 'x' | 'm' |
| | f_ardg | 'x' | 'm' |
| | f_dardg1dt | 'm' | 'x' |
| | f_dardg2dt | 'm' | 'x' |
| | f_dvirdgdt | 'm' | 'x' |
| | f_opening | 'm' | 'x' |
| | f_vlvl | 'x' | 'm' |
| | f_vrdg | 'x' | 'm' |
| &icefields_nml | f_aice | 'dm' | 'm' |
| | f_albice | 'x' | 'm' |
| | f_albsni | 'x' | 'm' |
| | f_albsno | 'x' | 'm' |
| | f_alidf | 'x' | |
| | f_alidf_ai | 'm' | |
| | f_alidr_ai | 'm' | |
| | f_alvdf | 'x' | |
| | f_alvdf_ai | 'm' | |
| | f_alvdr_ai | 'm' | |
| | f_congel | 'x' | 'm' |
| | f_daidtd | 'x' | 'm' |
| | f_daidtt | 'x' | 'm' |
| | f_dvidtd | 'x' | 'm' |
| | f_dvidtt | 'x' | 'm' |
| | f_dvsdtd | 'm' | |
| | f_dvsdtt | 'm' | |
| | f_dxt | False | True |
| | f_dxu | False | True |
| | f_dyf | False | True |
| | f_dyf | False | True |
| | f_evap_ai | 'x' | 'm' |
| | f_evap_ice_ai | 'm' | |
| | f_evap_snow_ai | 'm' | |
| | f_fcondtop_ai | 'x' | 'm' |
| | f_fhocn_ai | 'x' | 'm' |
| | f_flat_ai | 'x' | 'm' |
| | f.flatn_ai | 'x' | 'm' |
| | f_flwdn | 'x' | 'm' |
| | f_flwup_ai | 'x' | 'm' |
| | f_fmeltn_ai | 'x' | 'm' |
| | f_frazil | 'x' | 'm' |

| Group (continued) | Variable | ACCESS-CM2/ cice_in.nml | ./gadi/g/data/ hh5/tmp/cosima/ access-om2/ 1deg_jra55v13_- iaf_spinup1_B1/ output059/ice/ cice_in.nml |
|-------------------|--------------------|----------------------------|---|
| | f_fresh_ai | 'x' | 'm' |
| | f_fsalt_ai | 'x' | 'm' |
| | f_fsens | | 'x' |
| | f_fsens_ai | | 'm' |
| | f_fsurf_ai | 'm' | 'x' |
| | f_fswabs_ai | 'x' | 'm' |
| | f_fswdn | | 'm' |
| | f_fswfac | 'x' | 'm' |
| | f_fswthru_ai | 'x' | 'm' |
| | f_hi | | 'm' |
| | f_hs | | 'm' |
| | f_hte | False | True |
| | f_htn | False | True |
| | f_iage | | 'm' |
| | f_icepresent | 'x' | 'm' |
| | f_meltb | 'x' | 'm' |
| | f_meltl | 'x' | 'm' |
| | f_melts | | 'm' |
| | f_meltt | 'x' | 'm' |
| | f_rain_ai | 'x' | 'm' |
| | f_shear | 'x' | 'm' |
| | f_siage | 'm' | |
| | f_sialb | 'm' | |
| | f_sice | | 'm' |
| | f_sicompstren | 'm' | |
| | f_sidconcdyn | 'm' | |
| | f_sidconchth | 'm' | |
| | f_sidiivvel | 'm' | |
| | f_sidmassdyn | 'm' | |
| | f_sidmassevapsUBL | 'm' | |
| | f_sidmassgrowthbot | 'm' | |
| | f_sidmassgrowthwat | 'm' | |
| | f_sidmasslat | 'm' | |
| | f_sidmassmeltbot | 'm' | |
| | f_sidmassmelttop | 'm' | |
| | f_sidmassssi | 'm' | |
| | f_sidmassth | 'm' | |
| | f_sidmasstranx | 'm' | |
| | f_sidmasstrany | 'm' | |
| | f_sifb | 'm' | |
| | f_siflcondbot | 'm' | |
| | f_siflcondtop | 'm' | |
| | f_siflfwbot | 'm' | |
| | f_sifllatstop | 'm' | |
| | f_sifllwdtop | 'm' | |
| | f_sifllwutop | 'm' | |
| | f_siflsaltbot | 'm' | |
| | f_siflsenstop | 'm' | |
| | f_siflsensupbot | 'm' | |
| | f_siflswdbot | 'm' | |
| | f_siflswdtop | 'm' | |
| | f_siflswutop | 'm' | |
| | f_siforcecoriolx | 'm' | |

| Group (continued) | Variable | ACCESS-CM2/ cice_in.nml | ./gadi/g/data/ hh5/tmp/cosima/ access-om2/ 1deg_jra55v13_- iaf_spinup1_B1/ output059/ice/ cice_in.nml |
|---------------------|------------------|----------------------------|---|
| | f_siforcecoriol | 'm' | |
| | f_siforceintstrx | 'm' | |
| | f_siforceintstry | 'm' | |
| | f_siforcetiltx | 'm' | |
| | f_siforcetilty | 'm' | |
| | f_sig1 | 'm' | 'x' |
| | f_sig2 | 'm' | 'x' |
| | f_sihc | 'm' | |
| | f_sipr | 'm' | |
| | f_sisaltmass | 'm' | |
| | f_sisnconc | 'm' | |
| | f_sisnhc | 'm' | |
| | f sisn thick | 'dm' | |
| | f sispeed | 'dm' | |
| | f_sistrxtop | 'm' | |
| | f_sistrxubot | 'm' | |
| | f_sistrydtop | 'm' | |
| | f_sistryubot | 'm' | |
| | f_sitempbottop | 'm' | |
| | f_sitempsnic | 'm' | |
| | f_sitemptop | 'dm' | |
| | f_sithick | 'dm' | |
| | f_siuc | 'dm' | |
| | f_siv | 'dm' | |
| | f_sndmassmelt | 'm' | |
| | f_sndmasssnf | 'm' | |
| | f_snoice | 'x' | 'm' |
| | f_snow_ai | 'x' | 'm' |
| | f_snowfrac | 'm' | |
| | f_snowfranc | 'm' | |
| | f_strairx | 'x' | 'm' |
| | f_stairy | 'x' | 'm' |
| | f_strcorx | 'x' | 'm' |
| | f_strcory | 'x' | 'm' |
| | f_strength | 'x' | 'm' |
| | f_strintx | 'x' | 'm' |
| | f_strinty | 'x' | 'm' |
| | f_strocnx | 'x' | 'm' |
| | f_strocny | 'x' | 'm' |
| | f_strltx | 'x' | 'm' |
| | f_strlty | 'x' | 'm' |
| | f_tsfc | | 'm' |
| | f_uocn | 'x' | 'm' |
| | f_uvel | | 'm' |
| | f_vgrdb | | False |
| | f_vocn | 'x' | 'm' |
| | f_vsnon | 'm' | |
| | f_vvel | | 'm' |
| &icefields_pond_nml | f_apeffn | 'm' | 'x' |
| | f_apondn | 'm' | 'x' |
| | f_hpndn | 'm' | 'x' |
| &ponds_nml | frzpd | 'cesm' | 'hlid' |
| | hs0 | 0.03 | 0.0 |

| Group (continued) | Variable | ACCESS-CM2/ cice_in.nml | ./gadi/g/data/ hh5/tmp/cosima/ access-om2/ 1deg_jra55v13_- iaf_spinup1_B1/ output059/ice/ cice_in.nml |
|-------------------|------------------|----------------------------|---|
| | rfracmax | 0.85 | 1.0 |
| &setup_nml | diagfreq | 24 | 960 |
| | dt | 1800 | 3600 |
| | dumpfreq | 'm' | 'y' |
| | history_dir | '/HISTORY/' | '/OUTPUT/' |
| | incond_dir | '/HISTORY/' | '/OUTPUT/' |
| | istep0 | 17280 | 2067360 |
| | lcdf64 | | False |
| | npt | 1488 | 35 040.0 |
| | print_global | True | False |
| | print_points | True | False |
| | restart_ext | True | False |
| | use_leap_years | True | False |
| | use_restart_time | False | True |
| | year_init | 301 | 1 |
| &shortwave_nml | ahmax | 0.5 | 0.1 |
| | albicei | 0.36 | 0.44 |
| | albicev | 0.78 | 0.86 |
| | dalb_mlt | | -0.02 |
| | dt_mlt | | 1.0 |
| | r_snow | 1.5 | 0.0 |
| | tocnfrz | | -1.8 |
| &thermo_nml | chio | | 0.004 |
| | conduct | 'MU71' | 'bubbly' |
| | dsdt_slow_mode | -1.5×10^{-7} | -5×10^{-8} |
| | saltmax | 9.6 | |
| &tracer_nml | tr_iage | True | False |
| | tr_pond_topo | True | False |

References

- Abel, R., C. W. Böning, R. J. Greatbatch, H. T. Hewitt, and M. J. Roberts, 2017: Feedback of mesoscale ocean currents on atmospheric winds in high-resolution coupled models and implications for the forcing of ocean-only models. *Ocean Science Discussions*, 1–22, doi:10.5194/os-2017-24, URL <http://dx.doi.org/10.5194/os-2017-24>.
- Abernathy, R. P., I. Cerovecki, P. R. Holland, E. Newsom, M. Mazloff, and L. D. Talley, 2016: Water-mass transformation by sea ice in the upper branch of the Southern Ocean overturning. *Nature Geoscience*, **9** (8), 596–601, doi:10.1038/ngeo2749, URL <http://dx.doi.org/10.1038/ngeo2749>.
- Adcroft, A., C. Hill, and J. Marshall, 1997: Representation of topography by shaved cells in a height coordinate ocean model. *Monthly Weather Review*, **125**, 2293–2315.
- Archer, M., M. Roughan, S. Keating, and A. Schaeffer, 2017a: On the variability of the East Australian Current: Jet structure, meandering, and influence on shelf circulation. *Journal of Geophysical Research: Oceans*, doi:10.1002/2017jc013097, URL <http://dx.doi.org/10.1002/2017JC013097>.
- Archer, M. R., S. R. Keating, M. Roughan, W. E. Johns, R. Lumpkin, F. Beron-Vera, and L. K. Shay, 2018: The kinematic similarity of two western boundary currents revealed by sustained high-resolution observations. *Geophysical Research Letters*, doi:10.1029/2018gl078429, URL <http://dx.doi.org/10.1029/2018GL078429>.
- Archer, M. R., L. K. Shay, and W. E. Johns, 2017b: The surface velocity structure of the Florida Current in a jet coordinate frame. *Journal of Geophysical Research: Oceans*, doi:10.1002/2017jc013286, URL <http://dx.doi.org/10.1002/2017JC013286>.
- Atmadipoera, A., R. Molcard, G. Madec, S. Wijffels, J. Sprintall, A. Koch-Larrouy, I. Jaya, and A. Supangat, 2009: Characteristics and variability of the Indonesian throughflow water at the outflow straits. *Deep Sea Research Part I: Oceanographic Research Papers*, **56** (11), 1942–1954, doi:10.1016/j.dsr.2009.06.004, URL <http://dx.doi.org/10.1016/j.dsr.2009.06.004>.
- Bailey, D., E. Hunke, A. DuVivier, B. Lipscomb, C. Bitz, M. Holland, B. Briegleb, and J. Schramm, 2018: CESM CICE5 users guide, Release CESM CICE5. Tech. rep. URL <https://media.readthedocs.org/pdf/cesmcice/latest/cesmcice.pdf>.
- Bamber, J., M. van den Broeke, J. Ettema, J. Lenaerts, and E. Rignot, 2012: Recent large increases in freshwater fluxes from Greenland into the North Atlantic. *Geophysical Research Letters*, **39** (19), L19 501, doi:10.1029/2012gl052552, URL <http://dx.doi.org/10.1029/2012GL052552>.
- Barthélemy, A., H. Goosse, T. Fichefet, and O. Lecomte, 2017: On the sensitivity of Antarctic sea ice model biases to atmospheric forcing uncertainties. *Climate Dynamics*, **51** (4), 1585–1603, doi:10.1007/s00382-017-3972-7, URL <http://dx.doi.org/10.1007/s00382-017-3972-7>.
- Beckmann, A., and R. Döscher, 1997: A method for improved representation of dense water spreading over topography in geopotential-coordinate models. *Journal of Physical Oceanography*, **27** (4), 581–591, doi:10.1175/1520-0485(1997)027<0581:amfiro>2.0.co;2, URL [http://dx.doi.org/10.1175/1520-0485\(1997\)027<0581:AMFIRO>2.0.CO;2](http://dx.doi.org/10.1175/1520-0485(1997)027<0581:AMFIRO>2.0.CO;2).
- Behrendt, A., H. Sumata, B. Rabe, and U. Schauer, 2018: UDASH - Unified Database for Arctic and Subarctic Hydrography. *Earth System Science Data*, **10** (2), 1119–1138, doi:10.5194/essd-10-1119-2018, URL <https://www.earth-syst-sci-data.net/10/1119/2018/>.
- Behrens, E., A. Biastoch, and C. W. Böning, 2013: Spurious AMOC trends in global ocean sea-ice models related to subarctic freshwater forcing. *Ocean Modelling*, **69**, 39–49, doi:10.1016/j.ocemod.2013.05.004, URL <http://dx.doi.org/10.1016/j.ocemod.2013.05.004>.

REFERENCES

- Beljaars, A. C. M., 1995: The parametrization of surface fluxes in large-scale models under free convection. *Quarterly Journal of the Royal Meteorological Society*, **121** (522), 255–270, doi:10.1002/qj.49712152203, URL <https://rmets.onlinelibrary.wiley.com/doi/abs/10.1002/qj.49712152203>, <https://rmets.onlinelibrary.wiley.com/doi/pdf/10.1002/qj.49712152203>.
- Bentley, J. L., 1975: Multidimensional binary search trees used for associative searching. *Commun. ACM*, **18** (9), 509–517, doi:10.1145/361002.361007, URL <http://doi.acm.org/10.1145/361002.361007>.
- Bi, D., and S. Marsland, 2010: Australian Climate Ocean Model (AusCOM) users guide. CAWCR Technical Report 27, The Centre for Australian Weather and Climate Research. URL http://www.cawcr.gov.au/technical-reports/CTR_027.pdf.
- Bi, D., H. Yan, and A. Sullivan, 2016: ACCESS-CM2 development. *COSIMA workshop 26-27 May 2016, Hobart*, URL <http://cosima.org.au/wp-content/uploads/2016/06/BI-COSIMA-Hobart-20160526.ppt.pdf>.
- Bi, D., and Coauthors, 2013a: The ACCESS coupled model: description, control climate and evaluation. *Australian Meteorological and Oceanographic Journal*, **63** (1), 41–64.
- Bi, D., and Coauthors, 2013b: ACCESS-OM: the ocean and sea-ice core of the ACCESS coupled model. *Australian Meteorological and Oceanographic Journal*, **63** (1), 213–232.
- Bi, D., and Coauthors, 2019: Configuring the ACCESS-CM2 model for CMIP6 experiments. *AMOS Annual Meeting 2019 and the International Conference on Tropical Meteorology and Oceanography*.
- Bitz, C. M., and W. H. Lipscomb, 1999: An energy-conserving thermodynamic model of sea ice. *Journal of Geophysical Research: Oceans*, **104** (C7), 15 669–15 677, doi:10.1029/1999jc900100, URL <http://dx.doi.org/10.1029/1999JC900100>.
- Böning, C. W., E. Behrens, A. Biastoch, K. Getzlaff, and J. L. Bamber, 2016: Emerging impact of Greenland meltwater on deepwater formation in the North Atlantic Ocean. *Nature Geoscience*, **9** (7), 523–527, doi:10.1038/ngeo2740, URL <http://dx.doi.org/10.1038/NGEO2740>.
- Bouillon, S., T. Fichefet, V. Legat, and G. Madec, 2013: The elastic-viscous-plastic method revisited. *Ocean Modelling*, **71**, 2–12, doi:10.1016/j.ocemod.2013.05.013, URL <http://dx.doi.org/10.1016/j.ocemod.2013.05.013>.
- Brodeau, L., B. Barnier, S. K. Gulev, and C. Woods, 2017: Climatologically significant effects of some approximations in the bulk parameterizations of turbulent air-sea fluxes. *Journal of Physical Oceanography*, **47** (1), 5–28, doi:10.1175/jpo-d-16-0169.1, URL <http://dx.doi.org/10.1175/JPO-D-16-0169.1>.
- Caesar, L., S. Rahmstorf, A. Robinson, G. Feulner, and V. Saba, 2018: Observed fingerprint of a weakening Atlantic Ocean overturning circulation. *Nature*, **556** (7700), 191–196, doi:10.1038/s41586-018-0006-5, URL <https://doi.org/10.1038/s41586-018-0006-5>.
- Campin, J.-M., and H. Goosse, 1999: Parameterization of density-driven downsloping flow for a coarse-resolution ocean model in z-coordinate. *Tellus A: Dynamic Meteorology and Oceanography*, **51** (3), 412–430, doi:10.3402/tellusa.v51i3.13468, URL <http://dx.doi.org/10.3402/tellusa.v51i3.13468>.
- Capet, X., J. C. McWilliams, M. J. Molemaker, and A. F. Shchepetkin, 2008: Mesoscale to submesoscale transition in the California Current system. Part I: Flow structure, eddy flux, and observational tests. *Journal of Physical Oceanography*, **38** (1), 29–43, doi:10.1175/2007JPO3671.1, URL <http://dx.doi.org/10.1175/2007JPO3671.1>.

REFERENCES

- Cassano, J. J., and Coauthors, 2017: Development of the Regional Arctic System Model (RASM): Near-surface atmospheric climate sensitivity. *Journal of Climate*, **30** (15), 5729–5753, doi:10.1175/jcli-d-15-0775.1, URL <http://dx.doi.org/10.1175/JCLI-D-15-0775.1>.
- Cheon, W. G., Y.-G. Park, J. R. Toggweiler, and S.-K. Lee, 2014: The relationship of Weddell Polynya and open-ocean deep convection to the Southern Hemisphere Westerlies. *Journal of Physical Oceanography*, **44** (2), 694–713, doi:10.1175/jpo-d-13-0112.1, URL <http://dx.doi.org/10.1175/JPO-D-13-0112.1>.
- Colella, P., and P. R. Woodward, 1984: The Piecewise Parabolic Method (PPM) for gas-dynamical simulations. *Journal of Computational Physics*, **54** (1), 174–201, doi:10.1016/0021-9991(84)90143-8, URL [http://dx.doi.org/10.1016/0021-9991\(84\)90143-8](http://dx.doi.org/10.1016/0021-9991(84)90143-8).
- Colin de Verdière, A., and M. Ollitrault, 2016: A direct determination of the world ocean barotropic circulation. *Journal of Physical Oceanography*, **46** (1), 255–273, doi:10.1175/jpo-d-15-0046.1, URL <http://dx.doi.org/10.1175/JPO-D-15-0046.1>.
- Craig, A. P., S. A. Mickelson, E. C. Hunke, and D. A. Bailey, 2015: Improved parallel performance of the CICE model in CESM1. *The International Journal of High Performance Computing Applications*, **29** (2), 154–165, doi:10.1177/1094342014548771, URL <http://dx.doi.org/10.1177/1094342014548771>.
- Dai, A., T. Qian, K. E. Trenberth, and J. D. Milliman, 2009: Changes in continental freshwater discharge from 1948 to 2004. *Journal of Climate*, **22** (10), 2773–2792, doi:10.1175/2008jcli2592.1, URL <http://dx.doi.org/10.1175/2008JCLI2592.1>.
- Danabasoglu, G., and Coauthors, 2014: North Atlantic simulations in Coordinated Ocean-ice Reference Experiments phase II (CORE-II). Part I: Mean states. *Ocean Modelling*, **73**, 76–107, doi:10.1016/j.ocemod.2013.10.005, URL <http://dx.doi.org/10.1016/j.ocemod.2013.10.005>.
- Danabasoglu, G., and Coauthors, 2016: North Atlantic simulations in Coordinated Ocean-ice Reference Experiments phase II (CORE-II). Part II: Inter-annual to decadal variability. *Ocean Modelling*, **97**, 65–90, doi:10.1016/j.ocemod.2015.11.007, URL <http://dx.doi.org/10.1016/j.ocemod.2015.11.007>.
- Dansereau, V., J. Weiss, P. Saramito, and P. Lattes, 2016: A Maxwell elasto-brittle rheology for sea ice modelling. *The Cryosphere*, **10** (3), 1339–1359, doi:10.5194/tc-10-1339-2016, URL <http://dx.doi.org/10.5194/tc-10-1339-2016>.
- de Boyer Montégut, C., G. Madec, A. S. Fischer, A. Lazar, and D. Iudicone, 2004: Mixed layer depth over the global ocean: An examination of profile data and a profile-based climatology. *Journal of Geophysical Research*, **109** (C12), doi:10.1029/2004jc002378, URL <http://dx.doi.org/10.1029/2004JC002378>.
- de Lavergne, C., S. Falahat, G. Madec, F. Roquet, J. Nycander, and C. Vic, 2019: Toward global maps of internal tide energy sinks. *Ocean Modelling*, **137**, 52–75, doi:10.1016/j.ocemod.2019.03.010, URL <http://dx.doi.org/10.1016/j.ocemod.2019.03.010>.
- Delworth, T. L., and Coauthors, 2012: Simulated climate and climate change in the GFDL CM2.5 high-resolution coupled climate model. *Journal of Climate*, **25** (8), 2755–2781, doi:10.1175/jcli-d-11-00316.1, URL <http://dx.doi.org/10.1175/JCLI-D-11-00316.1>.
- Depoorter, M. A., J. L. Bamber, J. A. Griggs, J. T. M. Lenaerts, S. R. M. Ligtenberg, M. R. van den Broeke, and G. Moholdt, 2013: Calving fluxes and basal melt rates of Antarctic ice shelves. *Nature*, **502** (7469), 89–92, doi:10.1038/nature12567, URL <http://dx.doi.org/10.1038/nature12567>.
- Dix, M., and Coauthors, 2013: The ACCESS coupled model: Documentation of core CMIP5 simulations and initial results. *Australian Meteorological and Oceanographic Journal*, **63** (1), 83–99.

REFERENCES

- Donat-Magnin, M., N. C. Jourdain, P. Spence, J. Le Sommer, H. Gallée, and G. Durand, 2017: Ice-shelf melt response to changing winds and glacier dynamics in the amundsen sea sector, antarctica. *Journal of Geophysical Research: Oceans*, **122** (12), 10 206–10 224, doi:10.1002/2017jc013059, URL <http://dx.doi.org/10.1002/2017JC013059>.
- Donohue, K. A., K. L. Tracey, D. R. Watts, M. P. Chidichimo, and T. K. Chereskin, 2016: Mean Antarctic Circumpolar Current transport measured in Drake Passage. *Geophysical Research Letters*, **43** (22), 11,760–11,767, doi:10.1002/2016gl070319, URL <http://dx.doi.org/10.1002/2016GL070319>.
- Dorn, W., A. Rinke, C. Köberle, K. Dethloff, and R. Gerdes, 2018: HIRHAM–NAOSIM 2.0: The upgraded version of the coupled regional atmosphere-ocean-sea ice model for Arctic climate studies. *Geoscientific Model Development Discussions*, 1–30, doi:10.5194/gmd-2018-278, URL <http://dx.doi.org/10.5194/gmd-2018-278>.
- Döscher, R., and A. Beckmann, 2000: Effects of a bottom boundary layer parameterization in a coarse-resolution model of the North Atlantic Ocean. *Journal of Atmospheric and Oceanic Technology*, **17** (5), 698–707, doi:10.1175/1520-0426(2000)017<0698:eoabbl>2.0.co;2, URL [http://dx.doi.org/10.1175/1520-0426\(2000\)017<0698:EOABBL>2.0.CO;2](http://dx.doi.org/10.1175/1520-0426(2000)017<0698:EOABBL>2.0.CO;2).
- Downes, S. M., N. L. Bindoff, and S. R. Rintoul, 2009: Impacts of climate change on the subduction of mode and intermediate water masses in the Southern Ocean. *Journal of Climate*, **22** (12), 3289–3302, doi:10.1175/2008jcli2653.1, URL <http://dx.doi.org/10.1175/2008JCLI2653.1>.
- Downes, S. M., A. Gnanadesikan, S. M. Griffies, and J. L. Sarmiento, 2011: Water mass exchange in the Southern Ocean in coupled climate models. *Journal of Physical Oceanography*, **41** (9), 1756–1771, doi:10.1175/2011jpo4586.1, URL <http://dx.doi.org/10.1175/2011JPO4586.1>.
- Downes, S. M., and Coauthors, 2015: An assessment of Southern Ocean water masses and sea ice during 1988–2007 in a suite of interannual CORE-II simulations. *Ocean Modelling*, **94**, 67–94, doi:10.1016/j.ocemod.2015.07.022, URL <http://dx.doi.org/10.1016/j.ocemod.2015.07.022>.
- Dufour, C. O., A. K. Morrison, S. M. Griffies, I. Frenger, H. Zanowski, and M. Winton, 2017: Pre-conditioning of the Weddell Sea polynya by the ocean mesoscale and dense water overflows. *Journal of Climate*, **30** (19), 7719–7737, doi:10.1175/jcli-d-16-0586.1, URL <http://dx.doi.org/10.1175/JCLI-D-16-0586.1>.
- Dukowicz, J. K., and J. R. Baumgardner, 2000: Incremental remapping as a transport/advection algorithm. *Journal of Computational Physics*, **160** (1), 318–335, doi:10.1006/jcph.2000.6465, URL <http://dx.doi.org/10.1006/jcph.2000.6465>.
- Dunne, J. P., and Coauthors, 2012: GFDL’s ESM2 global coupled climate–carbon earth system models. Part I: Physical formulation and baseline simulation characteristics. *Journal of Climate*, **25** (19), 6646–6665, doi:10.1175/jcli-d-11-00560.1, URL <http://dx.doi.org/10.1175/JCLI-D-11-00560.1>.
- Durran, D., J. A. Weyn, and M. Q. Menchaca, 2017: Practical considerations for computing dimensional spectra from gridded data. *Monthly Weather Review*, **145** (9), 3901–3910, doi:10.1175/mwr-d-17-0056.1, URL <http://dx.doi.org/10.1175/MWR-D-17-0056.1>.
- Errico, R. M., 1985: Spectra computed from a limited area grid. *Monthly Weather Review*, **113** (9), 1554–1562, doi:10.1175/1520-0493(1985)113<1554:scfala>2.0.co;2, URL [http://dx.doi.org/10.1175/1520-0493\(1985\)113<1554:SCFALA>2.0.CO;2](http://dx.doi.org/10.1175/1520-0493(1985)113<1554:SCFALA>2.0.CO;2).
- Farneti, R., and Coauthors, 2015: An assessment of Antarctic Circumpolar Current and Southern Ocean meridional overturning circulation during 1958–2007 in a suite of interannual CORE-II simulations. *Ocean Modelling*, **93**, 84–120, doi:10.1016/j.ocemod.2015.07.009, URL <http://dx.doi.org/10.1016/j.ocemod.2015.07.009>.

REFERENCES

- Feng, M., X. Zhang, P. Oke, D. Monselesan, M. Chamberlain, R. Matear, and A. Schiller, 2016: Invigorating ocean boundary current systems around Australia during 1979–2014: As simulated in a near-global eddy-resolving ocean model. *Journal of Geophysical Research: Oceans*, **121** (5), 3395–3408, doi:10.1002/2016JC011842, URL <http://dx.doi.org/10.1002/2016JC011842>.
- Fetterer, F., K. Knowles, W. Meier, M. Savoie, and A. K. Windnagel, 2017, updated daily: Sea ice index, version 3. Tech. rep., NSIDC: National Snow and Ice Data Center, Boulder, Colorado, USA. doi:<https://doi.org/10.7265/N5K072F8>, URL <https://doi.org/10.7265/N5K072F8>.
- Fiedler, E. K., and Coauthors, 2019: Intercomparison of long-term sea surface temperature analyses using the GHRSST Multi-Product Ensemble (GMPE) system. *Remote Sensing of Environment*, **222**, 18–33, doi:10.1016/j.rse.2018.12.015, URL <http://dx.doi.org/10.1016/j.rse.2018.12.015>.
- Flato, G., and Coauthors, 2013: *Evaluation of Climate Models*, book section 9, 741866. Cambridge University Press, Cambridge, United Kingdom and New York, NY, USA, doi:10.1017/CBO9781107415324.020, URL www.climatechange2013.org.
- Fox-Kemper, B., R. Ferrari, and R. Hallberg, 2008: Parameterization of mixed layer eddies. Part I: Theory and diagnosis. *J. Phys. Oceanogr.*, **38** (6), 1145–1165, doi:10.1175/2007JPO3792.1.
- Frajka-Williams, E., and Coauthors, 2019: Atlantic meridional overturning circulation: Observed transport and variability. *Frontiers in Marine Science*, **6**, doi:10.3389/fmars.2019.00260, URL <http://dx.doi.org/10.3389/fmars.2019.00260>.
- Fritzner, S., R. Graversen, K. H. Christensen, P. Rostosky, and K. Wang, 2018: Impact of assimilating sea ice concentration, sea ice thickness and snow depth in a coupled ocean-sea ice modeling system. *The Cryosphere Discussions*, 1–27, doi:10.5194/tc-2018-171, URL <http://dx.doi.org/10.5194/tc-2018-171>.
- Ganachaud, A., and C. Wunsch, 2003: Large-scale ocean heat and freshwater transports during the world ocean circulation experiment. *Journal of Climate*, **16** (4), 696–705, doi:10.1175/1520-0442(2003)016<0696:LSOHA>2.0.CO;2.
- Gent, P. R., and J. C. McWilliams, 1990: Isopycnal mixing in ocean circulation models. *J. Phys. Oceanogr.*, **20** (1), 150–155, doi:10.1175/1520-0485(1990)020<0150:IMIOCM>2.0.CO;2.
- Giles, A., R. Massom, P. Heil, and G. Hyland, 2011: Semi-automated feature-tracking of East Antarctic sea ice from Envisat ASAR imagery. *Remote Sensing of Environment*, **115** (9), 2267–2276, doi:10.1016/j.rse.2011.04.027, URL <http://ecite.utas.edu.au/76076>, ISSN 0034-4257.
- Gill, A. E., 1982: *Atmosphere-Ocean Dynamics*, International Geophysics, Vol. 30. 1st ed., Academic Press, San Diego.
- Girard, L., J. Weiss, J. M. Molines, B. Barnier, and S. Bouillon, 2009: Evaluation of high-resolution sea ice models on the basis of statistical and scaling properties of Arctic sea ice drift and deformation. *Journal of Geophysical Research*, **114** (C8), doi:10.1029/2008jc005182, URL <http://dx.doi.org/10.1029/2008JC005182>.
- Goosse, H., and T. Fichefet, 2001: Open-ocean convection and polynya formation in a large-scale ice-ocean model. *Tellus A*, **53** (1), 94–111, doi:10.3402/tellusa.v53i1.12175, URL <https://doi.org/10.3402/tellusa.v53i1.12175>.
- Gordon, A. L., 1978: Deep Antarctic convection west of Maud Rise. *Journal of Physical Oceanography*, **8** (4), 600–612, doi:10.1175/1520-0485(1978)008<0600:dacwom>2.0.co;2, URL [http://dx.doi.org/10.1175/1520-0485\(1978\)008<0600:DACWOM>2.0.CO;2](http://dx.doi.org/10.1175/1520-0485(1978)008<0600:DACWOM>2.0.CO;2).
- Gregg, M. C., T. B. Sanford, and D. P. Winkel, 2003: Reduced mixing from the breaking of internal waves in equatorial waters. *Nature*, **422** (6931), 513–515, doi:10.1038/nature01507.

REFERENCES

- Gregory, J. M., and Coauthors, 2016: The flux-anomaly-forced model intercomparison project (FAFMIP) contribution to CMIP6: investigation of sea-level and ocean climate change in response to CO₂ forcing. *Geoscientific Model Development*, **9** (11), 3993–4017, doi:10.5194/gmd-9-3993-2016, URL <http://dx.doi.org/10.5194/gmd-9-3993-2016>.
- Griffies, S., 2004: *Fundamentals of Ocean Climate Models*. Princeton University Press, Princeton, USA.
- Griffies, S., 2015: A handbook for the GFDL CM2-O model suite. Technical Report 1, GFDL Climate Processes and Sensitivity Group, NOAA/GFDL Princeton, USA.
- Griffies, S., and R. Hallberg, 2000: Biharmonic friction with a Smagorinsky-like viscosity for use in large-scale eddy-permitting ocean models. *Monthly Weather Review*, **128**, 2935–2946.
- Griffies, S., M. J. Harrison, R. C. Pacanowski, and A. Rosati, 2008: A technical guide to MOM4. GFDL Ocean Group Technical Report 5, NOAA/Geophysical Fluid Dynamics Laboratory, 342 pp.
- Griffies, S. M., 1998: The Gent-McWilliams skew flux. *J. Phys. Oceanogr.*, **28** (5), 831–841, doi:10.1175/1520-0485(1998)028<0831:TGMSF>2.0.CO;2.
- Griffies, S. M., 2012: Elements of the Modular Ocean Model (MOM) 5 (2012 release with updates). Technical Report 7, NOAA/Geophysical Fluid Dynamics Laboratory Ocean Group.
- Griffies, S. M., and Coauthors, 2009: Coordinated ocean-ice reference experiments (COREs). *Ocean Modelling*, **26** (1-2), 1–46, doi:10.1016/j.ocemod.2008.08.007, URL <http://dx.doi.org/10.1016/j.ocemod.2008.08.007>.
- Griffies, S. M., and Coauthors, 2014: An assessment of global and regional sea level for years 1993–2007 in a suite of interannual CORE-II simulations. *Ocean Modelling*, **78**, 35–89, doi:10.1016/j.ocemod.2014.03.004, URL <http://dx.doi.org/10.1016/j.ocemod.2014.03.004>.
- Griffies, S. M., and Coauthors, 2015: Impacts on ocean heat from transient mesoscale eddies in a hierarchy of climate models. *Journal of Climate*, **28** (3), 952–977, doi:10.1175/jcli-d-14-00353.1, URL <http://dx.doi.org/10.1175/JCLI-D-14-00353.1>.
- Griffies, S. M., and Coauthors, 2016: OMIP contribution to CMIP6: experimental and diagnostic protocol for the physical component of the Ocean Model Intercomparison Project. *Geoscientific Model Development*, **9** (9), 3231–3296, doi:10.5194/gmd-9-3231-2016, URL <https://www.geosci-model-dev.net/9/3231/2016/>.
- Haarsma, R. J., and Coauthors, 2016: High Resolution Model Intercomparison Project (HighResMIP). *Geoscientific Model Development Discussions*, 1–35, doi:10.5194/gmd-2016-66, URL <http://dx.doi.org/10.5194/gmd-2016-66>.
- Haidvogel, D., J. McWilliams, and P. Gent, 1992: Boundary current separation in a quasigeostrophic, eddy-resolving ocean circulation model. *J. Phys. Oceanogr.*, **22**, 882–902.
- Hallberg, R., 2013: Using a resolution function to regulate parameterizations of oceanic mesoscale eddy effects. *Ocean Modelling*, **72**, 92 – 103, doi:<http://dx.doi.org/10.1016/j.ocemod.2013.08.007>, URL <http://www.sciencedirect.com/science/article/pii/S1463500313001601>.
- Hallberg, R., 2014: Numerical instabilities of the ice/ocean coupled system. *CLIVAR Exchanges*, **65** (19/2), 38–42, URL http://www.clivar.org/sites/default/files/documents/exchanges65_0.pdf.
- Hamman, J., B. Nijssen, A. Roberts, A. Craig, W. Maslowski, and R. Osinski, 2017: The coastal streamflow flux in the Regional Arctic System Model. *Journal of Geophysical Research: Oceans*, **122** (3), 1683–1701, doi:10.1002/2016jc012323, URL <http://dx.doi.org/10.1002/2016JC012323>.

REFERENCES

- Hammond, M. D., and D. C. Jones, 2016: Freshwater flux from ice sheet melting and iceberg calving in the Southern Ocean. *Geoscience Data Journal*, **3** (2), 60–62, doi:10.1002/gdj3.43, URL <http://dx.doi.org/10.1002/gdj3.43>.
- Hautala, S. L., J. Sprintall, J. T. Potemra, J. C. Chong, W. Pandoe, N. Bray, and A. G. Ilahude, 2001: Velocity structure and transport of the Indonesian Throughflow in the major straits restricting flow into the Indian Ocean. *Journal of Geophysical Research: Oceans*, **106** (C9), 19 527–19 546, doi:10.1029/2000JC000577, URL <https://agupubs.onlinelibrary.wiley.com/doi/abs/10.1029/2000JC000577>.
- Heil, P., R. Massom, I. Allison, and A. Worby, 2011: Physical attributes of sea-ice kinematics during spring 2007 off East Antarctica. *Deep-Sea Research. Part 2: Topical Studies in Oceanography*, **58** (9-10), 1158–1171, doi:10.1016/j.dsr2.2010.12.004, URL <http://ecite.utas.edu.au/76077>, iSSN 0967-0645.
- Heorton, H. D. B. S., M. Tsamados, S. T. Cole, A. M. G. Ferreira, A. Berbellini, M. Fox, and T. W. K. Armitage, 2019: Retrieving sea ice drag coefficients and turning angles from in situ and satellite observations using an inverse modeling framework. *Journal of Geophysical Research: Oceans*, **124** (8), 6388–6413, doi:10.1029/2018jc014881, URL <http://dx.doi.org/10.1029/2018JC014881>.
- Heuzé, C., K. J. Heywood, D. P. Stevens, and J. K. Ridley, 2013: Southern Ocean bottom water characteristics in CMIP5 models. *Geophysical Research Letters*, **40** (7), 1409–1414, doi:10.1002/grl.50287, URL <http://dx.doi.org/10.1002/grl.50287>.
- Heuzé, C., J. K. Ridley, D. Calvert, D. P. Stevens, and K. J. Heywood, 2015: Increasing vertical mixing to reduce Southern Ocean deep convection in NEMO3.4. *Geoscientific Model Development*, **8** (10), 3119–3130, doi:10.5194/gmd-8-3119-2015, URL <http://dx.doi.org/10.5194/gmd-8-3119-2015>.
- Hibler, W. D., 1979: A dynamic thermodynamic sea ice model. *Journal of Physical Oceanography*, **9** (4), 815–846, doi:10.1175/1520-0485(1979)009<0815:adtsim>2.0.co;2, URL [http://dx.doi.org/10.1175/1520-0485\(1979\)009<0815:ADTSIM>2.0.CO;2](http://dx.doi.org/10.1175/1520-0485(1979)009<0815:ADTSIM>2.0.CO;2).
- Hirschi, J. J.-M., and Coauthors, 2019: The Atlantic meridional overturning circulation in high resolution models. *Journal of Geophysical Research: Oceans*, **(submitted)**.
- Hobbs, W. R., R. Massom, S. Stammerjohn, P. Reid, G. Williams, and W. Meier, 2016: A review of recent changes in Southern Ocean sea ice, their drivers and forcings. *Global and Planetary Change*, **143**, 228–250, doi:10.1016/j.gloplacha.2016.06.008, URL <http://dx.doi.org/10.1016/j.gloplacha.2016.06.008>.
- Holliday, N. P., S. Bacon, S. A. Cunningham, S. F. Gary, J. Karstensen, B. A. King, F. Li, and E. L. McDonagh, 2018: Subpolar North Atlantic overturning and gyre-scale circulation in the summers of 2014 and 2016. *Journal of Geophysical Research: Oceans*, **123** (7), 4538–4559, doi:10.1029/2018jc013841, URL <http://dx.doi.org/10.1029/2018JC013841>.
- Holte, J., L. D. Talley, J. Gilson, and D. Roemmich, 2017: An Argo mixed layer climatology and database. *Geophysical Research Letters*, **44** (11), 5618–5626, doi:10.1002/2017gl073426, URL <http://dx.doi.org/10.1002/2017GL073426>.
- Hunke, E. C., 2001: Viscous–plastic sea ice dynamics with the EVP model: Linearization issues. *Journal of Computational Physics*, **170** (1), 18–38, doi:10.1006/jcph.2001.6710, URL <http://dx.doi.org/10.1006/jcph.2001.6710>.
- Hunke, E. C., 2010: Thickness sensitivities in the CICE sea ice model. *Ocean Modelling*, **34** (3-4), 137–149, doi:10.1016/j.ocemod.2010.05.004, URL <http://dx.doi.org/10.1016/j.ocemod.2010.05.004>.
- Hunke, E. C., and J. K. Dukowicz, 1997: An elastic–viscous–plastic model for sea ice dynamics. *Journal of Physical Oceanography*, **27** (9), 1849–1867, doi:10.1175/1520-0485(1997)027<1849:aevpmf>2.0.co;2, URL [http://dx.doi.org/10.1175/1520-0485\(1997\)027<1849:AEVPMF>2.0.CO;2](http://dx.doi.org/10.1175/1520-0485(1997)027<1849:AEVPMF>2.0.CO;2).

REFERENCES

- Hunke, E. C., and J. K. Dukowicz, 2002: The elastic–viscous–plastic sea ice dynamics model in general orthogonal curvilinear coordinates on a sphere—incorporation of metric terms. *Monthly Weather Review*, **130** (7), 1848–1865, doi:10.1175/1520-0493(2002)130<1848:tevpsi>2.0.co;2, URL [http://dx.doi.org/10.1175/1520-0493\(2002\)130<1848:TEVPSI>2.0.CO;2](http://dx.doi.org/10.1175/1520-0493(2002)130<1848:TEVPSI>2.0.CO;2).
- Hunke, E. C., W. H. Lipscomb, A. K. Turner, N. Jeffery, and S. Elliott, 2015: CICE: the Los Alamos Sea Ice Model documentation and software user’s manual version 5.1. Tech. Rep. LA-CC-06-012, Los Alamos National Laboratory, Los Alamos NM 87545. URL <http://oceans11.lanl.gov/trac/CICE/attachment/wiki/WikiStart/cicedoc.pdf?format=raw>.
- Hutchings, J. K., P. Heil, and W. D. Hibler, 2005: Modeling linear kinematic features in sea ice. *Monthly Weather Review*, **133** (12), 3481–3497, doi:10.1175/mwr3045.1, URL <http://dx.doi.org/10.1175/MWR3045.1>.
- Hutchings, J. K., A. Roberts, C. A. Geiger, and J. Richter-Menge, 2011: Spatial and temporal characterization of sea-ice deformation. *Annals of Glaciology*, **52** (57), 360–368, doi:10.3189/172756411795931769.
- Hutter, N., M. Losch, and D. Menemenlis, 2018: Scaling properties of Arctic sea ice deformation in a high-resolution viscous-plastic sea ice model and in satellite observations. *Journal of Geophysical Research: Oceans*, **123** (1), 672–687, doi:10.1002/2017jc013119, URL <http://dx.doi.org/10.1002/2017JC013119>.
- Ilicak, M., and Coauthors, 2016: An assessment of the Arctic Ocean in a suite of interannual CORE-II simulations. Part III: Hydrography and fluxes. *Ocean Modelling*, **100**, 141–161, doi:10.1016/j.ocemod.2016.02.004, URL <http://dx.doi.org/10.1016/j.ocemod.2016.02.004>.
- Iovino, D., S. Masina, A. Storto, A. Cipollone, and V. N. Stepanov, 2016: A $1/16^\circ$ eddying simulation of the global NEMO sea-ice–ocean system. *Geoscientific Model Development*, **9** (8), 2665–2684, doi:10.5194/gmd-9-2665-2016, URL <http://dx.doi.org/10.5194/gmd-9-2665-2016>.
- Ivanova, D. P., P. J. Gleckler, K. E. Taylor, P. J. Durack, and K. D. Marvel, 2016: Moving beyond the total sea ice extent in gauging model biases. *Journal of Climate*, **29** (24), 8965–8987, doi:10.1175/jcli-d-16-0026.1, URL <http://dx.doi.org/10.1175/JCLI-D-16-0026.1>.
- Ivanova, N., and Coauthors, 2015: Inter-comparison and evaluation of sea ice algorithms: towards further identification of challenges and optimal approach using passive microwave observations. *The Cryosphere*, **9** (5), 1797–1817, doi:10.5194/tc-9-1797-2015, URL <http://dx.doi.org/10.5194/tc-9-1797-2015>.
- Jackett, D. R., T. J. McDougall, R. Feistel, D. G. Wright, and S. M. Griffies, 2006: Algorithms for density, potential temperature, conservative temperature, and the freezing temperature of seawater. *Journal of Atmospheric and Oceanic Technology*, **23** (12), 1709–1728, doi:10.1175/jtech1946.1, URL <http://dx.doi.org/10.1175/JTECH1946.1>.
- Jayne, S. R., 2009: The impact of abyssal mixing parameterizations in an ocean general circulation model. *Journal of Physical Oceanography*, **39** (7), 1756–1775, doi:10.1175/2009jpo4085.1, URL <http://dx.doi.org/10.1175/2009JPO4085.1>.
- Jayne, S. R., and L. C. St. Laurent, 2001: Parameterizing tidal dissipation over rough topography. *Geophysical Research Letters*, **28** (5), 811–814, doi:10.1029/2000gl012044, URL <http://dx.doi.org/10.1029/2000GL012044>.
- Jin, M., and Coauthors, 2018: Effects of model resolution and ocean mixing on forced ice-ocean physical and biogeochemical simulations using global and regional system models. *Journal of Geophysical Research: Oceans*, **123** (1), 358–377, doi:10.1002/2017jc013365, URL <http://dx.doi.org/10.1002/2017JC013365>.

REFERENCES

- Jochum, M., 2009: Impact of latitudinal variations in vertical diffusivity on climate simulations. *Journal of Geophysical Research: Oceans*, **114 (C1)**, C01 010, doi:10.1029/2008JC005030.
- Johns, W. E., T. N. Lee, D. Zhang, R. Zantopp, C.-T. Liu, and Y. Yang, 2001: The Kuroshio east of Taiwan: Moored transport observations from the WOCE PCM-1 array. *Journal of Physical Oceanography*, **31 (4)**, 1031–1053, doi:10.1175/1520-0485(2001)031<1031:tkeotm>2.0.co;2, URL [http://dx.doi.org/10.1175/1520-0485\(2001\)031<1031:TKEOTM>2.0.CO;2](http://dx.doi.org/10.1175/1520-0485(2001)031<1031:TKEOTM>2.0.CO;2).
- Johnson, G. C., B. M. Sloyan, W. S. Kessler, and K. E. McTaggart, 2002: Direct measurements of upper ocean currents and water properties across the tropical Pacific during the 1990s. *Progress in Oceanography*, **52 (1)**, 31–61, doi:10.1016/s0079-6611(02)00021-6, URL [http://dx.doi.org/10.1016/S0079-6611\(02\)00021-6](http://dx.doi.org/10.1016/S0079-6611(02)00021-6).
- Kerry, C., B. Powell, M. Roughan, and P. Oke, 2016: Development and evaluation of a high-resolution reanalysis of the East Australian Current region using the Regional Ocean Modelling System (ROMS 3.4) and incremental strong-constraint 4-dimensional variational (IS4D-Var) data assimilation. *Geoscientific Model Development*, **9 (10)**, 3779–3801, doi:10.5194/gmd-9-3779-2016, URL <http://dx.doi.org/10.5194/gmd-9-3779-2016>.
- Khoei, A. R., and S. A. Gharehbaghi, 2007: The superconvergence patch recovery technique and data transfer operators in 3d plasticity problems. *Finite Elem. Anal. Des.*, **43 (8)**, 630–648, doi:10.1016/j.finel.2007.01.002, URL <http://dx.doi.org/10.1016/j.finel.2007.01.002>.
- Kim, J. G., E. C. Hunke, and W. H. Lipscomb, 2006: Sensitivity analysis and parameter tuning scheme for global sea-ice modeling. *Ocean Modelling*, **14 (1-2)**, 61–80, doi:10.1016/j.ocemod.2006.03.003, URL <http://dx.doi.org/10.1016/j.ocemod.2006.03.003>.
- Kim, W. M., R. J. Small, S. Yeager, G. Danabasoglu, H. Tsujino, and C. OMDP, 2018: A new dataset for forcing ocean sea-ice simulations: JRA55-do. 2018 OMWG Winter Meeting, URL <http://www.cesm.ucar.edu/events/wg-meetings/2018/presentations/omwg/kim.pdf>.
- Kimmritz, M., S. Danilov, and M. Losch, 2015: On the convergence of the modified elastic-viscous-plastic method for solving the sea ice momentum equation. *Journal of Computational Physics*, **296**, 90–100, doi:10.1016/j.jcp.2015.04.051, URL <http://dx.doi.org/10.1016/j.jcp.2015.04.051>.
- Kimmritz, M., M. Losch, and S. Danilov, 2017: A comparison of viscous-plastic sea ice solvers with and without replacement pressure. *Ocean Modelling*, **115**, 59–69, doi:10.1016/j.ocemod.2017.05.006, URL <http://dx.doi.org/10.1016/j.ocemod.2017.05.006>.
- Kirtman, B. P., and Coauthors, 2012: Impact of ocean model resolution on CCSM climate simulations. *Climate Dynamics*, **39 (6)**, 1303–1328, doi:10.1007/s00382-012-1500-3, URL <http://dx.doi.org/10.1007/s00382-012-1500-3>.
- Kiss, A. E., and Coauthors, 2020: ACCESS-OM2 v1.0: a global ocean-sea ice model at three resolutions. *Geoscientific Model Development*, **13 (2)**, 401–442, doi:10.5194/gmd-13-401-2020, URL <https://www.geosci-model-dev.net/13/401/2020/>.
- Kjellsson, J., and Coauthors, 2015: Model sensitivity of the weddell and ross seas, antarctica, to vertical mixing and freshwater forcing. *Ocean Modelling*, **94**, 141–152, doi:10.1016/j.ocemod.2015.08.003, URL <http://dx.doi.org/10.1016/j.ocemod.2015.08.003>.
- Kobayashi, S., and Coauthors, 2015: The JRA-55 reanalysis: General specifications and basic characteristics. *Journal of the Meteorological Society of Japan. Ser. II*, **93 (1)**, 5–48, doi:10.2151/jmsj.2015-001, URL <http://dx.doi.org/10.2151/jmsj.2015-001>.
- Koch-Larrouy, A., G. Madec, B. Blanke, and R. Molcard, 2008a: Water mass transformation along the Indonesian throughflow in an OGCM. *Ocean Dynamics*, **58 (3-4)**, 289–309, doi:10.1007/s10236-008-0155-4, URL <http://dx.doi.org/10.1007/s10236-008-0155-4>.

REFERENCES

- Koch-Larrouy, A., G. Madec, D. Iudicone, A. Atmadipoera, and R. Molcard, 2008b: Physical processes contributing to the water mass transformation of the Indonesian Throughflow. *Ocean Dynamics*, **58** (3-4), 275–288, doi:10.1007/s10236-008-0154-5, URL <http://dx.doi.org/10.1007/s10236-008-0154-5>.
- Koldunov, N. V., V. Aizinger, N. Rakowsky, P. Scholz, D. Sidorenko, S. Danilov, and T. Jung, 2019a: Scalability and some optimization of the Finite-volumE Sea ice-Ocean Model, version 2.0 (FESOM2). *Geoscientific Model Development Discussions*, 1–30, doi:10.5194/gmd-2018-334, URL <http://dx.doi.org/10.5194/gmd-2018-334>.
- Koldunov, N. V., and Coauthors, 2019b: Fast EVP solutions in a high-resolution sea ice model. *Journal of Advances in Modeling Earth Systems*, **11** (5), 1269–1284, doi:10.1029/2018ms001485, URL <http://dx.doi.org/10.1029/2018MS001485>.
- Kritsikis, E., M. Aechtner, Y. Meurdesoif, and T. Dubos, 2017a: Conservative interpolation between general spherical meshes. *Geoscientific Model Development*, **10** (1), 425–431, doi:10.5194/gmd-10-425-2017, URL <https://www.geosci-model-dev.net/10/425/2017/>.
- Kritsikis, E., M. Aechtner, Y. Meurdesoif, and T. Dubos, 2017b: Conservative interpolation between general spherical meshes. *Geoscientific Model Development*, **10** (1), 425–431, doi:10.5194/gmd-10-425-2017, URL <http://dx.doi.org/10.5194/gmd-10-425-2017>.
- Kurtz, N. T., and T. Markus, 2012: Satellite observations of Antarctic sea ice thickness and volume. *Journal of Geophysical Research: Oceans*, **117** (C8), doi:10.1029/2012jc008141, URL <http://dx.doi.org/10.1029/2012JC008141>.
- Kwok, R., 2018: Arctic sea ice thickness, volume, and multiyear ice coverage: losses and coupled variability (1958–2018). *Environmental Research Letters*, **13** (10), 105 005, doi:10.1088/1748-9326/aae3ec, URL <http://dx.doi.org/10.1088/1748-9326/aae3ec>.
- Kwok, R., and G. F. Cunningham, 2008: ICESat over Arctic sea ice: Estimation of snow depth and ice thickness. *Journal of Geophysical Research*, **113** (C8), doi:10.1029/2008jc004753, URL <http://dx.doi.org/10.1029/2008JC004753>.
- Kwok, R., E. C. Hunke, W. Maslowski, D. Menemenlis, and J. Zhang, 2008: Variability of sea ice simulations assessed with RGPS kinematics. *Journal of Geophysical Research*, **113** (C11), doi:10.1029/2008jc004783, URL <http://dx.doi.org/10.1029/2008JC004783>.
- Kwok, R., S. S. Pang, and S. Kacimi, 2017: Sea ice drift in the Southern Ocean: Regional patterns, variability, and trends. *Elem. Sci. Anth.*, **5** (0), 32, doi:10.1525/elementa.226, URL <http://dx.doi.org/10.1525/elementa.226>.
- Kwok, R., and D. A. Rothrock, 2009: Decline in Arctic sea ice thickness from submarine and ICESat records: 1958–2008. *Geophysical Research Letters*, **36** (15), n/a–n/a, doi:10.1029/2009gl039035, URL <http://dx.doi.org/10.1029/2009GL039035>.
- Kwok, R., L. Toudal Pedersen, P. Gudmandsen, and S. S. Pang, 2010: Large sea ice outflow into the Nares Strait in 2007. *Geophysical Research Letters*, **37** (3), doi:10.1029/2009gl041872, URL <http://dx.doi.org/10.1029/2009GL041872>.
- Large, W. G., J. C. McWilliams, and S. C. Doney, 1994: Oceanic vertical mixing: A review and a model with a nonlocal boundary layer parameterization. *Rev. Geophys.*, **32** (4), 363–403, doi:10.1029/94RG01872.
- Large, W. G., and S. Yeager, 2004: Diurnal to decadal global forcing for ocean and sea-ice models: The data sets and flux climatologies. Technical Note NCAR/TN-460+STR, NCAR. URL <http://dx.doi.org/10.5065/D6KK98Q6>.

REFERENCES

- Large, W. G., and S. G. Yeager, 2009: The global climatology of an interannually varying air-sea flux data set. *Climate Dynamics*, **33** (2), 341–364, doi:10.1007/s00382-008-0441-3, URL <http://dx.doi.org/10.1007/s00382-008-0441-3>.
- Laurindo, L. C., A. J. Mariano, and R. Lumpkin, 2017: An improved near-surface velocity climatology for the global ocean from drifter observations. *Deep Sea Research Part I: Oceanographic Research Papers*, **124**, 73–92, doi:10.1016/j.dsr.2017.04.009, URL <http://dx.doi.org/10.1016/j.dsr.2017.04.009>.
- Lee, H.-C., A. Rosati, and M. J. Spelman, 2006: Barotropic tidal mixing effects in a coupled climate model: Oceanic conditions in the Northern Atlantic. *Ocean Modelling*, **11** (3-4), 464–477, doi:10.1016/j.ocemod.2005.03.003, URL <http://dx.doi.org/10.1016/j.ocemod.2005.03.003>.
- Lemieux, J.-F., D. A. Knoll, B. Tremblay, D. M. Holland, and M. Losch, 2012: A comparison of the Jacobian-free Newton–Krylov method and the EVP model for solving the sea ice momentum equation with a viscous-plastic formulation: A serial algorithm study. *Journal of Computational Physics*, **231** (17), 5926–5944, doi:10.1016/j.jcp.2012.05.024, URL <http://dx.doi.org/10.1016/j.jcp.2012.05.024>.
- Lemieux, J.-F., and B. Tremblay, 2009: Numerical convergence of viscous-plastic sea ice models. *Journal of Geophysical Research*, **114** (C5), doi:10.1029/2008jc005017, URL <http://dx.doi.org/10.1029/2008JC005017>.
- Lemieux, J.-F., and Coauthors, 2015: The Regional Ice Prediction System (RIPS): verification of forecast sea ice concentration. *Quarterly Journal of the Royal Meteorological Society*, **142** (695), 632–643, doi:10.1002/qj.2526, URL <http://dx.doi.org/10.1002/qj.2526>.
- Leppäranta, M., 2011: *The Drift of Sea Ice*. 2nd ed., Springer, doi:10.1007/978-3-642-04683-4, URL <https://www.springer.com/gp/book/9783642046827>.
- Lindsay, R. W., J. Zhang, and D. A. Rothrock, 2003: Sea-ice deformation rates from satellite measurements and in a model. *Atmosphere-Ocean*, **41** (1), 35–47, doi:10.3137/ao.410103, URL <http://dx.doi.org/10.3137/ao.410103>.
- Lipscomb, W. H., and E. C. Hunke, 2004: Modeling sea ice transport using incremental remapping. *Monthly Weather Review*, **132** (6), 1341–1354, doi:10.1175/1520-0493(2004)132<1341:msitui>2.0.co;2, URL [http://dx.doi.org/10.1175/1520-0493\(2004\)132<1341:MSITUI>2.0.CO;2](http://dx.doi.org/10.1175/1520-0493(2004)132<1341:MSITUI>2.0.CO;2).
- Lipscomb, W. H., E. C. Hunke, W. Maslowski, and J. Jakacki, 2007: Ridging, strength, and stability in high-resolution sea ice models. *Journal of Geophysical Research*, **112** (C3), C03S91, doi:10.1029/2005jc00355, URL <http://dx.doi.org/10.1029/2005JC00355>.
- Locarnini, R. A., and Coauthors, 2013: World Ocean Atlas 2013, Volume 1: Temperature. NOAA Atlas NESDIS 73. URL https://data.nodc.noaa.gov/woa/WOA13/DOC/woa13_vol1.pdf.
- Losch, M., and S. Danilov, 2012: On solving the momentum equations of dynamic sea ice models with implicit solvers and the elastic–viscous–plastic technique. *Ocean Modelling*, **41**, 42–52, doi:10.1016/j.ocemod.2011.10.002, URL <http://dx.doi.org/10.1016/j.ocemod.2011.10.002>.
- Losch, M., A. Fuchs, J.-F. Lemieux, and A. Vanselow, 2014: A parallel Jacobian-free Newton–Krylov solver for a coupled sea ice-ocean model. *Journal of Computational Physics*, **257**, 901–911, doi:10.1016/j.jcp.2013.09.026, URL <http://dx.doi.org/10.1016/j.jcp.2013.09.026>.
- Lozier, M. S., and Coauthors, 2017: Overturning in the Subpolar North Atlantic Program: A new international ocean observing system. *Bulletin of the American Meteorological Society*, **98** (4), 737–752, doi:10.1175/bams-d-16-0057.1, URL <http://dx.doi.org/10.1175/BAMS-D-16-0057.1>.
- Lozier, M. S., and Coauthors, 2019: A sea change in our view of overturning in the subpolar north atlantic. *Science*, **363** (6426), 516–521, doi:10.1126/science.aau6592, URL <http://dx.doi.org/10.1126/science.aau6592>.

REFERENCES

- Lu, P., Z. Li, B. Cheng, and M. Leppäranta, 2011: A parameterization of the ice-ocean drag coefficient. *Journal of Geophysical Research*, **116** (C7), doi:10.1029/2010jc006878, URL <http://dx.doi.org/10.1029/2010JC006878>.
- Lumpkin, R., and K. Speer, 2007: Global ocean meridional overturning. *Journal of Physical Oceanography*, **37** (10), 2550–2562, doi:10.1175/jpo3130.1, URL <http://dx.doi.org/10.1175/JPO3130.1>.
- Manizza, M., C. Le Quéré, A. J. Watson, and E. T. Buitenhuis, 2005: Bio-optical feedbacks among phytoplankton, upper ocean physics and sea-ice in a global model. *Geophysical Research Letters*, **32** (5), L05603, doi:10.1029/2004gl020778, URL <http://dx.doi.org/10.1029/2004GL020778>.
- Martin, T., W. Park, and M. Latif, 2012: Multi-centennial variability controlled by Southern Ocean convection in the Kiel Climate Model. *Climate Dynamics*, **40** (7-8), 2005–2022, doi:10.1007/s00382-012-1586-7, URL <http://dx.doi.org/10.1007/s00382-012-1586-7>.
- Martinson, D. G., and C. Wamser, 1990: Ice drift and momentum exchange in winter Antarctic pack ice. *Journal of Geophysical Research*, **95** (C2), 1741, doi:10.1029/jc095ic02p01741, URL <http://dx.doi.org/10.1029/JC095iC02p01741>.
- Massonnet, F., H. Goosse, T. Fichefet, and F. Counillon, 2014: Calibration of sea ice dynamic parameters in an ocean-sea ice model using an ensemble Kalman filter. *Journal of Geophysical Research: Oceans*, **119** (7), 4168–4184, doi:10.1002/2013jc009705, URL <http://dx.doi.org/10.1002/2013JC009705>.
- Mathiot, P., A. Jenkins, C. Harris, and G. Madec, 2017: Explicit representation and parametrised impacts of under ice shelf seas in the z* coordinate ocean model NEMO 3.6. *Geoscientific Model Development*, **10** (7), 2849–2874, doi:10.5194/gmd-10-2849-2017, URL <http://dx.doi.org/10.5194/gmd-10-2849-2017>.
- Mazloff, M. R., P. Heimbach, and C. Wunsch, 2010: An eddy-permitting Southern Ocean state estimate. *Journal of Physical Oceanography*, **40** (5), 880–899, doi:10.1175/2009JPO4236.1, URL <http://dx.doi.org/10.1175/2009JPO4236.1>.
- McPhee, M., 2008: *Air-Ice-Ocean Interaction: Turbulent Ocean Boundary Layer Exchange Processes*. Springer New York, doi:10.1007/978-0-387-78335-2, URL <http://dx.doi.org/10.1007/978-0-387-78335-2>.
- Meehl, G. A., J. M. Arblaster, C. T. Y. Chung, M. M. Holland, A. DuVivier, L. Thompson, D. Yang, and C. M. Bitz, 2019: Sustained ocean changes contributed to sudden Antarctic sea ice retreat in late 2016. *Nature Communications*, **10** (1), 14, doi:10.1038/s41467-018-07865-9, URL <https://doi.org/10.1038/s41467-018-07865-9>.
- Meier, W., F. Fetterer, M. Savoie, S. Mallory, R. Duerr, and J. Stroeve, 2017: Noaa/nsidc climate data record of passive microwave sea ice concentration, version 3. Tech. rep., NSIDC: National Snow and Ice Data Center, Boulder, Colorado USA. doi:10.7265/N59P2ZTG, URL <https://doi.org/10.7265/N59P2ZTG>.
- Meier, W. N., G. Peng, D. J. Scott, and M. H. Savoie, 2014: Verification of a new NOAA/NSIDC passive microwave sea-ice concentration climate record. *Polar Research*, **33** (1), 21 004, doi:10.3402/polar.v33.21004, URL <http://dx.doi.org/10.3402/polar.v33.21004>.
- Merino, N., N. C. Jourdain, J. Le Sommer, H. Goosse, P. Mathiot, and G. Durand, 2018: Impact of increasing Antarctic glacial freshwater release on regional sea-ice cover in the Southern Ocean. *Ocean Modelling*, **121**, 76–89, doi:10.1016/j.ocemod.2017.11.009, URL <http://dx.doi.org/10.1016/j.ocemod.2017.11.009>.

REFERENCES

- Merino, N., J. Le Sommer, G. Durand, N. C. Jourdain, G. Madec, P. Mathiot, and J. Tournadre, 2016: Antarctic icebergs melt over the Southern Ocean: Climatology and impact on sea ice. *Ocean Modelling*, **104**, 99–110, doi:10.1016/j.ocemod.2016.05.001, URL <http://dx.doi.org/10.1016/j.ocemod.2016.05.001>.
- Miller, P. A., S. W. Laxon, D. L. Feltham, and D. J. Cresswell, 2006: Optimization of a sea ice model using basinwide observations of Arctic sea ice thickness, extent, and velocity. *Journal of Climate*, **19** (7), 1089–1108, doi:10.1175/jcli3648.1, URL <http://dx.doi.org/10.1175/JCLI3648.1>.
- Morales Maqueda, M. A., 2004: Polynya dynamics: a review of observations and modeling. *Reviews of Geophysics*, **42** (1), doi:10.1029/2002rg000116, URL <http://dx.doi.org/10.1029/2002RG000116>.
- Murray, R. J., 1996: Explicit generation of orthogonal grids for ocean models. *Journal of Computational Physics*, **126** (2), 251–273, doi:10.1006/jcph.1996.0136, URL <http://dx.doi.org/10.1006/jcph.1996.0136>.
- NAS, 2017: *Antarctic Sea Ice Variability in the Southern Ocean-Climate System: Proceedings of a Workshop*. The National Academies Press, National Academies of Sciences, Engineering, and Medicine, Washington, DC, doi:10.17226/24696, URL <https://www.nap.edu/catalog/24696/antarctic-sea-ice-variability-in-the-southern-ocean-climate-system>.
- Naughten, K., 2018: Modelling antarctic ice shelf, ocean, and sea ice interactions under present-day and future climate scenarios. Ph.D. thesis, Climate Change Research Centre (CCRC), Faculty of Science, University of New South Wales, URL https://www.unswworks.unsw.edu.au/primo-explore/fulldisplay?docid=unswworks_51321&context=L&vid=UNSWORKS&search_scope=unswworks_search_scope&tab=default_tab&lang=en_US.
- Naughten, K. A., K. J. Meissner, B. K. Galton Fenzi, M. H. England, R. Timmermann, H. H. Hellmer, T. Hattermann, and J. B. Debernard, 2018: Intercomparison of Antarctic ice-shelf, ocean, and sea-ice interactions simulated by MetROMS-iceshelf and FESOM 1.4. *Geoscientific Model Development*, **11** (4), 1257–1292, doi:10.5194/gmd-11-1257-2018, URL <https://www.geosci-model-dev.net/11/1257/2018/>.
- Newsom, E. R., C. M. Bitz, F. O. Bryan, R. Abernathey, and P. R. Gent, 2016: Southern Ocean deep circulation and heat uptake in a high-resolution climate model. *Journal of Climate*, **29** (7), 2597–2619, doi:10.1175/jcli-d-15-0513.1, URL <http://dx.doi.org/10.1175/JCLI-D-15-0513.1>.
- Nihashi, S., and K. I. Ohshima, 2015: Circumpolar mapping of Antarctic coastal polynyas and landfast sea ice: Relationship and variability. *Journal of Climate*, **28** (9), 3650–3670, doi:10.1175/jcli-d-14-00369.1, URL <http://dx.doi.org/10.1175/JCLI-D-14-00369.1>.
- Notz, D., F. A. Haumann, H. Haak, J. H. Jungclaus, and J. Marotzke, 2013: Arctic sea-ice evolution as modeled by Max Planck Institute for Meteorology's Earth system model. *Journal of Advances in Modeling Earth Systems*, **5** (2), 173–194, doi:10.1002/jame.20016, URL <http://dx.doi.org/10.1002/jame.20016>.
- Notz, D., A. Jahn, M. Holland, E. Hunke, F. Massonnet, J. Stroeve, B. Tremblay, and M. Vancoppenolle, 2016: The CMIP6 Sea-Ice Model Intercomparison Project (SIMIP): understanding sea ice through climate-model simulations. *Geoscientific Model Development*, **9** (9), 3427–3446, doi:10.5194/gmd-9-3427-2016, URL <https://www.geosci-model-dev.net/9/3427/2016/>.
- Nye, J. F., 1973: Is there any physical basis for assuming linear viscous behavior for sea ice? *AIDJEX Bull.*, **21**, 18–19, URL http://psc.apl.washington.edu/nonwp_projects/aidjex/files/AIDJEX-21.pdf.
- Ohshima, K. I., S. Nihashi, and K. Iwamoto, 2016: Global view of sea-ice production in polynyas and its linkage to dense/bottom water formation. *Geoscience Letters*, **3** (1), doi:10.1186/s40562-016-0045-4, URL <http://dx.doi.org/10.1186/s40562-016-0045-4>.

REFERENCES

- Oke, P. R., and Coauthors, 2013: Evaluation of a near-global eddy-resolving ocean model. *Geoscientific Model Development*, **6** (3), 591–615, doi:10.5194/gmd-6-591-2013, URL <http://www.geosci-model-dev.net/6/591/2013/>.
- Ollitrault, M., and A. Colin de Verdière, 2014: The ocean general circulation near 1000-m depth. *Journal of Physical Oceanography*, **44** (1), 384–409, doi:10.1175/jpo-d-13-030.1, URL <http://dx.doi.org/10.1175/JPO-D-13-030.1>.
- Pacanowski, R. C., and A. Gnanadesikan, 1998: Transient response in a z-level ocean model that resolves topography with partial cells. *Monthly Weather Review*, **126** (12), 3248–3270, doi:10.1175/1520-0493(1998)126<3248:triazl>2.0.co;2, URL [http://dx.doi.org/10.1175/1520-0493\(1998\)126<3248:TRIAZL>2.0.CO;2](http://dx.doi.org/10.1175/1520-0493(1998)126<3248:TRIAZL>2.0.CO;2).
- Park, H.-S., and A. L. Stewart, 2016: An analytical model for wind-driven Arctic summer sea ice drift. *The Cryosphere*, **10** (1), 227–244, doi:10.5194/tc-10-227-2016, URL <http://dx.doi.org/10.5194/tc-10-227-2016>.
- Pelichero, V., J.-B. Sallée, C. C. Chapman, and S. M. Downes, 2018: The southern ocean meridional overturning in the sea-ice sector is driven by freshwater fluxes. *Nature Communications*, **9** (1), 1789, doi:10.1038/s41467-018-04101-2, URL <https://doi.org/10.1038/s41467-018-04101-2>.
- Peng, G., W. N. Meier, D. J. Scott, and M. H. Savoie, 2013: A long-term and reproducible passive microwave sea ice concentration data record for climate studies and monitoring. *Earth System Science Data*, **5** (2), 311–318, doi:10.5194/essd-5-311-2013, URL <http://dx.doi.org/10.5194/essd-5-311-2013>.
- Pringle, D. J., H. Eicken, H. J. Trodahl, and L. G. E. Backstrom, 2007: Thermal conductivity of landfast Antarctic and Arctic sea ice. *Journal of Geophysical Research*, **112** (C4), C04017, doi:10.1029/2006jc003641, URL <http://dx.doi.org/10.1029/2006JC003641>.
- Rae, J. G. L., H. T. Hewitt, A. B. Keen, J. K. Ridley, A. E. West, C. M. Harris, E. C. Hunke, and D. N. Walters, 2015: Development of the Global Sea Ice 6.0 CICE configuration for the Met Office Global Coupled model. *Geoscientific Model Development*, **8** (7), 2221–2230, doi:10.5194/gmd-8-2221-2015, URL <https://www.geosci-model-dev.net/8/2221/2015/>.
- Rahmstorf, S., J. E. Box, G. Feulner, M. E. Mann, A. Robinson, S. Rutherford, and E. J. Schaffernicht, 2015: Exceptional twentieth-century slowdown in Atlantic Ocean overturning circulation. *Nature Climate Change*, **5**, 475 EP –, URL <https://doi.org/10.1038/nclimate2554>.
- Redi, M. H., 1982: Oceanic isopycnal mixing by coordinate rotation. *J. Phys. Oceanogr.*, **12** (10), 1154–1158, doi:10.1175/1520-0485(1982)012<1154:OIMBCR>2.0.CO;2.
- Renault, L., P. Marchesiello, S. Masson, and J. C. McWilliams, 2019a: Remarkable control of western boundary currents by eddy killing, a mechanical air-sea coupling process. *Geophysical Research Letters*, **46** (5), 2743–2751, doi:10.1029/2018gl081211, URL <http://dx.doi.org/10.1029/2018GL081211>.
- Renault, L., S. Masson, T. Arsouze, G. Madec, and J. C. McWilliams, 2020: Recipes for how to force oceanic model dynamics. *Journal of Advances in Modeling Earth Systems*, **12** (2), doi:10.1029/2019ms001715, URL <http://dx.doi.org/10.1029/2019MS001715>.
- Renault, L., S. Masson, V. Oerder, S. Jullien, and F. Colas, 2019b: Disentangling the mesoscale ocean-atmosphere interactions. *Journal of Geophysical Research: Oceans*, **124** (3), 2164–2178, doi:10.1029/2018jc014628, URL <http://dx.doi.org/10.1029/2018JC014628>.
- Renault, L., M. J. Molemaker, J. Gula, S. Masson, and J. C. McWilliams, 2016: Control and stabilization of the Gulf Stream by oceanic current interaction with the atmosphere. *Journal of Physical Oceanography*, doi:10.1175/JPO-D-16-0115.1, URL <http://dx.doi.org/10.1175/JPO-D-16-0115.1>.

REFERENCES

- Richter, O., D. E. Gwyther, B. K. Galton-Fenzi, and K. A. Naughten, 2020: The Whole Antarctic Ocean Model (WAOM v1.0): Development and evaluation. *Geoscientific Model Development Discussions*, **2020**, 1–40, doi:10.5194/gmd-2020-164, URL <https://gmd.copernicus.org/preprints/gmd-2020-164/>.
- Ridley, J. K., E. W. Blockley, A. B. Keen, J. G. L. Rae, A. E. West, and D. Schroeder, 2018: The sea ice model component of HadGEM3-GC3.1. *Geoscientific Model Development*, **11** (2), 713–723, doi: 10.5194/gmd-11-713-2018, URL <http://dx.doi.org/10.5194/gmd-11-713-2018>.
- Rintoul, S. R., 2018: The global influence of localized dynamics in the Southern Ocean. *Nature*, **558** (7709), 209–218, doi:10.1038/s41586-018-0182-3, URL <https://doi.org/10.1038/s41586-018-0182-3>.
- Rio, M.-H., S. Mulet, and N. Picot, 2014: Beyond GOCE for the ocean circulation estimate: Synergetic use of altimetry, gravimetry, and in situ data provides new insight into geostrophic and Ekman currents. *Geophysical Research Letters*, **41** (24), 8918–8925, doi:10.1002/2014gl061773, URL <http://dx.doi.org/10.1002/2014GL061773>.
- Roach, L. A., S. M. Dean, and J. A. Renwick, 2018: Consistent biases in Antarctic sea ice concentration simulated by climate models. *The Cryosphere*, **12** (1), 365–383, doi:10.5194/tc-12-365-2018, URL <http://dx.doi.org/10.5194/tc-12-365-2018>.
- Roberts, A., W. Maslowski, J. Jakacki, M. Higgins, A. Craig, J. Cassano, W. Gutowski, and P. Lettenmaier, 2011: High frequency and wavenumber ocean-ice-atmosphere coupling in the Regional Arctic Climate Model. *AGU Fall Meeting Abstracts*, 4.
- Roberts, A., and Coauthors, 2015: Simulating transient ice-ocean Ekman transport in the Regional Arctic System Model and Community Earth System Model. *Annals of Glaciology*, **56** (69), 211–228, doi:10.3189/2015aog69a760, URL <http://dx.doi.org/10.3189/2015AoG69A760>.
- Roberts, A. F., E. C. Hunke, R. Allard, D. A. Bailey, A. P. Craig, J.-F. Lemieux, and M. D. Turner, 2018: Quality control for community-based sea-ice model development. *Philosophical Transactions of the Royal Society A: Mathematical, Physical and Engineering Sciences*, **376** (2129), 20170344, doi: 10.1098/rsta.2017.0344, URL <http://dx.doi.org/10.1098/rsta.2017.0344>.
- Roberts, M. J., and Coauthors, 2019: Description of the resolution hierarchy of the global coupled HadGEM3-GC3.1 model as used in CMIP6 HighResMIP experiments. *Geoscientific Model Development Discussions*, 1–47, doi:10.5194/gmd-2019-148, URL <http://dx.doi.org/10.5194/gmd-2019-148>.
- Roquet, F., G. Madec, T. J. McDougall, and P. M. Barker, 2015: Accurate polynomial expressions for the density and specific volume of seawater using the TEOS-10 standard. *Ocean Modelling*, **90**, 29–43, doi:10.1016/j.ocemod.2015.04.002, URL <http://dx.doi.org/10.1016/j.ocemod.2015.04.002>.
- Röske, F., 2006: A global heat and freshwater forcing dataset for ocean models. *Ocean Modelling*, **11** (3-4), 235–297, doi:10.1016/j.ocemod.2004.12.005, URL <http://dx.doi.org/10.1016/j.ocemod.2004.12.005>.
- Sallée, J.-B., E. Shuckburgh, N. Bruneau, A. J. S. Meijers, T. J. Bracegirdle, and Z. Wang, 2013: Assessment of Southern Ocean mixed-layer depths in CMIP5 models: Historical bias and forcing response. *Journal of Geophysical Research: Oceans*, **118** (4), 1845–1862, doi:10.1002/jgrc.20157, URL <https://agupubs.onlinelibrary.wiley.com/doi/abs/10.1002/jgrc.20157>.
- Sallée, J.-B., N. Wienders, K. Speer, and R. Morrow, 2006: Formation of subantarctic mode water in the southeastern Indian Ocean. *Ocean Dynamics*, **56** (5-6), 525–542, doi:10.1007/s10236-005-0054-x, URL <http://dx.doi.org/10.1007/s10236-005-0054-x>.

REFERENCES

- Schmidt, M., 2007: A benchmark for the parallel code used in FMS and MOM-4. *Ocean Modelling*, **17** (1), 49–67, doi:10.1016/j.ocemod.2006.11.002, URL <http://dx.doi.org/10.1016/j.ocemod.2006.11.002>.
- Schmidtko, S., G. C. Johnson, and J. M. Lyman, 2013: MIMOC: A global monthly isopycnal upper-ocean climatology with mixed layers. *Journal of Geophysical Research: Oceans*, **118** (4), 1658–1672, doi:10.1002/jgrc.20122, URL <http://dx.doi.org/10.1002/jgrc.20122>.
- Schröder, D., D. L. Feltham, M. Tsamados, A. Ridout, and R. Tilling, 2019: New insight from CryoSat-2 sea ice thickness for sea ice modelling. *The Cryosphere*, **13** (1), 125–139, doi:10.5194/tc-13-125-2019, URL <http://dx.doi.org/10.5194/tc-13-125-2019>.
- Schroeter, S., W. Hobbs, N. L. Bindoff, R. Massom, and R. Matear, 2018: Drivers of Antarctic sea ice volume change in CMIP5 models. *Journal of Geophysical Research: Oceans*, doi:10.1029/2018jc014177, URL <http://dx.doi.org/10.1029/2018JC014177>.
- Schweiger, A., R. Lindsay, J. Zhang, M. Steele, H. Stern, and R. Kwok, 2011: Uncertainty in modeled Arctic sea ice volume. *Journal of Geophysical Research*, **116**, doi:10.1029/2011jc007084, URL <http://dx.doi.org/10.1029/2011JC007084>.
- Shirasawa, K., and R. G. Ingram, 1997: Currents and turbulent fluxes under the first-year sea ice in Resolute Passage, Northwest Territories, Canada. *Journal of Marine Systems*, **11** (1-2), 21–32, doi:10.1016/s0924-7963(96)00024-3, URL [http://dx.doi.org/10.1016/S0924-7963\(96\)00024-3](http://dx.doi.org/10.1016/S0924-7963(96)00024-3).
- Simmons, H. L., S. R. Jayne, L. C. S. Laurent, and A. J. Weaver, 2004: Tidally driven mixing in a numerical model of the ocean general circulation. *Ocean Model.*, **6** (3), 245–263, doi:10.1016/S1463-5003(03)00011-8.
- Sloyan, B. M., K. R. Ridgway, and R. Cowley, 2016: The east australian current and property transport at 27°S from 2012 to 2013. *Journal of Physical Oceanography*, **46** (3), 993–1008, doi:10.1175/JPO-D-15-0052.1, URL <http://dx.doi.org/10.1175/JPO-D-15-0052.1>, <http://dx.doi.org/10.1175/JPO-D-15-0052.1>.
- Smeed, D. A., and Coauthors, 2018: The North Atlantic Ocean is in a state of reduced overturning. *Geophysical Research Letters*, **45** (3), 1527–1533, doi:10.1002/2017gl076350, URL <http://dx.doi.org/10.1002/2017GL076350>.
- Smith, G. C., and Coauthors, 2015: Sea ice forecast verification in the Canadian Global Ice Ocean Prediction System. *Quarterly Journal of the Royal Meteorological Society*, **142** (695), 659–671, doi:10.1002/qj.2555, URL <http://dx.doi.org/10.1002/qj.2555>.
- Smith, W. H. F., and D. T. Sandwell, 1997: Global sea floor topography from satellite altimetry and ship depth soundings. *Science*, **277** (5334), 1956–1962, doi:10.1126/science.277.5334.1956, URL <http://www.sciencemag.org/content/277/5334/1956.abstract>, <http://www.sciencemag.org/content/277/5334/1956.full.pdf>.
- Spence, P., R. M. Holmes, A. M. Hogg, S. M. Griffies, K. D. Stewart, and M. H. England, 2017: Localized rapid warming of West Antarctic subsurface waters by remote winds. *Nature Climate Change*, **7** (8), 595–603, doi:10.1038/nclimate3335, URL <http://dx.doi.org/10.1038/nclimate3335>.
- Sprintall, J., S. E. Wijffels, R. Molcard, and I. Jaya, 2009: Direct estimates of the Indonesian Through-flow entering the Indian Ocean: 2004–2006. *Journal of Geophysical Research: Oceans*, **114** (C7), C07001, doi:10.1029/2008JC005257, URL <http://dx.doi.org/10.1029/2008JC005257>.
- Stewart, K., A. Hogg, S. Griffies, A. Heerdegen, M. Ward, P. Spence, and M. England, 2017: Vertical resolution of baroclinic modes in global ocean models. *Ocean Modelling*, **113**, 50–65, doi:10.1016/j.ocemod.2017.03.012, URL <http://dx.doi.org/10.1016/j.ocemod.2017.03.012>.

REFERENCES

- Stewart, K., and Coauthors, 2019: JRA55-do repeat year forcing. *in preparation, to be submitted to Ocean Modelling.*
- Storkey, D., and Coauthors, 2018: UK Global Ocean GO6 and GO7: a traceable hierarchy of model resolutions. *Geoscientific Model Development Discussions*, 1–43, doi:10.5194/gmd-2017-263, URL <http://dx.doi.org/10.5194/gmd-2017-263>.
- Stössel, A., D. Notz, F. A. Haumann, H. Haak, J. Jungclaus, and U. Mikolajewicz, 2015: Controlling high-latitude Southern Ocean convection in climate models. *Ocean Modelling*, **86**, 58–75, doi:10.1016/j.ocemod.2014.11.008, URL <http://dx.doi.org/10.1016/j.ocemod.2014.11.008>.
- Stössel, A., Z. Zhang, and T. Vihma, 2011: The effect of alternative real-time wind forcing on Southern Ocean sea ice simulations. *Journal of Geophysical Research*, **116 (C11)**, C11021, doi: 10.1029/2011jc007328, URL <http://dx.doi.org/10.1029/2011JC007328>.
- Sumata, H., R. Gerdes, F. Kauker, and M. Karcher, 2015a: Empirical error functions for monthly mean Arctic sea-ice drift. *Journal of Geophysical Research: Oceans*, **120 (11)**, 7450–7475, doi:10.1002/2015jc011151, URL <http://dx.doi.org/10.1002/2015JC011151>.
- Sumata, H., R. Kwok, R. Gerdes, F. Kauker, and M. Karcher, 2015b: Uncertainty of Arctic summer ice drift assessed by high-resolution SAR data. *Journal of Geophysical Research: Oceans*, **120 (8)**, 5285–5301, doi:10.1002/2015jc010810, URL <http://dx.doi.org/10.1002/2015JC010810>.
- Sumata, H., T. Lavergne, F. Girard-Ardhuin, N. Kimura, M. A. Tschudi, F. Kauker, M. Karcher, and R. Gerdes, 2014: An intercomparison of Arctic ice drift products to deduce uncertainty estimates. *Journal of Geophysical Research: Oceans*, **119 (8)**, 4887–4921, doi:10.1002/2013jc009724, URL <http://dx.doi.org/10.1002/2013JC009724>.
- Suresh, A., and H. Huynh, 1997: Accurate monotonicity-preserving schemes with Runge-Kutta time stepping. *Journal of Computational Physics*, **136 (1)**, 83–99, doi:10.1006/jcph.1997.5745, URL <http://dx.doi.org/10.1006/jcph.1997.5745>.
- Suzuki, T., D. Yamazaki, H. Tsujino, Y. Komuro, H. Nakano, and S. Urakawa, 2018: A dataset of continental river discharge based on JRA-55 for use in a global ocean circulation model. *Journal of Oceanography*, **74 (4)**, 421–429, doi:10.1007/s10872-017-0458-5, URL <https://doi.org/10.1007/s10872-017-0458-5>.
- Sweeney, C., A. Gnanadesikan, S. M. Griffies, M. J. Harrison, A. J. Rosati, and B. L. Samuels, 2005: Impacts of shortwave penetration depth on large-scale ocean circulation and heat transport. *J. Phys. Oceanogr.*, **35 (6)**, 1103–1119, doi:10.1175/JPO2740.1.
- Szanyi, S., J. V. Lukovich, D. G. Barber, and G. Haller, 2016: Persistent artifacts in the NSIDC ice motion data set and their implications for analysis. *Geophysical Research Letters*, **43 (20)**, 10,800–10,807, doi:10.1002/2016gl069799, URL <http://dx.doi.org/10.1002/2016GL069799>.
- Talley, L. D., 2013: Closure of the global overturning circulation through the Indian, Pacific, and Southern Oceans: Schematics and transports. *Oceanography*, **26 (1)**, 80–97, doi:10.5670/oceanog.2013.07, URL <https://doi.org/10.5670/oceanog.2013.07>.
- Tamura, T., and K. I. Ohshima, 2011: Mapping of sea ice production in the Arctic coastal polynyas. *Journal of Geophysical Research*, **116 (C7)**, doi:10.1029/2010jc006586, URL <http://dx.doi.org/10.1029/2010JC006586>.
- Tamura, T., K. I. Ohshima, A. D. Fraser, and G. D. Williams, 2016: Sea ice production variability in Antarctic coastal polynyas. *Journal of Geophysical Research: Oceans*, **121 (5)**, 2967–2979, doi:10.1002/2015jc011537, URL <http://dx.doi.org/10.1002/2015JC011537>.

REFERENCES

- Tamura, T., K. I. Ohshima, and S. Nihashi, 2008: Mapping of sea ice production for Antarctic coastal polynyas. *Geophysical Research Letters*, **35** (7), n/a–n/a, doi:10.1029/2007gl032903, URL <http://dx.doi.org/10.1029/2007GL032903>.
- Toyota, T., and N. Kimura, 2018: An examination of the sea ice rheology for seasonal ice zones based on ice drift and thickness observations. *Journal of Geophysical Research: Oceans*, doi:10.1002/2017JC013627, URL <http://dx.doi.org/10.1002/2017JC013627>.
- Tsamados, M., D. L. Feltham, and A. V. Wilchinsky, 2013: Impact of a new anisotropic rheology on simulations of Arctic sea ice. *Journal of Geophysical Research: Oceans*, **118** (1), 91–107, doi:10.1029/2012jc007990, URL <http://dx.doi.org/10.1029/2012JC007990>.
- Tseng, Y.-H., and Coauthors, 2016: North and equatorial Pacific Ocean circulation in the CORE-II hindcast simulations. *Ocean Modelling*, **104**, 143–170, doi:10.1016/j.ocemod.2016.06.003, URL <http://dx.doi.org/10.1016/j.ocemod.2016.06.003>.
- Tsujino, H., 2015a: On the use of JRA55 for driving ocean-sea ice models - biases, correction (adjustment), results from preliminary model run. *OMDP forcing mini workshop 29-30 Jan 2015, Grenoble, France*, URL http://www.clivar.org/sites/default/files/documents/wgomd/grenoble2015/OMDP_Grenoble2015_Tsujino.pdf.
- Tsujino, H., 2015b: Short description of a JRA-55 based surface atmospheric data set for driving ocean-sea ice models. Tech. rep., JMA Meteorological Research Institute. URL <https://mri-2.mri-jma.go.jp/owncloud/index.php/s/3d33d5a6ee3bd326abae2cecbea91bd0#pdfviewer>.
- Tsujino, H., 2016: JRA-55 based surface atmospheric data set for driving ocean-sea ice models. *OMDP extended meeting 14 January 2016, JAMSTEC, Yokohama, Japan*, URL http://www.clivar.org/sites/default/files/documents/wgomd/japan2016/OMDP_Meeting/Tsujino_OMDP2016.pdf.
- Tsujino, H., 2018: Results of testing several wind forcing methods based on JRA55-do-v1.3: Application to MRI ocean - sea-ice models, URL <https://jra55-do.slack.com/archives/C7LEZT4KY/p1524498479000123>, posted to Slack JRA55-do channel <https://jra55-do.slack.com>.
- Tsujino, H., and Coauthors, 2016: JRA-55 based data set for driving ocean - sea ice model (JRA55-do). *17 September 2016 ARP-OMDP joint session Qingdao, China*.
- Tsujino, H., and Coauthors, 2018a: JRA-55 based surface dataset for driving ocean - sea-ice models (JRA55-do). *Ocean Modelling*, **130**, 79–139, doi:10.1016/j.ocemod.2018.07.002, URL <http://dx.doi.org/10.1016/j.ocemod.2018.07.002>.
- Tsujino, H., and Coauthors, 2018b: *User manual for JRA-55 based surface dataset for driving ocean-sea-ice models (JRA55-do), version 1.3*. URL <https://mri-2.mri-jma.go.jp/owncloud/index.php/s/cSntssoesw4ATRT>.
- Tsujino, H., and Coauthors, 2019: *User manual of JRA-55 based surface dataset for driving ocean-sea-ice models (JRA55-do), version 1.4*. JMA Meteorological Research Institute, Tsukuba, Japan, URL https://climate.mri-jma.go.jp/~htsujino/docs/JRA55-do/v1_4-manual/User_manual_jra55_do_v1_4.pdf.
- Turner, A. K., E. C. Hunke, and C. M. Bitz, 2013: Two modes of sea-ice gravity drainage: A parameterization for large-scale modeling. *Journal of Geophysical Research: Oceans*, **118** (5), 2279–2294, doi:10.1002/jgrc.20171, URL <http://dx.doi.org/10.1002/jgrc.20171>.
- Uotila, P., H. Goosse, K. Haines, M. Chevallier, A. Barthélemy, C. Bricaud, J. Carton, and Coauthors, 2019: An assessment of ten ocean reanalyses in the polar regions. *Climate Dynamics*, **52** (1613), doi:10.1007/s00382-018-4242-z, URL <http://dx.doi.org/10.1007/s00382-018-4242-z>.

REFERENCES

- Uotila, P., D. Iovino, M. Vancoppenolle, M. Lensu, and C. Rousset, 2017: Comparing sea ice, hydrography and circulation between NEMO3.6 LIM3 and LIM2. *Geoscientific Model Development*, **10** (2), 1009–1031, doi:10.5194/gmd-10-1009-2017, URL <http://dx.doi.org/10.5194/gmd-10-1009-2017>.
- Uotila, P., S. O'Farrell, S. Marsland, and D. Bi, 2012: A sea-ice sensitivity study with a global ocean-ice model. *Ocean Modelling*, **51**, 1–18, doi:10.1016/j.ocemod.2012.04.002, URL <http://dx.doi.org/10.1016/j.ocemod.2012.04.002>.
- Uotila, P., S. O'Farrell, S. J. Marsland, and D. Bi, 2013: The sea-ice performance of the Australian climate models participating in the CMIP5. *Australian Meteorological And Oceanographic Journal*, **63** (1), 121–143.
- Urrego-Blanco, J. R., N. M. Urban, E. C. Hunke, A. K. Turner, and N. Jeffery, 2016: Uncertainty quantification and global sensitivity analysis of the Los Alamos sea ice model. *Journal of Geophysical Research: Oceans*, **121** (4), 2709–2732, doi:10.1002/2015jc011558, URL <http://dx.doi.org/10.1002/2015JC011558>.
- Valcke, S., T. Craig, and L. Coquart, 2013: OASIS3-MCT User Guide: OASIS3-MCT 2.0. CERFACS/CNRS SUC URA No1875, CERFACS TR/CMGC/13/17, CERFACS/CNRS. URL http://www.cerfacs.fr/oa4web/oasis3-mct/oasis3mct_UserGuide.pdf.
- Van Roekel, L., and Coauthors, 2018: The KPP boundary layer scheme for the ocean: Revisiting its formulation and benchmarking one-dimensional simulations relative to LES. *Journal of Advances in Modeling Earth Systems*, doi:10.1029/2018ms001336, URL <http://dx.doi.org/10.1029/2018MS001336>.
- Vaughan, D., and Coauthors, 2013: *Observations: Cryosphere*, book section 4, 317382. Cambridge University Press, Cambridge, United Kingdom and New York, NY, USA, doi:10.1017/CBO9781107415324.012, URL www.climatechange2013.org.
- Wang, G., H. H. Hendon, J. M. Arblaster, E.-P. Lim, S. Abhik, and P. van Rensch, 2019: Compounding tropical and stratospheric forcing of the record low Antarctic sea-ice in 2016. *Nature Communications*, **10** (1), 13, doi:10.1038/s41467-018-07689-7, URL <https://doi.org/10.1038/s41467-018-07689-7>.
- Wang, K., and C. Wang, 2009: Modeling linear kinematic features in pack ice. *Journal of Geophysical Research*, **114** (C12), doi:10.1029/2008jc005217, URL <http://dx.doi.org/10.1029/2008JC005217>.
- Wang, Q., S. Danilov, T. Jung, L. Kaleschke, and A. Wernecke, 2016a: Sea ice leads in the arctic ocean: Model assessment, interannual variability and trends. *Geophysical Research Letters*, **43** (13), 7019–7027, doi:10.1002/2016gl068696, URL <http://dx.doi.org/10.1002/2016GL068696>.
- Wang, Q., and Coauthors, 2016b: An assessment of the Arctic Ocean in a suite of interannual CORE-II simulations. Part I: Sea ice and solid freshwater. *Ocean Modelling*, **99**, 110–132, doi:10.1016/j.ocemod.2015.12.008, URL <http://dx.doi.org/10.1016/j.ocemod.2015.12.008>.
- Wang, Q., and Coauthors, 2016c: An assessment of the Arctic Ocean in a suite of interannual CORE-II simulations. Part II: Liquid freshwater. *Ocean Modelling*, **99**, 86–109, doi:10.1016/j.ocemod.2015.12.009, URL <http://dx.doi.org/10.1016/j.ocemod.2015.12.009>.
- Waters, J. K., and M. S. Bruno, 1995: Internal wave generation by ice floes moving in stratified water: Results from a laboratory study. *Journal of Geophysical Research*, **100** (C7), 13 635, doi:10.1029/95jc01220, URL <http://dx.doi.org/10.1029/95JC01220>.
- Weiss, J., 2003: Scaling of fracture and faulting of ice on Earth. *Surveys in Geophysics*, **24** (2), 185–227, doi:10.1023/A:1023293117309, URL <https://doi.org/10.1023/A:1023293117309>.

REFERENCES

- Weiss, J., 2017: Exploring the “solid turbulence” of sea ice dynamics down to unprecedented small scales. *Journal of Geophysical Research: Oceans*, **122** (8), 6071–6075, doi:10.1002/2017jc013236, URL <http://dx.doi.org/10.1002/2017JC013236>.
- Weiss, J., and V. Dansereau, 2017: Linking scales in sea ice mechanics. *Philosophical Transactions of the Royal Society A: Mathematical, Physical and Engineering Sciences*, **375** (2086), 20150352, doi:10.1098/rsta.2015.0352, URL <http://dx.doi.org/10.1098/rsta.2015.0352>.
- Weiss, J., and E. M. Schulson, 2009: Coulombic faulting from the grain scale to the geophysical scale: lessons from ice. *Journal of Physics D: Applied Physics*, **42** (21), 214017, URL <http://stacks.iop.org/0022-3727/42/i=21/a=214017>.
- Weiss, J., E. M. Schulson, and H. L. Stern, 2007: Sea ice rheology from in-situ, satellite and laboratory observations: Fracture and friction. *Earth and Planetary Science Letters*, **255** (1-2), 1–8, doi:10.1016/j.epsl.2006.11.033, URL <http://dx.doi.org/10.1016/j.epsl.2006.11.033>.
- Wijeratne, S., C. Pattiarchi, and R. Proctor, 2018: Estimates of surface and subsurface boundary current transport around Australia. *Journal of Geophysical Research: Oceans*, doi:10.1029/2017jc013221, URL <http://dx.doi.org/10.1029/2017JC013221>.
- Wijffels, S. E., and Coauthors, 2018: A fine spatial-scale sea surface temperature atlas of the Australian regional seas (SSTAARS): Seasonal variability and trends around Australasia and New Zealand revisited. *Journal of Marine Systems*, doi:10.1016/j.jmarsys.2018.07.005, URL <http://dx.doi.org/10.1016/j.jmarsys.2018.07.005>.
- Wilchinsky, A. V., and D. L. Feltham, 2006: Modelling the rheology of sea ice as a collection of diamond-shaped floes. *Journal of Non-Newtonian Fluid Mechanics*, **138** (1), 22–32, doi:10.1016/j.jnnfm.2006.05.001, URL <http://dx.doi.org/10.1016/j.jnnfm.2006.05.001>.
- Williams, K. D., and Coauthors, 2018: The Met Office Global Coupled Model 3.0 and 3.1 (GC3.0 and GC3.1) configurations. *Journal of Advances in Modeling Earth Systems*, **10** (2), 357–380, doi:10.1002/2017ms001115, URL <http://dx.doi.org/10.1002/2017MS001115>.
- Worby, A. P., C. A. Geiger, M. J. Paget, M. L. Van Woert, S. F. Ackley, and T. L. DeLiberty, 2008: Thickness distribution of Antarctic sea ice. *Journal of Geophysical Research*, **113** (C5), doi:10.1029/2007jc004254, URL <http://dx.doi.org/10.1029/2007JC004254>.
- Wu, Y., X. Zhai, and Z. Wang, 2017: Decadal-mean impact of including ocean surface currents in bulk formulas on surface air-sea fluxes and ocean general circulation. *Journal of Climate*, **30** (23), 9511–9525, doi:10.1175/jcli-d-17-0001.1, URL <http://dx.doi.org/10.1175/JCLI-D-17-0001.1>.
- Xu, Y., and L.-L. Fu, 2011: Global variability of the wavenumber spectrum of oceanic mesoscale turbulence. *Journal of Physical Oceanography*, **41** (4), 802–809, doi:10.1175/2010JPO4558.1, URL <http://dx.doi.org/10.1175/2010JPO4558.1>.
- Xu, Y., and L.-L. Fu, 2012: The effects of altimeter instrument noise on the estimation of the wavenumber spectrum of sea surface height. *Journal of Physical Oceanography*, **42** (12), 2229–2233, doi:10.1175/JPO-D-12-0106.1, URL <http://dx.doi.org/10.1175/JPO-D-12-0106.1>.
- Yang, R., M. Ward, and B. Evans, 2019: Parallel I/O in FMS and MOM5. *Geoscientific Model Development Discussions*, **2019**, 1–31, doi:10.5194/gmd-2019-257, URL <https://www.geosci-model-dev-discuss.net/gmd-2019-257/>.
- Zhang, J., and D. A. Rothrock, 2003: Modeling global sea ice with a thickness and enthalpy distribution model in generalized curvilinear coordinates. *Monthly Weather Review*, **131** (5), 845–861, doi:10.1175/1520-0493(2003)131<0845:mgswa>2.0.co;2, URL [http://dx.doi.org/10.1175/1520-0493\(2003\)131<0845:MGSIWA>2.0.CO;2](http://dx.doi.org/10.1175/1520-0493(2003)131<0845:MGSIWA>2.0.CO;2).

REFERENCES

- Zhang, R., R. Sutton, G. Danabasoglu, Y.-O. Kwon, R. Marsh, S. G. Yeager, D. E. Amrhein, and C. M. Little, 2019: A review of the role of the Atlantic Meridional Overturning Circulation in Atlantic multidecadal variability and associated climate impacts. *Reviews of Geophysics*, doi: 10.1029/2019rg000644, URL <http://dx.doi.org/10.1029/2019RG000644>.
- Zhang, Z., T. Vihma, A. Stössel, and P. Uotila, 2015: The role of wind forcing from operational analyses for the model representation of Antarctic coastal sea ice. *Ocean Modelling*, **94**, 95–111, doi: 10.1016/j.ocemod.2015.07.019, URL <http://dx.doi.org/10.1016/j.ocemod.2015.07.019>.
- Zilberman, N. V., D. H. Roemmich, and S. T. Gille, 2014: Meridional volume transport in the South Pacific: Mean and SAM-related variability. *Journal of Geophysical Research: Oceans*, **119** (4), 2658–2678, doi:10.1002/2013JC009688, URL <https://agupubs.onlinelibrary.wiley.com/doi/abs/10.1002/2013JC009688>.
- Zilberman, N. V., D. H. Roemmich, S. T. Gille, and J. Gilson, 2018: Estimating the velocity and transport of western boundary current systems: A case study of the East Australian Current near Brisbane. *Journal of Atmospheric and Oceanic Technology*, **35** (6), 1313–1329, doi:10.1175/jtech-d-17-0153.1, URL <http://dx.doi.org/10.1175/JTECH-D-17-0153.1>.
- Zweng, M., and Coauthors, 2013: World Ocean Atlas 2013, Volume 2: Salinity. NOAA Atlas NESDIS 74. URL https://data.nodc.noaa.gov/woa/WOA13/DOC/woa13_vol2.pdf.

Index

01deg_jra55v13_iaf, 33
01deg_jra55v13_ryf8485_spinup6, 33
1deg_jra55v13_iaf_spinup1_B1_lastcycle, 10
1deg_jra55v13_iaf_spinup1_B1, 10
BLCKX, 34, 36
BLCKY, 34, 36
MXBLCKS, 34
NCAT, 25
NTASK, 34, 36
a_rapid_mode, 86
absolute_wind, 32
accessom2.nml, 23, 28, 72, 89, 91, 98, 111
accessom2_nml, 72, 89, 90, 92, 99, 111
acor, 24, 74, 118
adams_bashforth_third, 24, 79
advect_gotm_method, 122, 128
advect_sweby_all, 122, 128
advection, 81
afkph_00, 129
afkph_90, 129
age_tracer_max_init, 79, 122
agm_closure_baroclinic, 17, 75, 103, 112, 119
agm_closure_buoy_freq, 17, 75, 103, 113, 119
agm_closure_eady_ave_mixed, 18, 75, 113
agm_closure_eady_cap, 18, 75, 113
agm_closure_eady_smooth_horz, 18, 75, 113
agm_closure_eady_smooth_vert, 18, 75, 113
agm_closure_eden_gamma, 75, 100, 101
agm_closure_eden_greatbatch, 75, 100, 101
agm_closure_grid_scaling, 18, 76, 113
agm_closure_length_bczone, 76, 100, 101, 103, 119
agm_closure_length_fixed, 76, 100, 101, 103, 119
agm_closure_length_rossby, 76, 100, 101, 103, 119
agm_closure_length, 17, 76, 103, 113, 119
agm_closure_lower_depth, 17, 76, 103, 113, 119
agm_closure_max, 18, 76, 103, 113, 119, 126
agm_closure_min, 18, 76, 103, 113, 119, 126
agm_closure_scaling, 17, 76, 103, 113, 119
agm_closure_upper_depth, 17, 76, 103, 113, 119
agm_closure, 17, 75, 103, 112, 119
agm_damping_time, 76, 100, 101
agm_smooth_space, 18, 76, 100, 101
agm_smooth_time, 18, 76, 100, 101
agm, 75, 100, 101, 103, 119
ahmax, 27, 86, 134
aice_cutoff, 72, 116
aice, 33
aidif, 24, 79
albedo_type, 27, 86
albicei, 27, 86, 134
albicev, 27, 86, 134
albsnowi, 27, 86
albsnowv, 27, 86
alt_gustiness, 31, 88
aredi_diffusivity_grid_scaling, 18, 76, 113
aredi_equal_agm, 18, 76, 103, 113, 119
aredi, 18, 76, 103, 113, 119, 126
aspect_rapid_mode, 86
athresh, 121
atm.nml, 88, 91, 97, 111, 115
atm_data_dir, 81
atm_data_format, 81
atm_data_type, 81
atmbndy, 81
atmos_npes, 116
auscom_ice_nml, 72, 93, 112, 116, 124
avg_sfc_temp_salt_eta, 77, 120
avg_sfc_velocity, 77, 120
background_diffusivity, 21, 79, 129
background_viscosity, 21, 79, 123
baroclinic_split, 24, 27, 75
barotropic_halo, 73, 117, 125
barotropic_leap_frog, 117
barotropic_pred_corr, 117
barotropic_split, 23, 75, 119, 126
barotropic_time_stepping_a, 23, 73, 117
barotropic_time_stepping_b, 73, 117
barotropic_time_stepping_mom4p0, 117
barotropic_time_stepping_mom4p1, 117
bg_diff_eq, 124
bg_diff_lat_dependence_nml, 124
bgc_data_dir, 86
bgc_flux_type, 86
bih_friction_scheme, 74
bmf_implicit, 24, 74, 118, 125
bottom_5point, 18, 37, 74, 75, 112
bryan_lewis_diffusivity, 79
bryan_lewis_lat_depend, 79, 123, 129
bryan_lewis_lat_transition, 129
build.sh, 34
buoyancy_crit, 51
bv_freq_smooth_vert, 76, 113
bvp_bc_mode, 76, 113
bvp_min_speed, 76, 113
bvp_speed, 76, 113
calc_strair, 81, 130
calc_tsfc, 81, 130
calendar, 116, 127
calving_insertion_thickness, 29
calvingspread, 77, 120, 127

INDEX

cap_fluxes, 130
cdbot_hi, 21, 74, 118, 125
cdbot_law_of_wall, 21, 68, 125
cdbot_lo, 21
cdbot_roughness_length, 74, 100, 101, 103, 118, 125
cdbot_roughness_uamp, 21, 74, 118, 125
cdbot, 21, 68, 74, 100, 101, 103, 118
charnock, 87
check_stocks, 116
checksum_required, 73, 93, 94, 112, 117
chio, 26, 86, 134
chk_a2i_fields, 87
chk_frzmlt_sst, 87, 108
chk_gfdl_roughness, 87
chk_i2a_fields, 87, 108
chk_i2o_fields, 72, 87, 108, 116
chk_o2i_fields, 72, 87, 108, 116
chl.nc, 28
cice_in.nml, 23, 34, 80, 90, 95, 104, 114, 130
clock_grain, 73, 112, 117
cmip_units, 75, 119
coefficient_ce, 78, 121, 128
compute_tmask_limit_on, 122
conduct, 26, 86, 134
config.yaml, 28, 34
construct_table_wrt_liq_and_ice, 123
convect_full_scalar, 118, 125
convect_full_vector, 118, 125
convect_ncon, 118
correct_adv_errors, 122, 129
cosw, 26, 33, 37, 81, 95, 130
coupler_nml, 116
coupling_nml, 87, 108–110
cprime_aiki, 125
cst_ocn_albedo, 27, 68, 87, 108–110
current_date, 116
dSdt_slow_mode, 39
dalb_mlt, 27, 86, 134
damp_coeff_3d, 121, 128
date_init, 127
date_manager_nml, 72, 89, 90, 92, 98, 99, 111
days_per_year, 85
days_to_increment, 118, 119, 126
days_to_restore, 121
days, 116, 127
dbuf, 85
debug_diag_manager, 73, 101, 102, 117, 124
debug_this_module_detail, 78, 122
debug_this_module, 73–79, 100–104, 118–123, 125, 126, 128, 129
debug, 75
decay_scale, 21, 79, 123, 129
deflate_level=-1, 67
deflate_level, 73, 99, 112, 117, 125
dfkph_00, 129
dfkph_90, 129
diag_file, 85
diag_manager_nml, 73, 99, 101, 102, 117, 124
diag_step, 73, 78, 79, 112, 113, 117, 122, 125, 128
diag_type, 85
diagfreq, 85, 95, 134
diff_cbt_iw, 79, 122, 123
diff_cbt_limit, 122
diff_cbt_min, 123, 129
diff_con_limit, 122, 129
discharge_combine_runoff_calve, 29
distribution_type, 34, 36, 80, 91, 95, 97, 107, 114
distribution_wght, 80, 130
do_advection_gotm, 123, 129
do_alltoallv, 80, 114, 124
do_alltoall, 80, 114, 124
do_area_weighted_flux, 117
do_atmos, 116
do_bitwise_exact_sum, 77, 79, 113, 120, 127
do_cap40, 87
do_eta_tendency, 120
do_flux_correction, 77, 120, 127
do_gm_skewson, 76, 113
do_highwind, 88
do_ice_once, 72, 116
do_ice, 116
do_land, 116
do_langmuir, 38, 129
do_neutral_diffusion, 76, 113
do_ocean, 116
do_override_stress_ofam, 120
do_runoff, 117
do_turbulence_gotm, 123, 129
do_wave, 126
domain_nml, 80, 91, 95, 97, 107, 114, 130
domains_stack_size, 73, 93, 112, 117, 124
double_diffusion, 79, 123
dpscale, 85
drag_coeff, 21
drag_dissipation_use_cbot, 79, 123, 129
dragio, 26, 81, 130
drhodz_min, 80, 129
drhodz_mom4p1, 18, 67, 76, 101, 103, 113, 119
drhodz_smooth_horz, 76, 100, 101, 103, 119
drhodz_smooth_vert, 76, 100, 102, 104, 119
dsdt_slow_mode, 86, 134
dt_atmos, 116
dt_cpld, 116, 127
dt_cpl, 124
dt_mlt, 27, 86, 134
dt_ocean, 119, 126

dt, 23, 85, 115, 134
 dump_last, 85
 dumpfreq_n, 85, 115
 dumpfreq, 85, 115, 134
 dynamics_nml, 81, 95, 130
 enable_simple_timers, 92
 energy_diag_step, 79, 113, 122, 128
 enforce_sw_frac, 77
 eos_linear, 74, 118
 eos_preteos10, 23, 74, 118
 epsln_bv_freq, 76, 113
 eq_lat_micom, 74, 118
 eq_vel_micom_aniso, 74, 118
 eq_vel_micom_iso, 74, 118
 equatorial_zonal, 74, 118
 eta_max, 23, 73, 117
 ew_boundary_type, 80
 f_aero, 81, 130
 f_aicen, 82, 91, 107
 f_aice, 82, 105–107, 131
 f_aisnap, 82
 f_albice, 82, 114, 131
 f_albpnd, 82
 f_albsni, 82, 114, 131
 f_albsno, 82, 114, 131
 f_alidf_ai, 131
 f_alidf, 131
 f_alidr_ai, 131
 f_alidr, 82
 f_alvdf_ai, 131
 f_alvdf, 131
 f_alvdr_ai, 131
 f_alvdr, 82
 f_alvl, 82, 131
 f_anglet, 83
 f_angle, 82
 f_aparticn, 82
 f_apeff_ai, 84, 105, 106
 f_apeffn, 84, 133
 f_apeff, 84, 105, 106
 f_apond_ai, 85, 105, 106
 f_apondn, 85, 133
 f_apond, 84, 105, 106
 f_araftn, 82
 f_ardgn, 82
 f_ardg, 82, 131
 f_aredistn, 82
 f_bgc_am_ml, 81, 130
 f_bgc_am_sk, 81, 130
 f_bgc_c_sk, 81, 130
 f_bgc_chl_sk, 81, 130
 f_bgc_dms_sk, 81, 130
 f_bgc_dmssp_ml, 81, 130
 f_bgc_dmspd_sk, 81, 130
 f_bgc_dmssp_sk, 81, 130
 f_bgc_n_sk, 81, 130
 f_bgc_nit_ml, 82, 130
 f_bgc_nit_sk, 82, 130
 f_bgc_sil_ml, 82, 130
 f_bgc_sil_sk, 82, 130
 f_bounds, 83
 f_bphi, 82, 130
 f_btin, 82, 130
 f_cdn_atm, 82, 131
 f_cdn_ocn, 82, 131
 f_congel, 68, 83, 105–107, 131
 f_coszen, 83
 f_daidtd, 83, 107, 131
 f_daidtt, 83, 107, 131
 f_dardg1dt, 82, 131
 f_dardg1ndt, 82
 f_dardg2dt, 82, 131
 f_dardg2ndt, 82
 f_divu, 83, 107
 f_drag, 82, 131
 f_dsnow, 83
 f_dvidtd, 83, 105–107, 131
 f_dvidtt, 83, 105–107, 131
 f_dvirdgdt, 82, 131
 f_dvirdgndt, 82
 f_dvsdtd, 131
 f_dvsdtt, 131
 f_dxt, 83, 131
 f_dxu, 83, 131
 f_dyf, 83, 131
 f_dyu, 83, 131
 f_evap_ai, 83, 114, 131
 f_evap_ice_ai, 131
 f_evap_snow_ai, 131
 f_evap, 83
 f_faero_atm, 82, 130
 f_faero_ocn, 82, 130
 f_fbri, 82, 105, 106, 130
 f_fcondtop_ai, 83, 114, 131
 f_fcondtopn_ai, 83, 114
 f_fhocn_ai, 83, 114, 131
 f_fhocn, 83
 f_flat_ai, 83, 114, 131
 f.flatn_ai, 83, 131
 f_flat, 83
 f_flwdn, 83, 114, 131
 f_flwup_ai, 83, 114, 131
 f_flwup, 83
 f_fmeltt_ai, 83, 96, 105
 f_fmelttn_ai, 83, 114, 131
 f_fn_ai, 82, 131

f_fnh_ai, 82, 131
 f_fnh, 82, 131
 f_fno_ai, 82, 131
 f_fno, 82, 131
 f_fn, 82, 130
 f_frazil, 68, 83, 105–107, 131
 f_fresh_ai, 83, 114, 132
 f_fresh, 83
 f_frz_onset, 83, 105–107
 f_frzmlt, 68, 83, 105–107
 f_fsalt_ai, 83, 96, 106, 107, 132
 f_fsalt, 83, 105–107
 f_fsens_ai, 83, 114, 132
 f_fsens, 83, 132
 f_fsil_ai, 82, 131
 f_fsil, 82, 131
 f_fsurf_ai, 83, 132
 f_fsurf_nai, 83, 114
 f_fswabs_ai, 83, 114, 132
 f_fswabs, 83
 f_fswdn, 83, 114, 132
 f_fswfac, 83, 114, 132
 f_fswthru_ai, 83, 114, 132
 f_fswthru, 83
 f_fy, 83
 f_grownet, 82, 131
 f_hbri, 82, 105, 106, 131
 f_hisnap, 83
 f_hi, 83, 105–107, 132
 f_hpond_ai, 85, 105, 106
 f_hpondn, 85, 133
 f_hpond, 85, 105, 106
 f_hs, 83, 91, 105–107, 132
 f_hte, 83, 132
 f_htn, 83, 132
 f_iage, 83, 132
 f_icepresent, 84, 114, 132
 f_ipond_ai, 85, 105, 106
 f_ipond, 85, 105, 106
 f_krdgn, 82
 f_meltb, 84, 114, 132
 f_meltl, 84, 114, 132
 f_melts, 84, 114, 132
 f_meltt, 84, 114, 132
 f_mlt_onset, 84, 105–107
 f_ncat, 84
 f_opening, 82, 96, 105, 131
 f_ppnet, 82, 131
 f_qref, 84
 f_rain_ai, 84, 114, 132
 f_rain, 84
 f_shear, 84, 107, 132
 f_siage, 132
 f_sialb, 132
 f_sice, 84, 114, 132
 f_sicomstren, 132
 f_sidconcdyn, 132
 f_sidconch, 132
 f_sidivvel, 132
 f_sidmassdyn, 132
 f_sidmassevapsubl, 132
 f_sidmassgrowthbot, 132
 f_sidmassgrowthwat, 132
 f_sidmasslat, 132
 f_sidmassmeltbot, 132
 f_sidmassmelttop, 132
 f_sidmassssi, 132
 f_sidmassth, 132
 f_sidmasstranx, 132
 f_sidmasstrany, 132
 f_sifb, 132
 f_siflcondbot, 132
 f_siflcondtop, 132
 f_siflfwbot, 132
 f_sifllatstop, 132
 f_sifllwdtop, 132
 f_sifllwutop, 132
 f_siflsaltbot, 132
 f_siflsenstop, 132
 f_siflsensupbot, 132
 f_siflswdbot, 132
 f_siflswdtop, 132
 f_siflswutop, 132
 f_siforcecoriolx, 132
 f_siforcecorioly, 133
 f_siforceintstrx, 133
 f_siforceintstry, 133
 f_siforcetiltx, 133
 f_siforcetilty, 133
 f_sig1, 84, 96, 106, 107, 133
 f_sig2, 84, 96, 106, 107, 133
 f_sihc, 133
 f_sinz, 84
 f_sipr, 133
 f_sisaltmass, 133
 f_sisnconc, 133
 f_sisnhc, 133
 f_sisnthick, 133
 f_sispeed, 133
 f_sistrxdtop, 133
 f_sistrxubot, 133
 f_sistrydtop, 133
 f_sistryubot, 133
 f_sitempbott, 133
 f_sitempsnic, 133
 f_sitemptop, 133

f_sithick, 133
 f_siui, 133
 f_siv, 133
 f_sndmassmelt, 133
 f_sndmasssnf, 133
 f_snoice, 84, 105–107, 133
 f_snow_ai, 84, 114, 133
 f_snowfracn, 133
 f_snowfrac, 133
 f_snow, 84
 f_sss, 84, 96, 105, 107
 f_sst, 84, 96, 105, 107
 f_strairx, 84, 107, 133
 f_strairy, 84, 107, 133
 f_strcorx, 84, 114, 133
 f_strcory, 84, 115, 133
 f_strength, 84, 133
 f_strintx, 84, 115, 133
 f_strinty, 84, 115, 133
 f_strocnx, 84, 115, 133
 f_strocny, 84, 115, 133
 f_strltx, 84, 115, 133
 f_strlty, 84, 115, 133
 f_tair, 84, 115
 f_tarea, 84
 f_tinz, 84
 f_tmask, 84
 f_tref, 84
 f_trsig, 84, 115
 f_tsfc, 84, 133
 f_tsnz, 84
 f_uarea, 84
 f_uocn, 84, 96, 105, 107, 133
 f_uvel, 84, 105–107, 133
 f_vgrdb, 84, 133
 f_vgrdi, 84
 f_vgrds, 84
 f_vicen, 84, 91, 107
 f_vlvl, 82, 114, 131
 f_vocn, 84, 96, 105, 107, 133
 f_vraftn, 82
 f_vrdgn, 82
 f_vrdg, 82, 114, 131
 f_vredistn, 82
 f_vsnon, 133
 f_vvel, 84, 105–107, 133
 field_table, 21, 22
 fields_from_atm, 108–110
 fields_from_ocn, 108–110
 fields_in, 73, 99, 101, 103, 117, 125
 fields_out, 73, 117, 125
 fields_to_ocn, 108–110
 filesset_write, 73, 112
 fixed_wave_dissipation, 80, 123
 fixmeltt, 72, 116
 flux_exchange_nml, 117
 fms_io_nml, 73, 93, 94, 112, 117
 fms_nml, 73, 93, 112, 117, 124
 forcing.json, 9, 28
 forcing_end_date, 72, 98, 99, 111
 forcing_nml, 31, 67, 81, 105–107, 114, 130
 forcing_start_date, 72, 98, 99, 112
 formdrag, 81
 frac_crit_cell_height, 23, 73, 117
 fraction_increment, 118, 119, 126
 frazil_factor, 72, 116
 frazil_heating_after_yphysics, 79
 frazil_heating_before_yphysics, 79, 122
 frazil_only_in_surface, 23, 74, 118, 125
 freezing_temp_preteos10, 23, 26, 74, 118, 125
 freezing_temp_simple, 74, 118, 125
 front_length_const, 78, 121
 front_length_deform_radius, 78, 121
 frzpdnd, 85, 133
 fyyear_init, 81, 130
 gfdl_surface_flux, 87
 gm_skewson_bvproblem, 76, 113
 gm_skewson_modes, 76, 113
 grid_file, 81, 130
 grid_format, 81
 grid_nml, 81, 130
 grid_type, 81
 gust_const, 31, 88
 gust_min, 31, 88
 highfreq, 31, 32, 39, 67, 105–107
 hist_avg, 85
 histfreq_n, 85
 histfreq, 85
 history_chunksize_x, 105–107, 115
 history_chunksize_y, 105–107, 115
 history_deflate_level, 105–107
 history_dir, 85, 134
 history_file, 85
 hi, 33
 horizontal-advection-scheme, 17
 hours, 117, 128
 hp1, 85
 hs0, 39, 85, 133
 hs1, 85
 hwf_diffusivity, 79, 123, 129
 hwf_min_diffusivity, 79, 123, 129
 hwf_n0_2omega, 79, 123, 129
 ice_diag.d, 34
 ice_fwflux, 87
 ice_ic, 33, 85
 ice_init.F90, 33

ice_model_nml, 117
 ice_ocean_timestep, 23, 24, 27, 37, 72, 89, 90, 92, 99, 111
 ice_pressure_on, 87
 ice_ref_salinity, 31
 ice_salt_concentration, 31, 127
 icefields_bgc_nml, 81, 105, 106, 130
 icefields_drag_nml, 82, 131
 icefields_mechred_nml, 82, 96, 105, 114, 131
 icefields_nml, 82, 91, 96, 105–107, 114, 131
 icefields_pond_nml, 84, 105, 106, 133
 iceform_adj_salt, 72, 116
 icemlt_factor, 72, 116
 iceruf, 27, 81, 130
 ige, 124
 igs, 124
 impose_init_from_restart, 119
 incond_dir, 85, 134
 incond_file, 85
 initialize_zero_eta, 128
 input.nml, 9, 72, 90, 92, 99, 112, 124
 input_ice.nml, 87, 91, 97, 108, 115
 input_ice_gfdl.nml, 87, 91, 97, 110, 115
 input_ice_monin.nml, 88, 91, 97, 111, 115
 interp_method, 80, 130
 io_layout, 75, 93, 94, 112, 117, 119, 126
 ire1, 124
 ire2, 124
 irs1, 124
 irs2, 124
 issue_oor_warnings, 73, 117, 124
 istep0, 85, 90, 95, 105–107, 134
 j09_bgmax, 21, 69, 79, 104, 113, 129
 j09_bgmin, 21, 69, 79, 104, 113, 129
 j09_diffusivity, 21, 79, 104, 113, 129
 j09_lat, 21, 79, 104, 114, 129
 jge, 124
 jgs, 124
 jre1, 124
 jre2, 124
 jrs1, 124
 jrs2, 124
 k_smag_aniso, 18, 37, 74, 75, 112, 118
 k_smag_iso, 18, 37, 74, 75, 112, 118
 kbl_standard_method, 79, 123, 129
 kcatbound, 25, 55, 81, 130
 kdyn, 25, 81
 kitd, 86
 kmt_file, 81, 130
 kmt_min, 16
 kmxic, 73, 116, 124
 krdg_partic, 25, 81
 krdg_redist, 81
 kstrength, 81
 ktherm, 26, 36, 86, 115
 lambda, 121
 land_model_heat_fluxes, 77, 120, 127
 lap_friction_scheme, 75, 119
 large_cfl_value, 73, 79
 lat_low_bgdiff, 124
 latpnt, 85, 107
 layer_nk, 74, 118
 layout, 36, 75, 93, 94, 112, 117, 119, 126
 lcdf64, 85, 105–107, 134
 limit_age_tracer, 79, 122
 limit_icemelt, 87
 limit_psi_velocity_scale, 78, 121
 limit_psi, 78, 121
 limit_salt_min, 121
 limit_salt, 121
 limit_temp_restore, 121
 limit_temp, 121
 linear_eos, 118
 linear_taper_diff_cbt_table, 129
 log_level, 72
 lonpnt, 85, 107
 make_exchange_reproduce, 80, 130
 make_tables.py, 72, 89, 91, 97, 111
 maskhalo_bound, 34, 80, 130
 maskhalo_dyn, 34, 80, 130
 maskhalo_remap, 34, 80, 130
 max_advection_velocity, 73, 103, 112, 117
 max_axes, 99, 101, 102, 117
 max_cfl_value, 73, 79
 max_cgint, 79, 122
 max_delta_salinity_restore, 30, 77, 93, 113, 120, 127
 max_drag_diffusivity, 129
 max_files, 99, 101, 102
 max_ice_thickness, 9, 23, 77, 120, 127
 max_num_axis_sets, 99, 101, 102
 max_tracers, 74, 118, 125
 max_wave_diffusivity, 80, 123
 maxraft, 25
 meltlimit, 87
 min_diss, 123, 129
 min_kblt, 78, 121
 min_thickness, 67, 100, 102, 104, 128
 min_tke, 123, 129
 minutes, 117, 128
 mixdownslope_mask_gfdl, 75, 112
 mixdownslope_npts, 23, 75, 112
 mixing_efficiency_n2depend, 80, 123
 mld, 51
 mom_oasis3_interface_nml, 9, 73, 99, 101, 103, 117, 125
 monin_obukhov_nml, 37, 73, 88, 99, 101, 103, 117, 125
 months, 117, 128

INDEX

mpp_io_nml, 73, 99, 112, 117, 125
mu_rdg, 25, 81
n_itts, 31
namcouple, 9
ncar_boundary_scaling_read, 74, 118, 125
ncar_boundary_scaling, 18, 67, 74, 101, 103, 112, 118
ncar_ocean_flux_orig, 31, 88
ncar_ocean_flux, 31, 88, 124
ncar_only_equatorial, 126
ncar_rescale_power, 18, 74, 118
ncar_vconst_4, 18, 74, 118
ncar_vconst_5, 74, 118
ncpus, 34
ndtd, 24, 25, 36, 85, 107, 115
ndte, 24, 25, 39, 71, 81
neutral_eddy_depth, 76, 113
neutral_linear_gm_taper, 126
neutral_physics_limit, 76, 113, 126
neutral_physics_simple, 126
neutral_sine_taper, 126
neutralrho_max, 67, 74, 100, 101, 103, 118
neutralrho_min, 67, 74, 100, 101, 103, 118
neutral, 37, 73, 88, 99, 101, 103, 117, 125
nit_data_type, 86
nmltab, 72, 89, 91, 97, 111
no_neg_q, 88
nphysics_util_zero_init, 17, 76, 113
npower, 121
nprocs, 34, 80, 91, 95, 97, 107, 114, 130
npt, 85, 115, 134
ns_boundary_type, 80
nsteps_adv, 117
nsteps_dyn, 117
nsubset, 80, 124, 130
num_fields_in, 73, 99, 101, 103, 117, 125
num_fields_out, 73, 117, 125
num_runoff_caps, 88, 115
number_bc_modes, 76, 113
ocean.nc, 11
ocean_adv_vel_diag_nml, 73, 112, 117, 125
ocean_advection_velocity_nml, 73, 103, 112, 117
ocean_albedo_nml, 73, 99, 101, 103, 125
ocean_albedo_option, 27, 68, 73, 99, 101, 103, 125
ocean_barotropic_nml, 73, 100, 101, 103, 112, 117, 125
ocean_bbc_nml, 74, 100, 101, 103, 118, 125
ocean_bbc_ofam_nml, 118, 125
ocean_bih_friction_nml, 74
ocean_bih_tracer_nml, 74
ocean_bihcst_friction_nml, 74
ocean_bihgen_friction_nml, 74, 101, 103, 112, 118, 125
ocean_convect_nml, 21, 74, 118, 125
ocean_coriolis_nml, 74, 118
ocean_density_nml, 74, 100, 101, 103, 118
ocean_domains_nml, 74, 118, 125
ocean_form_drag_nml, 74, 125
ocean_frazil_nml, 74, 100, 101, 103, 118, 125
ocean_grid.nc, 21
ocean_grids_nml, 75, 100, 101, 103, 126
ocean_hgrid.nc, 13
ocean_ice_salt_limit, 31, 77, 102, 113, 120
ocean_increment_eta_nml, 75, 118, 126
ocean_increment_tracer_nml, 75, 118, 126
ocean_increment_velocity_nml, 75, 119, 126
ocean_lap_friction_nml, 75, 119
ocean_lap_tracer_nml, 75
ocean_lapcst_friction_nml, 75
ocean_lapgen_friction_nml, 75, 112, 126
ocean_mixdownslope_nml, 23, 75, 100, 112, 119
ocean_model_nml, 75, 93, 94, 112, 119, 126
ocean_momentum_source_nml, 75, 119, 126
ocean_npes, 117
ocean_nphysicsC, 17
ocean_nphysics_mom4p0_nml, 119
ocean_nphysics_mom4p1_nml, 119
ocean_nphysics_nml, 17, 75, 100, 101, 103, 112, 119
ocean_nphysics_util_nml, 17, 75, 100, 101, 103, 112, 119, 126
ocean_nphysicsa_nml, 76, 119, 126
ocean_nphysicsb_nml, 76, 119
ocean_nphysicsc_nml, 76, 100, 102, 113, 119
ocean_ofam_diag_nml, 120
ocean_operators_nml, 76, 100, 102, 104, 120, 126
ocean_overexchange_nml, 23, 76, 100, 102, 104, 120, 126
ocean_overflow_nml, 23, 77, 120, 126
ocean_overflow_ofp_nml, 77, 120, 126
ocean_polar_filter_nml, 77, 100, 102, 104
ocean_pressure_nml, 77, 100, 102, 104, 120, 127
ocean_rivermix_nml, 77, 100, 102, 104, 120, 127
ocean_riverspread_nml, 77, 104, 120, 127
ocean_rough_nml, 27, 77, 87, 120, 127
ocean_sbc_nml, 77, 93, 94, 102, 113, 120, 127
ocean_sbc_ofam_nml, 120, 127
ocean_shortwave_csiro_nml, 77, 120, 127
ocean_shortwave_gfdl_nml, 28, 77, 100, 102, 104, 120, 127
ocean_shortwave_jerlov_nml, 78, 121
ocean_shortwave_nml, 78, 121
ocean_sigma_transport_nml, 23, 38, 78, 113, 127
ocean_solo_nml, 127
ocean_sponges_eta_nml, 78
ocean_sponges_eta_ofam_nml, 121
ocean_sponges_tracer_nml, 78, 121, 128
ocean_sponges_tracer_ofam_nml, 121
ocean_sponges_velocity_nml, 78, 121
ocean_sponges_velocity_ofam_nml, 121

ocean_submesoscale_nml, 18, 78, 100, 102, 104, 113, 121, 128
 ocean_tempsalt_nml, 78, 100, 102, 104, 122, 128
 ocean_thickness_nml, 78, 100, 102, 104, 122, 128
 ocean_topog_nml, 100, 102, 104, 128
 ocean_tracer_advect_nml, 78, 100, 102, 104, 122, 128
 ocean_tracer_diag_nml, 78, 113, 122, 128
 ocean_tracer_nml, 79, 100, 102, 104, 122, 128
 ocean_velocity_diag_nml, 79, 100, 102, 104, 113, 122, 128
 ocean_velocity_nml, 79, 122, 128
 ocean_vert_chen_nml, 122
 ocean_vert_const_nml, 122
 ocean_vert_gotm_nml, 122, 128
 ocean_vert_kpp_iow_nml, 79, 100, 102, 104, 123, 129
 ocean_vert_kpp_mom4p1_nml, 79, 123, 129
 ocean_vert_kpp_nml, 123
 ocean_vert_mix_nml, 79, 104, 113, 123, 129
 ocean_vert_tidal_nml, 21, 79, 123, 129
 ocean_vgrid.nc, 11
 ocean_xlandinsert_nml, 80, 123, 129
 ocean_xlandmix_nml, 80, 123, 129
 oceanmixed_file, 81
 oceanmixed_ice, 81
 ocn_albedo, 27, 87
 ocn_data_dir, 81
 ocn_data_format, 81
 old_dtaudy, 88
 optics_manizza, 28, 77, 120
 optics_morel_antoine, 77, 120
 overexch_check_extrema, 126
 overexch_npts, 76, 100, 102, 104, 120
 overexch_weight_far, 76, 100, 102, 104, 120
 overflow_umax, 76, 100, 102, 104, 120
 payu, 34
 pbott_offset, 117
 phi_c_slow_mode, 86
 phi_i_mushy, 86
 phi_snow, 86
 pndaspect, 85
 pointer_file, 85
 ponds_nml, 26, 85, 133
 pop_icediag, 73, 87, 116
 potrho_max, 74, 118
 potrho_min, 74, 118
 pottemp_2nd_iteration, 78
 pottemp_equal_contemp, 23, 67, 69, 78, 100, 102, 104, 122, 128
 ppm_hlimiter, 17
 ppm_vlimiter, 17
 precip_factor, 87
 precip_units, 81
 pred_corr_gamma, 23, 73
 print_global, 85, 134
 print_points, 85, 134
 processor_shape, 34, 36, 80, 114, 130
 r_ice, 86
 r_pnd, 86
 r_snow, 86, 134
 rac_rapid_mode, 86
 raoult_sat_vap, 88, 124
 rayleigh_damp_exp_from_bottom, 75, 119, 126
 rayleigh_damp_exp_scale, 119
 rayleigh_damp_exp_time, 119
 read_basin_mask, 78, 122, 128
 read_chl, 28, 77
 read_depth, 120, 127
 read_mixdownslope_mask, 75, 112
 read_rescale_rho0_mask, 128
 read_restore_mask, 77
 read_rho0_profile, 126
 read_roughness, 21, 80, 123
 read_tide_speed, 21, 80, 118, 125
 read_wave_dissipation, 80, 123
 reading_roughness_amp, 21, 80, 123
 reading_roughness_length, 80, 123
 redsea_gulfbay_sfifx, 23, 36, 73, 93, 112, 124
 regularize_psi, 76, 113
 reinit_ts_with_ideal, 122
 remap_depth_to_s_init, 79, 122
 remap_weights_file, 88
 rescale_mass_to_get_ht_mod, 78, 122, 128
 rescale_rho0_basin_label, 128
 rescale_rho0_mask_gfdl, 128
 rescale_rho0_value, 128
 restart_aero, 86
 restart_age, 86
 restart_bgc, 86
 restart_dir, 85
 restart_ext, 85, 134
 restart_file, 85
 restart_format, 85, 105–107
 restart_fy, 86
 restart_hbrine, 86
 restart_lvl, 86
 restart_period, 72, 89, 90, 92, 98, 99, 112
 restart_pond_cesm, 86
 restart_pond_lvl, 86
 restart_pond_topo, 86
 restart, 33, 85, 90, 95–97, 105–107
 restore_bgc, 86
 restore_ice, 81
 restore_mask_gfdl, 77, 120
 restore_mask_ofam, 120, 127
 restore_sst, 81
 restrict_polar_visclat, 75, 112

restrict_polar_visc_ratio, 75, 112
 restrict_polar_visc, 75, 112
 revised_evp, 25, 81
 rfracmax, 39, 85, 134
 rfracmin, 85
 rho0, 11
 ricr, 79, 123
 river_diffuse_salt, 77, 120, 127
 river_diffuse_temp, 77, 120, 127
 river_diffusion_thickness, 77
 river_diffusivity, 77
 river_insertion_thickness, 29, 77, 120
 river_temp_ofam, 120, 127
 rossby_radius_max, 76, 100, 102, 104, 119
 rossby_radius_min, 76, 100, 102, 104, 119
 rotate_winds, 87
 rough_scheme, 27, 77, 88, 120, 127
 roughness_amp.nc, 21
 roughness_cdbot.nc, 21
 roughness_heat, 88
 roughness_min, 88
 roughness_moist, 88
 roughness_mom, 88
 roughness_scale, 80, 123, 129
 rsnw_mlt, 86
 runoff_caps_ie, 32, 89, 115
 runoff_caps_is, 32, 89, 111, 115
 runoff_caps_je, 33, 89, 111, 116
 runoff_caps_js, 33, 89, 116
 runoff_caps, 32, 89, 111, 115
 runoff_insertion_thickness, 29
 runoff_nml, 88, 111, 115
 runoff_salinity, 77, 120
 runoffspread, 77, 113, 120
 runtype, 85, 90, 95–97, 105–107
 s_max_limit, 78
 s_max, 78, 122, 128
 s_min_limit, 78, 122, 128
 s_min, 78, 128
 salinity_restore_limit_lower, 30
 salinity_restore_limit_upper, 30
 salt_correction_scale, 77, 120, 127
 salt_restore_as_salt_flux, 30, 77
 salt_restore_tscale, 30, 77, 93, 94, 113, 120, 127
 salt_restore_under_ice, 30, 77, 120, 127
 salt_sfc_restore.nc, 30
 saltmax, 134
 sat_vapor_pres_nml, 123
 seconds, 117, 128
 secs_to_increment, 118, 119, 126
 secs_to_restore, 121
 send_after_ocean_update, 73, 117, 125
 send_before_ocean_update, 73, 117, 125
 set_state_var, 33
 setup_nml, 85, 90, 91, 95–97, 105–107, 115, 134
 sfix_hours, 124
 sfkph_00, 129
 sfkph_90, 129
 shelf_depth_cutoff, 80, 123, 129
 shortwave_nml, 39, 86, 134
 shortwave, 26, 27, 39, 86
 show_all_bad_values, 123
 shuffle, 73, 117, 125
 sigma_advection_on, 127
 sigma_advection_sgs_only, 38, 127
 sigma_diffusion_on, 127
 sigma_diffusivity_ratio, 127
 sigma_just_in_bottom_cell, 127
 sigma_umax, 38, 127
 sign_stflx, 73, 116
 sil_data_type, 86
 sinw, 26, 33, 37, 81, 95, 130
 skl_bgc, 86
 smax_psi, 76, 113
 smax, 126
 smooth_advect_transport_num, 78, 113, 121, 128
 smooth_advect_transport, 78, 121, 128
 smooth_blmc, 79, 123, 129
 smooth_eta_diag_laplacian, 23, 73, 117
 smooth_eta_t_biharmonic, 73, 125
 smooth_eta_t_laplacian, 23, 73, 125
 smooth_hblt, 78, 121
 smooth_pbdt_biharmonic, 73, 117, 125
 smooth_pbdt_laplacian, 23, 73, 118, 125
 smooth_psi_num, 78, 113, 121, 128
 smooth_psi, 76, 78, 113, 121, 128
 smooth_ri_kmax_eq_kmu, 79, 123, 129
 smooth_sigma_thickness, 127
 smooth_sigma_velocity, 127
 smooth_velmicom, 127
 snowpatch, 27
 spec_ice, 117
 sss_data_type, 81
 sst_data_type, 81
 st_edges_ocean, 11
 st_ocean, 11
 submeso_advect_flux, 78, 121, 128
 submeso_advect_limit, 78, 122, 128
 submeso_advect_upwind, 78, 122, 128
 submeso_advect_zero_bdy, 78, 122, 128
 submeso_diffusion_biharmonic, 18, 78, 122, 128
 submeso_diffusion_scale, 18, 78, 122, 128
 submeso_diffusion, 18, 78, 122, 128
 submeso_limit_flux, 128
 submeso_skew_flux, 78, 122, 128
 surface_flux_nml, 32, 88, 124

surface_height_split, 75
 sw_edges_ocean, 11
 sw_ocean, 11
 swidth, 126
 t_max_limit, 78
 t_max, 78
 t_min_limit, 78, 122, 128
 t_min, 78, 122, 128
 taumin, 121
 temp_restore_tscale, 77, 127
 temperature_variable, 23, 78, 104
 tfrz_option, 26, 81, 114, 130
 thermo_nml, 86, 115, 134
 thickness_dzt_min_init, 128
 thickness_dzt_min, 128
 thickness_method, 78
 thickness_sigma_layer, 38, 127
 thickness_sigma_max, 127
 thickness_sigma_min, 38, 127
 threading_read, 73
 threading_write, 73, 112
 tide_speed_data_on_t_grid, 80, 123
 tideamp.nc, 21
 time_tendency, 24, 75
 tmask_neutral_on, 76, 113, 126
 tmask_sigma_on, 127
 tmelt, 73, 116
 tocnfrz, 26, 86, 134
 topog.nc, 16, 17
 topog_latest.nc, 16
 tr_aero, 86
 tr_bgc_am_sk, 86
 tr_bgc_c_sk, 86
 tr_bgc_chl_sk, 86
 tr_bgc_dms_sk, 87
 tr_bgc_dmspd_sk, 87
 tr_bgc_dmspp_sk, 87
 tr_bgc_sil_sk, 87
 tr_brine, 87
 tr_fy, 86
 tr_iage, 86, 134
 tr_lvl, 86
 tr_pond Cesm, 86
 tr_pond_lvl, 86
 tr_pond_topo, 86, 134
 tracer_conserve_days, 79, 122, 128
 tracer_mix_micom, 38, 76, 100, 102, 104, 119, 127
 tracer_nml, 86, 134
 trestore, 81
 truncate_eta, 23, 74
 truncate_velocity_value, 79, 122
 truncate_velocity, 79
 truncate_verbose, 79, 122, 128
 turb_blayer_min, 76, 113
 update_dzwu_k0, 122
 update_ocn_f, 81
 uresidual2_max, 118, 125
 uresidual, 21, 74, 125
 use_adaptive_restore, 121
 use_diff_cbt_table, 79, 123
 use_drag_dissipation, 21, 80
 use_full_patm_for_sea_level, 9, 23, 77, 120, 127
 use_geothermal_heating, 28, 74, 100, 101, 103, 118
 use_hard_thump, 121
 use_hblt_equal_mld, 78, 122
 use_ioaice, 73, 116
 use_lag_fluxes, 117
 use_leap_years, 85, 134
 use_legacy_barotropic_halos, 74, 118, 125
 use_legacy_div_ud, 76, 100, 102, 104, 120, 126
 use_legacy_methods, 80, 123, 129
 use_mixing_ratio, 88
 use_normalising, 121
 use_nphysicsa, 17, 75, 119
 use_nphysicsb, 75, 119
 use_nphysicsc, 17, 75, 112, 119
 use_ocnslope, 9, 87
 use_psi_legacy, 78, 122, 128
 use_rayleigh_damp_table, 75, 119
 use_restart_time, 85, 91, 134
 use_shortwave_csiro, 78, 121
 use_shortwave_gfdl, 78, 121
 use_shortwave_jerlov, 78, 121
 use_tempsalt_check_range, 79, 122, 128
 use_this_module, 17, 74–80, 100, 102, 104, 112, 113, 118–123, 125–129
 use_umask, 87
 use_virtual_temp, 88
 use_waterflux, 30, 77
 use_wave_dissipation, 21, 80, 123
 ustар_min, 26, 81
 vconst_1, 126
 vconst_2, 126
 vconst_3, 126
 vconst_4, 126
 vconst_5, 126
 vconst_6, 126
 vconst_7, 126
 vel_mico_iso, 37
 vel_micom_aniso, 18, 37, 74, 118
 vel_micom_bih, 74
 vel_micom_bottom, 18, 37, 74, 112, 118
 vel_micom_iso, 18, 74, 75, 112, 118
 vel_micom_lap_diag, 74, 118
 vel_micom_lap, 23, 74
 vel_micom, 38, 76, 100, 102, 104, 119, 127

INDEX

velocity_advect_centered, 24
verbose_cfl, 73, 117, 125
verbose_init, 123, 129
verbose_truncate, 74, 118
vert_diff_back_via_max, 79, 123
vert_mix_scheme, 18, 79, 123
vertical-advection-scheme, 17
vertical_coordinate, 11, 75
visc_cbu_iw, 79, 122, 123
visc_cbu_limit, 122
visc_cbu_min, 123, 129
visc_con_limit, 122, 129
visc_crit_scale, 18, 74, 112, 118
viscosity_ncar_2000, 126
viscosity_ncar_2007, 75, 112, 126
viscosity_ncar, 75, 112, 126
viscosity_scale_by_rossby_power, 75, 112
viscosity_scale_by_rossby, 75, 112
waterflux_tavg, 127
wave_energy_flux_max, 80, 123
write_a_restart, 123, 129
write_ic, 85
xgrid_nml, 80, 114, 124, 130
xlandmix_kmt, 129
ycycle, 81
year_init, 86, 134
years, 128
z0b, 123, 129
z0s, 123, 129
zbgc_nml, 24, 86
zcoh1, 88
zcoq1, 88
zero_heat_fluxes, 77, 120
zero_net_salt_correction, 77, 120, 127
zero_net_salt_restore, 30, 31, 77, 120, 127
zero_net_water_correction, 77, 120, 127
zero_net_water_couple_restore, 77, 120, 127
zero_net_water_coupler, 30, 77, 120, 127
zero_net_water_restore, 77, 120, 127
zero_pressure_force, 77, 100, 102, 104, 120, 127
zero_surface_stress, 77, 120
zero_tendency_explicit_a, 79, 122, 128
zero_tendency_explicit_b, 79, 122, 128
zero_tendency_implicit, 79, 122, 128
zero_tendency, 74, 79, 125
zero_tracer_advect_horz, 122
zero_tracer_advect_vert, 122
zero_tracer_source, 79, 122
zero_water_fluxes, 77, 120
zfkph_00, 129
zfkph_90, 129
zmax_pen, 28, 67, 77, 100, 102, 104, 120, 121, 127
FIXME, 16, 25, 30, 31, 41, 44, 45, 48, 55, 62
ISSUE, 55
ISSUE (closed), 55
Rayleigh drag, 21, 38
TEOS-10, 23
TODO, 1, 7, 8, 11, 13, 14, 16, 17, 21, 23–34, 37, 41–43, 48–51, 54–56, 58–61, 63, 70, 72, 124
Warnings 13, 16–18, 21, 23, 24, 26, 27, 30, 31, 33